**universität
wien**

DISSERTATION

Titel der Dissertation

**A Geographic Information Science Approach to Flood Hazard Assessment:
Land Cover/Land Use and Climate Change Perspectives
of the Gorganrood Watershed (Iran)**

Verfasser

Masoud Minaei

angestrebter akademischer Grad

Doktor der Naturwissenschaften (Dr. rer.nat.)

Wien, 2015

This collection is dedicated to

My loving family,

My dear parents and brothers

My country (Iran),

All with peace and love!

Acknowledgements

Abstract

GISci or GIScience as the abbreviation of Geographic Information Science contains the existing technologies and research areas of geographic information systems (GIS), remote sensing, cartography and quantitative spatial analysis that provide a powerful collection for natural hazard studies. In the case of natural hazard and hydrological studies, flood hazards are the most common and destructive of all natural disasters. This fact is also true for the Gorganrood watershed –as our case study- in the Northeast of Iran. Flood as a hazard that cause tremendous losses and social disruption worldwide each year, need to be delineated and identified for possible measures to mitigate potential impacts. To study about the flood, Land Cover Land Use (LCLU) and climate are two most important factors influencing hydrological conditions of watersheds.

This study will use GIScience to assess changes of LCLU and climate change (CC) on the hydrological regime of the Gorganrood watershed. To reach to this goal, firstly hydro-meteorological studies were analyzed spatially and temporally. The trends in the precipitation, Max, Min, Mean temperature and discharge series were detected. Then, in the LCLU section the LCLU maps were provided using pixel-based and GEOBIA remote sensing and afterward several spatio-temporal analysis were applied on the maps to know the status and dynamics of LCLU. Afterward, the floods characteristics extracted from discharge series and the relations among these characteristics and LCLU and CC were examined statistically. In addition, to provide deeper knowledge regarding LCLU impacts on runoff series four SWAT model based on LCLU maps were constructed. Afterward, the Minimum, maximum and mean of simulated series were analyzed.

Results of our study show great ability of GIScience to manage different sections of flood hazards related studies. Finally, the relations and contribution percentages of LCLU and CC in each floods characteristics for each sub-basin were detected. In this regard, this study can be so useful and have a significant role to improve the managers' decision-making process regarding the floods. It also provided a deep knowledge and base for the flood hazards in the region and related researches in the future.

Zusammenfassung

"Geographic Information Science" (GIScience oder GISci) - auf Deutsch „geographische Informationswissenschaft" – umfasst die technologischen und wissenschaftlichen Bereiche von Geographischen Informationssystemen (GIS), Fernerkundung, Kartographie und räumlicher Statistik. Diese Werkzeuge stellen in der Erforschung von Naturgefahren und hydrologischen Untersuchungen eine wertvolle Methodensammlung dar.

Unter den Naturgefahren sind Überflutungen die häufigste und zerstörerischte aller Naturkatastrophen. Das gilt auch für das Einzugsgebiet des Gorganroods im Norden Irans, der für diese Untersuchung als Fallstudie dient. Nachdem durch Unwetter und dazugehörige Schäden nicht nur Menschen sondern auch die Wirtschaft in Leidenschaft gezogen wird, soll das Ziel sein, dies bestmöglich vorherzusagen und versuchen die Auswirkungen zu minimieren. Bodenbedeckung und Bodennutzung (engl. Land Cover Land Use (LCLU)) und klimatische Faktoren haben die größten Auswirkungen auf die hydrologischen Eigenschaften eines Einzugsgebietes.

Diese Studie benutzte Daten aus GIScience um die Flächenbeschaffenheit und die klimatische Veränderungen (CC) des Goorganrood Einzugsgebietes näher zu untersuchen. Auch hydrometeorologische Studien in dieser Region hinsichtlich räumlicher und temporärer Einflussnahme wurden herangezogen. Des Weitern wurden Niederschlagmessungen, Temperaturschwankungen (Min., Max., Durchschnitt) und diesbezügliche Trends miteinbezogen.

In diesem Zusammenhang und mit Hilfe der örtliche LCLU, wurde eine spezielle LCLU-Karte auf Pixel-Basis und in globaler Form erstellt. Auf diese Karte wurden dann die räumlichen Temperatur-Schwankungen dargestellt und weiter analysiert um das dynamisches Verhalten der LCLU zu bestimmen. Danach wurden die Flut-Charakteristiken aus den Niederschlagsmengen extrahiert und das Verhältnis zwischen diesen Charakteristiken, LCLU und CC wurden statistisch geprüft. Zusätzlich um die LCLU-Auswirkungen genauer zu verstehen, wurden einige SWAT-Modelle auf die LCLU-Karte angewandt. Daraufhin wurden die Minimal-, Maximal- und die Durchschnittswerte der simulierten Werte genauer analysiert.

Das Resultat dieser Studie zeigt, dass GIScience eine sehr gute Basis bietet, um die Überflutungsgefahren-Studien zu ergänzen. Es lassen sich die Relation und prozentuelle Aufteilung des LCLU und CC bei jeder Flut bewerten. Mit diesen Daten lassen sich Entscheidungen bei Unwetter und Flutkatastrophen besser treffen. Auch die Vorhersagen solche Katastrophen in den mit dieser Methode untersuchten Regionen wären genauer möglich.

Contents

List of Figures

List of Tables

Glossary of Abbreviations

ASTER	Advanced Spaceborne Thermal Emission and Reflection Radiometer
AVHRR	Advanced Very High Resolution Radiometer
CC	Climate Change
CP	Change Point
DEM	Digital Elevation Model
EDA	Exploratory Data Analysis
ESRI	Environmental Systems Research Institute
ETM+	Enhanced Thematic Mapper Plus
GCPs	Ground Control Points
GEOBIA	Geographic Object Based Image Analysis
GIS	Geographic Information System
GISci	Geographic Information Science
GIScience	Geographic Information Science
GNDVI	Green Normalized Difference Vegetation Index
GS	Ehlers and Gram-Schmidt
H	Homogeneities
HPF	High Pass Filter
IDW	Inverse distance weighting
IRS	Indian Remote Sensing satellite
LC	Land Cover
LCLU	Land Cover/Land Use
LCLUC	Land Cover/Land Use Change
LCUC	Land Cover/Use Change
LU	Land Use
LWM	Land and Water Mask
M-HIS	Modified Intensity-Hue-Saturation
MK	Mann-Kendall
MSS	Multispectral Scanner
NDBI	Normalized Difference Build-up Index
NDGRVI	Normalized Difference Green Red Vegetation Index
NDMI	Normalized Dry Matter Index
NDVI	Normalized Difference Vegetation Index
NOAA	National Oceanic Atmospheric Administration
OLI/TIRS	Operational Land Imager / Thermal Infrared Sensor
PCA	Principle Component Analysis
PCC	Post Classification Comparison

POT	Peak-Over-Threshold
Prcp	Precipitation
PW	Pre-whitened series
RS	Remote Sensing
SC	Serial Correlation
SCA	Snow Cover Area
Sen'	Sen's Slope Estimator
SLAVI	Specific Leaf Area Vegetation Index
S-MK	Seasonal Considered Mann-Kendall
STDDEV	Standard Deviation
SWAT	Soil and Water Assessment Tool
TFPW	Trend Free Pre-Whitening
TM	Thematic Mapper
TMax	Maximum Temperature
TMean	Mean Temperature
TMin	Minimum Temperature
TSA	Trend Spatial Analysis
UI	Uniform Intensity

Chapter 1

General Introduction

This chapter introduces the outline of this research, which intends to deal with flood hazards assessment in relation to land cover land use and climate change. The chapter explains the problem and background, express research motivation, questions, objectives and a general research planned methodology within this work. Finally, it will conclude by the structure of the thesis.

1.1.   Introduction

GISci or GIScience as the abbreviation of Geographic Information Science contains the existing technologies and research areas of geographic information systems (GIS), remote sensing, cartography and quantitative spatial analysis (Walsh, 2015). GIScience, therefore, addresses fundamental issues in the use of digital technology to handle geographic information; namely, information about places, activities and phenomena on and near the surface of the Earth that are stored in maps or images (http://www.geo.oregonstate.edu/gcert).

In the case of natural hazard and hydrological studies, flood hazards are the most common and destructive of all natural disasters (Kellens, Terpstra, & De Maeyer, 2013). This fact is also true for the Gorganrood watershed –as our case study- in the Northeast of Iran. The estimation of floods has been at the heart of hydrological research since its beginnings (Rogger et al., 2012). Floods are the basis for building flood protection measures and performing integrated flood management to protect people's lives and property. To mitigate potential impacts of flood as a hazard, floods characteristics in each region must be identified and necessary measures must be delineated. Each year, flood disasters cause tremendous losses and social disruption worldwide. In the last two decades major flood events have further raised the awareness of national and international authorities to the importance of reducing flood risks (Rogger et al., 2012; Uddin, Gurung, Amarnath, & Shrestha, 2013).

To study about the flood, some factors are always in account. The factors can be divided in two categories: Meteorological and physical characteristics. Land Cover

Land Use (LCLU) and climate are two most important factors influencing hydrological conditions of watersheds. Land use/cover changes have impacts on surface runoff, infiltration and soil water redistribution in the hydrological processes (De Roo, Odijk, Schmuck, Koster, & Lucieer, 2001; De Roo, Schmuck, Perdigao, & Thielen, 2003). On the other hand, climate change can change the flood characteristics like, peak flows, runoff or aggravating current flood problems or creating new situations and new types of problems-such as floods in different parts of the year, or new types of floods (Muzik, 2001; Naess, Bang, Eriksen, & Vevatne, 2005).

This study will use GIScience to assess changes of LCLU and climate change (CC) on the hydrological regime of the Gorganrood watershed. In particular, the study will examine the impact of land cover/use change (LCUC) and CC on floods. In this regard, this study can be so useful and have a significant role to improve the managers' decision-making process.

1.2.   Background

Flood hazards are the most common and destructive of all natural disasters (Kellens et al., 2013). Previous research has improved understanding of individual factors but many complex interactions need to be addressed for flood mitigation in practice (www.floodsite.net, 2013).

In previous studies, some have investigated the impacts of urbanization on watershed hydrology e.g. (Du et al., 2012; Sim & Balamurugan, 1991; Suriya & Mudgal, 2012). Some studies used "paired catchment" approach (Merz & Bloschl, 2005; Merz, Bloschl, & Humer, 2008). Such studies studied land cover and climate effects (Bronstert, Niehoff, & Burger, 2002; J. Z. Li, Feng, & Wei, 2013; Z. Li, Liu, Zhang, & Zheng, 2009; Liu, Liu, Ren, Fischer, & Xu, 2011; Loukas, Vasiliades, & Dalezios, 2004; Muzik, 2002; Ouellet, Saint-Laurent, & Normand, 2012). These studies have suggested that although the impact of climate change on flood risk is acknowledged, comprehensive modeling effort, such as necessity of regional assessments, has yet to be seen (Kwon, Sivakumar, Moon, & Kim, 2011) and many complex interactions need to be addressed for flood mitigation in practice (www.floodsite.net, 2013).

In addition, in the Gorganrood watershed floods, LCLU and CC studies are not popular and just some studies with different point of view of ours have been conducted in the case of floods. For example regarding river morphology and physical structure (e.g. Mikaeili A.R, Abdoli A, and S.M (2005); Hosseinzadeh and Jahadi Toroghi (2007); Mohammadi, Alaghmand, and Mosaedi (2008); Mohammadi, Mosaedi, and Alaghmand (2007). Yamani, Eyvazi, and Jahadi (2010) investigated the types of floods that flow in this basin. Modaresi, Araghinejad, Ebrahimi, and Kholghi (2010) assessed

Climate Change using statistical tests in the Gharehsu basin. The flood impacts on the environment and structures studied by Sepehry and Liu (2006) that search and determined land cover change caused by the 2001 flood. Tjerry, Jessen, Morishita, and Enggrob (2006) investigated providing flood maps and to assess the hydraulic impact of debris flow. Hosseini Asl, Matkan, Javid, and Pourali (2008) prepared a GIS database for the Madarsoo basin based on the available information. Some studies are in the case of early warning systems. For instance, Matkan, Shakiba, Pourali, and Azari (2009) provided a flood early warning system based on NOAA/AVHRR satellite images. Ghalkhani, Golian, Saghafian, Farokhnia, and Shamseldin (2013) studied on real time flood routing. In addition, some studies were done by Ghezelsofloo, Deiminiat, Shojaee, and Lotfi (2010); Poozesh-Shirazi, Refahi, and Shahooei (2000); Zanganeh, Mosaedi, Meftah Halghi, and Dehghani (2011).

Regarding the LCUC and CC impacts, it appears that people only studied about land use impact on the flood. Hadiani and Ebadi (2007) studied land use change impact on design floods and consequent results on hydraulic structures in Madarsoo watershed. They believe that when designing hydraulic structures, the predicting the discharge of flood is necessary. Most hydraulic structures were destructed because of the lack of resistance against floods with flow rates more than design floods. They compared land use and land capacity maps and satellite images of previous years and mention that the changes in land uses are clear enough in this area. Comparing obtained results showed that the flow rate of design floods of hydraulic structures in field study at land capacity condition were 30 to 70 percent less than the discharge of design floods in the present land use condition. Furthermore, considering the change of land using during passing the time, the evaluation of design flood's flow rate with respect to useful lifetime and stability of structures is not certain. Thus, land use changes already exist in the region and should be consider in the design flood estimation.

While, based upon researches where land use change has an impact on floods, Abbaszadeh Tehrani, Makhdoum, and Mahdavi (2011) studied the land use change impact on the surface runoff in the Dough watershed. They chose and processed suitable Landsat TM images (of 1998) for producing a land use map. 30 years statistical data of rainfall was gathered for the region. They assessed the flood status based on current land use (1998) with the land capability condition and different soil moisture. Results showed that land use impact decreases with increasing the flood return period.

According to the literature, research discovered that land use change has an impact on floods in the region. The studies do not pay attention to CC impacts on floods. Also in these studies they used only the one year land use map and we cannot understand the Land Use/Cover Change impacts on the floods from past to present. They did not consider the climate change impacts too.

As far as the literature was reviewed, there is no implementation of flood hazard assessment in relation to LCUC and CC by using a comprehensive approach included

GIS, Remote Sensing and statistical analysis. In this study, GIS therefore serves as a major framework that will be combined with remote sensing and statistical analysis to perform many processes of geodatabase management, analysis and visualization.

1.3. Research motivation

Many scientists believed that the LCUC and CC impacts on floods in different watersheds should be investigated to explore their impacts on floods. With this in mind, the overall objective of this research is to analyze the past and current situation of LCLU and CC trends and conditions in the study area, using GIScience and spatio-temporal statistical methods, to explore these trends and impacts on flood hazards.

This research will provide updated information on the effect of climate change, climate variability and LCLUC on floods characteristics in the study area. It is obvious that the result of this research has great importance for decision-making authorities to mitigate flood hazards.

1.4. Research questions

- What and where are the changes in LCLU of Gorganrood watershed?
- At what rate and when does the LCLU change from past to present?
- Are there changes in hydro-meteorological data in the basin?
- Which factor(s) control floods from the past to the present?

1.5. Objectives

- To map and analyze LCLU changes and dynamics in the study area.
- To detect trends in hydro-meteorological data.
- To investigate LCUC and CC impacts on floods within the catchment.

1.6. Methodology

1.6.1. Study area

The study area is located in the northeastern part of Iran and covers an area of 5500 km^2 (Fig 1.1). It is located between the latitude of 36° 57' and 37° 47'N and the longitude of 55° 08' and 56° 25'E. It contains upstream of Gorganrood watershed. The altitude range is between 15 to 2541 meters above sea level. This region is very

important in several viewpoints. Firstly, there are valuable agricultural lands, products and soils. Secondly, living of about 600 thousand people who are under floods risks in the study area (Statistical-Center-of-Iran, 2006). Thirdly, locating Golestan national park as a UNESCO heritage site in this region with valuable and old forests, high diversity of flora and fauna and endangered species that can be suffered from floods, CC and LCLUC. Moreover, the study area is a geographically complex region that has a remarkable climate variation: the plains are located in the east and center; to the southern parts, region is covered by dense forests and after that, dry highlands. Northern part is mostly hills with semi-arid condition (Delbari, Afrasiab, & Jahani, 2013).
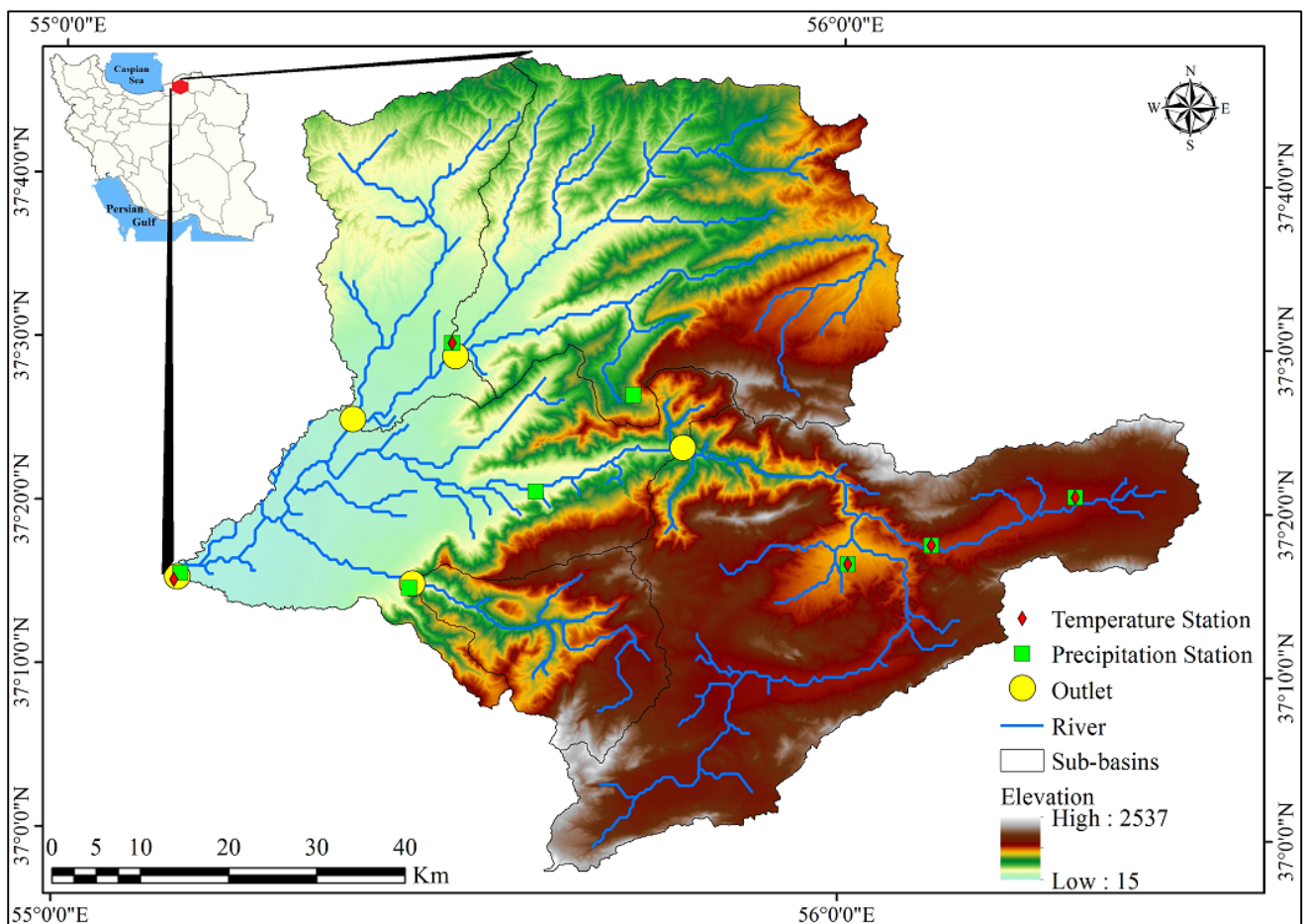
Fig. 1.1. Study area and station locations in the northeast of Iran.

This research will be done based on different methods of GIScience. Therefore, the first part of the present work is to create a geodatabase that contains required geographic data to answer the questions. This may involve providing, classifying and creation of LCLU maps, digitizing analog maps, obtaining data from a variety of sources and formats, data quality control regarding the task, coordinate system and so on (ESRI, 2001). Second part is providing land use/cover maps and doing spatio-temporal analysis. The third part is LUCC and CC impact assessment using statistical analysis of the results (Fig 1.2).
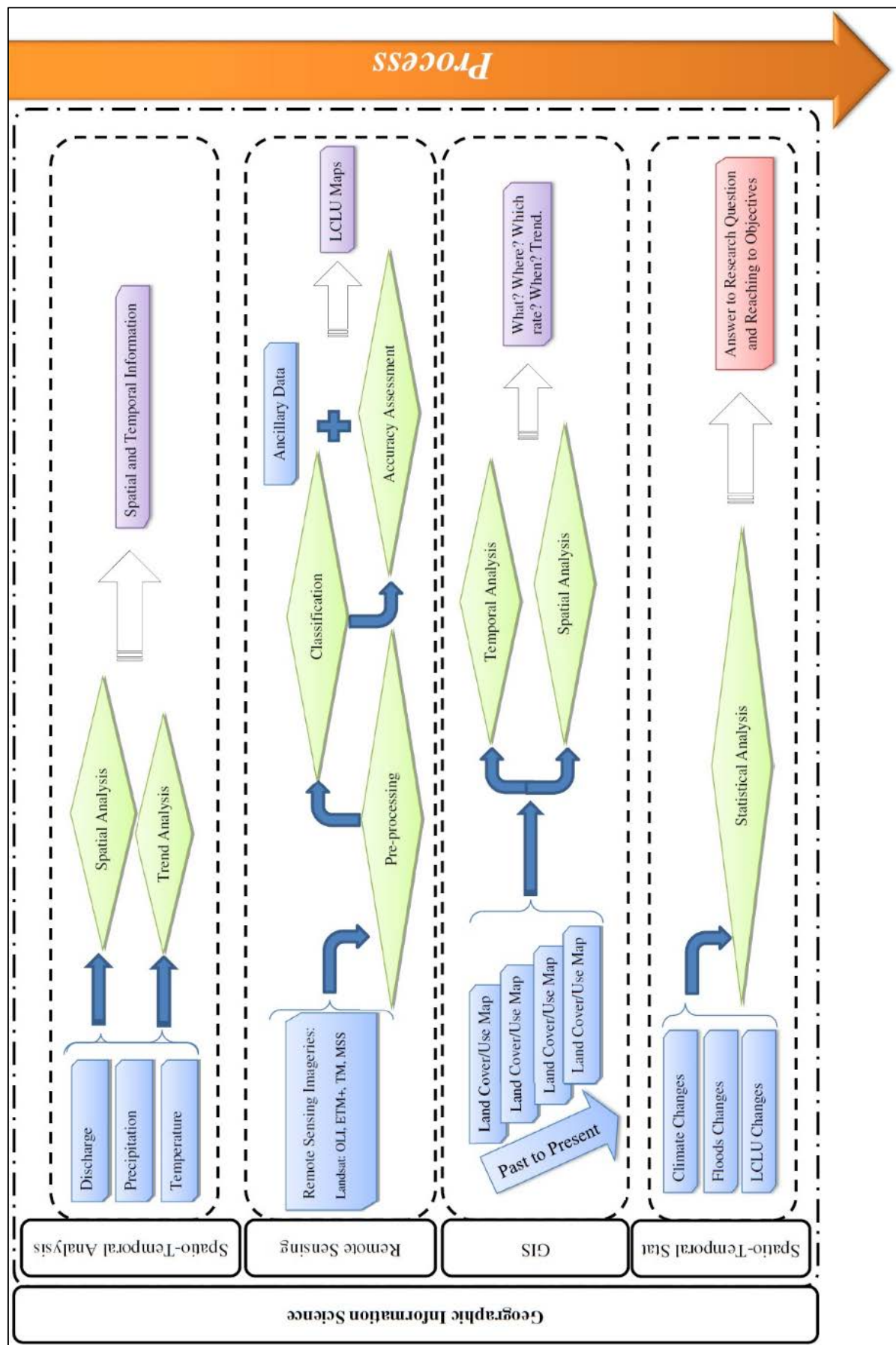
Fig. 1.2. Methodology flowchart

1.6.2. Trend analysis

Investigation of climate and floods trends will help to identify the hydrological processes of the watershed. In this regard, to implement trend analysis we should investigate the data quality and then a trend test will be used to detect trends.

1.6.2.1.   Data control

Data are the backbone of any attempt to detect trends or other changes and should be quality-controlled before commencing an analysis of change (Zbigniew W. Kundzewicz & Robson, 2004). To reach to this goal, exploratory data analysis (EDA) will used to identify such features as data problems like outliers, gaps, homogeneities and independencies. Homogenous data are often required in climate studies; otherwise the trend analysis will be biased (Nie et al., 2012; Salarijazi, Akhond-Ali, Adib, & Daneshkhah, 2012). In addition, homogeneity and breaks in all situations are not detectable by one single test (A. El Kenawy, López-Moreno, Stepanek, & Vicente-Serrano, 2013). To test the homogeneity we will used popular Pettitt, Alexandersson's SNHT and Buishand tests. As well, autocorrelation will checked to detect serial correlation. In this regard, Box-Pierce, Ljung-Box and McLeod-Li tests with 95% confidence interval will used. Thereupon, time series with serial correlation will pre-whitened by Trend Free Pre-Whitening (TFPW) method.

1.6.2.2.   Trend test

The rank-based nonparametric Mann-Kendall (MK) test has been commonly used to assess the significance of monotonic trends in hydro-meteorological time series (e.g. Gocic and Trajkovic (2013); Yue and Pilon (2004)). This test will be used to detect trends in the discharge and climate data. The Mann-Kendall test statistic has been shown to be more robust than parametric tests when dealing with skewed data and outliers in a data series (Z. W. Kundzewicz, Pinskwar, & Brakenridge, 2013).

1.6.3. Land use/cover change detection and analysis

The hydrologic effects of LCLU changes have been thoroughly described by De Roo et al. (2003) and summarized in De Roo et al. (2001). The three most important parameters controlled by land cover are the saturated hydraulic conductivity at the soil surface, the canopy capacity and the canopy enhancement factor (Woods, Schmidt, & Collins, 2009).

Given the importance of the impacts of changing patterns of land use/cover on water resources, it is difficult to arrive at a statement that would be universally accepted,

as land use/cover change is a complex phenomenon that varies greatly from place to place and from time to time. Although it may seem overwhelming in its complexity, it is still essential to quantify its impact on water management systems in order to obtain optimal mitigation and integrated water resources management strategies to cope with present and future risks of extreme flood events (Kuntiyawichai, 2012).

Over the past decades, remote sensing (RS) has played a large role in studying land use / land cover change detection. LCLU change detection studies are becoming demanding tasks with the availability of a suite of wide range sensors operating at various imaging scales and scope of using various techniques as well as increasing ways for monitoring effective and accurate LCLU change. Considerable research has been directed at the various components of LCLU change including the accuracy assessment, which is drawing an equal attention by scientists nowadays (Das, 2009). In this regard, the following methods will be used to provide the land use/land cover information:

1.6.3.1. Providing LCLU maps using Remote Sensing

Remote Sensing data are a valuable source of data for LCLU maps creating and updating efficiently. Thus, aerial photos and satellite imagery (MSS, TM, ETM+ and OLI/TIRS) will be selected to investigate LUCC and landscape change of the study area. Afterwards, images will be pre-processed, including atmospheric and geometry rectifications. Secondly, some types of classes including bare land, built-up, farmland, forest, range and water will be detected. Last, the interpreted results will be revised until the classification results are satisfying. In the next step, we will analyze the land use/cover changes using different spatial analysis.

1.6.4. LCUC and CC impact assessment

To evaluate the effect of land use/cover changes and climate change on the floods characteristics of the basin we will investigate their relationships and impacts using statistical analysis. In this regard, we will investigate the contribution of climate and LCLU categories on the different floods characteristics in whole watershed and sub-basins.

1.7. Expected innovation

The Gorganrood watershed is one of the most vulnerable flooding areas in Iran. For the local and national governments the management and control of flood hazards in the region have considerable importance. Based on past studies many complex interactions need to be addressed for flood mitigation and regional assessments. In this regard, for

the first time in the Gorganrood watershed a comprehensive approach will investigate the LCLU and CC impacts on the basin's floods. Different dimensions of LCLU changes will be assessed and visualized. Hydro-meteorological data will be investigated to detect their properties, spatial variability and temporal trends. Investigating of daily hydro-climatological data will show trends of floods and climate conditions from past to present that is very important in the hazard management in the watershed and is as a guide to the future conditions. We will evaluate the relations between different LCLU and floods to determine the type and amount of impacts of various LCLU classes and their changes on the watershed's floods. The relations and impacts between climatic factors and floods will be evaluated, too.

By understanding these impacts and relations, we discover knowledge in the case of controller factor of floods in Gorganrood basin. This knowledge will open a new window in front of managers and decision makers. It will improve the quality and accuracy of the decision-making process and type of flood resisting activities. In conclusion, the thesis provides specific guidance concerning the how to manage flood hazards based on LCLU and CC impacts on the watershed's floods.

1.8.   Structure of dissertation

This thesis consists of the following seven chapters to achieve the objectives of the research that are as follow:

Chapter 1, Introduction: Present an overview of the problem and background and outlines such as research motivation, research questions, objectives and a brief about the research methodology.

Chapter 2, Hydro-meteorological Spatio-Temporal analysis: contains scientific review of the previous works and researches in case of hydro-meteorological trend analysis. Afterwards time series will be investigated in daily, monthly and yearly scales and trends will be detected.

Chapter 3, Remote Sensing Detection and Spatio-temporal LCLU Change Analysis: In this chapter, the remotely sensed data will be classified and several spatio-temporal analysis will applied on the outcomes.

Chapter 4, Flood hazards, Climate Change and LCLU Relationship Assessment: In this chapter the floods and their characteristics will be detect and the relations among them, LCLU and CC will be investigated.

Chapter 5, Conclusion and Summary: In this section the general conclusion, answers of objectives, limitation and recommendations will be presented.

Appendix, Geostatistical Modeling of Air Temperature Using Landsat Thermal Remote Sensing: This appendix regarding the goal of first chapter of the thesis for spatio-temporal analysis of hydro-meteorological data tries to investigate the interpolation of temperature using Landsat thermal band. It also will investigate the impacts of snow-covered areas in the thermal bands images on the interpolation.

Chapter 2

Hydro-Meteorological Spatio-Temporal Analysis

This chapter is the first step in GIScience approach to flood hazard assessment. Time series of hydro-meteorological data in daily, monthly and yearly scale will be investigated to detect trends. These data are precipitation, maximum temperature, minimum temperature, mean temperature and discharge. The result of this chapter will shows the general condition in stations in watershed.

2.1. Introduction

Potential changes in climate will likely accompanied by changes in possible flood hazards (Muzik, 2002). Climate change is referred to as large variations in climate averages, which exist for decades or even longer periods (Gocic & Trajkovic, 2013). It seems to be the foremost global challenge facing humans currently, even though it seems that not all places in the world are affected (Obot, Chendo, Udo, & Ewona, 2010). Therefore, evaluation and analysis of changes in hydro-meteorological data are a considerable process and difficult in climate change detection. The detection of changes in long time series of hydro-meteorological data has received much interest in various parts of the world in the last decades because of their importance in many eco-hydrological process and natural disasters like floods (Buishand, De Martino, Spreeuw, & Brandsma, 2013; Gocic & Trajkovic, 2013; Zbigniew W. Kundzewicz & Robson, 2004; Obot et al., 2010).

Amid climate change affected factors, the precipitation pattern is probably one of the most useful indicators to reflect and show the effects of climate change (F. Wu, Wang, Cai, & Li, 2013). Precipitation is a climate parameter that affects the way and manner man lives (Obot et al., 2010). Its positive influences on all forms of societies, ecological systems, economy and water cycle as well as its destructive impacts on the world by encouraging of natural hazards make related researches important and indispensable (Obot et al., 2010; F. Wu et al., 2013). There is an extensive literature on precipitation trend analysis. In this regard, a study of Buishand et al. (2013) for 6 indices of precipitation in the Netherlands revealed significant increase. Zhang et al. (2013b) analyzed for 590 stations in China, changing characteristics of eight precipitation

indices covering a period of 1960–2005 using the modified Mann–Kendall (MK) trend test and linear regression. They found both wetting and drying tendencies.

Soltani, Saboohi, and Yaghmaei (2012) investigated long-term annual and monthly trends in rainfall amount, number of rainy days and maximum precipitation in 24 hour at 33 synoptic stations in Iran. Their results indicated that there are no significant linear trends in monthly rainfall at most of the synoptic stations in Iran. Joseph, Ting, and Kumar (2000) studied spatio–temporal variability of precipitation over the United States using 30-years, gridded hourly precipitation dataset. Río, Herrero, Fraile, and Penas (2011) analyzed the spatial distribution of rainfall trends from 1961-2006 in 533 Spanish weather stations. Hossein Tabari and Hosseinzadeh Talaee (2011) assessed the annual and seasonal precipitation trends of 41 stations in Iran for the period 1966–2005. Their results indicated a decreasing trend in annual precipitation at about 60% of the stations. Among other studies in Iran and the world can point to the followings: (Abghari, Tabari, & Hosseinzadeh Talaee, 2013; Berezovskaya, Yang, & Kane, 2004; Gocic & Trajkovic, 2013; Hartmann & Andresky, 2013; Hasan & Schorr, 2012; Houston, 2006; Jin Huang, Sun, & Zhang, 2013; Kriegel et al., 2013; López-Moreno et al., 2014; Łupikasza, Hänsel, & Matschullat, 2011; Santos & Fragoso, 2013; Shifteh Some'e, Ezani, & Tabari, 2012; Soo Chin, Aik Song, & Leong Keong, 2010; Hossein Tabari, Abghari, & Hosseinzadeh Talaee, 2012; Hossein Tabari, Somee, & Zadeh, 2011; Velpuri & Senay, 2013; Xu, Milliman, & Xu, 2010).

Coupled with precipitation, temperature is one of the most important and most discussed indicators of global change (Capparelli et al., 2013). Many policy makers and the general public are believed that they already feel the effects of global warming where they live (Capparelli et al., 2013). In addition, temperature changes as a cause of changes in the precipitation regime are important for water resources management and management of water-related natural hazards (Zhang, Li, Singh, & Xiao, 2013; Zhang, Li, Singh, & Xu, 2013). Capparelli et al. (2013) studied spatio-temporal trends of 1167 station temperature records for the United State from 1898 through 2008. They found that more than 50% of all stations experienced a significant trend over the last century. Moreover, their results revealed significant cooling and warming trends. In USA, Safeeq, Mair, and Fares (2013) examined trends in minimum and maximum temperatures in the Oahu Island during the two periods of 1969–2007 and 1983–2007 and found a strong spatial and temporal variability in the temperature trends.

Ahmed El Kenawy, López-Moreno, and Vicente-Serrano (2012) for 19 observatories (1920–2006) and 128 stations (1960 to 2006) performed an assessment of long-term change and variation of temperature in the north of Spain. They distinguished strongest trends in summer and spring. In spatial aspect, coastlands stations showed more trends than inland one. Kousari, Ahani, and Hendi-zadeh (2013) implemented Mann-Kendall and Sen's slope to detect trends of maximum air temperature in three time scales, including annual, seasonal and monthly time series in 32 synoptic stations

in the whole of Iran during 1960–2005. Some more researches in this issue are as follows: (A. El Kenawy et al., 2013; Fortin & Hétu, 2014; Gocic & Trajkovic, 2013; Kriegel et al., 2013; López-Moreno et al., 2014; Martínez, Serra, Burgueño, & Lana, 2010; Saboohi, Soltani, & Khodagholi, 2012; Hossein Tabari, Hosseinzadeh Talaee, Ezani, & Shifteh Some'e, 2012; Hossein Tabari et al., 2011; H. Tabari & Talaee, 2011; Unkašević & Tošić, 2013; Viola, Liuzzo, Noto, Lo Conti, & La Loggia, 2014; Y. Wang, Ren, & Zhang, 2014; C. Wu, Huang, Yu, Chen, & Ma, 2014).

In concert with precipitation and temperature, analysis of trends in hydrological data time series are thought to be an important tool for tracing and understanding of climate changes (Kliment, Matouskava, Ledvinka, & Kralovec, 2011). This analysis could be exploitable in hydrological risk assessment such as flood protection studies, too. Hence, has been an academic focus in recent years on it. Douglas, Vogel, and Kroll (2000) assessed flood flows and low flows time series trends using regional average Kendall's S trend test. They found evidence of upward trends in low flows, but no trends in flood flows. Jha and Singh (2013) performed trend analysis of high flow and seven-day low flow events for 25 years since 1982 in Peninsular Malaysia using Spearman's rank test and standard normal homogeneity test. Abghari et al. (2013) analyzed temporal trends in discharge and precipitation time series for 40 years since 1969 in west of Iran. Their results showed different trends and a strong relationship between river discharge and precipitation at the annual scale and in most of the months. Moreover, several other studies have been performed by whole around the world scientist (Berezovskaya et al., 2004; Bormann, Pinter, & Elfert, 2011; Cunderlik & Ouarda, 2009; Danneberg, 2012; Gebremicael, Mohamed, Betrie, van der Zaag, & Teferi, 2013; Hasan & Schorr, 2012; Ishak, Rahman, Westra, Sharma, & Kuczera, 2013); Kriegel et al. (2013); (Z. J. Li & Li, 2008; Petrow & Merz, 2009; Tian, Ma, Lei, & Jiang, 2010; Velpuri & Senay, 2013; H. Wang et al., 2011; Xu et al., 2010).

A considerable amount of literature has been published on natural hazards related research like as floods, landslides, debris flows and so on. In climate change studies, Moreover, both global and regional studies are necessary and make clear evidence and causes (Gocic & Trajkovic, 2013; Zbigniew W. Kundzewicz & Robson, 2004; Renard et al., 2008; F. Wu et al., 2013). In line with these and in addition to mentioned context detecting spatial and temporal trends in long time series of hydro-meteorological data is a vital part of clime change and natural hazard studies that should be investigated (Capparelli et al., 2013; Gocic & Trajkovic, 2013; Zbigniew W. Kundzewicz & Robson, 2004).

According to necessity of regional and local scale studies and conducted country scale studies in Iran it seemed necessary to carry out detailed and medium scaled researches. In addition, previous published studies did not cover entire of the study area. They did not pay attention to all factors together and the time scales are different and mostly monthly and yearly. In this regard, the main goal of the current chapter is to

implement a systematic and comprehensive investigation on the spatio-temporal variability of the five hydro-meteorological daily, monthly and yearly data at the different stations in the northeast of Iran as an important hazardous region during 1956-2010. These are the areas where many recent disastrous floods took place. The main objectives of this study are: (1) to explore and fix the quality of the data as detecting outliers, identifying of inhomogeneity, serial correlation in time series, pre-whitening and so on using different methods such as Pettitt, SNHT, Buishand and free pre-whitening (TFPW) and other statistical methods. (2) To analyze possible temporal trends and patterns of variables in detail. (3) Using nonparametric Mann-Kendall test and Sen's slope estimator to detect and quantify the significance of changes. (4) To investigate spatial distribution of trends in the region. The outcome of this study quantifies and visualizes the hydro-meteorological trends in the Gorganrood watershed and it has great importance for decision-making authorities to risk assessment and flood hazard mitigation of the region.

2.2.   Methodology

2.2.1. Study area and data collection

The main study area is located in the northeastern part of Iran and covers an area of 5500 km^2 (Fig 2.1). It is located between the latitude of 36° 57' and 37° 47'N and the longitude of 55° 08' and 56° 25'E. It contains upstream of Gorganrood watershed. To better understanding of conditions, we add more stations from out of main study area for the precipitation and temperature. In this regard, study area increased to 15000 km^2 (Fig 2.1). It is included the latitude of 36° 30' and 38° 07'N and the longitude of 53° 59' and 56° 25'E. It contains most of Gorganrood watershed and parts of Atrak and Gharasoo basins. The altitude range is between -30 to 3678 meters above sea level.

According to the definition of the World Meteorological Organization (WMO), data for a 30-year period are recommended because they provide stable and reproducible monthly means (Benavides et al., 2007). Furthermore, to have a better spatial cover of the area some stations with less than 30 years was used too. In addition, having the reliable data and good quality data sets are essential and were considered. Therefore, data of 18 stations for different hydro-meteorological parameters from Iran Meteorological Organization and Ministry of Energy were collected (Table 2.1; Fig 2.1). The data were structured by hydrological years, starting in October and ending in September. For precipitation and temperature, longest period has been since 1953 to 2013 in Gorgan station and shortest from 1992-2012. In discharge series, longest period is from 1955 to 2011 and shortest from 1983 to 2011 in Gonbad and Haji-ghushan stations, respectively. In the present study, series of daily, monthly and yearly precipitation (Prcp), Maximum (TMax), Mean (TMean), Minimum (TMin) of air

temperature and discharge were analyzed and descriptive statistics of them are presented in Table 2.1 too.
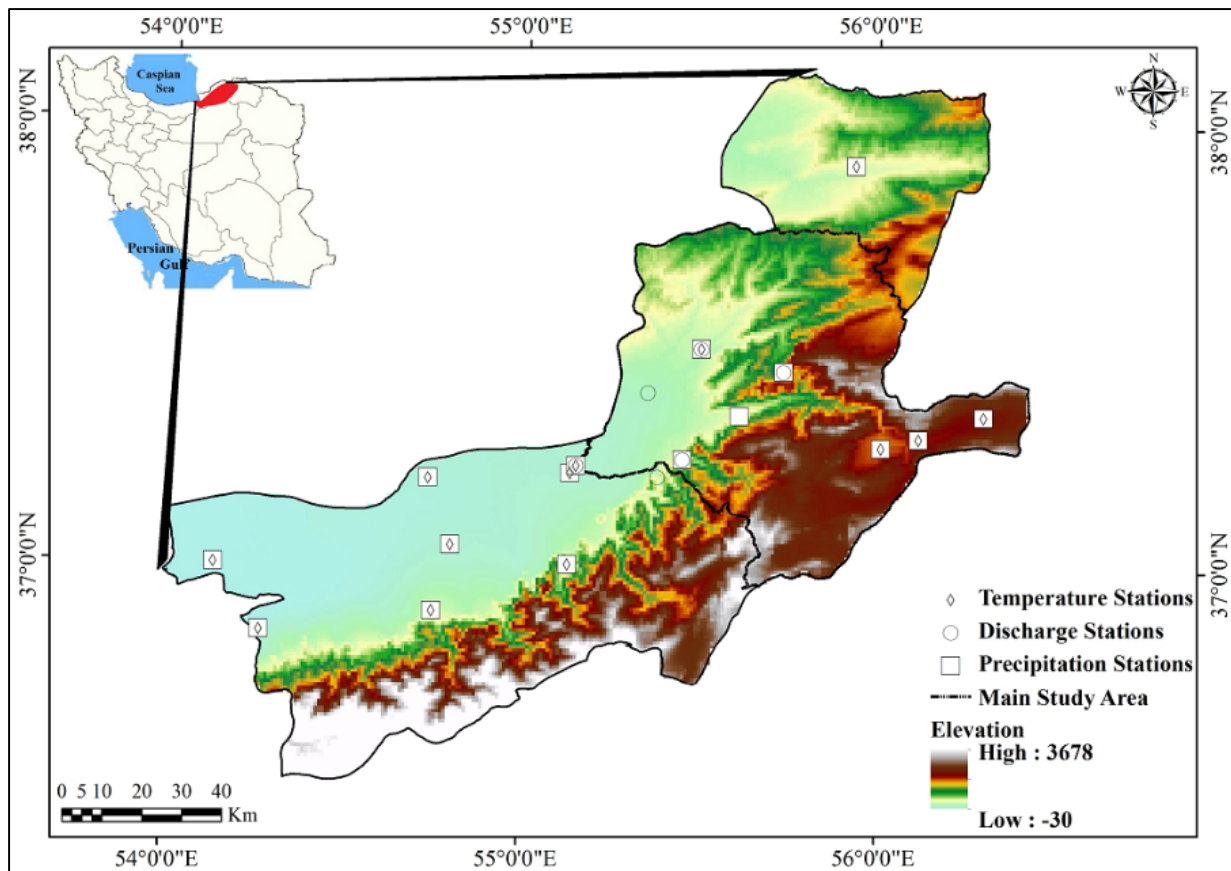
Fig. 2.1. Study area and stations location in the Northeast of Iran.

Table 2.1. Geographical properties of hydro-meteorological stations.

Station name	Latitude	Longitude	Elevation	TMax	TMin	TMean	Prcp	Discharge
Araz-kuse	37.21	55.13	34	25.3±8.04	10.7±7.2	17.5±7.5	37.3±29.3	*
Bahalke-dashli	37.05	54.8	24	24.07±8.2	10.4±7.5	17.1±7.7	36.3±27.3	*
Cheshme-khan	37.3	56.11	1250	19.6±8.9	3.8±7.3	11.7±8.04	19.6±20.2	*
Dasht	37.28	56.01	1000	19.8±8.6	4.2±7.7	10.8±8.3	13.5±16.8	*
Fazel-abad	36.9	54.75	210	23.5±7.8	10.9±6.8	17.3±7.2	56.8±33.2	*
Gonbad	37.23	55.15	37.2	24.3±8.6	11.4±7.4	18.02±7.9	39.4±31.8	7.08±8.3
Gorgan	36.85	54.26	13.3	22.8±7.8	12.6±7.2	17.7±7.4	49.3±36.7	*
Maraveh-tape	37.91	55.93	190	25.3±8.9	10.9±7.3	18.1±8.03	29.6±24.8	*
Ramian	37.01	55.13	200	22.8±8.01	10.7±6.6	16.7±7.2	72.8±54.3	*
Robat-gharabil	37.35	56.3	1450	21.3±9.8	3.01±8.04	12.1±8.7	15.6±16.3	*
Sad-gorgan	37.2	54.73	12	24.7±8.5	11.2±7.8	17.4±8.09	24.8±24.3	*
Tamar	37.5	55.5	132	24.6±8.09	11.05±6.6	16.7±7.3	42.3±35.1	1.5±1.6
Ghafar-haji	37	54.13	-22	22.7±7.7	11.1±7.8	16.1±7.6	37.9±29.4	*
Galikash	37.25	55.45	250	*	*	*	62.7±44.2	2.5±2.4
Pishkamar	37.35	55.61	976	*	*	*	43.7±38.6	*
Tangrah	37.45	55.73	330	*	*	*	59.4±44.7	1.5±2.5
Haji-ghushan	37.4	55.35	90	*	*	*	*	1.9±2.6

2.2.2. Data quality control

Data are the backbone of any attempt to detect trends or other changes and should be quality-controlled before commencing an analysis of change (Zbigniew W. Kundzewicz & Robson, 2004). To reach to this goal, exploratory data analysis (EDA)

used to identify such features as data problems like outliers, gaps, homogeneities and independencies. More information about the EDA can be found in Zbigniew W. Kundzewicz and Robson (2004) and Cleveland (1994). All the time series was controlled for outliers. The next step in the data quality assessment was filling the missing data. In case of our datasets missing data, we filled the small gaps using regression methods with high correlated close stations. And in order to avoid creating more inhomogeneities into the series for the stations with some bigger gaps, consistent with the ability of the XLSTAT software to deal with missing data they would not be filled.

Homogenous data are often required in climate studies; otherwise the trend analysis will be biased (Nie et al., 2012). In addition, homogeneity and breaks in all situations are not detectable by one single test (A. El Kenawy et al., 2013). To test the homogeneity we used popular Pettitt, Alexandersson's SNHT and Buishand tests. More information regarding homogeneity tests could be found in these references: (Alexandersson, 1986; Bormann et al., 2011; Buishand, 1982; Kang & Yusof, 2012; Pettitt, 1979; Santos & Fragoso, 2013; Wijngaard, Klein Tank, & Können, 2003). Using different mentioned tests, homogeneity has been tested for all time-series of temperature, precipitation and discharge daily, monthly and yearly data. According to the results of homogeneity test and Santos and Fragoso (2013) method homogenized and inhomogenized series were determined.

As well, autocorrelation was checked to detect serial correlation. In this regard, Box-Pierce, Ljung-Box and McLeod-Li tests with 95% confidence interval were used. Detailed description of the methods could be found in Box and Pierce (1970), Ljung and Box (1978), McLeod and Li (1983), respectively. Thereupon, time series with serial correlation was pre-whitened by Trend Free Pre-Whitening (TFPW) method. TFPW (Yue, Pilon, Phinney, & Cavadias, 2002) is a popular method to remove the lag-1 autocorrelation (Douglas et al., 2000; Hartmann & Andresky, 2013; Jha & Singh, 2013; Kousari et al., 2013; Kriegel et al., 2013; Petrow & Merz, 2009). Serial effects of time series were corrected as $Y_t = X_t - r_1 X_{t-1}$ where X_t is raw data time series. Pre-whitening reduced r_1 to near zero (Douglas et al., 2000; Hartmann & Andresky, 2013; Yue et al., 2002). Finally, the trend analyses were then performed on the both normal and pre-whitened time series of the data.

2.2.3. Trend analysis methods

Trend detection tests in hydro-climatological data can be classified as parametric and non-parametric methods (Chebana, Ouarda, & Duong, 2013; Gocic & Trajkovic, 2013; Ishak et al., 2013; Xu et al., 2010). Non-parametric tests do not need to normal distributed data and they should be only independence (Abghari et al., 2013; Gocic & Trajkovic, 2013; López-Moreno et al., 2014). In this regard, in this research the Mann-Kendall (MK) test as the main method and Sen's slope approach as two nonparametric

test (Bormann et al., 2011) were used to detect time series trends and their trends significant. Furthermore, we used seasonal Mann-Kendall test (12-month seasonality) to consider seasonality in the data series.

2.2.3.1. Mann-Kendall trend test

The MK as a trend detector test is commonly used to detect significant trends in hydrological and meteorological time series (Cunderlik & Ouarda, 2009; Jin Huang et al., 2013; Mann, 1945) and it is recommended by the World Meteorological Organization too (Shifteh Some'e et al., 2012; Zhang, Li, Singh, & Xiao, 2013). The MK test is simple, robust and can deal with missing values and values below a detection limit (Shifteh Some'e et al., 2012). The normalized test statistics Z for the MK test is computed by:

$$Z = \begin{cases} \frac{s-1}{\sqrt{Var\,(s)}} & if\ S > 0 \\ 0 & if\ S = 0 \\ \frac{s+1}{\sqrt{Var\,(s)}} & if\ S < 0 \end{cases} \qquad (Eq\ 2.1)$$

$$S = \sum_{i=1}^{N-1}\sum_{j=i+1}^{N} sgn(x_j - x_i) \qquad (Eq\ 2.2)$$

$$sgn\,(x_j - x_i) = \begin{cases} +1\ if\ (x_j - x_i) > 0 \\ 0\quad if\ (x_j - x_i) = 0 \\ -1\ if\ (x_j - x_i) < 0 \end{cases} \qquad (Eq\ 2.3)$$

$$Var(S) = \frac{1}{18}[n(n-1)(2n+5) - \sum_{t=1}^{m} t_i(t_i - 1)(2t_i + 5)] \qquad (Eq\ 2.4)$$

Where S is a MK statistic and Var is variance; n is the number of data points, t_i is the extent of any tie for i value and m is the number of tied values (Cunderlik & Ouarda, 2009; Gebremicael et al., 2013; Gocic & Trajkovic, 2013; Hartmann & Andresky, 2013; Jin Huang et al., 2013; Ishak et al., 2013; Shifteh Some'e et al., 2012).

A positive value of Z indicates existing of an increasing trend and a negative value indicates a decreasing trend. The null hypothesis H_0 that there is no trend in the records is either accepted or rejected depending if the computed Z statistics is less or more than the critical value of Z-statistics at the 5% significance level (Cunderlik & Ouarda, 2009; Gebremicael et al., 2013; Gocic & Trajkovic, 2013; Hartmann & Andresky, 2013; Jin Huang et al., 2013; Shifteh Some'e et al., 2012).

2.2.3.2. Sen's slope estimator

Sen's slope estimator was developed by Sen in 1968 and is used by many researchers (Bormann et al., 2011; Ishak et al., 2013; Kousari et al., 2013; Kriegel et al., 2013; Hossein Tabari & Hosseinzadeh Talaee, 2011, 2013).

If a linear trend is present in a time series, then the slope estimates of N pairs of data are first computed by

$$Q_i = \frac{x_j - x_k}{j-k} for \quad i = 1, \dots, N \qquad \text{(Eq 2.5)}$$

Where x_j and x_k are data values at times j and $k(j > k)$, respectively. The median of these *N* values of Q_i is Sen's estimator of slope. Eq 2.6 computes Sen's estimator if N is odd:

$$Q_{med} = Q_{[(N+1)/2]} \qquad \text{(Eq 2.6)}$$

Afterward Sen's estimator is computed by Eq 2.7 if N is even,

$$Q_{med} = {}^1\!/_2 \left(Q_{N/2} + Q_{[(N+2)/2]} \right) \qquad \text{(Eq 2.7)}$$

Finally, *Q_{med}* is tested with a two-sided test at the 100(1-α) percentage confidence interval and the true slope may be obtained with the nonparametric test (Gocic & Trajkovic, 2013; Salmi, Määttä, Anttila, Ruoho-Airola, & Amnell, 2002; Hossein Tabari & Hosseinzadeh Talaee, 2011, 2013).

In this work, the confidence interval was computed at confidence level of a = 0.05 as follows:

$$C_\alpha = Z_{1-\alpha/2}\sqrt{Var(S)} \qquad \text{(Eq 2.8)}$$

Where *Var(S)* has been defined in Eq 2.4 and *$Z_{1-\alpha/2}$* is obtained from the standard normal distribution. Then, *$M_1 = (N-C\alpha)/2$* and *$M_2 = (N + C\alpha)/2$* are computed. The lower and upper bounds of the confidence interval, *Qmin* and *Qmax*, are the M_1^{th} largest and the (M2 + 1)[th] largest of the *N* ordered slope estimates *Q_i*. If *M_1* is not a whole number, the lower border is interpolated. Correspondingly, if *M_2* is not a whole number the upper border is interpolated (Gocic & Trajkovic, 2013; Salmi et al., 2002; Hossein Tabari & Hosseinzadeh Talaee, 2011, 2013).

2.3.   Results and discussion

More descriptive analysis was applied on the data after data quality control and analysis. A linear regression model was used with nearby and best correlated series to fill the small gaps in data. Afterward, autocorrelation was checked to detect serial correlation. Thereupon, time series with serial correlation was pre-whitened by TFPW method. Moreover, homogeneity of the data was checked. In addition, series with

breaks were detected and under this circumstances trend analysis were done on these series before and after the breaks.

The results of statistical tests on the daily, monthly and yearly data are presented in the tables. Serial correlation (SC), homogeneity (H), seasonality considered Mann-Kendall (S-MK), Mann-Kendall (MK), Sen's slope estimator (Sen'), pre-whitened series (PW) and detected breaks and theirs Change Point (CP) direction are some columns of the following tables. The "-" in the SC and H columns means that data need to be pre-whitened and data are not homogenized, respectively and the "+" means vice versa of minus sign. The "Y" and "N" in the trends columns indicate that significant trend is detected or not. The rows that do not need calculation are marked by "*", too. It should be recalled that all daily, monthly and yearly trends were calculated in five percent significant level.

2.3.1. Spatio-temporal trends in precipitation

In daily analysis, all the stations shown trends but just 16 percent of the stations show significant trends and the trends were positive, but not strong (Table 2.2). As shown in Table 2.2 Dasht and Robat-gharabil stations had increasing trends and the Dasht was strongest one. In analyzing the change points and their direction in daily data, 58% of the stations showed trends that about 43% was raising breaks and around 57% downward breaks. In broken series just Sad-gorgan station showed significant trend (positive) in the second part.

In monthly series, trends were detected in all stations, but in 95% significant level, only Sad-gorgan, Tamar and Dasht station, means about 19% of stations, had trends that two-thirds of them were increasing. Detected trends in monthly data were stronger than daily data's trends. While, with regarding to seasonality in the data, 37.5% of the stations showed significant trends include Dasht, Gorgan, Robat-gharabil, Sad-gorgan, Tamar and Tangrah. Almost 33% of trended stations were negative (Table 2.3). Same as daily series Dasht had the biggest trend in monthly series as well. Results of break detection test detect breaks in 37.5% of the stations, although among them just 33% showed rising breaks. With investigation of broken series, first sections of Bahalke-dashli and Pishkamar and second section of Sad-gorgan showed significant trends (totally positive) (Table 2.3).

Finally, on the annual data 12.5% of the stations (Dasht and Tamar) showed significant positive trends and there was not negative trends, although all the stations showed trends. Detected breaks in the yearly series reduced to 31% and 60% of them were downward (Table 2.4). The yearly results in this region differs from that of Hossein Tabari and Hosseinzadeh Talaee (2011) who found negative trends in annual precipitation in 60% of stations and just in north-west of Iran. Furthermore, our detailed results are different with outputs of Shifteh Some'e et al. (2012) which just investigate

the seasonal and yearly precipitation time series in Gorgan station in our study area and had found decreasing trends in the north east of Iran. Because, in daily, monthly and yearly series we did not detect significant trends and only seasonality considered test present significant trends that the intensity of them is different in this station. In analyzing broken series, first section of Bahalke-dashli (positive trend) second section of the Gorgan station (negative trend) showed significant trends (Table 2.4).

Table 2.2. Results of statistical trend analysis of daily precipitation time series.

Station	SC	H	Tests	Total trend		Section1 / Trend	Section 2/ Trend	CP Direction/ Row Number
				Normal	PW			
Araz-kuse	-	+	MK	0.018/Y	0.018/N	*	*	*
			Sen'	5.4E-5	5.4E-5	*	*	
Bahalke-dashli	-	-	MK	0.009/N	0.009/N	-0.022/N	-0.016/N	-/3872
			Sen'	2.5E-5	2.5E-5	0	0	
Cheshme-khan	-	+	MK	0.014/Y	0.014/N	*	*	*
			Sen'	3.1E-5	3.1E-5	*	*	
Dasht	-	-	MK	0.075/Y	0.075/Y	-0.040/N	0.027/N	+/4808
			Sen'	0	0	1.4E-5	7.1E-5	
Fazel-abad	-	+	MK	0.009/N	0.009/N	*	*	*
			Sen'	7.9E-5	7.9E-5	*	*	
Gonbad	-	-	MK	-0.014/N	-0.014/N	-0.013/N	0.025/N	-/2927
			Sen'	4.9E-5	4.9E-5	0	0	
Gorgan	-	-	MK	-0.021/Y	-0.021/N	0.029/N	-0.027/N	-/10680
			Sen'	2.3E-5	2.3E-5	3.8E-5	3.1E-5	
Maraveh-tape	-	+	MK	0.001/N	0.001/N	*	*	*
			Sen'	4.3E-5	4.3E-5	*	*	
Ramian	-	+	MK	-0.007/N	-0.007/N	*	*	*
			Sen'	9.7E-5	9.7E-5	*	*	
Robat-gharabil	-	-	MK	0.049/Y	0.049/Y	0.004/N	0.001/N	+/4185
			Sen'	3.8E-5	3.8E-5	0	2.2E-5	
Sad-gorgan	-	-	MK	-0.006/N	-0.006/N	-0.017/N	0.184/Y	-/9579
			Sen'	2.1E-5	2.1E-5	5.7E-5	0	
Tamar	-	-	MK	-0.022/Y	-0.022/N	-0.052/N	0.022/N	+/1214
			Sen'	8.4E-5	8.4E-5	0	9.9E-5	

Table 2.3. Results of statistical trend analysis of monthly precipitation time series.

Station	SC	H	Tests	Total trend		S-MK	Section1 / Trend	Section 2/ Trend	CP Direction/ Row Number
				Normal	PW				
Araz-kuse	-	+	MK	0.033/N	0.033/N	0.057/N	*	*	*
			Sen'	0.007	0.007		*	*	
Bahalke-dashli	-	-	MK	-0.071/Y	-0.071/N	-0.066/N	0.18/Y	-0.026/N	- / 126
			Sen'	-0.018	-0.018		0.256	-0.008	
Cheshme-khan	-	+	MK	0.011/N	0.011/N	0.023/N	*	*	*
			Sen'	0	0		*	*	
Dasht	-	-	MK	0.28/Y	0.28/Y	0.29/Y	-0.134/N	0.068/N	+/149
			Sen'	0.055	0.055		0	0.041	
Fazel-abad	-	+	MK	-0.015/N	-0.015/N	-0.003/N	*	*	*
			Sen'	-0.006	-0.006		*	*	
Gonbad	-	+	MK	0.015/N	0.015/N	0.017/N	*	*	*
			Sen'	0.003	0.003		*	*	
Gorgan	-	-	MK	-0.065/Y	-0.065/N	-0.09/Y	0.07/N	-0.03/N	- /342
			Sen'	-0.014	-0.014		0.03	-0.01	
Maraveh-tape	-	+	MK	0.017/N	0.017/N	0.008/N	*	*	*
			Sen'	0.003	0.003		*	*	
Ramian	-	+	MK	-0.033/N	-0.033/N	-0.04/N	*	*	*
			Sen'	-0.024	-0.024		*	*	
Robat-gharabil	-	+	MK	0.088/Y	0.088/N	0.115/Y	*	*	*
			Sen'	0.006	0.006		*	*	
Sad-gorgan	-	-	MK	-0.114/Y	-0.114/Y	-0.11/Y	0.01/N	0.41/Y	-/316
			Sen'	-0.018	-0.018		0.002	0.115	
Tamar	-	-	MK	0.123/Y	0.123/Y	0.162/Y	0.047/N	-0.014/N	+/254
			Sen'	0.033	0.033		0.019	-0.007	
Ghafar-haji	-	+	MK	-0.034/N	-0.034/N	-0.027/N	*	*	*
			Sen'	-0.008	-0.008		*	*	
Galikash	-	+	MK	0.025/N	0.023/N	0.047/N	*	*	*
			Sen'	0.011	0.01		*	*	
Pishkamar	-	-	MK	-0.014/N	-0.014/N	-0.008/N	0.225/Y	0.1/N	- / 117
			Sen'	-0.004	-0.004		0.444	0.037	
Tangrah	-	+	MK	0.056/N	0.056/N	0.083/Y	*	*	*
			Sen'	0.025	0.025		*	*	

Table 2.4. Results of statistical trend analysis of yearly precipitation time series

Station	SC	H	Tests	Total trend		Section1 / Trend	Section 2/ Trend	CP Direction/ Row Number
				Normal	PW			
Araz-kuse	+	+	MK	0.05/N	*	*	*	*
			Sen'	0.7	*	*	*	
Bahalke-dashli	+	-	MK	-0.21/N	*	0.6/Y	-0.04/N	-/11
			Sen'	-2.9	*	44.3	-1	
Cheshme-khan	+	+	MK	-0.06/N	*	*	*	*
			Sen'	-0.5	*	*	*	
Dasht	-	-	MK	0.63/Y	0.63/Y	0.3/N	0.49/N	+/13
			Sen'	12.5	12.5	9.1	20.2	
Fazel-abad	+	+	MK	0.029/N	*	*	*	*
			Sen'	0.45	*	*	*	
Gonbad	+	+	MK	0.02/N	*	*	*	*
			Sen'	0.3	*	*	*	
Gorgan	-	-	MK	-0.25/Y	-0.25/N	0.16/N	-0.14/Y	-/30
			Sen'	-3.02	-3.02	5.8	-2.1	
Maraveh-tape	+	+	MK	-0.04/N	*	*	*	*
			Sen'	-0.5	*	*	*	
Ramian	+	+	MK	-0.02/N	*	*	*	*
			Sen'	-0.8	*	*	*	
Robat-gharabil	-	+	MK	0.15/N	0.15/N	*	*	*
			Sen'	1.2	1.2	*	*	
Sad-gorgan	-	-	MK	-0.12/N	-0.12/N	0.13/N	0.17/N	-/27
			Sen'	-1.7	-1.7	2.8	14.2	
Tamar	+	-	MK	0.29/Y	*	-0.03/N	0.0/N	+/22
			Sen'	4.9	*	-1.6	0.19	
Ghafar-haji	+	+	MK	-0.06/N	*	*	*	*
			Sen'	-0.9	*	*	*	
Galikash	+	+	MK	0.024/N	*	*	*	*
			Sen'	0.57	*	*	*	
Pishkamar	-	+	MK	-0.05/N	-0.05/N	*	*	*
			Sen'	-1.02	-1.02	*	*	
Tangrah	+	+	MK	0.12/N	*	*	*	*
			Sen'	2.8	*	*	*	

Furthermore, spatial distribution of trends and their trend direction in measuring gauges for the precipitation time series are through Fig 2.2. As shown in Fig 2.2 in daily time series stations in the mountainous region (semi-arid) present trends that it is increasing. For monthly series, stations with trends appear in the lowlands. Among them stations in the east, have positive trends while Sad-gorgan located in the west has negative trend. In seasonal MK that takes into account the seasonality in the time series the number of stations with trends increased. Same as the monthly map, stations in the east have positive trends while stations in the west have negative trends. Spatial distribution of trends in yearly data is similar to monthly ones, but there are no trends in the west of the region. Moreover, to interpolate the trends the Inverse Distance Whitening (IDW) model was used. Three-dimensional model was used to visualize the intensity and direction of the trends in the whole study area, too. This 3D modeling and visualization make conditions more clear and comprehensible (Fig 2.3). As can be seen from the Fig 2.3, the intensity of the trends in the east of the study area is considerable especially in the highlands regions.
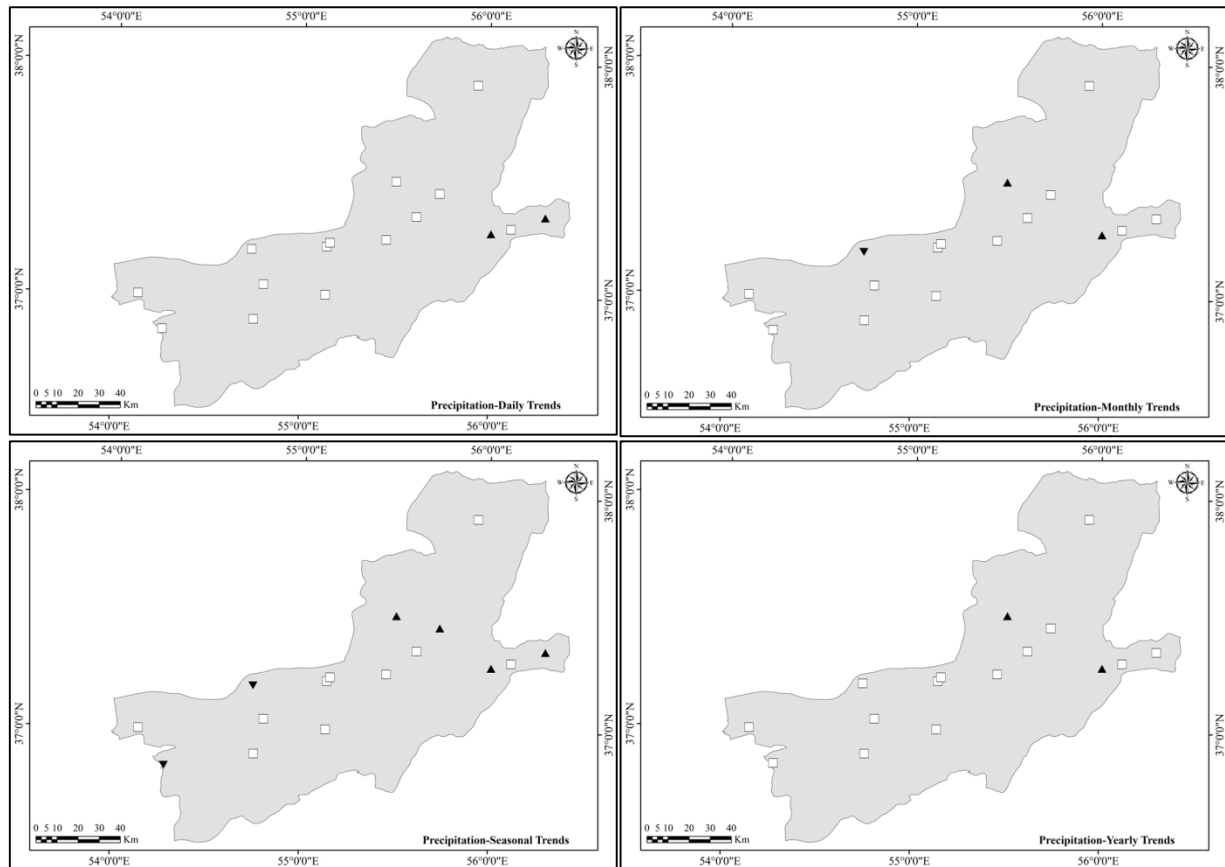
Fig. 2.2. Trend directions in precipitation data as daily, monthly and yearly. The squares show no-trend and triangles present the rise/fall of trends.
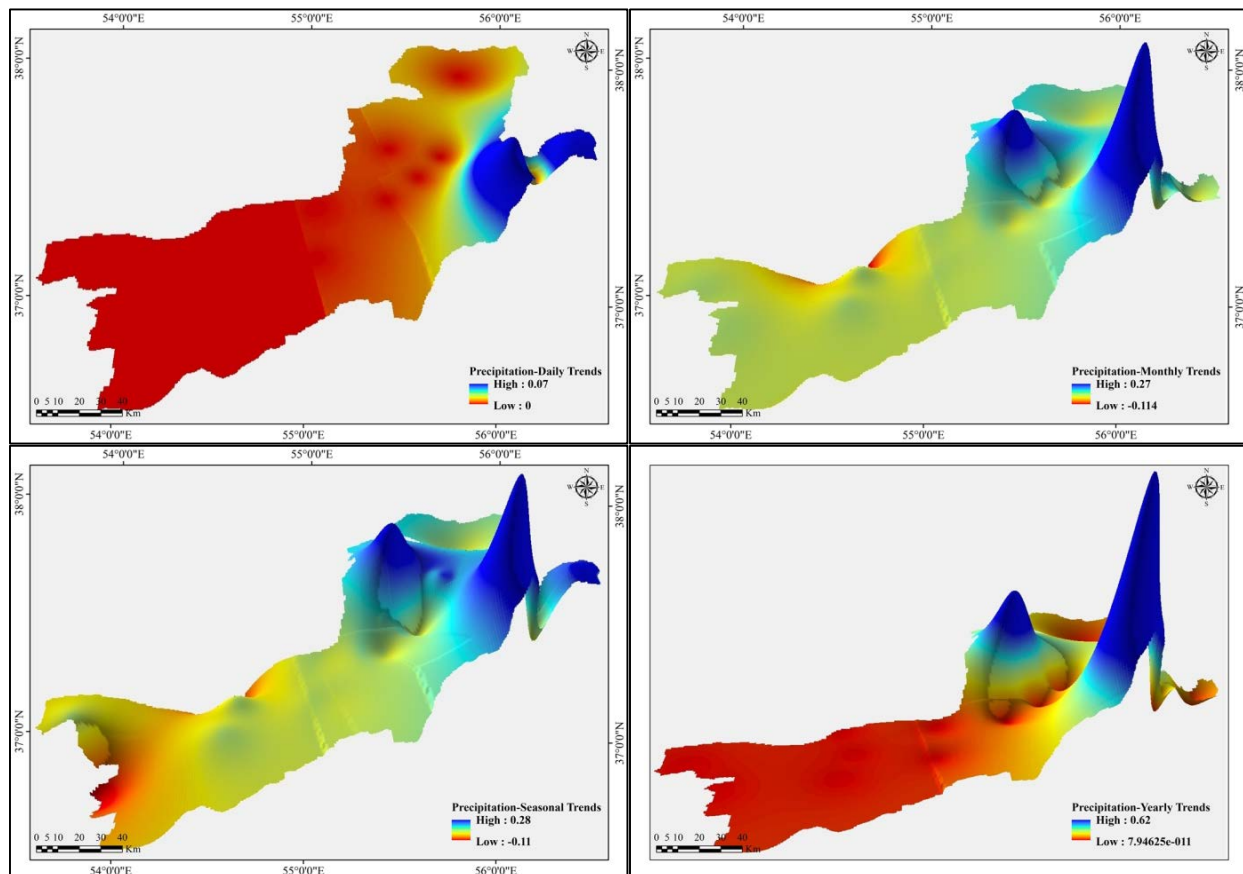
Fig. 2.3. 3D spatial distribution of trends intensity in precipitation time series

2.3.2. Spatio-temporal trends in temperature

2.3.2.1. Maximum temperature

The outputs of statistical trend analysis of maximum temperature series are briefly described in Tables 2.5-2.7. According to the Table 2.5 Mann-Kendall test, detect trends in Fazel-abad, Maraveh and Sad-gorgan. Trends in first and third one was positive and in the second one negative and among them Maraveh had the biggest trend. In monthly scale, only Sad-gorgan station showed trend and it was increasing. While, with considering seasonality about 54% of stations showed trends. In these amounts, 15% had negative trends. Between trends detected stations Sad-gorgan shown more trend than others. In concern with yearly data, Fazel-abad (biggest trend amount), Gorgan, Maraveh, Sad-gorgan and Ghafar-haji had trends and they were increased in all. Therefore, in yearly scale 61% of the stations did not have trends. This is similar to that Saboohi et al. (2012) said.

Table 2.5. Daily trend analysis results of TMax variable

Station	SC	H	Tests	Total trend		Section1 / Trend	Section 2/ Trend	CP Direction/ Row Number
				Normal	PW			
Araz-kuse	-	-	MK	0.029/Y	0.029/N	-0.033/N	-0.006/N	+ / 2771
			Sen'	1.6E-4	1.6E-4	-4.6E-4	9.7E-6	
Bahalke-dashli	-	-	MK	-0.01/N	-0.01/N	0.029/Y	0.062/Y	-/11030
			Sen'	4.4E-5	4.4E-5	1.1E-4	5.6E-4	
Cheshme-khan	-	-	MK	0.013/Y	0.013/N	0.005/N	-0.013	+/1314
			Sen'	0	0	0	0	
Dasht	-	-	MK	0.02/Y	0.02/N	-0.035/Y	0.004/N	+/6340
			Sen'	9.8E-5	9.8E-5	-1.9E-4	0	
Fazel-abad	-	-	MK	0.036/Y	0.036/Y	-0.005/N	0.013/N	+/8603
			Sen'	1.09E-4	1.09E-4	2.7E-5	0	
Gonbad	-	-	MK	0.018/Y	0.018/N	-0.071/N	-0.026/N	+/1505
			Sen'	1.1E-4	1.1E-4	-0.002	-2.2E-4	
Gorgan	-	-	MK	0.017/Y	0.017/N	-0.022/N	0.011/N	+/14734
			Sen'	1.1E-4	1.1E-4	-7.9E-6	8.2E-5	
Maraveh-tape	-	-	MK	-0.044/Y	-0.044/Y	0.019/N	-0.002/N	-/4404
			Sen'	-1.9E-4	-1.9E-4	1.9E-4	0	
Ramian	-	-	MK	0.023/Y	0.023/N	-0.035/N	-0.030/N	+/4632
			Sen'	0	0	-3.07E-4	-1.3E-4	
Robat-gharabil	-	-	MK	-0.001/N	-0.001/N	0.048/Y	0.053/Y	+/5866
			Sen'	0	0	3.8E-4	3.6E-4	
Sad-gorgan	-	-	MK	0.041/Y	0.041/Y	-0.010/N	-0.031/N	+/8958
			Sen'	1.2E-4	1.2E-4	3.3E-5	-1.5E-4	
Tamar	-	-	MK	-0.008/N	-0.008/N	0.010/N	0.049/Y	-/3964
			Sen'	7.2E-5	7.2E-5	0	2.9E-4	

Table 2.6. Monthly and seasonality considered TMax trend analysis.

Station	SC	H	Tests	Total trend		S-MK	Section1 / Trend	Section 2/ Trend	CP Direction/ Row Number
				Normal	PW				
Araz-kuse	-	+	MK	0.03/N	0.03/N	0.096/Y	*	*	*
			Sen'	0.002	0.002		*	*	
Bahalke-dashli	-	+	MK	-0.01/N	-0.01/N	-0.047/N	*	*	*
			Sen'	-7.4E-4	-7.4E-4		*	*	
Cheshme-khan	-	+	MK	0.016/N	0.016/N	0.04/N	*	*	*
			Sen'	0.001	0.001		*	*	
Dasht	-	+	MK	0.033/N	0.033/N	0.029/N	*	*	*
			Sen'	0.006	0.006		*	*	
Fazel-abad	-	+	MK	0.054/N	0.054/N	0.153/Y	*	*	*
			Sen'	0.005	0.005		*	*	
Gonbad	-	+	MK	-0.01/N	-0.01/N	-0.026/N	*	*	*
			Sen'	-6.1E-4	-6.1E-4		*	*	
Gorgan	-	-	MK	0.041/N	0.041/N	0.083/Y	-0.15/Y	-0.164/Y	+/446
			Sen'	0.002	0.002		-0.014	-0.023	
			MK	-0.052/N	-0.052/N		*	*	

				Normal	PW				
Maraveh-tape	-	+	Sen'	-0.006	-0.006	-0.139/Y	*	*	*
Ramian	-	+	MK	0.036/N	0.036/N	0.069/N	*	*	*
			Sen'	0.004	0.004		*	*	
Robat-gharabil	-	+	MK	-0.002/N	-0.002/N	-0.016/N	*	*	*
			Sen'	0	0		*	*	
Sad-gorgan	-	+	MK	0.061/Y	0.061/Y	0.196/Y	*	*	*
			Sen'	0.005	0.005		*	*	
Tamar	-	+	MK	0.033/N	0.033/N	0.1/Y	*	*	*
			Sen'	0.002	0.002		*	*	
Ghafar-haji	-	+	MK	0.036/N	0.036/N	0.1/Y	*	*	*
			Sen'	0.002	0.002		*	*	

Table 2.7. Yearly TMax trend analysis results.

Station	SC	H	Tests	Total trend		Section1 / Trend	Section 2/ Trend	CP Direction/ Row Number
				Normal	PW			
Araz-kuse	+	+	MK	0.1/N	*	*	*	*
			Sen'	0.01	*	*	*	
Bahalke-dashli	-	+	MK	-0.16/N	-0.16/N	*	*	*
			Sen'	-0.01	-0.01	*	*	
Cheshme-khan	+	+	MK	0.19/N	*	*	*	*
			Sen'	0.02	*	*	*	
Dasht	+	+	MK	0.13/N	*	*	*	*
			Sen'	0.032	*	*	*	
Fazel-abad	+	-	MK	0.4/Y	*	0.17/N	0.49/Y	+/20
			Sen'	0.05	*	0.03	0.1	
Gonbad	-	+	MK	-0.01/N	-0.01/N	*	*	*
			Sen'	-0.002	-0.002	*	*	
Gorgan	+	-	MK	0.2/Y	*	-0.001/N	0.1/N	+/44
			Sen'	0.019	*	0	0.02	
Maraveh-tape	+	-	MK	0.3/Y	*	0/N	-0.13/N	-/13
			Sen'	-0.079	*	-0.01	-0.03	
Ramian	+	+	MK	0.09/N	*	*	*	*
			Sen'	0.027	*	*	*	
Robat-gharabil	+	+	MK	-0.015/N	*	*	*	*
			Sen'	-0.006	*	*	*	
Sad-gorgan	-	-	MK	0.36/Y	0.36/Y	0.15/N	-0.046/N	+/27
			Sen'	0.05	0.05	0.03	-0.01	
Tamar	+	+	MK	0.16/N	*	*	*	*
			Sen'	0.02	*	*	*	
Ghafar-haji	+	-	MK	0.24/Y	*	0.05/N	-0.16/N	+/31
			Sen'	0.019	*	0.005	-0.02	

Directions and intensity of trends in case of maximum temperature time series are shown spatially in the Fig 2.4 and 2.5. In the first place, trend directions related to each station are presented and the second one present 3D spatial distribution and intensity of trends in the study area. Fig 2.4 firstly shows that for daily series maximum temperature in western lowlands had increasing trends, but in the arid hilled region in the north-east it has decreasing trend. Secondly, analyzing of monthly data set just detect positive trend in one station in the west. With considering seasonality in monthly series, more trends were detected in the region especially in the west that all were positive. For the yearly time series, gauges with trends gathered more in the east (all positive) and northeast station showed positive trend. As well, three-dimensional investigation of trend intensity showed that positive trends are stronger than negative ones. The intensity in the seasonality considered and yearly sections is clearer and sharp.
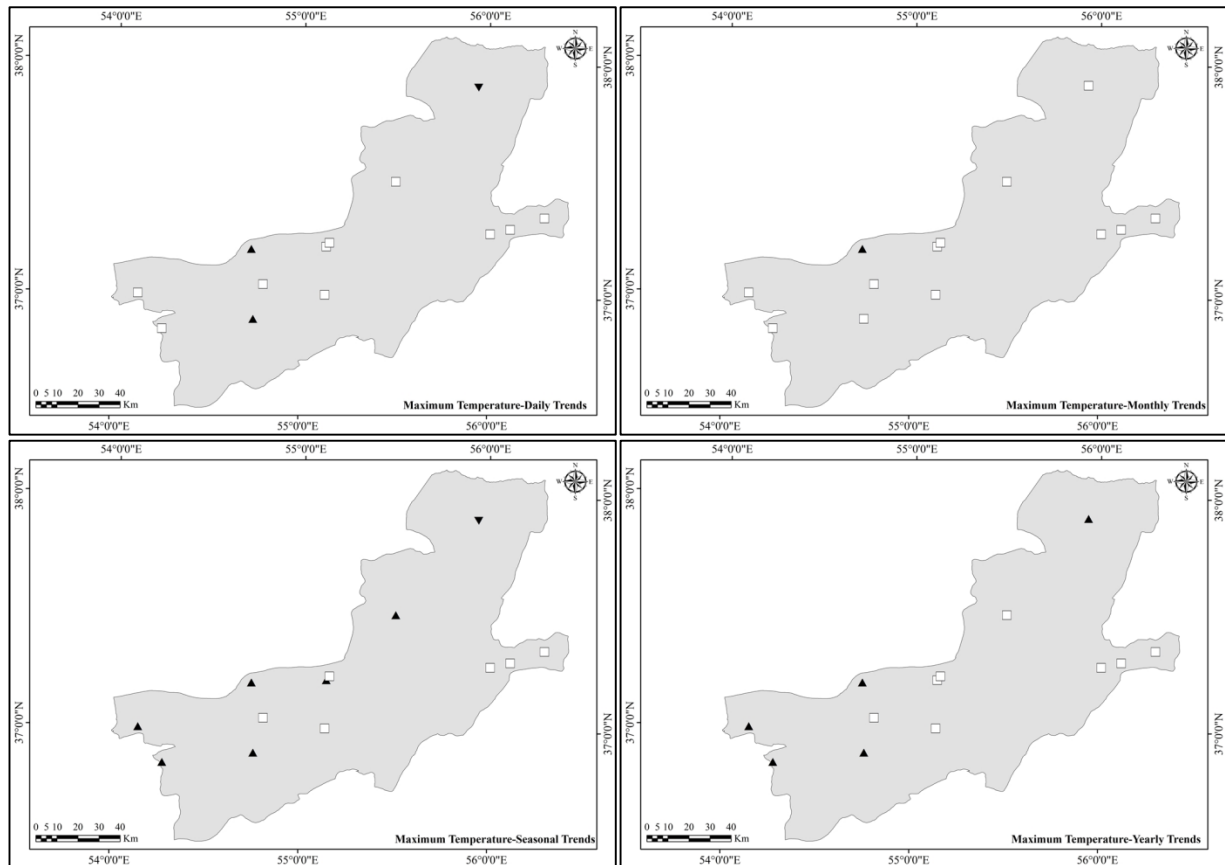
Fig. 2.4. Trend directions in maximum temperature data as daily, monthly, seasonality considered and yearly.
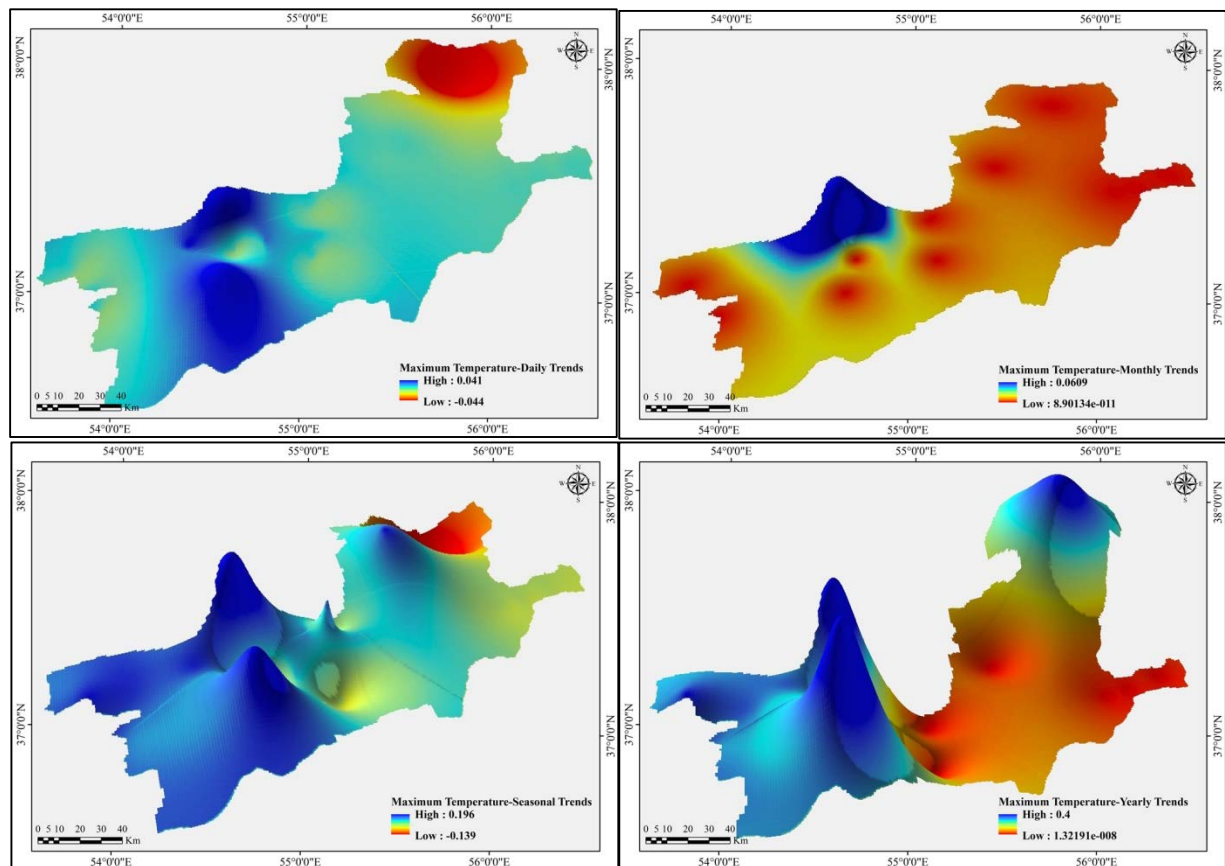
Fig. 2.5. 3D spatial distribution of trends intensity in maximum temperature time series

2.3.2.2. Minimum temperature

For the minimum temperature, results are presented in the tables 2.8-2.10. According to the Table 2.8 for daily data trends at $p<0.05$ were found in the Araz-kuse, Bahalke-dashli (strongest trend), Maraveh-tape, Ramian, Robat-gharabil, Sad-gorgan and Tamar (Six positive and one negative). Significant trends in monthly time series were found just for Bahalke-dashli and Gonbad (both positive and approximately similar). On the contrary, in seasonality considered test about 70% of the stations had shown trends (totally positive) that Bahalke-dashli and Maraveh-tape were biggest. On annual scale, Araz-kuse, Bahalke-dashli, Gonbad, Maraveh-tape, Ramian, Tamar and Ghafar-haji (as the biggest one) have shown positive trends. likewise, Saboohi et al. (2012) detect positive trends for the minimum temperature in most of the stations. The location of the measuring gauges and direction of trends for minimum temperature series are displayed in Fig 2.6 and Fig 2.7 present the intensity of the trends in the regions as a 3D model.

Fig 2.6 presents that for daily series there were significant positive trends in the north band of study area and one negative trend in the mountainous semi-arid region. From this figure, we can see that just two stations in the lowlands present trends in monthly scale. Taking into account seasonality in monthly series create similar results to daily scale, except that spatial distribution is vaster and all trends are positive. In yearly data, the number of stations with trends was reduced and all of them are in the north part and all positive. As Fig 2.7 shows, there is a significant difference between the detected trends. Trends are weak in daily and monthly scale whereas in seasonality considered and yearly sections trends are strong and intense.

Table 2.8. Daily statistical results for TMin trend analysis.

Station	SC	H	Tests	Total trend		Section1 / Trend	Section 2/ Trend	CP Direction/ Row Number
				Normal	PW			
Araz-kuse	-	-	MK	0.046/Y	0.046/Y	-0.017/N	0.006/N	+/8281
			Sen'	1.2E-4	1.2E-4	-3.6E-5	0	
Bahalke-dashli	-	-	MK	0.076/Y	0.076/Y	-0.033/N	0.033/Y	+/4260
			Sen'	2.5E-4	2.5E-4	-2.8E-4	1.3E-4	
Cheshme-khan	-	-	MK	0.021/Y	0.021/N	-0.033/N	0.002/N	+/8234
			Sen'	0	0	-1.3E-4	3.5E-5	
Dasht	-	-	MK	0.033/Y	0.033/N	-0.062/Y	0.0/N	+/5569
			Sen'	1.6E-4	1.6E-4	-5.4E-4	0	
Fazel-abad	-	-	MK	0.003/N	0.003/N	0.024/N	0.070/Y	-/3674
			Sen'	0	0	2.1E-4	2.2E-4	
Gonbad	-	-	MK	0.008/N	0.008/N	-0.056/N	-0.035/Y	+/1858
			Sen'	3.5E-5	3.5E-5	-0.001	-2.7E-4	
Gorgan	-	-	MK	0.007/N	0.007/N	-0.014/N	-0.033/N	+/15090
			Sen'	4.7E-5	4.7E-5	0	-2.6E-4	
Maraveh-tape	-	-	MK	0.07/Y	0.07/Y	0.01/N	0.005/N	+/6400
			Sen'	2.5E-4	2.5E-4	5.6E-5	0	
Ramian	-	-	MK	0.055/Y	0.055/Y	0.014/N	0.018/N	+/4991
			Sen'	1.8E-4	1.8E-4	5.5E-5	0	
Robat-gharabil	-	-	MK	-0.018/Y	-0.018/Y	0.022/N	0.152/Y	-/10263
			Sen'	6.4E-5	6.4E-5	6.7E-5	0.002	
Sad-gorgan	-	-	MK	0.029/Y	0.029/Y	-0.010/N	-0.029/N	+/9312
			Sen'	6.2E-5	6.2E-5	0	-1.08E-4	
Tamar	-	-	MK	0.057/Y	0.057/Y	-0.012/N	-0.023/N	+/6674
			Sen'	1.8E-4	1.8E-4	0	-6.5E-5	

Table 2.9. Minimum temperature monthly and seasonality considered statistical analysis outputs.

Station	SC	H	Tests	Total trend		S-MK	Section1 / Trend	Section 2/ Trend	CP Direction/ Row Number
				Normal	PW				
Araz-kuse	-	+	MK	0.054/N	0.054/N	0.17/Y	*	*	*
			Sen'	0.004	0.004		*	*	
Bahalke-dashli	-	+	MK	0.08/Y	0.08/Y	0.3/Y	*	*	*
			Sen'	0.007	0.007		*	*	
Cheshme-khan	-	+	MK	0.024/N	0.024/N	0.1/Y	*	*	*
			Sen'	0.002	0.002		*	*	
Dasht	-	+	MK	0.038/N	0.038/N	0.044/N	*	*	*
			Sen'	0.007	0.007		*	*	
Fazel-abad	-	+	MK	0.01/N	0.01/N	-0.008/N	*	*	*
			Sen'	0.001	0.001		*	*	
Gonbad	-	-	MK	0.081/Y	0.081/Y	0.29/Y	0.017/N	0.002/N	+/391
			Sen'	0.005	0.005		0.002	0	
Gorgan	-	+	MK	-0.001/N	-0.001/N	0.001/N	*	*	*
			Sen'	0	0		*	*	
Maraveh-tape	-	+	MK	0.078/Y	0.078/N	0.3/Y	*	*	*
			Sen'	0.008	0.008		*	*	
Ramian	-	+	MK	0.06/N	0.06/N	0.16/Y	*	*	*
			Sen'	0.006	0.006		*	*	
Robat-gharabil	-	+	MK	-0.01/N	-0.01/N	-0.08/N	*	*	*
			Sen'	-0.002	-0.002		*	*	
Sad-gorgan	-	+	MK	0.03/N	0.03/N	0.1/Y	*	*	*
			Sen'	0.003	0.003		*	*	
Tamar	-	+	MK	0.06/N	0.06/N	0.17/Y	*	*	*
			Sen'	0.006	0.006		*	*	
Ghafar-haji	-	+	MK	0.064/Y	0.064/N	0.2/Y	*	*	*
			Sen'	0.005	0.005		*	*	

Table 2.10. Minimum temperature yearly trend analysis outputs.

| Station	SC	H	Tests	Total trend		Section1 / Trend	Section 2/ Trend	CP Direction/ Row Number
				Normal	PW			
Araz-kuse	-	-	MK	0.4/Y	0.4/Y	0.19/N	0.12/N	+/27
			Sen'	0.067	0.067	0.067	0.04	
Bahalke-dashli	-	-	MK	0.58/Y	0.58/Y	0.25/N	0.37/N	+/14
			Sen'	0.06	0.06	0.05	0.05	
Cheshme-khan	-	+	MK	0.21/N	0.21/N	*	*	*
			Sen'	0.03	0.03	*	*	
Dasht	+	+	MK	0.14/N	*	*	*	*
			Sen'	0.042	*	*	*	
Fazel-abad	-	+	MK	0/N	0/N	*	*	*
			Sen'	3.08E-4	3.08E-4	*	*	
Gonbad	-	-	MK	0.46/Y	0.46/Y	-0.08/N	0.27/N	+/33
			Sen'	0.04	0.04	-0.007	0.036	
Gorgan	+	+	MK	-0.06/N	*	*	*	*
			Sen'	-0.004	*	*	*	
Maraveh-tape	+	-	MK	0.46/Y	*	0.2/N	0.23/N	+/18
			Sen'	0.09	*	0.04	0.09	
Ramian	+	-	MK	0.5/Y	*	0.23/N	0.24/N	+/12
			Sen'	0.05	*	0.06	0.02	
Robat-gharabil	+	+	MK	-0.14/N	*	*	*	*
			Sen'	-0.037	*	*	*	
Sad-gorgan	-	-	MK	0.35/Y	0.35/N	0.14/N	-0.013/N	+/27
			Sen'	0.04	0.04	0.04	0	
Tamar	-	-	MK	0.57/Y	0.57/Y	0.44/Y	0.017/N	+/30
			Sen'	0.14	0.14	0.29	0.008	
Ghafar-haji	-	-	MK	0.6/Y	0.6/Y	0.57/Y	0.39/N	+/20
			Sen'	0.06	0.06	0.59	0.04	
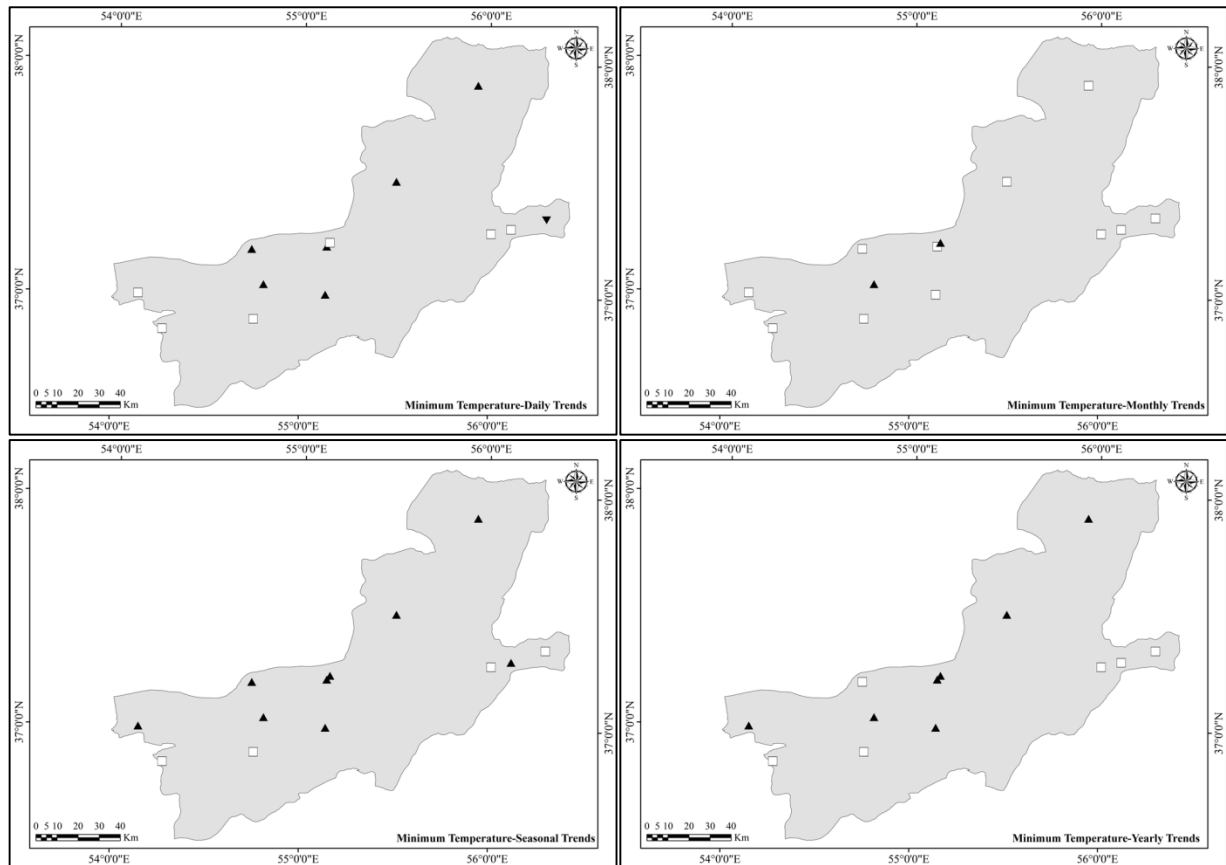
Fig. 2.6. Trend direction in minimum temperature data as daily, monthly, seasonality considered and yearly.
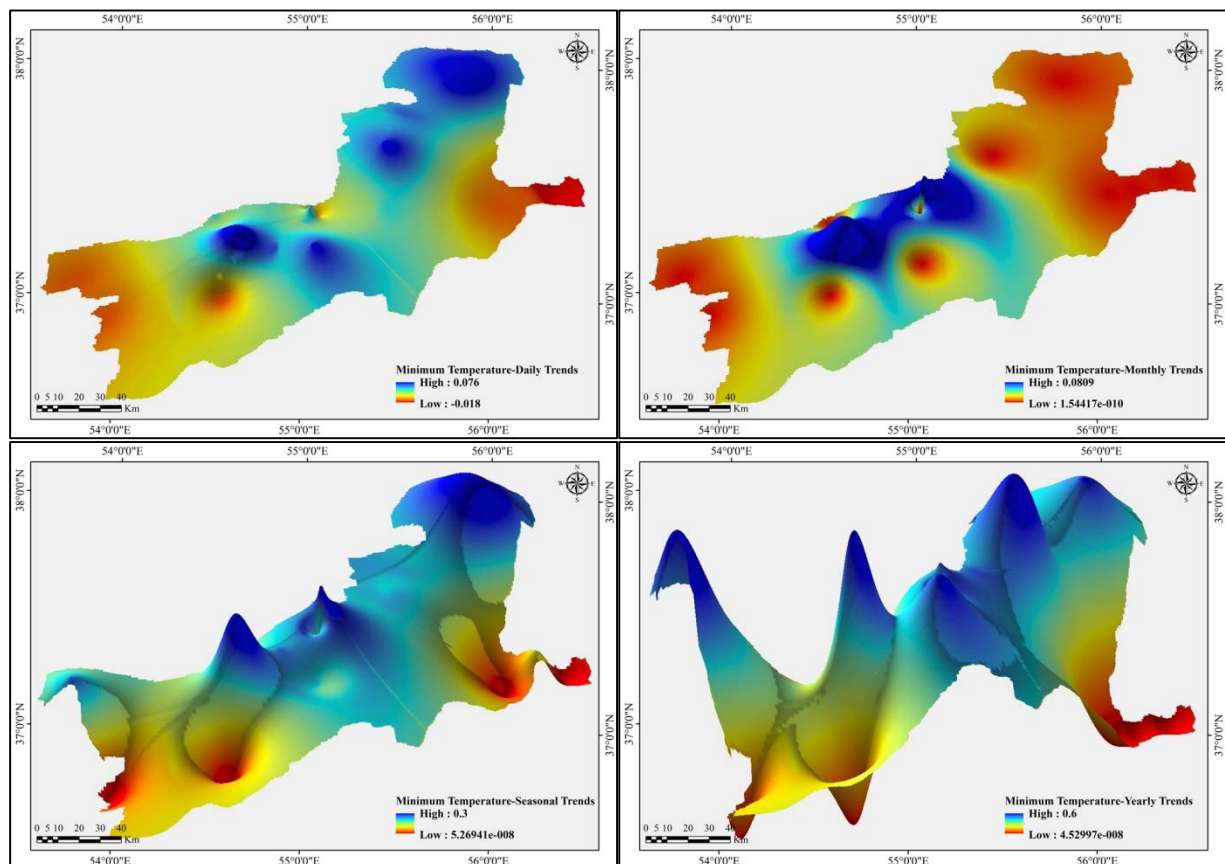
Fig. 2.7. Three-dimensional spatial distribution of trend intensity in minimum temperature time series

2.3.2.3. Mean temperature

Table 2.11 shows daily scale results for mean temperature. According to the table, in 41% of the stations trends were detected (all positive and biggest trends in Araz-kuse and Dasht). In monthly time series, Araz-kuse, Sad-gorgan, Tamar (trend more than others) and Ghafar-haji has shown trends (positive) (Table 2.12). While, Bahalke-dashli, Dasht and Ramian stations that shown trends in daily data in monthly scale were without trend. Moreover, with considering seasonality Mann-Kendall detected trends in 61% of the stations (positive) (Table 2.12). Likewise, Araz-kuse, Bahalke-dashli, Ramian, Sad-gorgan, Tamar and Ghafar-haji in $P < 0.05$ founded with trends (positive) in yearly scale (Table 2.13). Among seasonality considered and yearly trend analysis results Ghafar-haji has shown the strongest trend. According to the detected trends, the results of this section are in the same way with Hossein Tabari, Hosseinzadeh Talaee, et al. (2012) that found positive trends for some parts of Iran. Moreover, spatial distribution and direction of trends in stations and spatial 3D model of trends intensity can be found in Fig 2.8 and Fig 2.9.

Fig 2.8 provides that in daily analyze five station showed positive trends (four in wet lowlands and one in semi-arid region). In case of monthly series, although, four gauges in the north band showed positive trends, with considering seasonality in data the number of trended stations increased and more distributed in the area (all positive). Yearly results are similar to the monthly with seasonality except in mountainous stations. Detected trends can be compared in Fig 2.9. It is apparent from this figure that from daily series to yearly data the intensity of trends rose.

Table 2.11. Trend analysis outputs of daily TMean.

Station	SC	H	Tests	Total trend		Section1 / Trend	Section 2/ Trend	CP Direction/ Row Number
				Normal	PW			
Araz-kuse	-	-	MK	0.066/Y	0.066/Y	0.022/N	0.016/N	+/4998
			Sen'	2.01E-4	2.01E-4	1.4E-4	8.4E-5	
Bahalke-dashli	-	-	MK	0.033/Y	0.033/Y	-0.017/N	0.014/N	+/4257
			Sen'	1.4E-4	1.4E-4	-1.6E-4	5.1E-5	
Cheshme-khan	-	-	MK	0.02/Y	0.02/N	-0.021/N	0.002	+/8234
			Sen'	6.05E-5	6.05E-5	-4.6E-5	4.2E-5	
Dasht	-	-	MK	0.061/Y	0.061/Y	-0.029/N	0.018/N	+/5951
			Sen'	3.3E-4	3.3E-4	-2.3E-4	3.1E-4	
Fazel-abad	-	-	MK	0.021/Y	0.021/N	-0.035/Y	0.019/N	+/8629
			Sen'	6.07E-5	6.07E-5	-1.1E-4	1.6E-4	
Gonbad	-	-	MK	0.015/N	0.015/N	-0.042/N	-0.032/N	+/1858
			Sen'	9.03E-5	9.03E-5	-9.8E-4	-2.6E-4	
Gorgan	-	-	MK	0.013/Y	0.013/N	-0.020/N	-0.005/N	+/14734
			Sen'	7.2E-5	7.2E-5	-2.05E-5	-3.2E-5	
Maraveh-tape	-	-	MK	0.006/N	0.006/N	-0.033/Y	-0.047/Y	+/6399
			Sen'	7.3E-6	7.3E-6	-2.2E-4	-3.8E-4	
Ramian	-	-	MK	0.039/Y	0.039/Y	-0.014/N	-0.01/N	+/4639
			Sen'	1.4E-4	1.4E-4	-9.4E-5	2.7E-5	
Robat-gharabil	-	-	MK	-0.009/N	-0.009/N	0.043/Y	0.028/N	+/5862
			Sen'	-1.07E-5	-1.07E-5	3.4E-4	1.7E-4	
Sad-gorgan	-	-	MK	0.038/Y	0.038/Y	-0.009/N	-0.025/N	+/8958
			Sen'	1.1E-4	1.1E-4	2.2E-5	-1.2E-4	
Tamar	-	-	MK	0.022/Y	0.022/N	-0.044/Y	-0.007/N	+/6319
			Sen'	7.6E-5	7.6E-5	-2.9E-4	-1.5E-5	

Table 2.12. TMean variable monthly and seasonality considered statistical analysis outputs.

Station	SC	H	Tests	Total trend		S-MK	Section1 / Trend	Section 2/ Trend	CP Direction/ Row Number
				Normal	PW				
Araz-kuse	-	-	MK	0.102/Y	0.102/Y	0.23/Y	0.164/N	0.018/N	+/91
			Sen'	0.008	0.008		0.068	0.002	
Bahalke-dashli	-	+	MK	0.042/N	0.042/N	0.04/N	*	*	*
			Sen'	0.003	0.003		*	*	
Cheshme-khan	-	+	MK	0.025/N	0.025/N	0.095/Y	*	*	*
			Sen'	0.002	0.002		*	*	
Dasht	-	-	MK	0.079/N	0.079/N	0.17/Y	-0.054/N	0.056/N	+/177
			Sen'	0.01	0.01		-0.006	0.02	
Fazel-abad	-	+	MK	0.027/N	0.027/N	0.075/Y	*	*	*
			Sen'	0.002	0.002		*	*	
Gonbad	-	+	MK	0.036/N	0.036/N	0.043/N	*	*	*
			Sen'	0.002	0.002		*	*	
Gorgan	-	+	MK	0.01/N	0.01/N	0.04/N	*	*	*
			Sen'	5.4E-4	5.4E-4		*	*	
Maraveh-tape	-	+	MK	0.005/N	0.005/N	0.04/N	*	*	*
			Sen'	4.9E-4	4.9E-4		*	*	
Ramian	-	+	MK	0.05/N	0.05/N	0.13/Y	*	*	*
			Sen'	0.006	0.006		*	*	
Robat-gharabil	-	+	MK	-0.01/N	-0.01/N	-0.054/N	*	*	*
			Sen'	-9.3E-4	-9.3E-4		*	*	
Sad-gorgan	-	-	MK	0.1/Y	0.1/Y	0.2/Y	0.23/Y	0.034/N	+/95
			Sen'	0.008	0.008		0.1	0.003	
Tamar	-	-	MK	0.161/Y	0.161/Y	0.192/Y	0.143/N	0.023/N	+/160
			Sen'	0.012	0.012		0.03	0.002	
Ghafar-haji	-	-	MK	0.135/Y	0.135/Y	0.325/Y	0.079/N	0.027/N	+/91
			Sen'	0.009	0.009		0.02	0.002	

Table 2.13. Statistical results for yearly TMean trend analysis.

| Station	SC	H	Tests	Total trend		Section1 / Trend	Section 2/ Trend	CP Direction/ Row Number
				Normal	PW			
Araz-kuse	-	-	MK	0.39/Y	0.39/Y	0.3/N	0.27/N	+/27
			Sen'	0.05	0.05	0.1	0.057	
Bahalke-dashli	+	-	MK	0.35/Y	*	0.46/N	0.16/N	+/7
			Sen'	0.026	*	0.079	0.01	
Cheshme-khan	-	+	MK	0.2/N	0.2/N	*	*	*
			Sen'	0.02	0.02	*	*	
Dasht	+	-	MK	0.24/N	*	-0.34/N	0.4/N	+/16
			Sen'	0.05	*	-0.12	0.4	
Fazel-abad	-	-	MK	0.2/Y	0.2/N	-0.02/N	0.22/N	+/29
			Sen'	0.02	0.02	-0.003	0.1	
Gonbad	-	-	MK	0.2/Y	0.2/N	-0.1/N	0.29/N	+/34
			Sen'	0.02	0.02	-0.01	0.05	
Gorgan	+	+	MK	0.09/N	*	*	*	*
			Sen'	0.008	*	*	*	
Maraveh-tape	+	+	MK	0.048/N	*	*	*	*
			Sen'	0.007	*	*	*	
Ramian	+	-	MK	0.32/Y	*	-0.23/N	0.07/N	+/12
			Sen'	0.04	*	-0.04	0.02	
Robat-gharabil	+	+	MK	-0.13/N	*	*	*	*
			Sen'	-0.02	*	*	*	
Sad-gorgan	-	-	MK	0.4/Y	0.4/Y	0.22/N	-0.066/N	+/27
			Sen'	0.05	0.05	0.06	-0.015	
Tamar	-	-	MK	0.48/Y	0.48/Y	0.46/N	0.14/N	+/14
			Sen'	0.09	0.09	0.42	0.017	
Ghafar-haji	-	-	MK	0.5/Y	0.5/Y	0.55/Y	0.32/N	+/25
			Sen'	0.05	0.05	0.24	0.04	
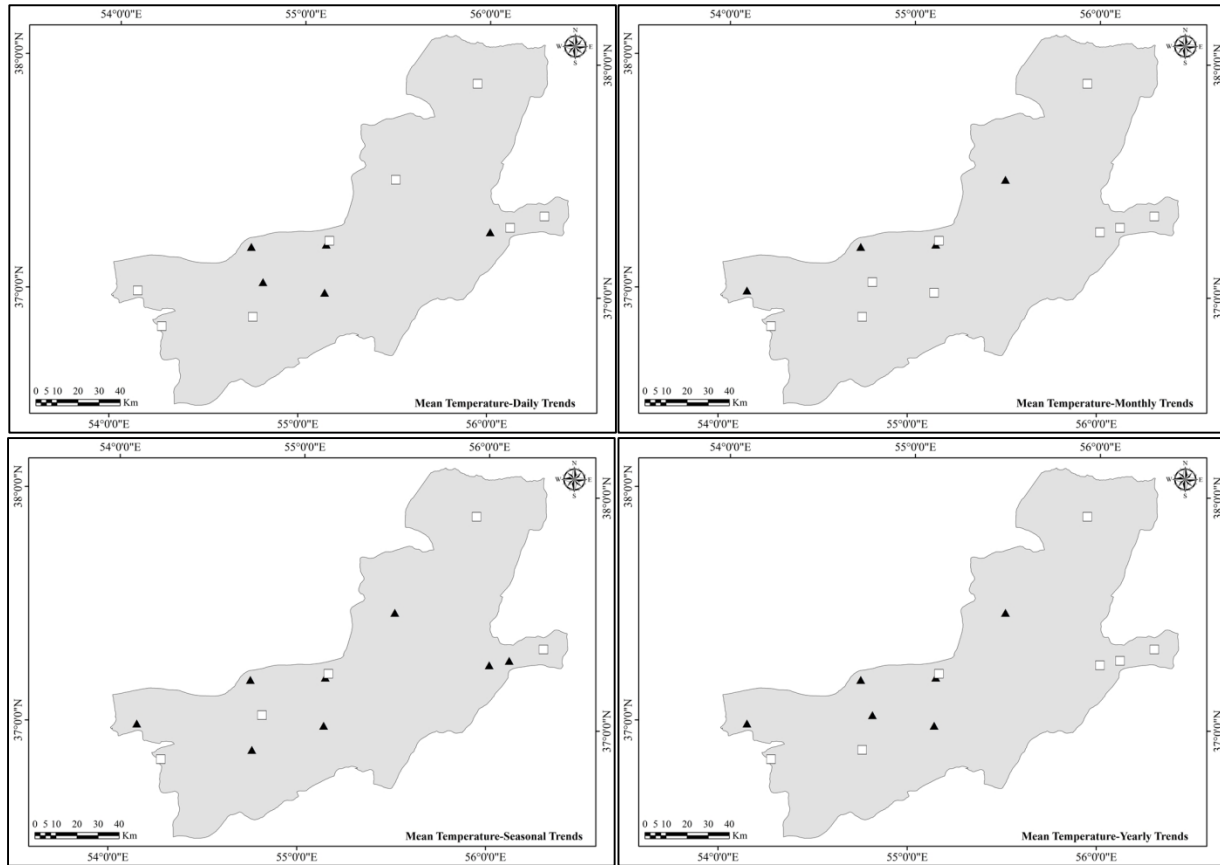
Fig. 2.8. Trends directions in mean temperature data as daily, monthly, seasonality considered and yearly.
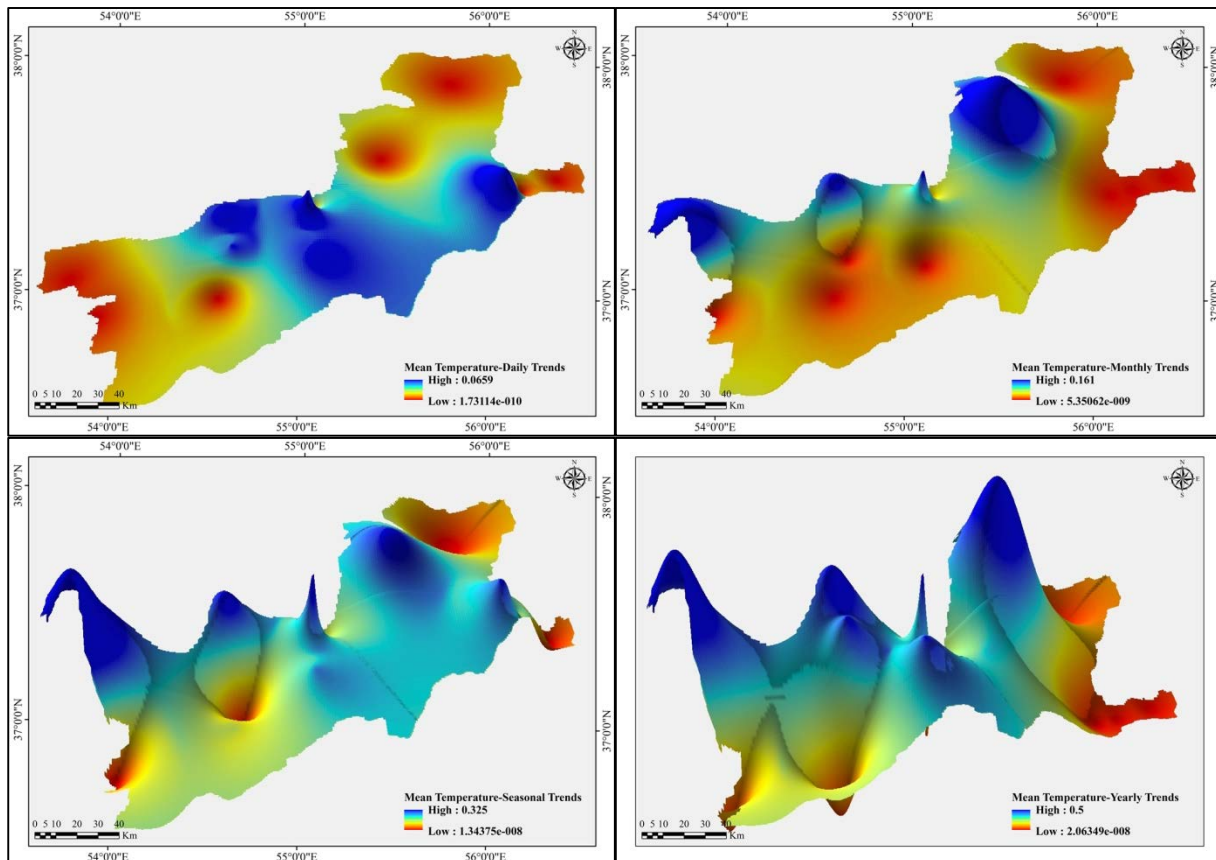
Fig. 2.9. 3D spatial distribution of trends intensity in mean temperature time series

2.3.3. Spatio-temporal trends in discharge

In discharge measuring stations about 80% of the daily time-series have shown trends (totally negative) that can be seen in the Table 2.14. In normal trend analysis and pre-whitened data, Haji-ghushan showed more trends than others did and trends were similar. Because of breaks were detected in the time series trends for data before and after the break were carried out that results are in Table 2.14. In monthly scale there is trends in the Tangrah and Haji-ghushan stations (Negative). In the same way, results with considering seasonality in data trends were detected in Tangrah and Haji-ghushan stations (approximately similar trend amount), but their amount is different than monthly outputs (Table 2.15). Although in yearly scale, no stations had shown trends (Table 2.16). Trend direction, however, for daily, monthly and seasonality considered statistical results are presented in Fig 2.10. As shown in this figure around all stations, have negative trends in daily data. In monthly series trends are negative, but just two stations showed trends and considering the seasonality just detect trends in one more station (all negative). In addition, in yearly scale no station showed trends. Additionally, it should be mentioned that our results is somehow different than the results of Abghari et al. (2013) that study yearly river flows in some parts in the west of Iran. Spatial 3D modeling of the trend intensity can be found in Fig 2.11, too.

Table 2.14. Trend analysis outputs of daily discharge.

Station	SC	H	Tests	Total trend		Section1 / Trend	Section 2/ Trend	CP Direction/ Row Number
				Normal	PW			
Tangrah	-	-	MK	-0.096/Y	-0.096/Y	0.077/Y	-0.072/Y	-/9213
			Sen'	2.5E-5	2.5E-5	2.7E-5	1.5E-4	
Galikash	-	-	MK	-0.034/Y	-0.034/Y	0.107/Y	-0.049/Y	-/11337
			Sen'	2.02E-5	2.02E-5	7.7E-5	-4.01E-5	
Haji-ghushan	-	-	MK	-0.24/Y	-0.24/Y	-0.07/Y	0.049/N	-/8501
			Sen'	3.3E-5	3.3E-5	-4.07E-5	3.8E-6	
Gonbad	-	-	MK	-0.039/Y	-0.039/N	0.15/Y	-0.017/N	-/15954
			Sen'	1.1E-4	1.1E-4	4.04E-4	-1.7E-5	
Tamar	-	-	MK	-0.097/Y	-0.097/Y	0.045/Y	-0.038/N	-/10497
			Sen'	3.4E-5	3.4E-5	7.2E-5	-1.9E-5	

Table 2.15. Monthly and seasonality considered discharge trend analysis outputs.

Station	SC	H	Tests	Total trend		S-MK	Section1 / Trend	Section 2/ Trend	CP Direction/ Row Number
				Normal	PW				
Tangrah	-	-	MK	-0.095/Y	-0.095/Y	-0.13/Y	0.1/N	-0.044/N	-/351
			Sen'	-5.8E-4	-5.8E-4		0.001	-4.8E-4	
Galikash	-	+	MK	-0.02/N	-0.02/N	-0.041/N	*	*	*
			Sen'	-2.02E-4	-2.02E-4		*	*	
Haji-ghushan	+	+	MK	-0.12/Y	*	-0.15/Y	*	*	*
			Sen'	-0.002	*		*	*	
Gonbad	-	-	MK	0.038/N	0.038/N	0.073/N	-0.013/N	-0.124/Y	+/149
			Sen'	9.7E-4	9.7E-4		-8.9E-4	-0.006	
Tamar	-	+	MK	-0.02/N	-0.02/N	-0.056/N	*	*	*
			Sen'	-1.8E-4	-1.8E-4		*	*	

Table 2.16. Statistical results for yearly discharge trend analysis.

Station	SC	H	Tests	Total trend		Section1 / Trend	Section 2/ Trend	CP Direction/ Row Number
				Normal	PW			
Tangrah	+	+	MK	-0.13/N	*	*	*	*
			Sen'	-0.014	*	*	*	
Galikash	+	+	MK	-0.005/N	*	*	*	*
			Sen'	-6.9E-4	*	*	*	
Haji-ghushan	+	+	MK	-0.16/N	*	*	*	*
			Sen'	-0.02	*	*	*	
Gonbad	-	-	MK	0.069/N	0.069/N	0.2/N	-0.29/N	+/12
			Sen'	0.01	0.01	0.1	-0.1	
Tamar	+	+	MK	-0.055/N	*	*	*	*
			Sen'	-0.003	*	*	*	
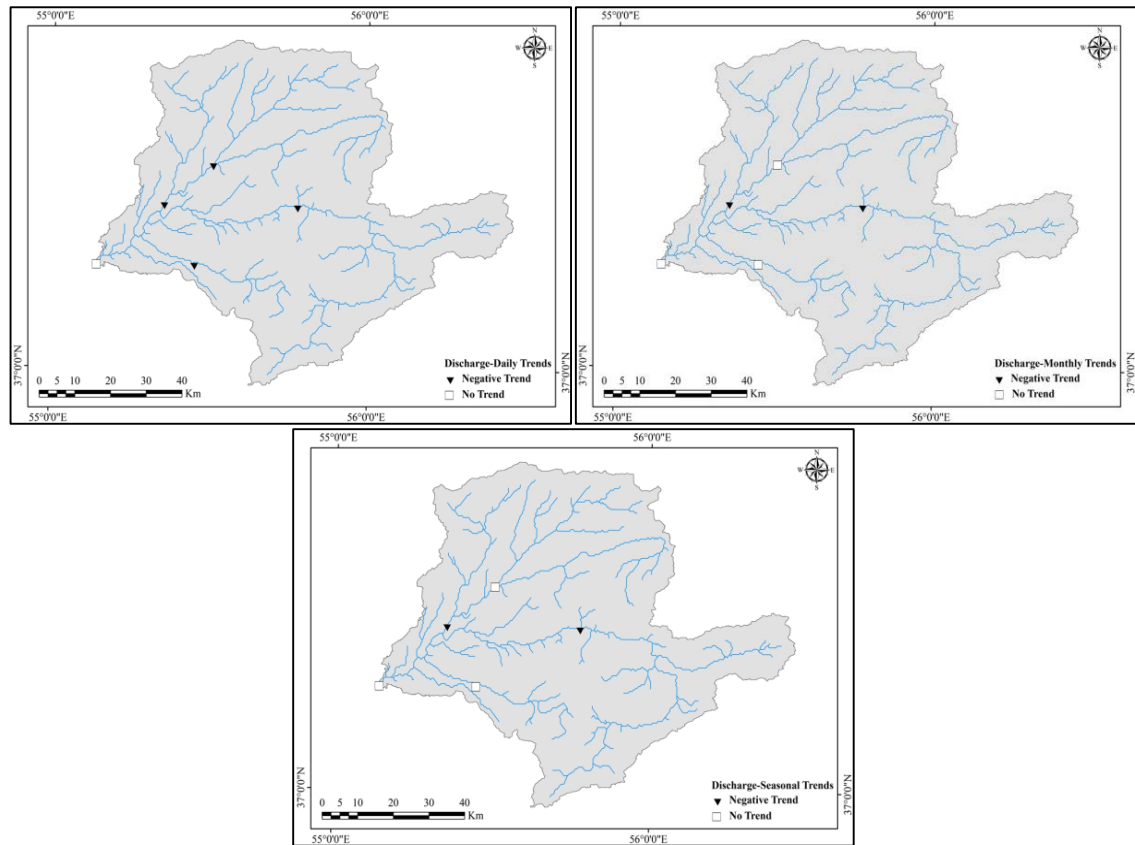
Fig. 2.10. Trend directions in discharge time series as daily, monthly and seasonality considered.
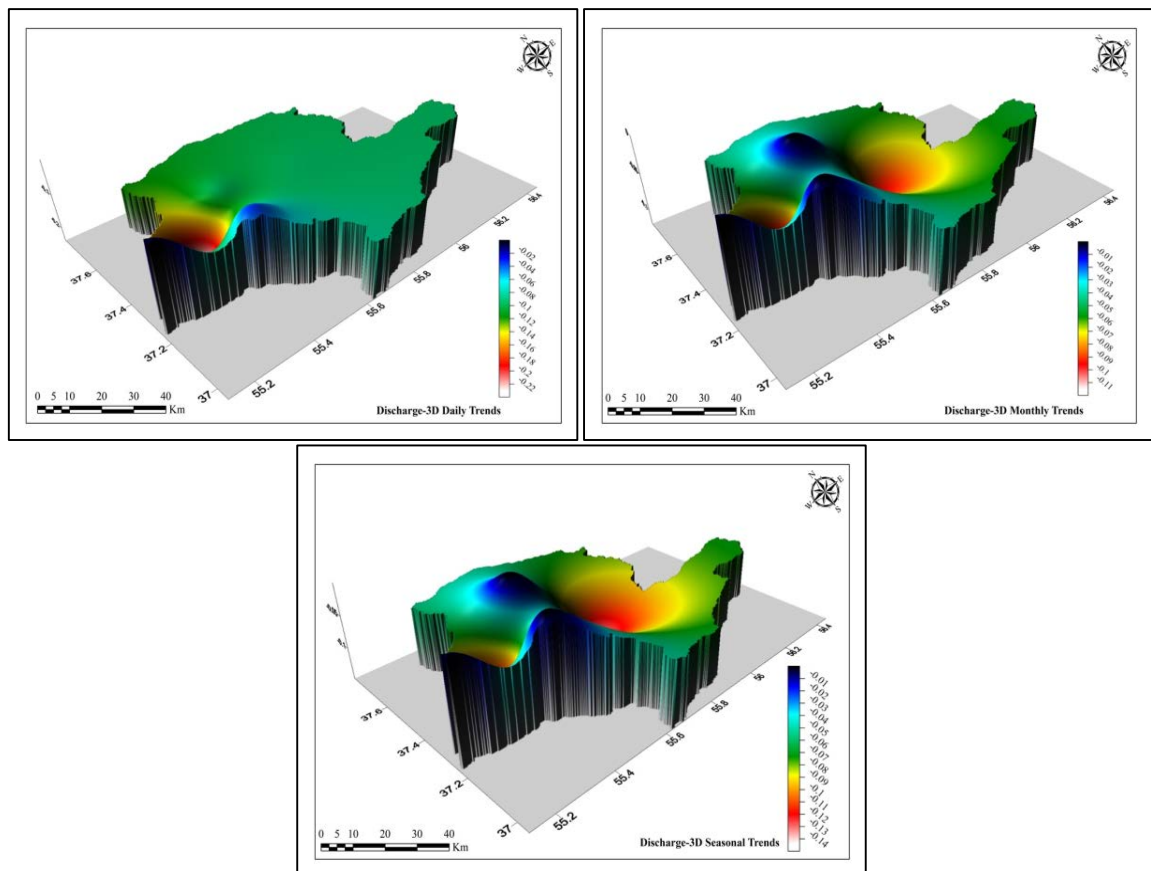
Fig. 2.11. 3D spatial distribution of trends intensity in discharge time series

2.4.   Conclusion

Climate variability was investigated in country scale in Iran recently by some researchers; but investigating these variations in local and regional scale is very important to provide better understanding of conditions. This section of thesis analyzes the behavior of the daily, monthly and yearly hydro-meteorological data in the northeast of Iran for trends in long historical data series. The data were controlled for homogeneity and auto-correlation and the TFPW technique was applied to pre-process the data series prior to the trend analysis in order to decrease the serial correlation in long time series. Afterwards, the non-parametric Mann–Kendall test and Sen's slope estimator were used to explore the precipitation, temperature and discharge trends.

Statistical and spatial analyzing the precipitation time-series over the study area have shown detected trends, their directions and intensity in each station and entire the region for precipitation data. In daily analysis, all the stations shown trends but just 16 percent of the stations show significant trends and the trends were positive, but not strong. In analyzing the change points and their direction in daily data, 58% of the stations showed trends that just Sad-gorgan station showed significant trend (positive) in the second part. In monthly series, trends were detected in all stations but in 95%, significant level only about 19% of stations, had trends that two-thirds of them were increasing. Detected trends in monthly data were stronger than daily data's trends. While, with regarding to seasonality in the data, 37.5% of the stations showed significant trends. With investigation of broken series, first sections of Bahalke-dashli and Pishkamar and second section of Sad-gorgan showed significant trends (entirely positive). Finally, on the annual data 12.5% of the stations showed significant positive trends and there was not negative trends, although all the stations showed trends.

In temperature, maximum series experienced some trends but they are small and just in the monthly seasonality considered time series a station in the main study area had increasing trend. While, minimum temperature endured significant trend changes in all time scales. In the plains regions the minimum of temperature increased while in the eastern highlands one station shows decreasing trends in all time scales but significant only in daily series. However, in mean temperature the stations that show significant trends generally experienced increase. In case of trend intensity, they are more intense in the yearly scale and among temperatures stronger in minimum temperature.

Statistical and spatial results of discharge trend analysis have shown decreasing trends in daily series. In daily analysis, 80% of discharge time series have shown negative trend. In monthly series, this percent amount reduced and 40% had presented trends. As well, in seasonality considered MK the results were similar to monthly ones (negative) but different amount of trends. Different from daily, monthly and seasonality considered outputs; yearly series did not shows a significant trend.

In general, this research shows that, there are trends in time series that means we will experience changes in the normal and stable conditions. Daily precipitation increased in some stations that could increase the risk of flash floods. The monthly changes in the trends could be evidence on variation of the floods distribution and concentrations during the year. Temperature characteristics in the basin have their great role in sustainability of environment and happening flood hazards. Whereas, changing of discharge amount could have its complex impact on the natural hazards consist floods. Overall, these results indicate the necessity of more local studies to understand climate and environmental changes. In addition, the evidence from this study revealed that there are climatological and environmental changes in the study area.

Research Question: Are there changes in hydro-meteorological data in the basin?

Yes, the results of time series analysis show that there are several changes in the hydro-meteorological time series.

Chapter 3

Remote Sensing Detection and Spatio-temporal LCLU Change Analysis

This chapter will cover the integration of GIS and remote sensing to provide deep knowledge about the LCLU status and dynamics during 1972 to 2014 in the study area. It will illustrate pixel-based and GEOBIA classification techniques to provide LCLU maps. A comprehensive spatio-temporal analysis of LCLU changes and dynamics characteristics will cover the rest of the chapter. The results of this section will contribute in establishing flood hazard analysis.

3.1.   Introduction

Land cover Land Use (LCLU) change studies have become an essential part of present plans for dealing with environment and natural resource management in all around the world by national and local organizations (Thilagavathi, Subramani, & Suresh, 2015). As a result of population growth and urbanization, agricultural and built up expansion and reduce in forest and range areas, different types of Land Cover Land Use (LCLU) changes taking place at intensive levels in developing countries (Adhikari, Southworth, & Nagendra, 2014; Lambin et al., 2001). Dingle Robertson and King (2011) in the same way with Chapin Iii et al. (2000) are believed to grate influence of the LCLU changes in earth. LCLU change is progressive, widespread and an accelerating process mainly driven by anthropogenic derangements and natural phenomenon, which in turn drives changes that impact humans (Berakhi, Oyana, & Adu-Prah, 2014). Humans play a major role as forces of change in the environment, imposing changes at all levels ranging from global to local (Berakhi et al., 2014). In our study area, the conditions are approximately the same with other parts of the world. In 2006 based on the census statistics, about 600 thousand people lived in six city and more than 500 villages located in this region (Statistical-Center-of-Iran, 2006). In this regard, as it is clear in Fig 3.1 to better understanding of environmental changes and

finding the influence of LCLU changes on the related features like floods timely detection of LCLU changes is necessary (Qin, Niu, Chen, Li, & Ban, 2013).

```
              ┌────────────────────┐
              │ Climate Change     │
              │ (CC)               │
              └────────────────────┘

┌──────────────────────────────┐        ┌──────────────────────────┐
│ Land Cover Land Use (LCLU):  │◄──────►│ Hazards:                 │
│                              │        │    • Floods              │
│    ┌──────────────┐          │        │    • Landslides          │
│    │ LCLU Time B  │          │        │                          │
│    └──────────────┘          │        └──────────────────────────┘
│ ┌──────────────┐  │          │
│ │ LCLU Time A  │             │        ┌──────────────────────────┐
│ └──────────────┘             │        │   • Population Increase   │
│    ┌──────────────┐          │        │   • Agricultural          │
│    │ LCLU Time C  │◄─────────┼────────│     expansion             │
│    └──────────────┘          │        │   • Settlement            │
└──────────────────────────────┘        │     Expansion             │
                                         │   • Government Policy     │
                                         │   • Others                │
                                         └──────────────────────────┘
```
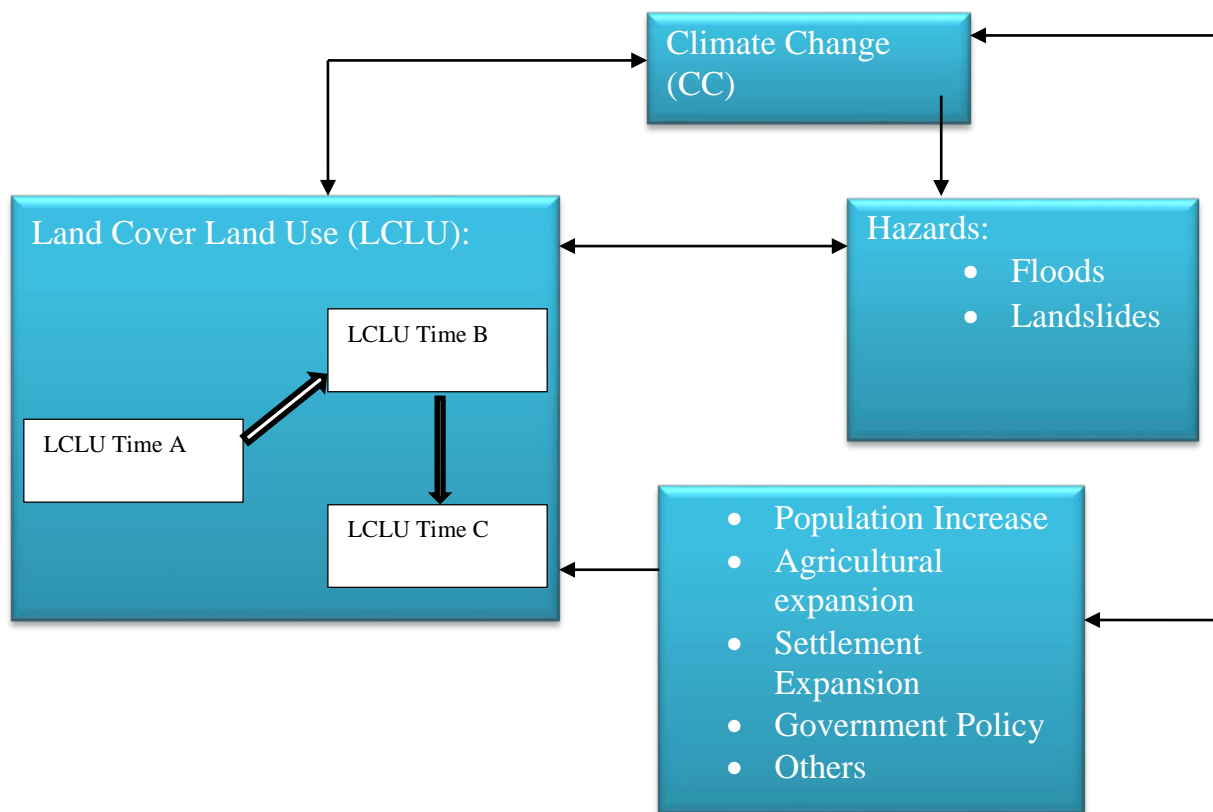
Fig. 3.1. Flowchart of LCLU and its relations (Adapted from Berakhi et al. (2014))

Under these circumstances LCLU change is a major issue of global environmental change and an important field in this area of research nowadays (Yesmin, Mohiuddin, Uddin, & Shahid, 2014). As a consequence, there is a general effort to develop reliable methods in order to identify and monitor LCLU changes (Kolios & Stylios, 2013). At the present time, it is widely known that LCLU changes can be monitored at different scales using Remote Sensing (RS) satellite imageries (Kolios & Stylios, 2013). In other words, satellite remote sensing is the most frequent data source for detection, quantification and mapping of LCLU patterns and changes because of its repetitive data acquisition, digital format suitable for computer processing and accurate geo-referencing procedures (Abd El-Kawy, Rød, Ismail, & Suliman, 2011). Monitoring and Change detection Using RS required the use of several multi-date (sometimes multi sensor) images to evaluate the differences occurring in LCLU between the acquisition dates of images that are due to various environmental conditions and human actions (Abd El-Kawy et al., 2011).

Since 1970 decade to present multispectral remote sensing images taken from the earth been prepared by several satellites like Landsat, ASTER, IRS and so on. These images are widely used in the geographical studies encompass LCLU mapping and change detection (Qin et al., 2013). In LCLU change detection studies a lot of sensor's

images were used, but the Landsat images are particular because they provide the longest datasets of imagery (Abd El-Kawy et al., 2011). The continuity of the Landsat program since 1972 and sufficient spatial resolution as well as its usefulness for large areas make it as a key milestone in the LCLU studies (Abd El-Kawy et al., 2011; Rogan & Chen, 2004). Henceforth, up to the present time, a lot of researches used Landsat images for change detection all around the world (e.g. Canty, Niemeyer, Richter, and Stein (1999); Davids and Doulgeris (2007); Jano, Jefferies, and Rockwell (1998); Matinfar and Roodposhti (2013); Nemmour and Chibani (2010); Ololade, Annegarn, Limpitlaw, and Kneen (2008); Son et al. (2014); Vorovencii (2014); Xiaolu and Bo (2011); Zelinski, Henderson, and Smith (2014); Zhu and Woodcock (2014)).

An adequate understanding of landscape phenomena, imaging properties and methodology employed for information extraction in relation to the aim of analysis are the key factors for successful use of satellite remote sensing for LCLU change detection (Abd El-Kawy et al., 2011; Yang & Lo, 2002). Numerous change detection techniques have been created and developed and many have been summarized and reviewed and used for monitoring changes in LCLU from remotely sensed data, such as spectral mixture analysis, Li Strahler canopy model, image differencing, post-classification comparison (PCC), principle components analysis and vegetation index differencing (Abd El-Kawy et al., 2011; D. Lu, Mausel, Brondízio, & Moran, 2004; Mas, 1999). The PCC method, which is recognize as the most accurate change detection technique, detects LCLU changes by comparing independently produced classifications of images from different dates (Abd El-Kawy et al., 2011; D. Lu et al., 2004; Qin et al., 2013; Yang & Lo, 2002). It can provide a complete matrix of change directions that provide "From - to" change information (D. Lu et al., 2004; Singh, 1989; Yang & Lo, 2002). It has an extra advantage whereupon minimizing the problems associated with multi-temporal images recorded under different atmospheric and environmental conditions (Abd El-Kawy et al., 2011; Singh, 1989). This means images from different dates are distinctly classified and hence, multi-dates images do not need adjustment for direct comparability (Abd El-Kawy et al., 2011; Singh, 1989).

In light of these considerations and based on the important of study area in case of agricultural products, residents, urban expansion and geo-hazards (e.g. floods) some studies have been performed for understanding LCLU changes status. For example, Saghafian, Farazjoo, Sepehry, and Najafinejad (2006) assessed the impact of land use on the floods based on the available maps from 1967 and 1996. They believed that the most changes were happened between ranges and farmlands. Sepehry and Liu (2006) used remote sensing to evaluate the different change detection methods in analysis of land use changes caused by August 2001 flood. They illustrated that among image differencing techniques the Change Vector Analysis method provides best results. Salman Mahini, Feghhi, Nadali, and Riazi (2009) used artificial neural network and post classification comparison to detect tree cover changes in the Golestan province.

They used TM and ETM+ images of 1987 and 2001 and identified forest increased and decreased lands. Their results showed that the tree cover reduction is 59528 hectare while the increase is about 35000 hectare. Furthermore, some studies like Saadat et al. (2011) try to provide a method to create accurate land use land cover maps using ancillary data or Abbaszadeh Tehrani, Makhdoum, and Mahdavi (2011) who provided the land use land cover map of 1998 in Dough watershed for the flood analysis. Nevertheless, in comparison with wide interest in LCLU change detection all over the world, as it is clear few researchers have studied LCLU changes in this region. Moreover, none of these researches did cover entire study area of this research. In addition, they have not recognized changes in a long period comprehensively. Some of them just provide one land cover map or analyze the changes between two dates.

In spite of these studies, the condition and pattern of LCLU changes since 40 years ago were still not completely understand. Hence, it is desirable to carry out a comprehensive LCLU change research to answer related questions. In this study, we attempt to analyze the LCLU changes in the study area from 1972 to 2014 using different sections of Geographic Information Science (GISci).

3.2.   Materials and methods

Change detection of the LCLU provides the substance for better understanding of dealings and interactions between human and environment to better management of the resources, both today and in the future (D. Lu et al., 2004). Change detection studies used remote sensing data as a crucial source of information (D. Lu et al., 2004). Consequently, based on data sources there is various ways to detect changes in the earth surface using imageries. Several change detection methods and algorithms have been developed up to the present time. One of these methods is very common that called PCC method. Since, one of the main goal of our study is detecting the changes among classes and preparing change matrix we choose this method. Classification of the images is the main step in PCC method and we used different ways to classify satellite images. Steps in the detection and analysis of LCLU changes showed in the Fig 3.2.

3.2.1. Study region

As mentioned in the first chapter the study area is located in the northeastern part of Iran and covers an area of 5500 km^2. In addition, for this section, study area buffered using a 1.5 km distance and all the images were subset to this buffer boundary. This buffer covered entire of the study area even in the boundary to have a classification that is more accurate (Fig 3.3).

3.2.2. Data-sets

In selection of appropriate remote sensing images various factors such as complexity of the area, coverage of the study area, study goals and user's requirement and data availability should consider (D. S. Lu, Li, Kuang, & Moran, 2014). Mentioned factors lead us to use Landsat images. Four multi-temporal cloud free L1T Landsat MSS, TM, ETM+ and OLI_TIRS images (Path/Row 162/34) from 1972 to 2014 distributed by the Land Processes Distributed Active Archive Center (LP DAAC) were used as the fundamental data for LCLU classification. In addition, to support the classification some ancillary data were used that can be listed as shown in Table 3.1 along with main Landsat data. In addition, a field trip was carried out to better understanding the study area and collecting GCPs for validation and training samples. In case of Google Earth, Yahoo and Bing satellite images it should be mentioned that in different regions of study area each one provide more up-to-dated images and with better resolution. In this regard, we highly recommend using all of them together simultaneously to increase accuracy.
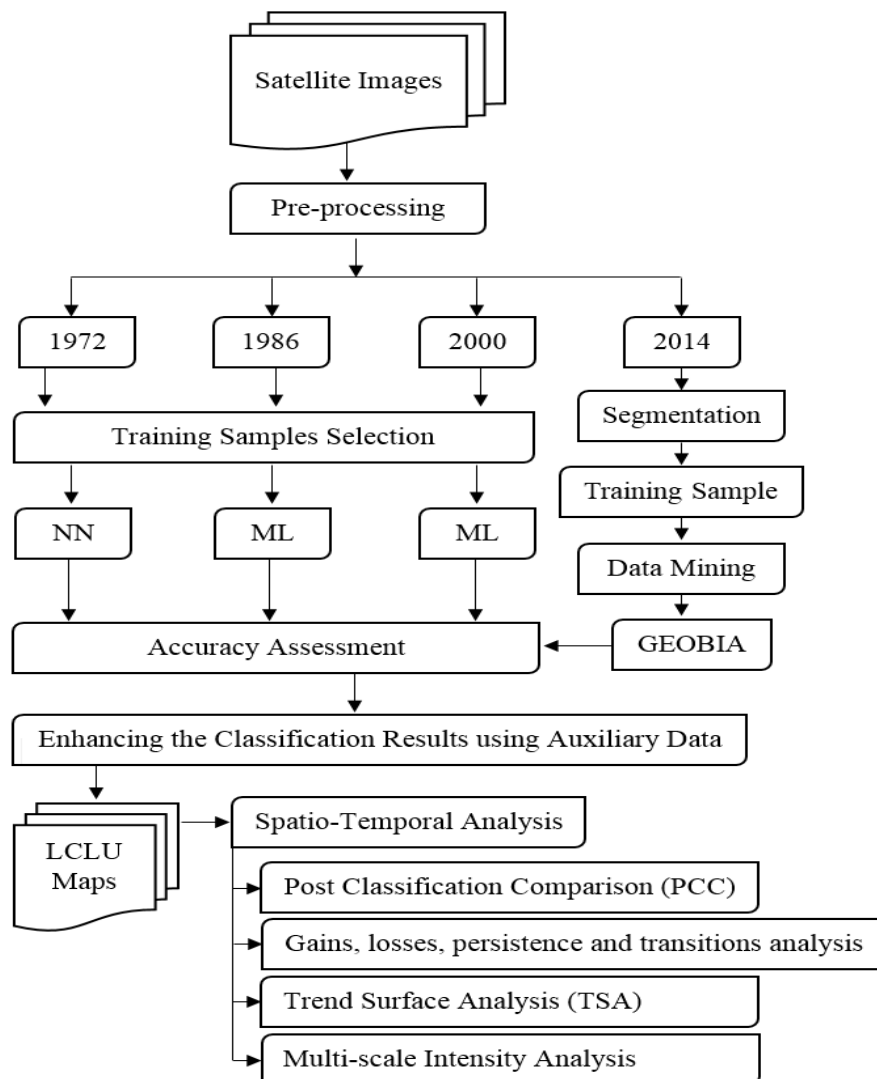
Fig. 3.2. LCLU analysis Methodology flowchart. NN = Neural Network, ML = Maximum Likelihood, GEOBIA = Geographic Object Based Image Analysis.
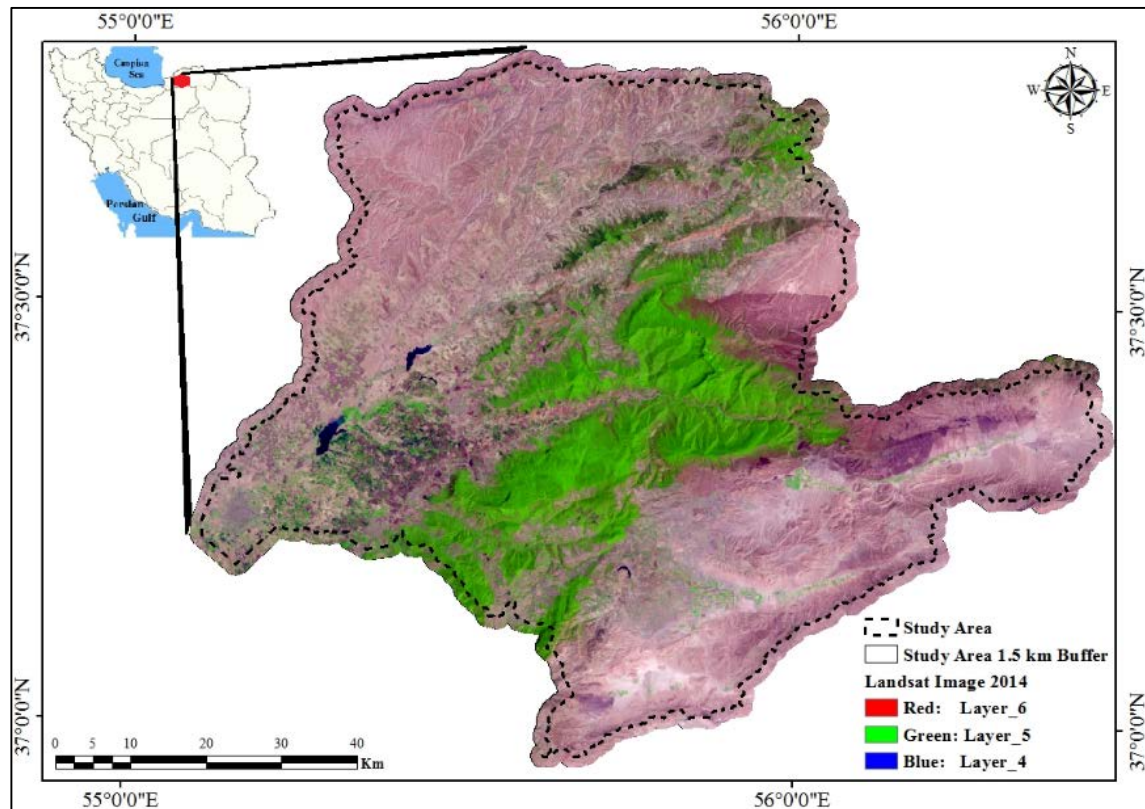
Fig. 3.3. LCLU change analysis area in the northeast of Iran.

Table 3.1. Main characteristics of data used in LCLU change detection

Data Name	Acquisition date	Resolution	Full Area Coverage
Landsat/MSS	1972/09/20	60 m	Yes
Landsat/TM	1986/05/19	30 m	Yes
Landsat ETM+	2000/07/20	30 m (Pan 15)	Yes
Landsat OLI/TIRS	2014/07/19	30 m (pan 15)	Yes
Aster	2001/07/18	15 m	No
CORONA	1970/05/27	~ 2.1 m	No
QuickBird	2005	0.6 m	No
Aerial Photo	1970	~ 1.9 m	No
DEM (Aster)		30 m	Yes
Topographic Map			No
GIS Thematic Maps			Yes/No
Google/Yahoo/Bing historical and up to date images			Yes/No

3.2.3. Image preprocessing and pan-sharpening

The four L1T Landsat images were convert to the radiance and after that reflectance with formula 3.1 and 3.2; more details regards formula can be found in the (Exelis VIS, 2015; USGS, 2013a, 2013b).

$$L_\lambda = Gain * Pixel\ value + offset \qquad (Eq\ 3.1)$$

$$\rho_\lambda = \frac{\pi L_\lambda d^2}{ESUN_\lambda \sin\theta} \qquad (Eq\ 3.2)$$

Where L_λ is radiance in units of watts/ (meter squared * steradian * μm); d is Earth-Sun distance in astronomical unit; $ESUN_\lambda$ is solar irradiance in units of w/(meter squared * μm) and θ is sun elevation in degrees. We also applied dark object subtraction model (Chavez, 1989) as a widely applied methodology on the images to reduce atmospheric effects (Kolios & Stylios, 2013).

Pan-sharpening techniques have confirmed by several researchers that are useful tools to enhance the process and results of image processing and provide better understanding of the observed earth surface (Saadat et al., 2011; Yuhendra, Alimuddin, Sumantyo, & Kuze, 2012). Numerous methods offered for Pan-sharpening of satellite images, for example: high pass filter (HPF), modified intensity-hue-saturation (M-IHS), Ehlers and Gram-Schmidt (GS) (ArcGIS Help, 2014; Yuhendra et al., 2012). GS pan-sharpening method has become one of the most prevalent approaches to pan-sharpening multispectral lower resolution images (Maurer, 2013). Thereupon, imageries of 2000 and 2014 that had pan bands were pan-sharpened with GS pan-sharpening algorithm.

3.2.4. Classification

Since, RS has become a fundamental source of data in geographical studies (e.g. LCLU change researches) various classification methods were developed to extract information from imageries. These methods can be classified in two main sections: pixel based and object based. Pixel based could be unsupervised (based on cluster analysis) or supervised. The latter one can consider statistical algorithm (e.g. Maximum Likelihood) or non-statistical algorithm (e.g. Neural Network, support vector machine and so on) (D. S. Lu et al., 2014). Each of them has their advantages and disadvantages, so we tried them on our images and choose the best output. On other hand, object based classification is more new classification method and overcome some special problems like salt-and-pepper in pixel based classification (Blaschke, 2010). We used pixel-based classification for the 1972 to 2000 images and GEOBIA for the 2014 image.

3.2.4.1.   Pixel-based classification

To recognize LCLU changes obviously it is extremely vital to determine the number of LCLU classes and best way to detect them (Kolios & Stylios, 2013). with this in mind, based on the study area condition and some other researches with Landsat images like Nutini, Boschetti, Brivio, Bocchi, and Antoninetti (2013), Pakhale and Gupta (2010), Yoon, Cho, Jeong, and Park (2003), G. Wu, Gao, Wang, Wang, and Xu (2015) we had choose six classes include: built-up, farmland, bare land, Range, forest and water. These six classes were subsequently used for the both per pixel and object based classification.

For each one of the mentioned classes training areas were carefully selected in the different band combination color composites of each image using different sources

include field GCPs, CORONA, QuickBird and Aster imageries, aerial photos, topographic maps and Google Earth, Yahoo and Bing satellite maps as references. Afterward, the training samples were tested in case of separability to know how well the selected samples are separated. Separation results are between 0-2 for comparison of each couple, which a very good separation is characterized by 1.9-2 and a very low separation is represented with values less than 1 (Kolios & Stylios, 2013).

Supervised classifications using the maximum likelihood, neural network, support vector machine and other classifiers were carried out on the images as soon as classes and training samples were finalized. Then we have checked the accuracy of the classification results based on the overall accuracy and Kappa coefficient to assess the quality of the classified images. For this accuracy assessment, we collect different samples using mentioned auxiliary data sources and used confusion matrix to provide accuracy measurements and then select the best classification output at the end. Table 3.2 presents the selected classifier algorithm for each image.

Table 3.2. Methods of classification selected for each date.

Image	Classifier
1972	Neural Network
1986	Maximum Likelihood
2000	Maximum Likelihood
2014	GEOBIA

For the implementation of the neural network classifier on the 1972 image, we kept constant: the training threshold contribution/rate/momentum/interactions respectively 0.9, 0.2, 0.9 and 1000. In contrast, we tried different activation functions (Logistic and Hyperbolic) and changed the number of hidden layers (one and two according to Kolios and Stylios (2013)). Finally, the combination of the constant elements with one hidden layer and logistic function provides the best result.

3.2.4.2. Geographic Object Based Image Analysis

In the last two decades, advances in earth observation sensors, computer technology and GIS science, led to the development of "Geographic Object-based Image Analysis (GEOBIA)" as an alternative to the traditional pixel-based image analysis method (Addink, Van Coillie, & de Jong, 2012; Gao & Mas, 2008). Ma et al. (2015) believe "GEOBIA is a systematic framework for geographic object identification, which combines pixels with the same semantic information into an object, thereby generating an integrated geographic object". GEOBIA is a newly developed area of Geographic Information Science and remote sensing in which automatic segmentation of images into objects of similar spectral, temporal and spatial characteristics is undertaken (Rabia & Terribile, 2013). In contrast to traditional image analysis, GEOBIA works more similar the human eye–brain combination does (Addink et al., 2012). The latter uses the object's properties such as color, square fit, texture, shape and occurrence to other image

objects and many other properties to interpret and analyze what we see (Addink et al., 2012; Rabia & Terribile, 2013).

3.2.4.2.1. Segmentation

GEOBIA starts by segmenting the image grouping together pixels into objects and next uses a wide range of object properties to classify the objects or to extract object's properties from the image (Addink et al., 2012; Blaschke, Feizizadeh, & Holbling, 2014; Witharana, Civco, & Meyer, 2014). Multi-resolution segmentation is a popular method of segmentation in the remote sensing (Blaschke et al., 2014). To create objects from pixels some parameters are important include: scale, color and shape, while with the shape compactness and smoothness are important too (Dingle Robertson & King, 2011). Normally, in most of studies up to present time, parameter's value selection has been done frequently by trial and error method (Dingle Robertson & King, 2011). We also used ESP tool (Dragut, Tiede, & Levick, 2010) to calculate prefer size for scale parameter. Hence, as well as ESP, different values were tested for them regards to different geographical objects classes and finally scale, shape and compactness optimal selected values were 75, 0.5 and 0.9, respectively. Created objects based on mentioned settings were used for further analysis. For more details on segmentation parameters, we refer the reader to pertinent literature (e.g., Baatz and Schäpe (2000); Blaschke (2010); Lang (2008); Z. Wang, Jensen, and Im (2010)).

3.2.4.2.2. Data mining

Generally, the methodology process is images segmentation, training object sampling, data mining of the samples, evaluation of data mining output, image classification and classification accuracy assessment. The whole process graphically presented in Fig 3.4.
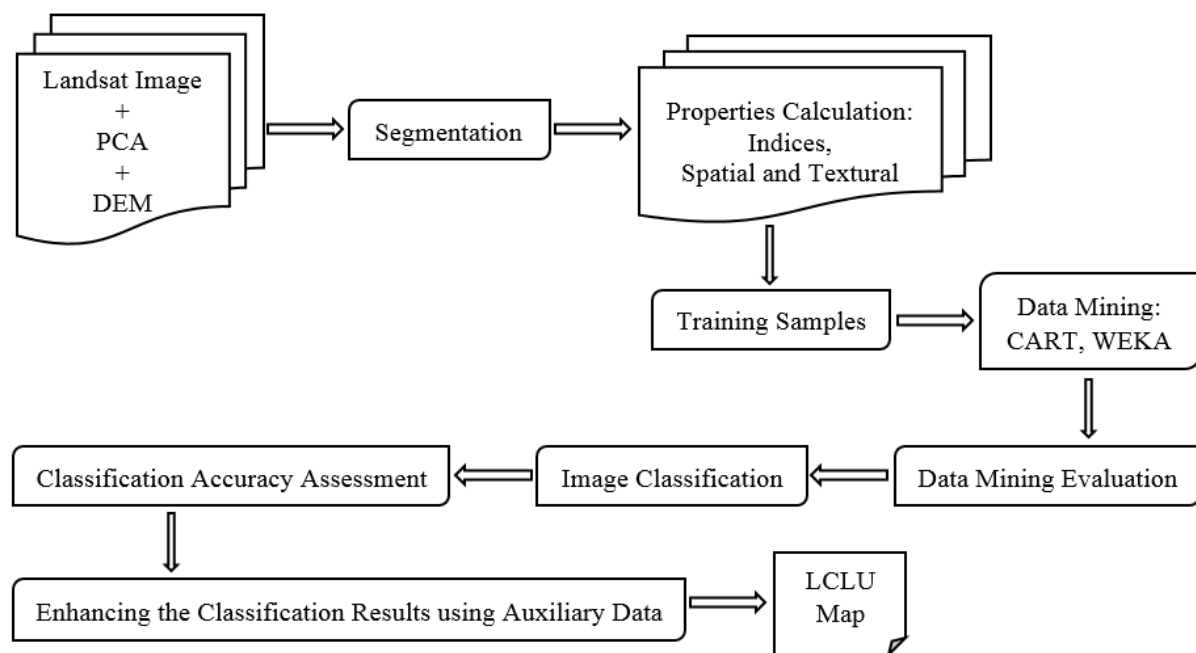
Fig. 3.4. GEOBIA and data mining procedure flowchart

To provide the input for data mining section segmentation were applied on the datasets. Then the data were parameterized based on the requirement of the LCLU classification. In this way to detect different classes in the image and preparing good criteria for data mining process, we were calculated brightness, Max.diff index, principle component analysis (PCA) and different indices contain NDVI, NDGRVI, NDBI, GNDVI, LWM, NDMI and SLAVI from the 2014 image. The slope and aspects were derived from the DEM too. Moreover, we provided different spatial, textural and spectral characteristics of the objects to be used in the data mining process (115 properties). List of the all characteristics of the objects that used in the data mining process are in the Table 3.3.

Table 3.3. List of the properties and indices used in the data mining

Name of Attributes	Name of Attributes	Name of Attributes
Mean and STDDEV of B1	Mean and STDDEV of B5-OVER-B4	Brightness
Mean and STDDEV of B2	Mean and STDDEV of B4-OVER-B6	Max Diff
Mean and STDDEV of B3	Mean and STDDEV of B4-OVER-B5	Modified mean brightness
Mean and STDDEV of B4	Mean and STDDEV of B3-OVER-B4	Elliptic fit
Mean and STDDEV of B5	Mean and STDDEV of DEM	Compactness
Mean and STDDEV of B6	Mean and STDDEV of ASPECT	Width
Mean and STDDEV of B7	Mean and STDDEV of SLOPE	Asymmetry
Mean and STDDEV of B8	STDDEV of area represented by segments	Density
Mean and STDDEV of B9	Length width only main line	Rectangular fit
Mean and STDDEV of PCA1	Relative border to image border	Length
Mean and STDDEV of PCA2	Average area represented by segment	Length width
Mean and STDDEV of PCA3	STDDEV curvature only main line	Average branch length
Mean and STDDEV of PCA4	Length of longest edge (polygon)	Volume
Mean and STDDEV of PCA5	Average length of edges (polygon)	Perimeter (polygon)
Mean and STDDEV of PCA6	Polygon self-intersection (polygon)	Length thickness
Mean and STDDEV of PCA7	Radius of smallest enclosing ellipse	Shape index
Mean and STDDEV of TC Wetness	Area excluding inner polygons	Thickness
Mean and STDDEV of TC Greenness	Length of main line regarding cycles	Number of segments
Mean and STDDEV of TC Brightness	Area including inner polygons	Maximum branch length
Mean and STDDEV of SLAVI[1]	Number of inner objects (polygon)	Area
Mean and STDDEV of NDVI[2]	STDDEV of length of edges (polygon)	Border index

Mean and STDDEV of NDMI[3]	Radius of largest enclosed ellipse	Width only main line
Mean and STDDEV of NDGRVI[4]	Degree of skeleton branching	Compactness (polygon)
Mean and STDDEV of NDBI[5]	Length of main line no cycle	Number of pixels
Mean and STDDEV of LWM[6]	Curvature length only main line	Roundness
Mean and STDDEV of GNDVI[7]	Border Length	Main direction
Mean and STDDEV of B7-OVER-B3	Number of edges (polygon)	

[1.] Specific Leaf Area Vegetation Index, [2.] Normalized Difference Vegetation Index, [3.] Normalized Dry Matter Index, [4.] Normalized Difference Green Red Vegetation Index, [5.] Normalized Difference Build-up Index, [6.] Land and Water Mask, [7.] Green Normalized Difference Vegetation Index.

Afterward the 4495 samples for different classes as bare land, built-up, farmland, forest, range and water were choose to provide classification rule-sets by data miners.

Rule-sets play an important role in classification of remotely sensed data in GEOBIA. The data mining section involves the choice and use of intelligent techniques in order to take out patterns of interest for the effective production of knowledge (Vieira et al., 2012). The term knowledge here understood as behavior patterns for each class of interest. We used two data mining packages WEKA (Hall et al., 2009) and CART (M. G. Dan Steinberg, 2006; P. C. Dan Steinberg, 1997; Leo Breiman 1984) to mining the data and creating rule set.

CART is a nonparametric method that uses a systematic procedure to found ripping rules (Waheed, Bonnell, Prasher, & Paulet, 2006). It includes seven single-variable splitting criteria, called: Gini, Sym-Gini, Twoing, Ordered Twoing, Class Probability for classification trees, Least Squares and Least Absolute Deviation for regression trees and also one multi-variable splitting criterion, the Linear Combinations method (M. G. Dan Steinberg, 2006). The Gini splitting criteria is the default method. Twoing is also a unique procedure of CART that is normally used for computer modeling and is more suitable for classification problems with many classes (M. G. Dan Steinberg, 2006; Waheed et al., 2006). More details of CART could be fined for example in M. G. Dan Steinberg (2006); P. C. Dan Steinberg (1997); Leo Breiman (1984); Salford System (2015); Waheed et al. (2006).

On the other hand, the J48 decision tree algorithm was applied using Waikato Environment for Knowledge Analysis (WEKA) that has a collection of machine learning algorithms for data mining (Biswal, Ghosh, Sharma, & Joshi, 2013; Hall et al., 2009; Sharma, Ghosh, & Joshi, 2013; Vieira et al., 2012). The J48 algorithm is an implementation of C4.5 that select a property to divide the data into two sub groups based on the highest normalized information gain (difference in the concept of information entropy). Procedure replication on each subset will apply until all cases in this subset fit to the same class. As a result, this procedure will create a leaf node in the decision tree (Kramer, 2014; Vieira et al., 2012). More comprehensive details of the WEKA and J48 could be found in the Biswal et al. (2013); Hall et al. (2009); Sharma et al. (2013); Vieira et al. (2012); Waikato (2015).

To found the best knowledge model we evaluated the data mining results. To reach this goal, a standard statistics tool recognized as cross validation were selected. The k-fold cross validation entails separating a dataset into k accidentally complementary

subsets (Vieira et al., 2012). We used 10-fold cross validation among the training samples. In this case, 10 percent of the data are for test and 90% are for training. In addition, other measurements about the accuracy and errors in the data mining were used to approve the data mining results. Afterward, the prepared rulesets by machine learning algorithms were applied on the image. For the purpose of quality assessment, we have checked the accuracy of the classification results based on the overall accuracy and Kappa coefficient. For this accuracy assessment, as pixel based methods we collect different samples using mentioned auxiliary data sources and used confusion matrix to provide accuracy measurements and then select the best classification output at the end.

Although, at the end of classification and accuracy assessment of created LCLU maps the results were acceptable, but using the auxiliary data we tried to increase the quality of classification as much as possible.

3.2.5. Accuracy assessment

As has been noted, accuracy assessment was applied on the LCLU maps produced from pixel based and object based classifications. Kappa coefficient, overall accuracy, producers and user accuracies was calculated for the outputs maps. To calculate these we collect different samples for each class from each image using available auxiliary data sources. For the old-time images include 1972 and 1986 image test sampling was done using CORONA satellite images, aerial photos and old topographic maps. While, in case of images since 2000 to 2014 more than previous sources ASTER and QuickBird images, thematic maps as well as historical and up-to-date Google, Bing and Yahoo satellite images were used.

3.2.6. Land cover/use change analysis

In this research, Post Classification Comparison (PCC) change detection method was applied. PCC is the most obvious method of change detection, which detects changes between determined classes (Madugundu, Al-Gaadi, Patil, & Tola, 2014; Shalaby & Tateishi, 2007). In other words, PCC has been found to offer precise statement of changes in the land and it is frequently rated highly among numerous alternatives such as principle components analysis, image differencing and multi-date classification (Dingle Robertson & King, 2011). In addition, PCC let us to know from-to class changes using provided change matrix (Madugundu et al., 2014). Furthermore, the individual classification of each image decreases the influence of multi-temporal effects because of sensor or atmospheric differences (Madugundu et al., 2014; Shalaby & Tateishi, 2007). In order to apply PCC on the maps we firstly change the maps resolution to the best one (15 m) and clip them with 150 meters smaller buffer of the study area. Then cross-tabulation were applied on the provided LCLU maps of the 1972,

1986, 2000 and 2014 on the pixel basis to create overall change maps as well as matrices of changes.

In addition, gains, losses, persistence and transitions among categories were analyzed to understand the nature and extent of the LCLU changes (Abino, Kim, Jang, Lee, & Chung, 2015). Furthermore, trend surface analysis (TSA) of the changes was used to investigate transitions between classes in different time intervals. This spatial tool, by fitting a polynomial trend surface tries to state underlying pattern of complex changes (Abino et al., 2015). Since there are, six classes and each class could have five maximum number of relations with other categories; we used fifth-order polynomial to improve the visualization of conversions.

3.2.6.1. Intensity analysis

Jinliang Huang, Pontius Jr, Li, and Zhang (2012) and Mallinis, Koutsias, and Arianoutsou (2014) believed even though from-to change matrices and the measures of loss, gain, swap and persistence, make available precious information, they do not make it possible to consider all time points concurrently and thus they do not allow highest understanding of the land surface change process. The multi-scale intensity analysis (Aldwaik & Pontius Jr, 2012) organized into three levels includes interval, category and transition that are in a top–bottom approach (Mallinis et al., 2014; Pontius et al., 2013) (Fig 3.5).
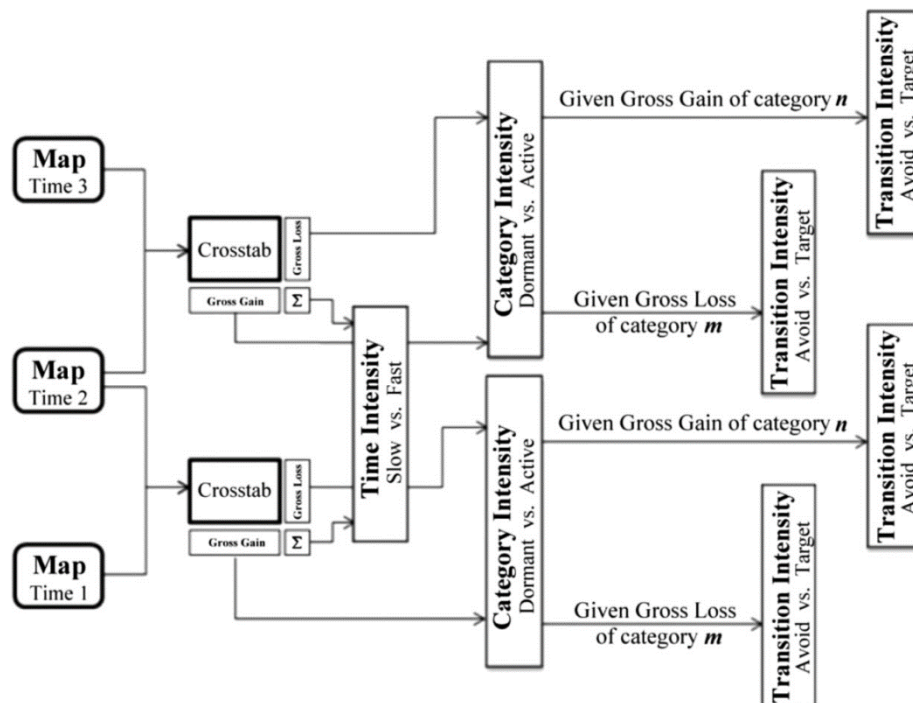

Fig. 3.5. Three level of intensity analysis (Aldwaik & Pontius Jr, 2012)

The interval level assesses variation of the size and rate of changes amongst time intervals. In other words, interval level comparing the observed annual change

intensity S_t (Eq 3.3) during each time interval $[Y_t, Y_{t+1}]$ to a uniform annual change U (Eq 3.4), during the entire extent of the study (Jinliang Huang et al., 2012; Mallinis et al., 2014; Pontius et al., 2013).

$$S_t = \frac{Area\ of\ change\ during\ interval\ [Y_t, Y_{t+1}]}{(Duration\ of\ interval\ [Y_t, Y_{t+1}]) * (Area\ of\ study\ region)}\ 100\% \qquad (Eq\ 3.3)$$

$$U = \frac{area\ of\ change\ during\ all\ intervals}{Duration\ of\ all\ intervals * (Area\ of\ study\ region)}\ 100\% \qquad (Eq\ 3.4)$$

For any specific time interval, category level evaluates how the intensities of change vary between categories and identifying active and dormant categories in each interval (Jinliang Huang et al., 2012; Mallinis et al., 2014). G_{tj} calculates the intensity of a category's annual gross gains as a percent of the size of the category at the end of the time interval $[Y_t, Y_{t+1}]$ (Eq 3. 5). Moreover, intensity of a category's annual gross loss as a percent of the size of the category at the beginning of the time interval is L_{ti}, which were calculated using Eq 3.6 (Jinliang Huang et al., 2012; Mallinis et al., 2014; Pontius et al., 2013). Afterward, the interval-specific uniform hypothesized intensity of change (S_t) should be compared with intensities obtained from equations. This S_t intensity would exist, if the overall interval change had been distributed equally throughout the landscape (Mallinis et al., 2014).

$$G_{tj} = \frac{Area\ of\ annual\ gain\ of\ category\ j\ during\ interval\ [Y_t, Y_{t+1}]}{Area\ of\ category\ j\ at\ Y_{t+1}}\ 100\% \qquad (Eq\ 3.5)$$

$$L_{ti} = \frac{Area\ of\ annual\ loss\ of\ category\ i\ during\ interval\ [Y_t, Y_{t+1}]}{Area\ of\ category\ i\ at\ Y_t}\ 100\% \qquad (Eq\ 3.6)$$

The transition level, which similarly consists of two groups, one group testing intensities of transitions to the specific gaining category and the other assessing intensities of transitions from the particular losing category, evaluates how the intensities of the transition among categories vary at each time interval (Aldwaik & Pontius Jr, 2012; Jinliang Huang et al., 2012; Mallinis et al., 2014). In fact, the transition intensity analysis of the gaining category examines sizes of the transitions of the particular category, given the amount of its gain. In addition, the analysis of the losing category assesses the sizes of the transitions from the losing category relative to the stock of the other categories (Aldwaik & Pontius Jr, 2012; Jinliang Huang et al., 2012; Mallinis et al., 2014).

Transition level concern with four equations. Eq 3.7 gives the declared intensity with which category n obtains from category i and it named R_{tin}. R_{tin} would equal W_{tn} if category n were to acquire with the similar intensity from each not i categories Eq 3.8 (Mallinis et al., 2014; Pontius et al., 2013). Concerning the loss of category m, Eq 3.8 gives the observed V_{tm} intensity of annual transition from category m to category j during interval according to the size of category j at the end of the interval time. Eq 3.10

presents the hypothesized Q_{tmj} uniform intensity of annual transition from category m to every non-m categories throughout every interval dependent to the amount of all non-m categories at the subsequent time point within every time interval (Mallinis et al., 2014; Pontius et al., 2013).

$$R_{tin} = \frac{\text{Area of annual transition from } i \text{ to } n \text{ during interval } [Y_t, Y_{t+1}]}{\text{Area of } i \text{ at } Y_t} 100\% \qquad \text{(Eq 3.7)}$$

$$W_{tn} = \frac{\text{Area of annual gain of category } n \text{ during interval } [Y_t, Y_{t+1}]}{\text{Area of not category } n \text{ at } Y_t} 100\% \qquad \text{(Eq 3.8)}$$

$$Q_{tmj} = \frac{\text{Area of annual transition from } m \text{ to } j \text{ during interval } [Y_t, Y_{t+1}]}{\text{Area of } j \text{ at } Y_{t+1}} 100\% \qquad \text{(Eq 3.9)}$$

$$V_{tm} = \frac{\text{Area of annual loss from category } m \text{ during interval } [Y_t, Y_{t+1}]}{\text{Area of not category } m \text{ at } Y_{t+1}} 100\% \qquad \text{(Eq 3.10)}$$

Moreover, at every levels, the intensity analysis method examines for the stationarity of patterns through time intervals (Aldwaik & Pontius Jr, 2012; Mallinis et al., 2014). Stationarity have different definitions in each level of intensity analysis that could be found in the (Aldwaik & Pontius Jr, 2012; Jinliang Huang et al., 2012). More detailed description and explanation of intensity analysis could be found in Aldwaik and Pontius Jr (2012, 2013); Jinliang Huang et al. (2012); Mallinis et al. (2014); Pontius et al. (2013).

3.3. Results and discussion

3.3.1. Pixel-based classification

Maximum likelihood and neural network classifier algorithms carried out supervised classification of the 1972, 1986 and 2000 images. For evaluation of the classifications, well-distributed random samples points were extracted from Auxiliary data, official maps and Google-Earth, Yahoo and Bing satellite maps. The Fig 3.6 showed the results of 1972, 1986 and 2000 image classifications. In addition, the accuracy assessment results of the presented classifications include kappa coefficient and overall accuracy are summarized in the Table 3.4. Nevertheless, to enhance quality of prepared maps, previously mentioned auxiliary data and visual interpretation were integrated with classification results in the GIS environment.

Table 3.4. Selected classifiers for each image as well as overall accuracy and Kappa coefficient statistics results.

Image	Classifier	Overall Accuracy	Kappa
1972	Neural Network	95.9	0.93
1986	Maximum Likelihood	89.8	0.88
2000	Maximum Likelihood	91.3	0.90
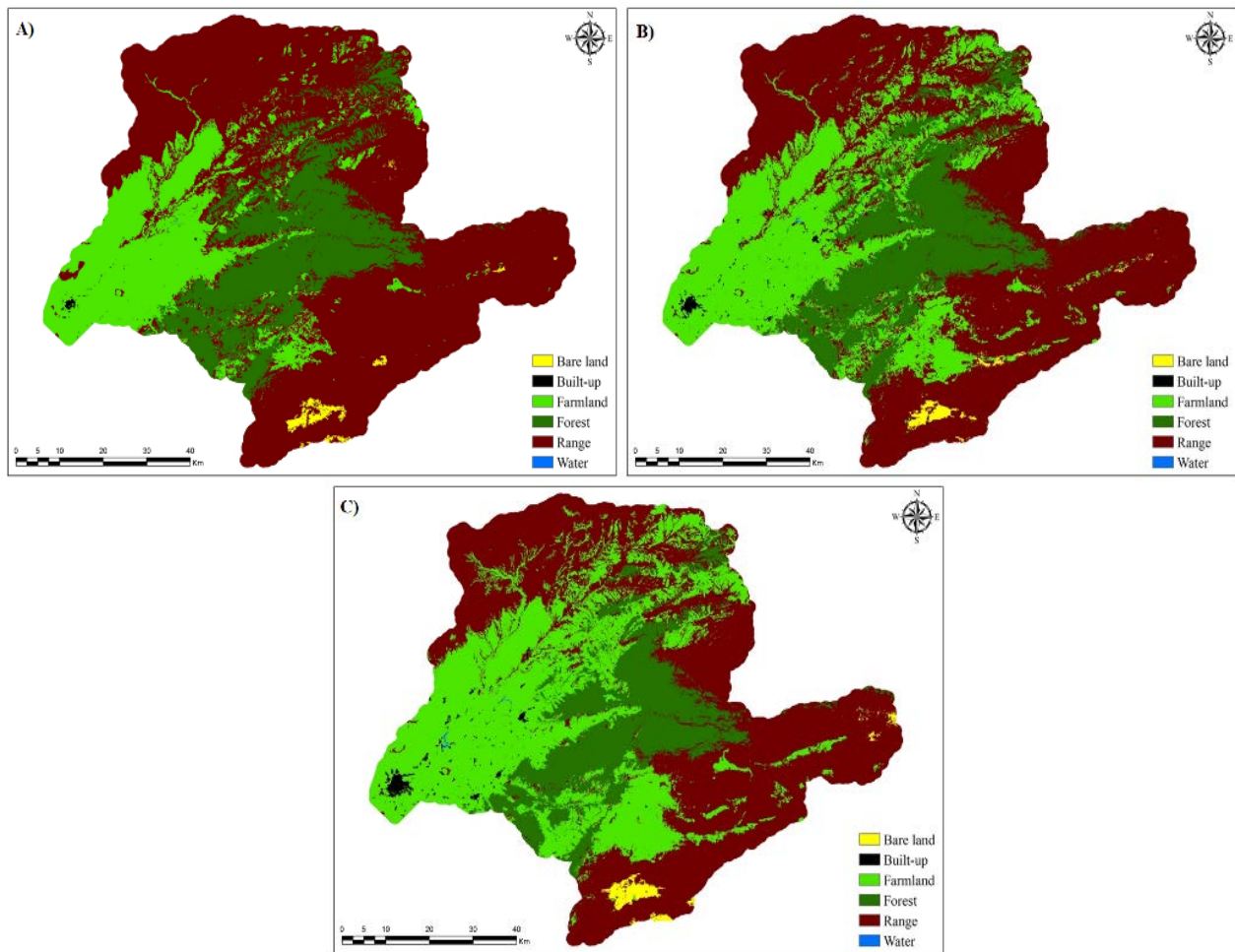
Fig. 3.6. Classification results A) 1972, B) 1986 and C) 2000.

3.3.2. GEOBIA classification

As mentioned before we chose 4495 samples after segmentation and imported them to both CART and WEKA. The data miners processed the data and detected important attributes to building their decision trees. These attributes are listed in the Table 3.5.

Table 3.5. List of attributes used by CART and WEKA

Attributes	CART	WEKA	Attributes	CART	WEKA
STDDEV of B1	✓	✓	Mean and STDDEV of B6	✓	-
Mean of B8	✓	✓	Mean and STDDEV of PCA6	✓	✓
STDDEV of B9	✓	✓	Mean and STDDEV of TC Greenness	✓	✓
STDDEV of PCA1	✓	-	Mean of B3-OVER-B4	✓	✓
STDDEV of PCA3	✓	✓	Mean and STDDEV of DEM	✓	✓
Mean of PCA4	✓	✓	STDDEV of ASPECT	✓	-
Mean of PCA5	✓	✓	Average area represented by segment	✓	-
STDDEV of PCA5	✓	-	Length of longest edge (polygon)	✓	✓
Mean of PCA7	✓	✓	Average length of edges (polygon)	✓	✓
STDDEV of PCA7	-	✓	Mean and STDDEV of NDGRVI	-	✓
STDDEV of SLAVI	✓	✓	Brightness	✓	✓
Mean of NDMI	✓	✓	Max Diff	✓	✓
Mean of GNDVI	✓	✓	Modified mean brightness	✓	✓
Mean of SLOPE	✓	✓	Border Length	✓	-
Mean of TC Wetness	-	✓	Mean of B7	-	✓
Asymmetry	-	✓	Mean of NDVI	-	✓
Mean LWM	-	✓			

Applying Gini and J48 algorithms on the training set data presented in Table 3.3 using CART and WEKA machine learning tools were bring us to decision trees based on attributes listed in Table 3.5. Figs 3.7 and 3.8 show the decision trees generated by CART and WEKA. To have precise decision trees, cross validation were applied on the data mining process. The overall accuracy of the CART and WEKA were 96.21 and 96.92, respectively. As it is clear, the accuracies are good and acceptable and we should just evaluate the results after the applying decision trees on the 2014 image.

Fig. 3.7. Schematic decision tree created using CART data mining.

Fig. 3.8. Schematic decision tree created using WEKA data mining.

After applying the decision trees on the image, we evaluate the results accuracy using test samples and creating confusion matrix. To reach to this goal we collect 150 randomly distributed separate samples for accuracy assessment and test the classification results of both methods with the same sample test collection (the results are presented in the Table 3.6). According to the results, both methods have the same accuracy and both are acceptable. Therefore, the WEKA output was selected and the post processing corrections were applied on it to provide more accurate final LCLU map 2014 (Fig 3.9).

Table 3.6. Overall accuracy and Kappa coefficient statistics of image classification using different data mining methods.

Image	Data Miner	Overall Accuracy	Kappa
2014	WEKA (J48)	94.05	0.9069
2014	CART (GINI)	94.03	0.9072
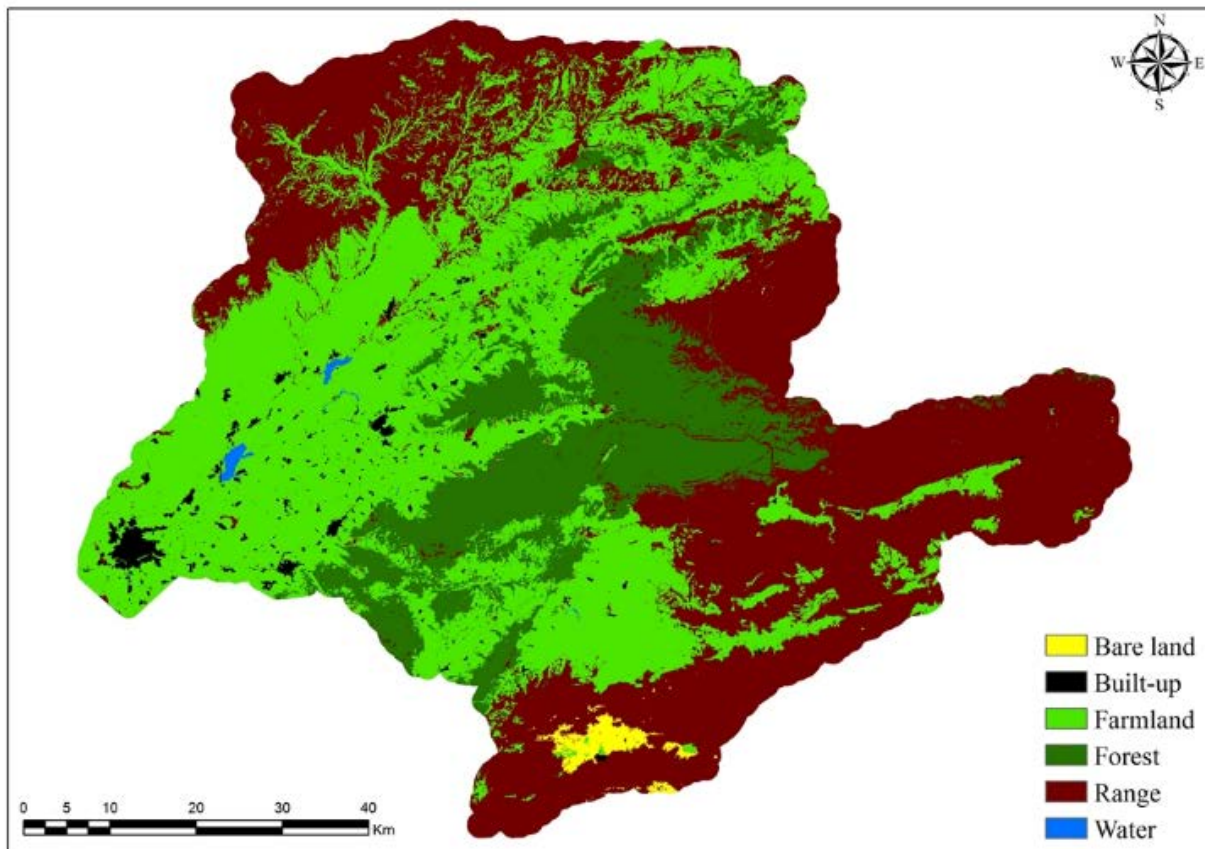
Fig. 3.9. LCLU 2014 classification result

3.3.3. LCLU change analysis

3.3.3.1.   LCLU status and dynamics between 1972 and 2014

The results of the classification process at each year provide an overall estimate of LCLU distribution in the study area. As shown in Figs. 3.6 and 3.9 and can be seen more clearly from Table 3.7 and Fig 3.10 different classes have different area and spatial extent during these years. It is apparent from tables and figures that at 1972, 1986 and 2000 the rangeland is dominant land cover with ~60%, 50% and 45% area, respectively. Farmland and forest as the most expanded land covers have follow range LC during 1972 to 2000. From the chart, it can be seen that there is a significant difference between 2014 and past dates, because no more the ranges are the most dominant land cover and replaced by farmland (40%). In 2014, farmlands followed by range and forest respectively. While, in the whole dates the water and built-up land covers are the smallest classes (maximum 1.45% and 0.19%).

Table 3.7. Summary of class's surface areas per hectares and percent of the total area in different years.

LCLU class	1972		1986		2000		2014	
	Area (ha)	(%)	Area (ha)	(%)	Area (ha)	(%)	Area (ha)	(%)
Bare land	4,404.78	0.70	4,084.52	0.65	5,759.80	0.92	4,305.24	0.69
Built-up	819.07	0.13	2,646.88	0.42	5,050.67	0.81	9,057.29	1.45
Farmland	125,379.09	20.02	182,633.27	29.16	224,809.31	35.90	255,753.59	40.84
Forest	122,614.20	19.58	119,333.86	19.06	106,020.83	16.93	106,267.82	16.97
Range	372,998.45	59.56	317,440.78	50.69	284,351.40	45.41	249,663.40	39.87
Water	20.57	0.00	96.95	0.02	244.28	0.04	1,188.97	0.19

Afterward, spatial analyses were implemented on the created LCLU maps to provide more detailed information about LCLUCs in study area among different classes and the change and persistence lands (Fig 3.11). To better understanding of changes, Fig 3.12 presents the summary of class's changes during the study period. The graph shows that there has been a steep decrease and increase in the rangelands and farmlands, respectively. The rangelands reduced from 372 thousand hectares to less than 250 thousand hectares. Whereas, farmlands from 125 thousand hectares reached to more than 255 thousand hectares. It also reveals that forests suffer from a decreasing gradual change until 2000 (lost ~ 17000 hectares); while since 2000 to 2014 it experienced a slow increase (something less than 250 ha). On the other hand, on small categories built-up and water classes increased too. Built-up increased 11 times since 1972 and now is about 9000 hectares and water class with areas 1200 hectares in 2014 experienced a 57 times increase from 1972. Finally, bare lands experienced some fluctuations and after these 42 years are approximately same.
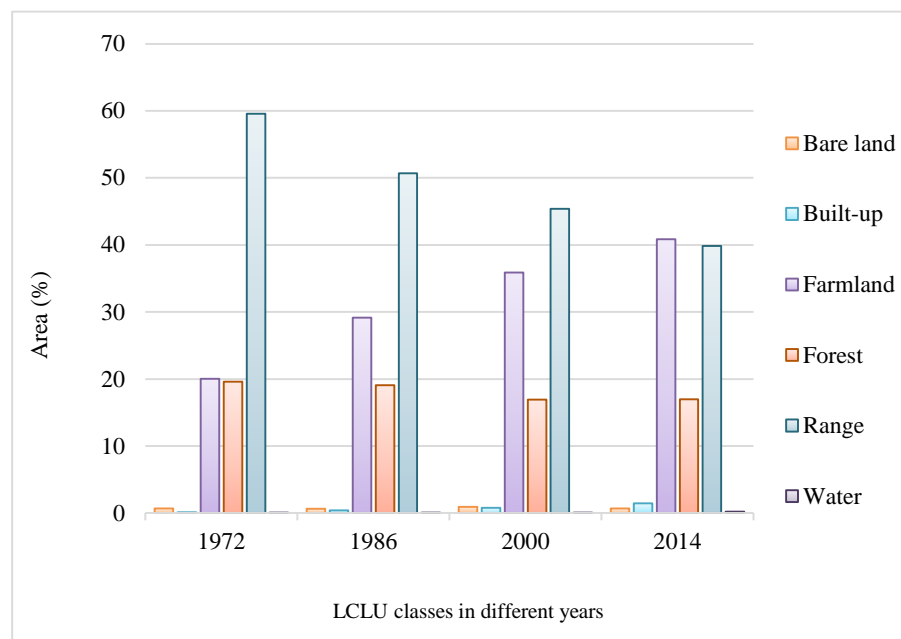
Fig. 3.10. Area of LCLU classes for different dates.

However, all previously mentioned changes are among one class. Transformation of LCLU changes as gains and losses between classes are presented in Fig 3.13 and Tables 3.8-3.10 as transition matrixes. Gains are presented by positive value, while losses are showed by negative rates. As shown in Fig 3.13, major substitutes per hectares contain gains of farmland and losses of the range class. Whereas, in change percentage graphs, water and built-up have the most gains, and built-up and farmland have the minimal losses.
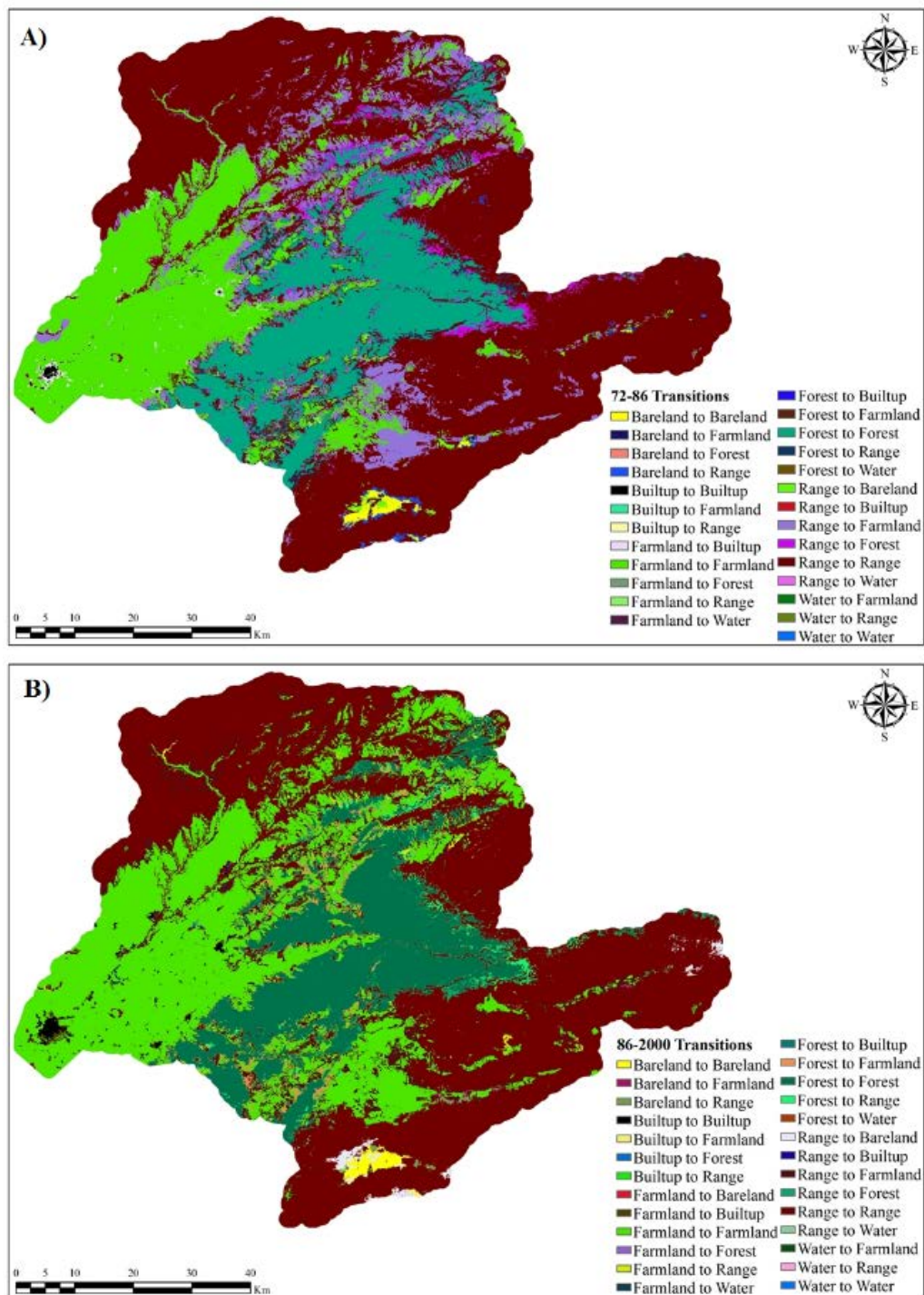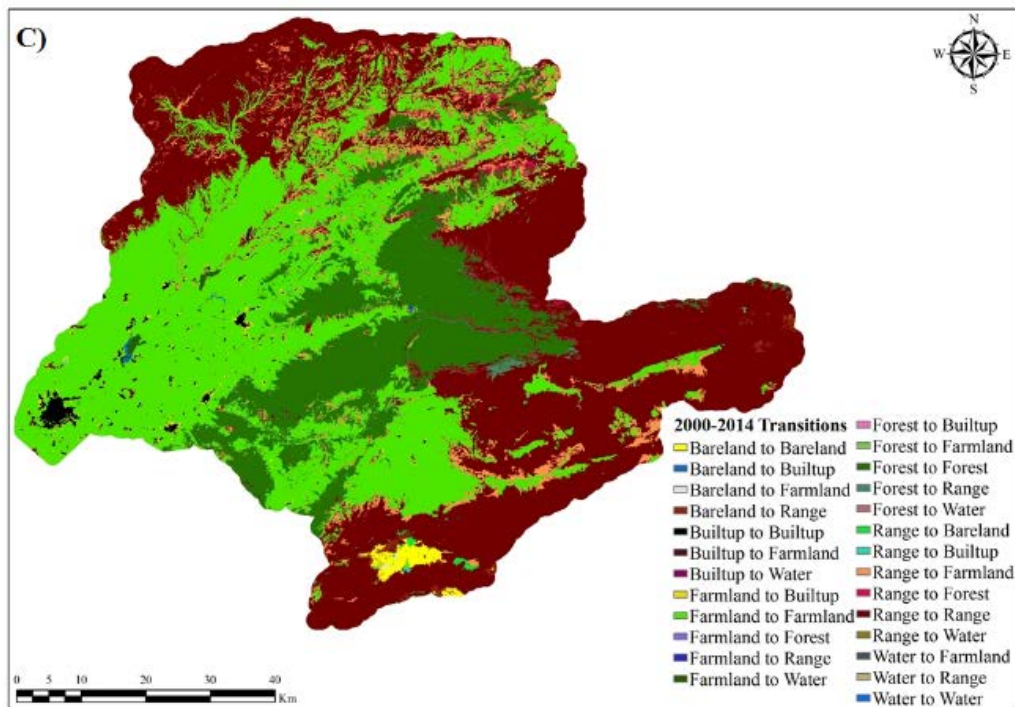
Fig. 3.11. LCLU persistence and changes during time. A) Transitions from 1972 to 1986, B) Transitions from 1986 to 2000, and C) 2000-2014 transitions.

From 1972 to 1986, rangeland as the biggest class was largely converted into farmland class (~ 50000 ha) in the north and south of the Golestan national park and forest (~ 5000 ha). The latter conversion could be related to establishing Golestan national park in 1976 and providing different resource of energy for the local population. Nevertheless, more than 8000 ha of the forest class during these years converted to farmlands too that are near the built-up areas are and flat regions, predominantly. Farmland class conversion was primarily to built-up (about 1600 ha) and then water (72 ha) Land cover up that are concentrated in the plain section of the region. However, the expansion of built-up area is not just limited to farmlands, ant it takes 169 ha from ranges and 15 ha from forest during 1972 to 1986. All things considered, range to farmland is the largest transformation and the farmlands had the biggest gains from other classes.

From 1986 to 2000 same as before, range and forest classes were primarily converted to farmland (~ 35000 ha and ~8500 h, respectively), and a part of farmlands subsequently converted into built-up (1877 ha). In comparison to the first period, transition from range to farmlands reduced. Vice versa, transition from forest to farmlands did not reduced. At the same time, built-up and water areas increased gains from range and farmland categories (~ 350 and 70 ha) respectively. It should be mentioned that, range category as the biggest loser gains around 5000 hectares from forests.
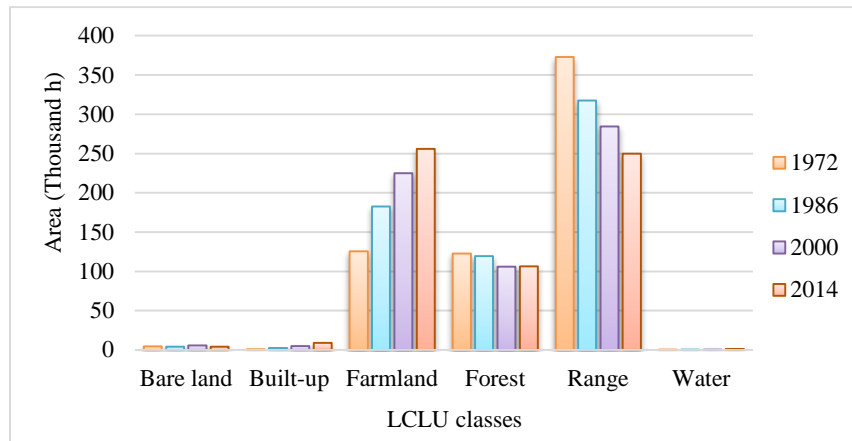
Fig. 3.12. LCLU classes' area changes during time.

Table 3.8. Transmission matrix of LCLU (hectares) over the 1972 to 1986 period.

1972/1986	Bare land	Built-up	Farmland	Forest	Range	Water
Bare land	2,412.90	0.00	97.92	1.46	1,892.49	0.00
Built-up	0.00	813.10	4.36	0.00	1.59	0.00
Farmland	0.00	1,647.85	121,218.54	250.29	2,188.66	73.68
Forest	0.00	14.89	8,672.58	105,659.64	8,263.12	3.96
Range	1,671.61	171.00	52,638.18	13,422.46	305,094.69	0.49
Water	0.00	0.00	1.58	0.00	0.18	18.81

In 2000 to 2014 period, as the same as two previous interval, the most obvious transition happened in range, farmlands and forest. The conversion from range to farmland does not have a tangible reduction as the first to second date and it is just 1/3 of it. While, built-up category have a considerable expansion about 1600 ha that gain from farmland and range category. Likewise, water category gains about 900 ha mostly from farmlands.
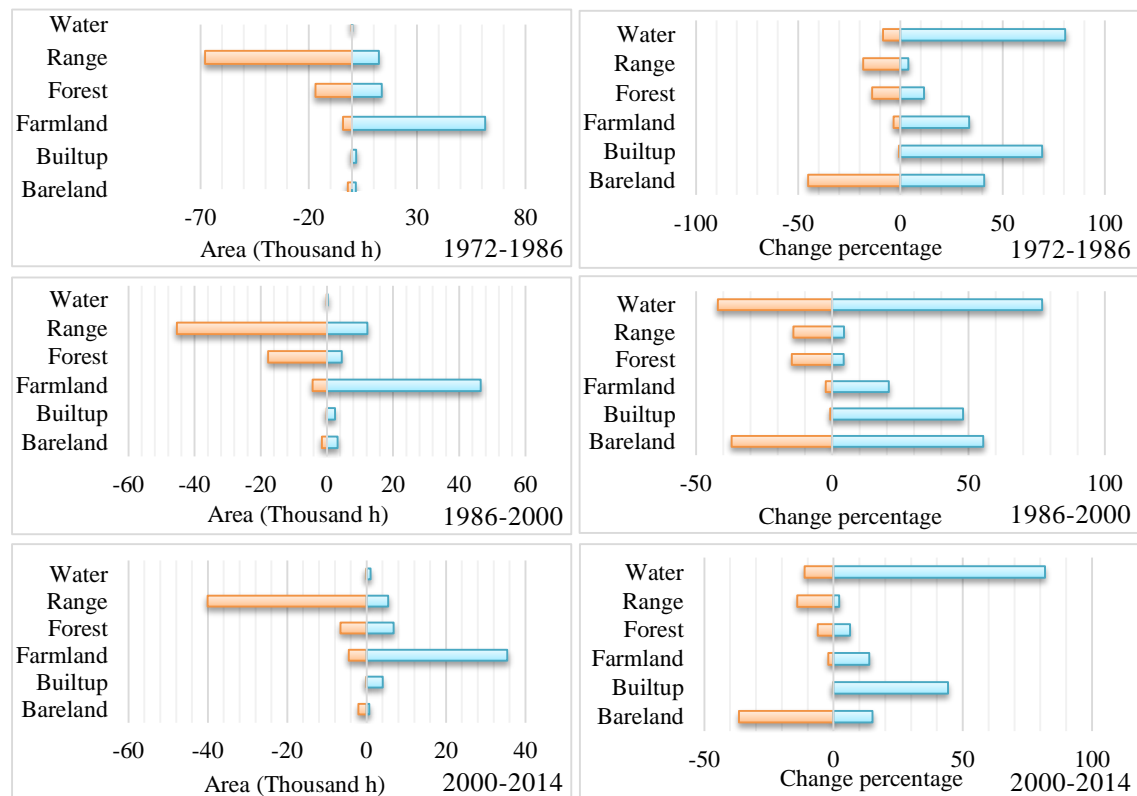
Fig. 3.13. Gains and losses in land cover classes by area (ha), 1972-1986, 1986-2000 and 2000-2014.

Table 3.9. Transmission matrix of LCLU (hectares) over the 1986 to 2000 period.

1986/2000	Bare land	Built-up	Farmland	Forest	Range	Water
Bare land	2,574.05	0.00	250.02	0.00	1,260.45	0.00
Built-up	0.00	2,626.99	19.40	0.05	0.45	0.00
Farmland	1.19	1,896.86	178,317.59	241.74	1,998.20	177.68
Forest	0.00	0.79	8,759.79	101,589.62	8,983.62	0.05
Range	3,184.56	525.98	37,423.89	4,189.43	272,106.61	10.31
Water	0.00	0.00	38.63	0.00	2.07	56.25

Table 3.10. Transmission matrix of LCLU (hectares) over the 2000 to 2014 period.

	Bare land	Built-up	Farmland	Forest	Range	Water
Bare land	3,654.56	8.89	122.83	0.00	1,973.52	0.00
Built-up	0.00	5,041.91	1.06	0.00	0.00	7.70
Farmland	0.00	3,431.99	220,323.20	18.65	131.45	904.05
Forest	0.00	1.76	3,265.58	99,467.51	3,285.97	0.02
Range	650.68	572.74	32,013.77	6,781.66	244,272.30	60.28
Water	0.00	0.00	27.18	0.00	0.18	216.92

Must be remembered, albeit LCLU changes are important but areas where no changes happened and known as persistence should be considered (Abino et al., 2015). To aid in the understanding the persistence lands a graph (Fig. 3.14) was created based on the persistence maps. Fig 3.14 revealed that percent of unchanged areas in the range

and forest categories reduced during these 42 years. While, the other categories and the total status show more stable LCLUs from past to present. Abino et al. (2015) and Rogan and Chen (2004) believed visual interpretation of LCLU conversions and persistence maps can be challenging if the place of changes are not bunched. In this regard, spatial trend of change analysis could be very useful. Regarding the major conversion among classes, 10 TSA map for each time interval were created.
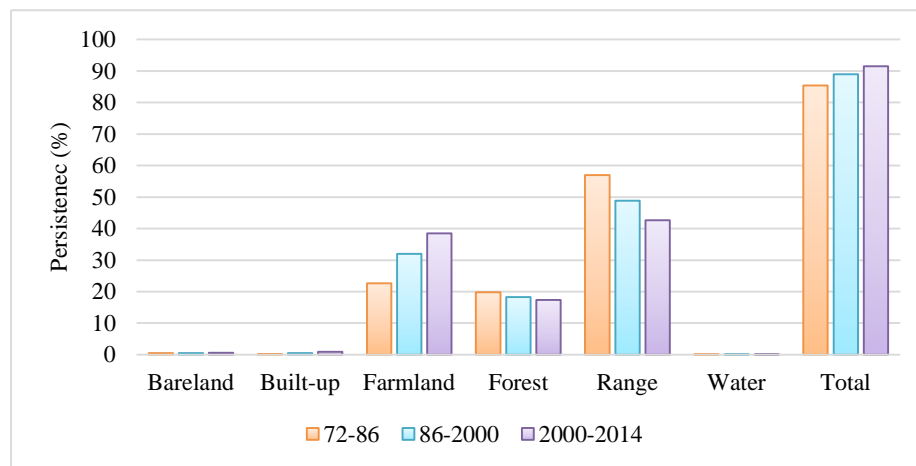
Fig. 3.14. Persistence lands per class and totally over 1972 to 2014 period.

The TSA maps are range, forest, farmland and bare land to all other classes and transitions from all classes to each of the categories separately (Figs 3.15-3.17). These maps simulate the generalized location of conversion among LCLU of interest and other categories.
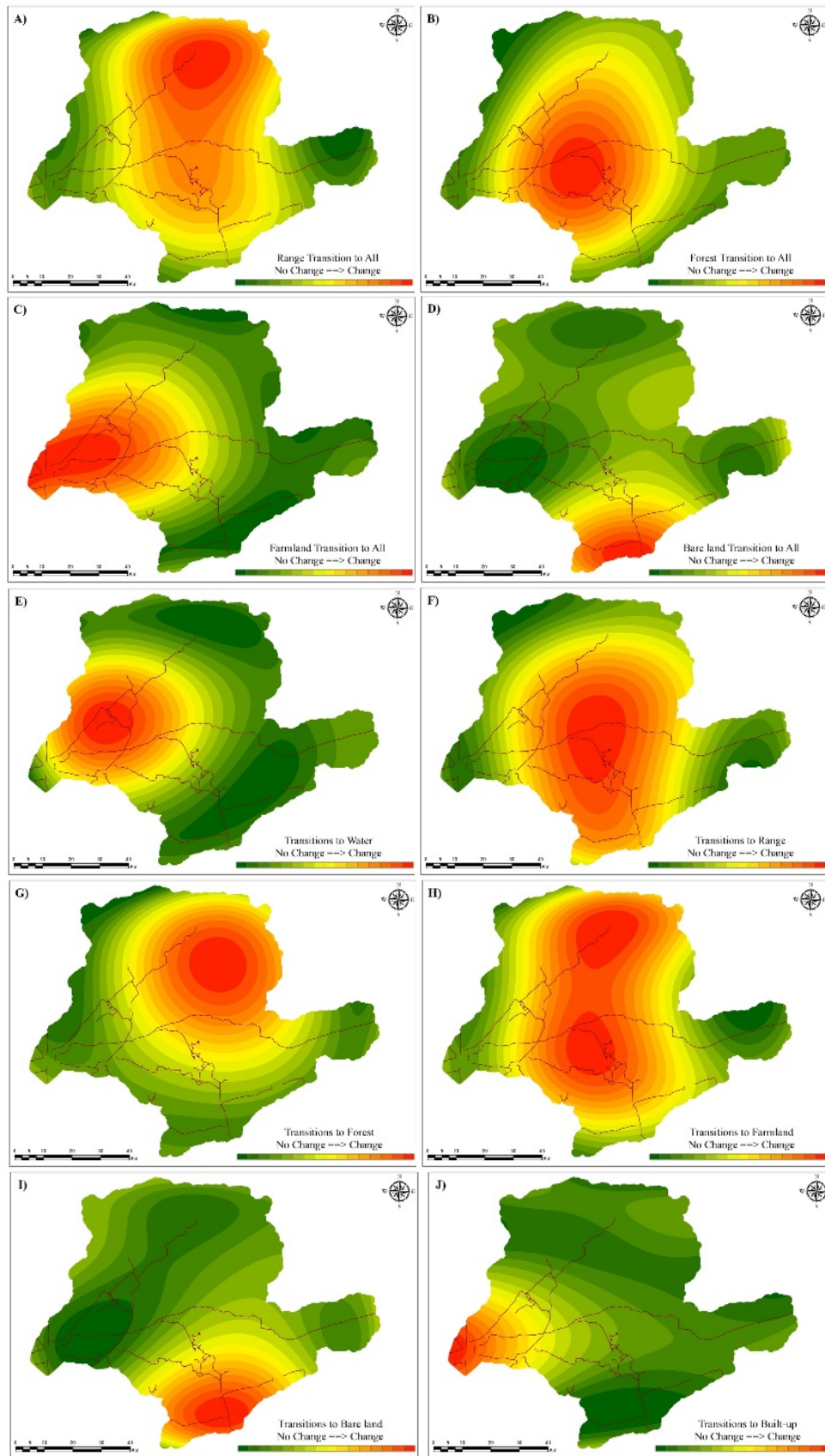
Fig. 3.15. Trend surface analysis of major transitions between LCLU categories in 1972 to 1986 and main road network. A) Range Transition to all, B) Forest transition to all, C) Farmland dtransition to all, D) Bare land transition to all, E) Transition to Water, F) Transition to Range, G) Transition to Forest, H) Transition to Farmland, I) Transition to Bare land, J) Transition to Built-up.

The maps are presented by colors from green to red that means a range from no-change to change. From the Fig 3.15, (A) and (F) we can see that range are affected in the north to the center of the region, while based on parts (D) and (I), the bare lands conversions are mostly concentrated in the south. (B) and (G) sections shows forests lost in the center of the area and gains in the northeast part. Built-up transitions are mostly in the low lands and in western part. Farmlands decreased in the low lands mostly by the built-up and water class in the east and center. Based on the (H), farmlands in a big area in the center to the north and south borders.

LCLU transition trends from 1986 to 2000 are presented in Fig 3.16. The range transition is approximately the same with previous date but in the (B) image, the forest hot spot of trends moved northwards. In the (C) image farmlands transitions increased in the northeast and the range of the bare lands changes extend in the south. Transitions to water are limited and transition to range moved eastwards. Forest trend did not change a lot but the farmlands that had to hot spots are joined together and create a more concentration in north direction. Finally, trends in (I) and (J) images remained approximately unchanged.

Fig 3.17 presents the LCLU conversion trends from 2000 to 2014. In (A) image, range transition hot spot moved northeastwards and have less contribution in the center and south parts. In the (B), Forest transitions focused more in the center. In (C), farmlands hot spot moved to the center of low lands. In (D), extend of the bare lands reduced and in (F) the extent and amount of transition of ranges reduced too. In (E) water conversions is almost similar with past. In (G) and (H), trends experienced a retreat from the center and moved to northeast and north, respectively. In addition, trends in (I) and (J) are the same as before just (J) have a west-east expansion in the center of transitions.

Fig. 3.16. Trend surface analysis of major transitions between LCLU categories in 1986 to 2000 and main road network. A) Range Transition to all, B) Forest transition to all, C) Farmland dtransition to all, D) Bare land transition to all, E) Transition to Water, F) Transition to Range, G) Transition to Forest, H) Transition to Farmland, I) Transition to Bare land, J) Transition to Built-up.
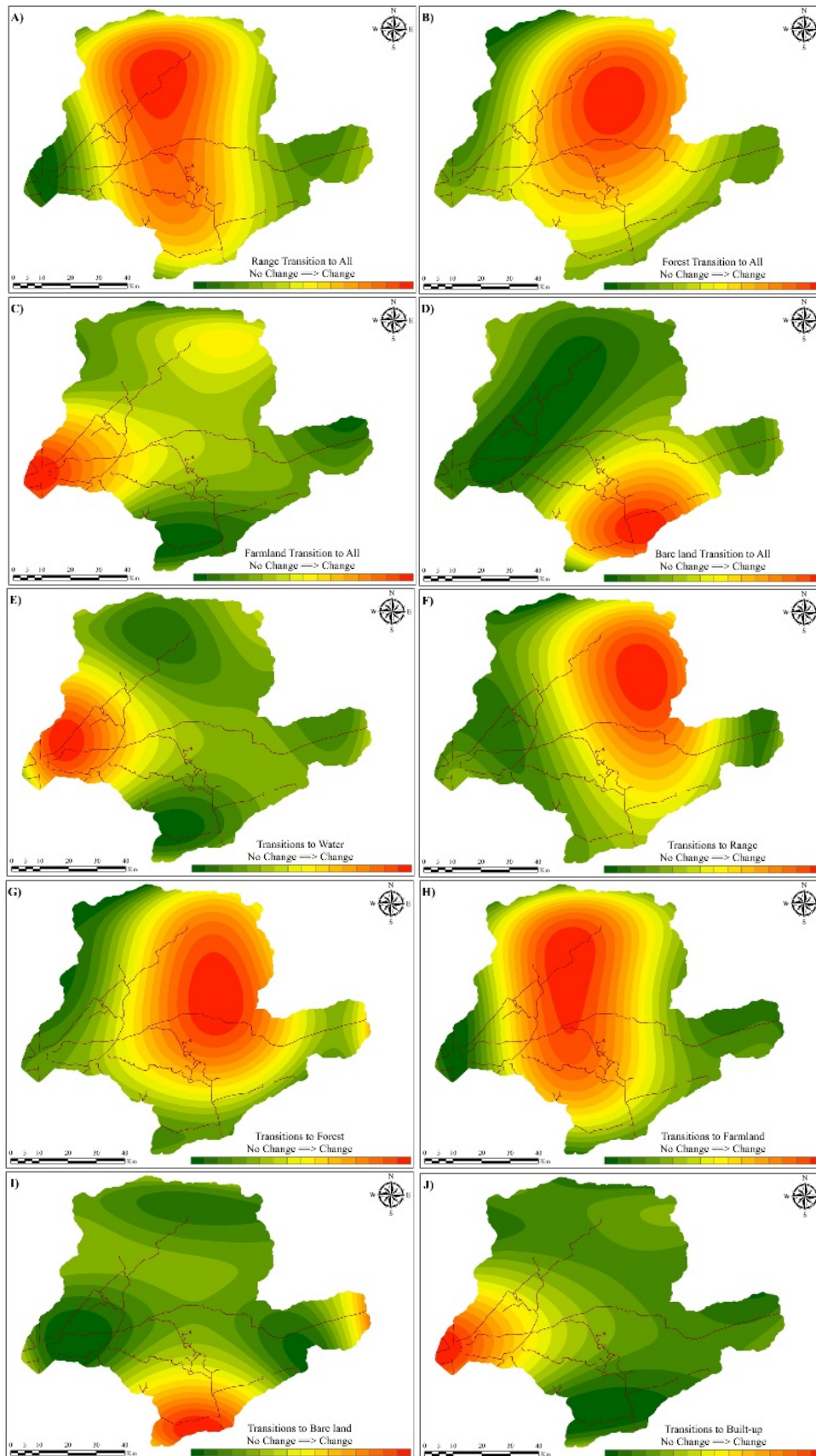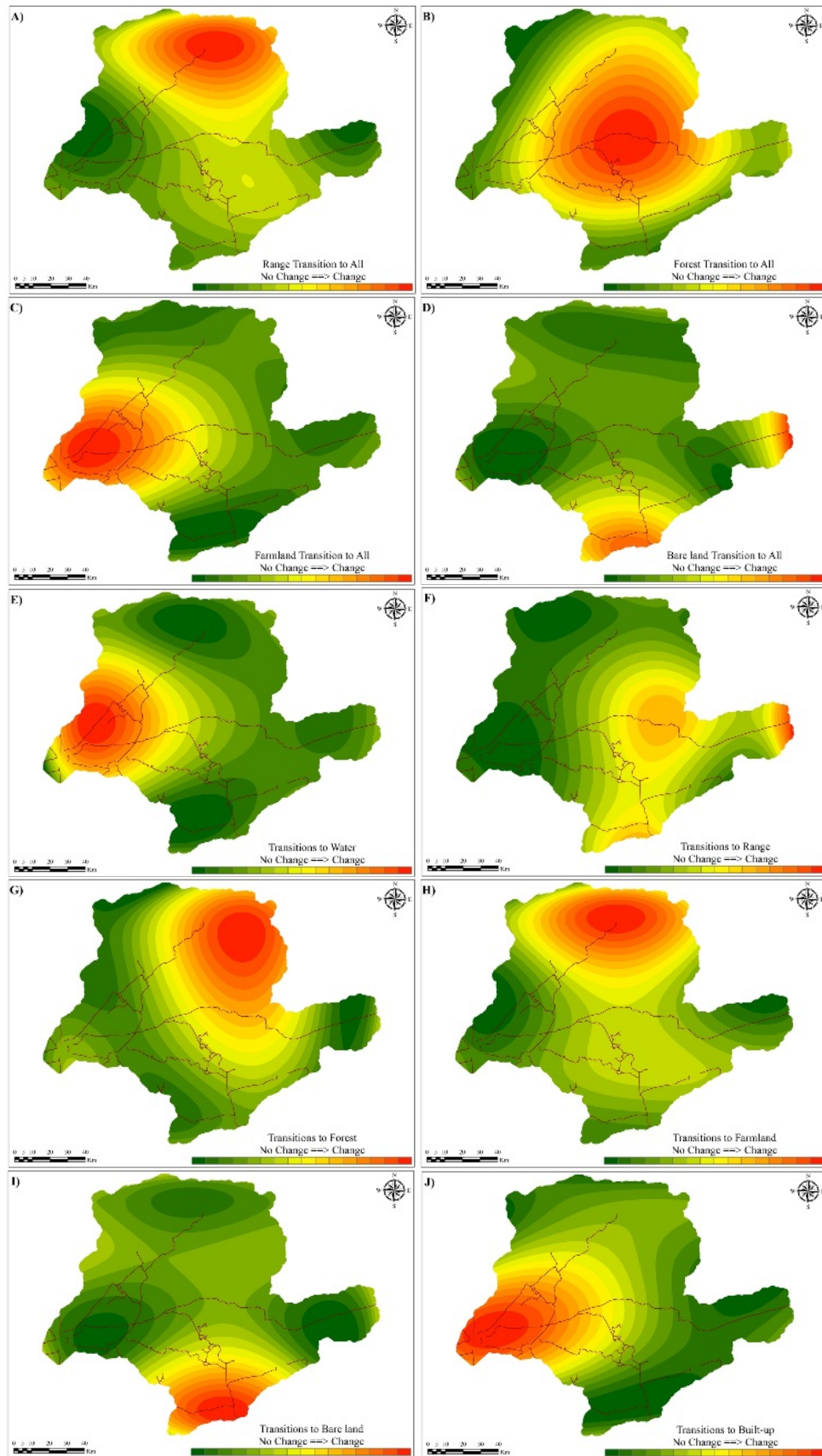
Fig. 3.17. Trend surface analysis of major transitions between LCLU categories in 2000 to 2014 and main road network. A) Range Transition to all, B) Forest transition to all, C) Farmland transition to all, D) Bare land transition to all, E) Transition to Water, F) Transition to Range, G) Transition to Forest, H) Transition to Farmland, I) Transition to Bare land, J) Transition to Built-up.

3.3.3.2.   LCLU intensity analysis

Intensity analysis is an accounting framework that computes intensity of changes among LCLU types (Aldwaik & Pontius Jr, 2012; Enaruvbe & Pontius, 2015). The ratio of the amount of a conversion to the size of LCLU type that is involved in the conversion is called Change intensity (Enaruvbe & Pontius, 2015). Fig 3.18 shows the interval level intensity analysis results. According to threshold of Uniform Intensity (UI) that is 0.81% of the annual rate of change, 1972-1986 is the fastest time interval and the annual rate reduced in the two next time interval so that its reach to 0.61%. This means that changes are not stationary at this interval analysis.
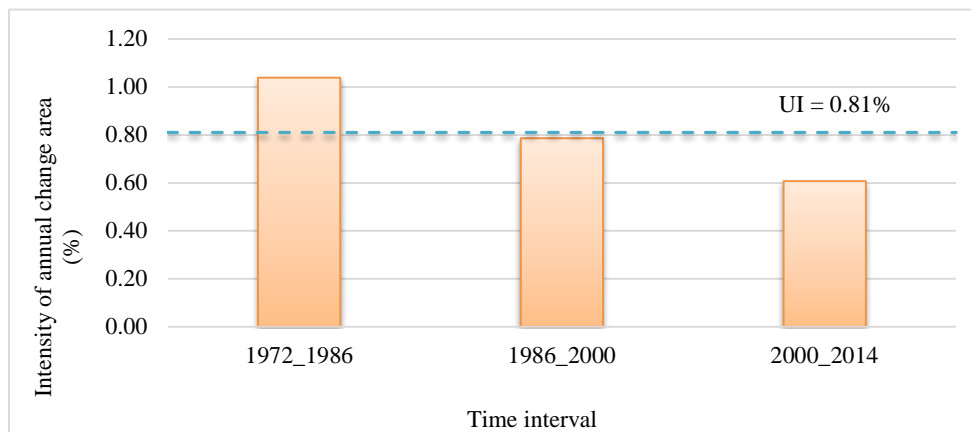
Fig. 3.18. Intensity analysis for three time intervals: 1972-1986, 1986-2000 and 2000-2014. Columns show annual area of change's intensity during each time interval.

The next step in intensity analysis is the category level. In the category level the UI value for first, second and third time intervals were 1.04%, 0.79% and 0.61% respectively. In all three periods, bare land, built-up, farmland and water gains are relatively active compare to uniform intensity but with some difference patterns in value of intensity. Bare land (~3% to ~1%), built-up (~5% to about 3%) and farmland intensity (2.40% to 0.99%) reduced. While, water intensity is almost stable with some increase from 5.76% to 5.84%. In contrast with mentioned class, gains of forest and range categories are relatively dormant compared to uniform and this condition increased during the time. Based on the Aldwaik and Pontius Jr (2012) in case of stability or in other word stationarity of categories, bare land, built-up, farmland and water are stationary in terms of gains.

In the same fashion losses intensity are presented in Fig 3.19. In first interval, bare land and range are active losers and other classes are relatively dormant in loss intensity. In 1986-2000 period, forest and water joined to range and bare and active loser classes reached to four, whereas built-up and farmland are dormant. Bare land, range and water are three relatively active losers in the third time interval. In this interval, forest, farmland and built-up are relatively more dormant, respectively. Nevertheless, for the

category level intensity analysis of losses the bare land and range categories are stationary.
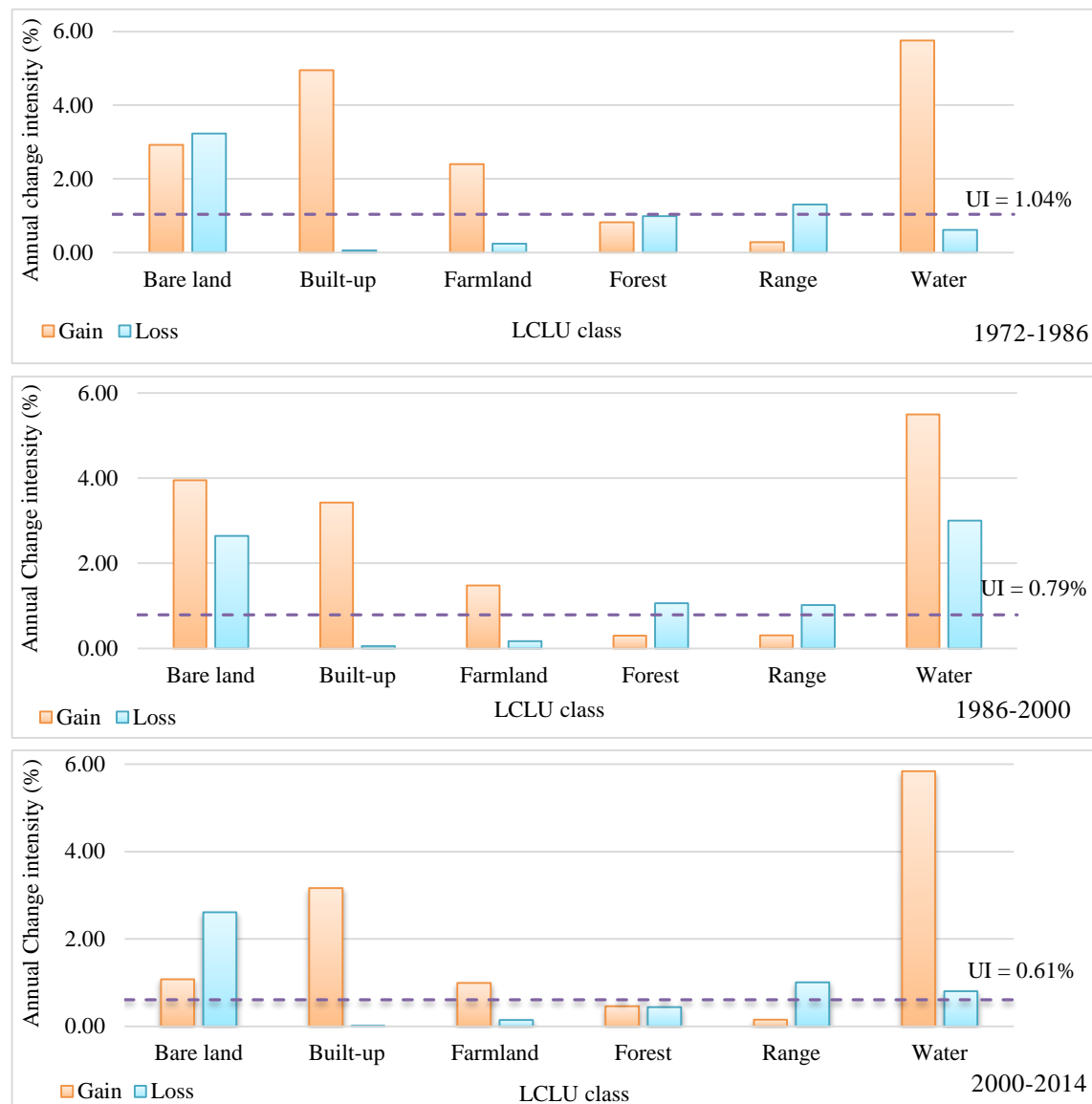
Fig. 3.19. Category intensity analysis in three time intervals: 1972-1986, 1986-2000 and 2000-2014. Columns show intensity of annual gain and losses within each category.

Analysis of intensity of transition level among the LCLU classes is more complicated than two previous level. In three interval dates, some targeting and targeted groups did not change: transitions to bare land, built-up, forest and water are stationary, from range (intensities during three dates = 0.03, 0.07 and 0.02 percent), farmland (0.09, 0.07 and 0.11 percent), range (0.26, 0.09 and 0.17 percent) and farmland (0.0, 0.01 and 0.03 percent) respectively. Transitions to farmland and range vary during the time so for better understanding the intensities graphs are presented in the Fig 3.20.
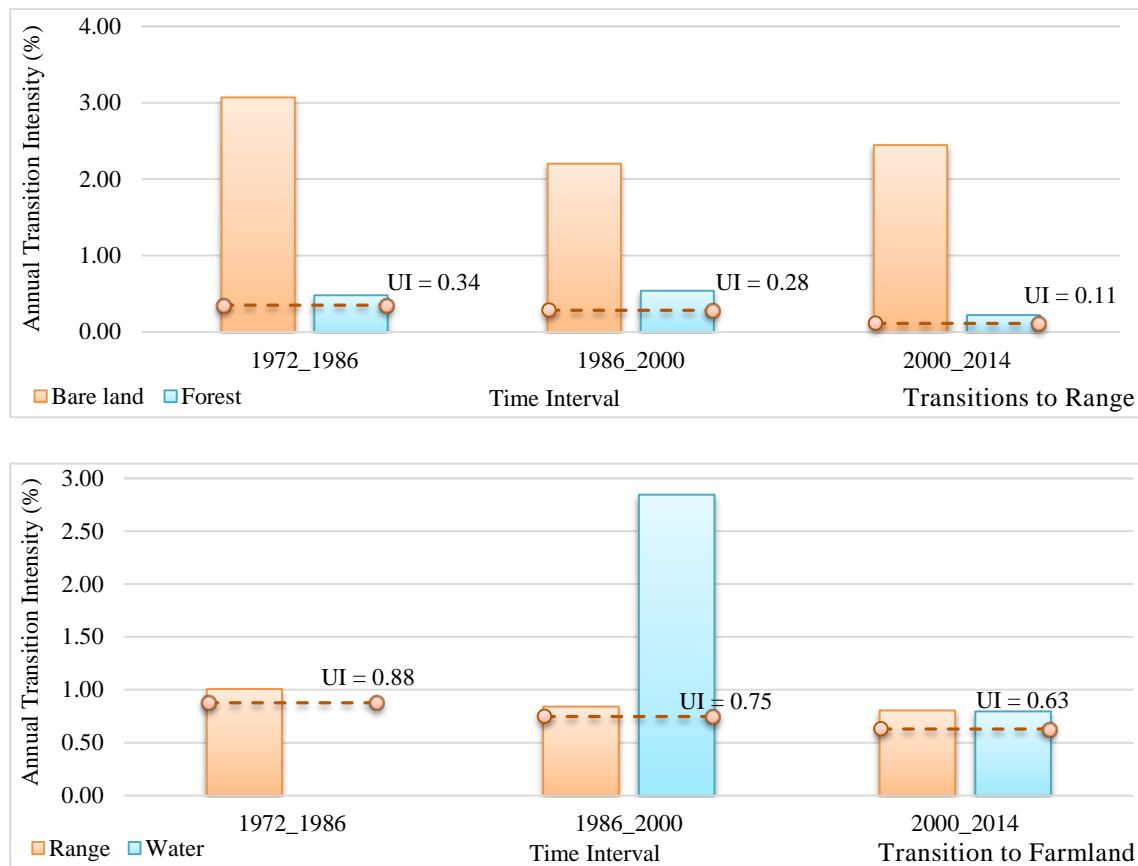
Fig. 3.20. Intensity analysis of transitions to range and farmland categories during three intervals. Columns show intensity of annual transitions in related categories.

Fig 3.20 presents the active classes in transition level analysis for range and farmlands. Range mostly gains from bare land and forest categories and the intensity of transition in both of these classes are reduced, but the bare land is more targeted by the range for gains. In addition, both transitions from bare land and forest to range are stationary too. Transitions to farmland are from range and water classes but just transitions from range are stationary. In 1972-1986 period, the farmlands just targeted the range but this category start to gain from water class too.

Analysis of transitions from each categories to other shows that in bare land category transitions are stationary to range and intensities are 0.04%, 0.03% and 0.06% during 1972-1986, 1986-2000 and 2000-2014, respectively. Transition from built-up is just to water in 2000-2014 and is not stationary. Transition from water is to farmland and is stationary but the intensity is zero. Presentation of transition intensity analysis from range, forest and farmland to other categories as can be seen from Fig 3.21 show that ranges loss lands to bare land and farmland categories intensively and with stationarity, but this intensity is reduced. Forest losses are stationary to the farmland, but water and range classes gain from it in 1972-1986 and 2000-2014. In other words, farmlands gains permanently from forest, but forest are targeted differently in 1972-1986 by water and it has finished in 1986-2000 and replaced by range in 2000-2014. Nevertheless, farmlands intensively and with stationarity loss to the water and built-up.

Built-up gain intensity reduced in 1986-2000 but increased again in 2000-2014, while the water gain is intense in all the times.
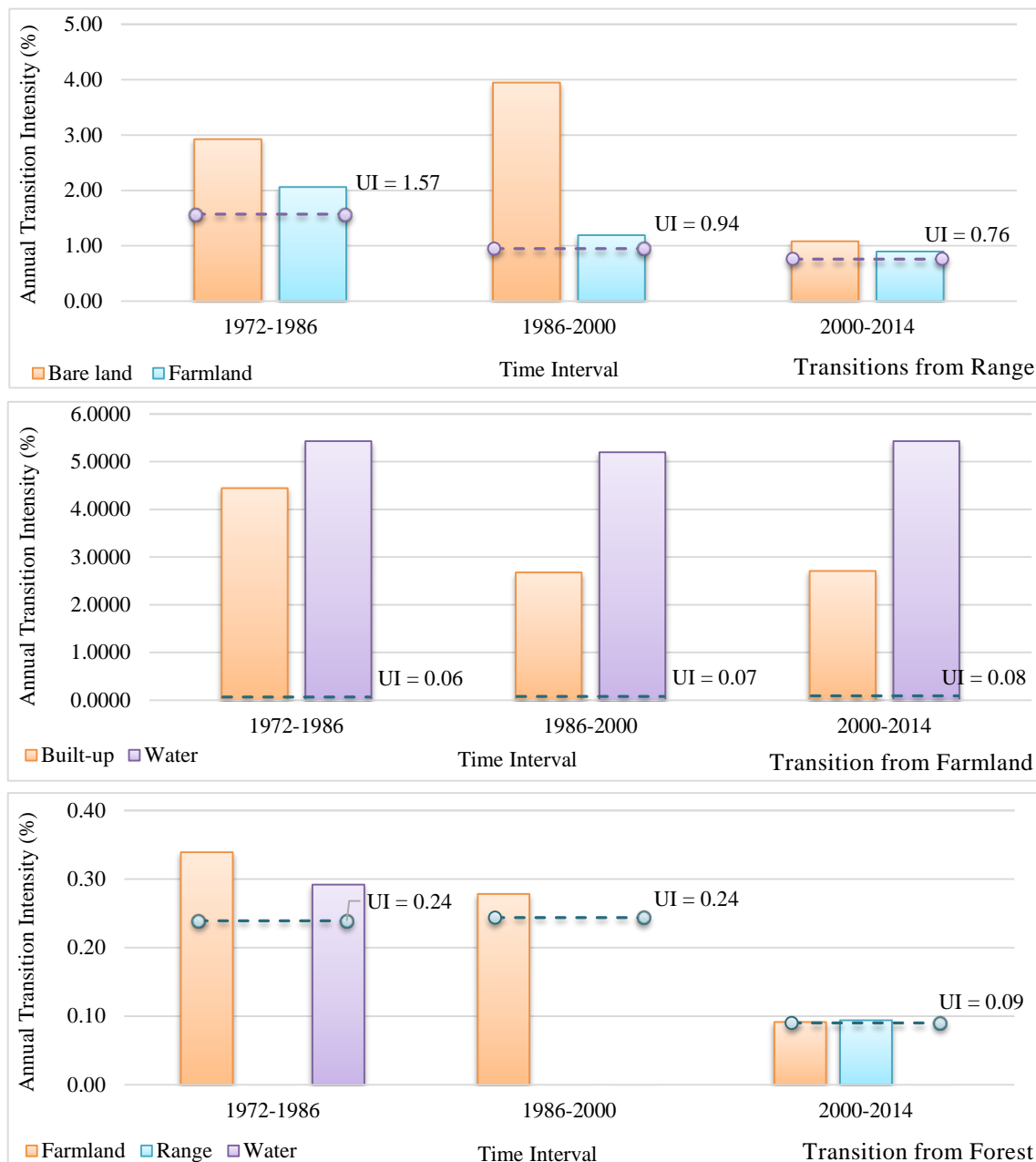
Fig. 3.21. Intensity analysis of transition from range, forest and farmland during 1972-1986, 1986-2000 and 2000-2014. Columns show intensity of annual transitions in related categories.

3.4.   Conclusion

This study set out to determine the LCLU status and changes since 1972 to 2014 during 42 years in the northeast of Iran. Based on the pixel based and GEOBIA remote sensing we clarify the status of LCLU during this period. Afterward, with creating transition matrix, trend surface analysis and intensity analysis in different levels the spatio-temporal dynamics and characteristics of changes were investigated. This study

has identified in 1972, 1986 and 2000 the rangeland is dominant land cover. Farmland and forest as the most expanded land covers have follow range LC during 1972 to 2000. There is a significant difference between 2014 and past dates, because range class no more is the most dominant land cover and replaced by farmland. In 2014, farmlands followed by range and forest respectively. While, in the whole dates the water and built-up land covers are the smallest classes.

This study has shown that regarding the changes there has been a steep decrease and increase in the rangelands and farmlands, respectively. It also reveals that forests suffer from a decreasing gradual change until 2000, while since 2000 to 2014 it experienced a slow increase. On the other hand, on small categories built-up and water classes increased too. Built-ups increased 11 times since 1972. Finally, bare lands experienced some fluctuations and after these 42 years are approximately same. The research has also shown that in case of gains and losses, farmland is the biggest gainer while range is the biggest loser per area. Whereas, in gains and losses percentage, water and built-up have the most gains, and built-up and farmland have the minimal losses. The investigation of gains and losses has shown that the most obvious transition happened between ranges, farmlands, forests that the farmlands mostly gains from both, and forest and ranges have some mutual relations too. Farmland class conversion was primarily to built-up in whole the period and water mostly get lands from farmlands too.

Trend surface analysis revealed that the ranges in the north and northeast are mostly changed to farmland, which means farmlands movement direction is to the north and northeast and finally changes are more concentrated there. Built-ups are mostly developed in the low lands, and movement direction is to the east and we have increased of built-ups in the northeast and south highlands. Regarding the forest transitions, it almost concentrated in the center of area in the whole of its boundaries from north to south to farmlands, built-ups and sometimes ranges. The investigation of intensities has shown that in interval level the 1972-1986 is an active period of changes comparing to uniform intensity. In category level built-up, farmland, and water are active gainers comparing to uniform intensity. Moreover, in transition level, targeted groups are mostly stable and just range and farmland and a little bit forest target groups are changed.

The results of this study indicate that, a great amount of changes happened in the region that affects the ecosystem services and human life consequently. Increase in farmlands and built-up and decrease of forests and ranges could increase different types of natural hazards and specially floods that are predominant in this region. The findings of this study suggest that with this knowledge of LCLU changes more plans and programs should be develop to manage the future of the watershed. Further studies, moreover, regarding the role of LCLU changes in future ecosystem services and natural

hazards would be interesting to extends our knowledge to confront with future more efficient.

What and where are the changes in LCLU of Gorganrood watershed?

Almost, changes happened among all categories. Using pixel-based and object-based Remote Sensing and PCC method, the LCLU maps and change matrix created and the changes and place of changes were detected.

At what rate and when does the LCLU change from past to present?

The changes in the first decade are faster and more intense than other decades but in all 42 years period, the region experienced several different changes.

Chapter 4

Flood hazards, Climate Change and LCLU Relationship Assessment

This chapter will investigate the discharge time series to provide floods database and floods characteristics. Afterward, the outcomes of previous chapters will contribute to establish a statistical relationship assessment among the provided floods characteristics and LCLU and climate change. The results of this chapter will explain the relations among them and will provide a great knowledge regarding impacts of CC and LCLU on the floods characteristics.

4.1.   Introduction

In the case of natural hazard and hydrological studies, flood hazards are the most common and destructive of all natural disasters (Kellens et al., 2013). This fact is also true for the Gorganrood watershed - as our case study - in the Northeast of Iran. Analysis and understanding of floods is one of the main parts of hydrological research since its beginnings (Rogger et al., 2012). Flood as a hazard that cause tremendous losses and social disruption worldwide each year, need to be delineated and identified for possible measures to mitigate potential impacts. Each year, flood disasters cause tremendous losses and social disruption worldwide. In the last two decades major flood events have further raised the awareness of national and international authorities to the importance of reducing flood risks (Rogger et al., 2012; Uddin et al., 2013).

To study about the flood, some factors are always in account. The factors can be divided in two categories: Meteorological and physical characteristics. Land cover land use (LULC) and climate are two most important factors influencing hydrological conditions of watersheds. Land use/cover changes have impacts on surface runoff, infiltration and soil water redistribution in the hydrological processes (De Roo et al., 2001; De Roo et al., 2003). On the other hand, climate change can change the flood characteristics like, peak flows, runoff or aggravating current flood problems or creating

new situations and new types of problems-such as floods in different parts of the year, or new types of floods (Muzik, 2001; Naess et al., 2005).

Previous research has improved understanding of individual factors but many complex interactions need to be addressed for flood mitigation in practice (www.floodsite.net, 2013). In previous studies, some have investigated the impacts of urbanization on watershed hydrology (Du et al., 2012; Sim & Balamurugan, 1991; Suriya & Mudgal, 2012). Some studies used "paired catchment" approach (Merz & Bloschl, 2005; Merz et al., 2008).

Such studies studied land cover and climate effects (Bronstert et al., 2002; J. Z. Li et al., 2013; Z. Li et al., 2009; Liu et al., 2011; Loukas et al., 2004; Muzik, 2002; Ouellet et al., 2012). These studies have suggested that although the impact of climate change on flood risk is acknowledged, more comprehensive efforts for regional assessments is necessary (Kwon et al., 2011) and many complex interactions need to be addressed for flood mitigation in practice (www.floodsite.net, 2013). In addition, in the Gorganrood watershed floods, LCLU and CC studies are not popular and just some studies with different point of view of ours have been conducted in the case of floods. For example Hosseinzadeh and Jahadi Toroghi (2007); Mikaeili A.R et al. (2005); Mohammadi et al. (2008); Mohammadi et al. (2007) made research concerning river morphology and physical structures.

Hadiani and Ebadi (2007) studied land use change impact on design floods and consequent results on hydraulic structures in Madarsoo watershed. They believe that when designing hydraulic structures, the predicting the discharge of flood is necessary. Most hydraulic structures were destructed because of the lack of resistance against floods with flow rates more than calculated design floods as the hypothetical floods used for planning. They compared land use and land capacity. Yamani et al. (2010) investigated the types of floods that flow in this basin. Modaresi et al. (2010) assessed Climate Change using statistical tests in the neighborhood basin called Gharehsou basin. The flood impacts on the environment and structures studied by Sepehry and Liu (2006) that search and determined land cover change caused by the 2001 flood. Tjerry et al. (2006) investigated providing flood maps and to assess the hydraulic impact of debris flow.

Hosseini Asl et al. (2008) prepared a GIS database for the Madarsoo basin based on the available information. Moreover, some studies are in the case of early warning systems. For instance Matkan et al. (2009) provided a flood early warning system based on NOAA/AVHRR satellite images. Ghalkhani et al. (2013) studied on real time flood routing. In addition, Poozesh-Shirazi et al. (2000), Zanganeh et al. (2011) and Ghezelsofloo et al. (2010) did some studies related too.

Based on the literature review analysis of the impact of CC and LCLUC on the floods, characteristics include flood peaks and numbers of floods have not been done in the study area. The aim of this research is to assess and compare the impact of CC and

LCLUC on the mentioned floods characteristics in the Gorganrood watershed. Observed daily discharge data are employed to obtain floods peaks and frequency. This section organized as follow: the study area, data sets, floods characteristics detection, statistical analysis, results and the discussion are presented at the end.

4.2.   Methodology

4.2.1. Study area and datasets

The study region in this section is the main study area (Fig 4.1). For the statistical section of this study, two types of the data were used: Hydro-meteorological and Land Cover/Land Use (LCLU) change data. Daily hydro-meteorological data of nine stations in the study area were obtained from Iranian Meteorological Organization and Ministry of Energy (Table 4.1; Fig 4.1). The data were structured by hydrological years, starting in October and ending in September. For precipitation and temperature, longest period has been since 1953 to 2013 in Gorgan station and shortest from 1992-2012. Whereas, in discharge series the longest period is from 1955 to 2011 in Gonbad station; and shortest from 1983 to 2011 in Haji-ghushan station. The LCLU data were provided by the classification of four cloud free, L1T Landsat images of the path/row 162/34 from 1972 to 2014 using pixel-based and object based remote sensing. The land cover maps include bare land, built-up, farmland, forest, range and water. The description of images, classification methods and classification accuracy are presented in Table 4.2. In addition, for the SWAT modeling section Aster DEM and DSMW FAO soil database were add to the previously mentioned data.
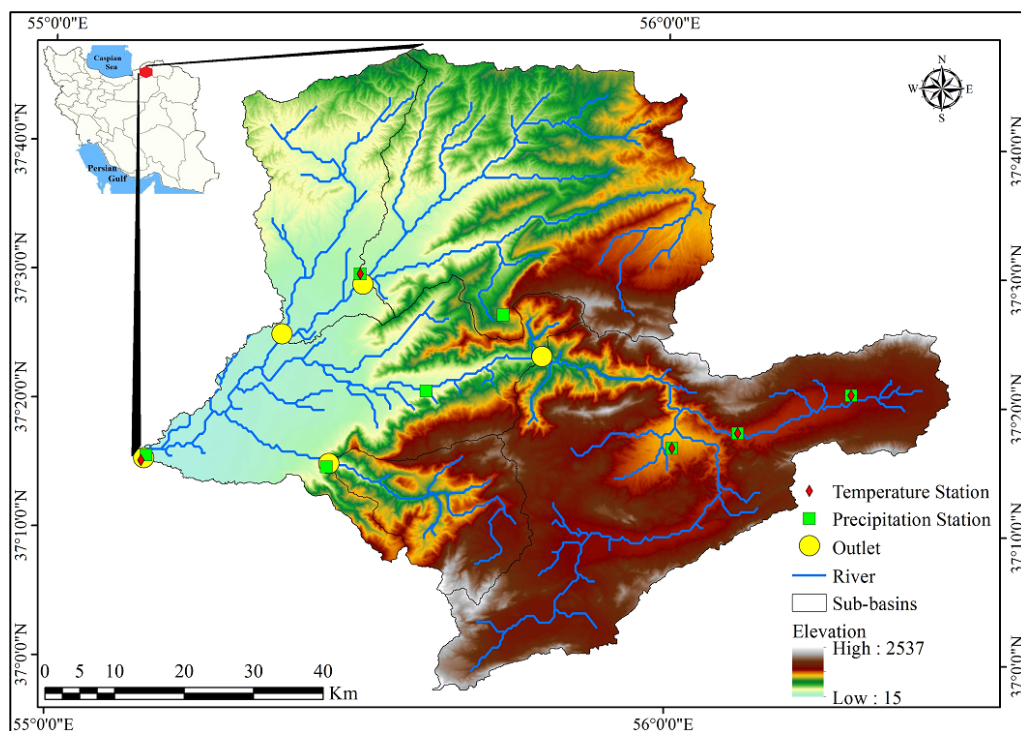

Fig. 4.1. Study area and stations location in the northeast of Iran.

Table 4.1. Descriptive statistics (mean and standard deviation) of monthly hydro-climatological time series during the study period

Station name	TMax	TMin	TMean	Prcp	Discharge
Cheshme-khan	19.6±8.9	3.8±7.3	11.7±8.04	19.6±20.2	*
Dasht	19.8±8.6	4.2±7.7	10.8±8.3	13.5±16.8	*
Robat-gharabil	21.3±9.8	3.01±8.04	12.1±8.7	15.6±16.3	*
Gonbad	24.3±8.6	11.4±7.4	18.02±7.9	39.4±31.8	7.08±8.3
Tamar	24.6±8.09	11.05±6.6	16.7±7.3	42.3±35.1	1.5±1.6
Galikash	*	*	*	62.7±44.2	2.5±2.4
Tangrah	*	*	*	59.4±44.7	1.5±2.5
Pishkamar	*	*	*	43.7±38.6	*
Haji-ghushan	*	*	*	*	1.9±2.6

Table 4.2. Images properties, classification methods and accuracy of remote sensing process and provided LCLU maps.

Image	Satellite/Sensor	Classifier	Overall Accuracy	Kappa
1972	Landsat/MSS	Neural Network	95.9	0.93
1986	Landsat/TM	Maximum Likelihood	89.8	0.88
2000	Landsat/ETM+	Maximum Likelihood	91.3	0.90
2014	Landsat/OLI-TIRS	GEOBIA	94.05	0.90

4.2.2. Floods detection

Floods have several characteristics and in this research, we want to investigate relationship of LCLU and climate changes with floods hazards, considering the peak values and number of floods. This is because the CC and LCLU changes can have significant impacts on the mentioned characteristics. The first step in this process is floods detection. To reach to this goal we used Peak-Over-threshold (POT) method using WETSPRO package (Willems, 2009).

River flow gauging data can be mostly gathered in groups based on different orders of greatness of the subflow reaction to precipitation (Willems, 2009). These two groups are quick flow and slow flow (baseflow) components. Whiles, the quick flow group might be split up to overland flow and interflow (Willems, 2009). Observed series of total runoff were split in sub-flows. These were done by subflow separation technique (T. Chapman, 1999; T. G. Chapman, 1991; Eckhardt, 2005; Willems, 2009). The filter aims to split the total flow time series $q(t)$ in the subflow or slow flow component series $b(t)$ and the quick flow series $f(t)$. in addition, a new filter parameter w add to the base filter by the Willems (2009) to get better results. The recession constant, is another parameter in this procedure that should be determined. Finally by detecting the baseflow and interflow the amount of overland flow were achieved. After separating the baseflow, interflow and overland flow in each discharge station the floods detection is the next step. In this regard, using POT method and adjustment of the value of parameters include max ratio difference, independency period and minimum peak height occurred floods have been detected. More information about the WETSPRO and floods detection process could be found in Willems (2009), http://www.kuleuven.be/wieiswie/en/person/u0009249 (2014) and (http://www.kuleuven.be/hydr/pwtools.htm, 2014). The summaries of results are presented in the Table 4.3 and Fig 4.2. As it is clear from the "Flood Importance" chart in the Fig 4.2 floods characteristics, have the great role in the Gonbad watershed. Then, the Tangrah and Tamar stations follow it and Haji-ghushan and Galikash are the last

ones respectively. In the case of mean of peaks, the Gonbad is the first one, Haji-ghushan is the second one and after that Tangrah, Galikash and Tamar, respectively. Gonbad is the most under attack sub-basin followed by Tamar, Haji-ghushan, Galikash and Tangrah. For the maximum of peaks, as a list the Gonbad have the biggest one in the top of list and then the Tangrah, Tamar, Haji-ghushan and Galikash are listed.

Table 4.3. Summary of flood hazards characteristics

Station name	Total Number of Floods	Mean of Peaks	Maximum of peaks
Gonbad	208	54.04	1035.4
Tamar	129	24.69	531.06
Galikash	47	38.79	339.3
Tangrah	42	44.96	777
Haji-ghushan	79	50.75	492.66
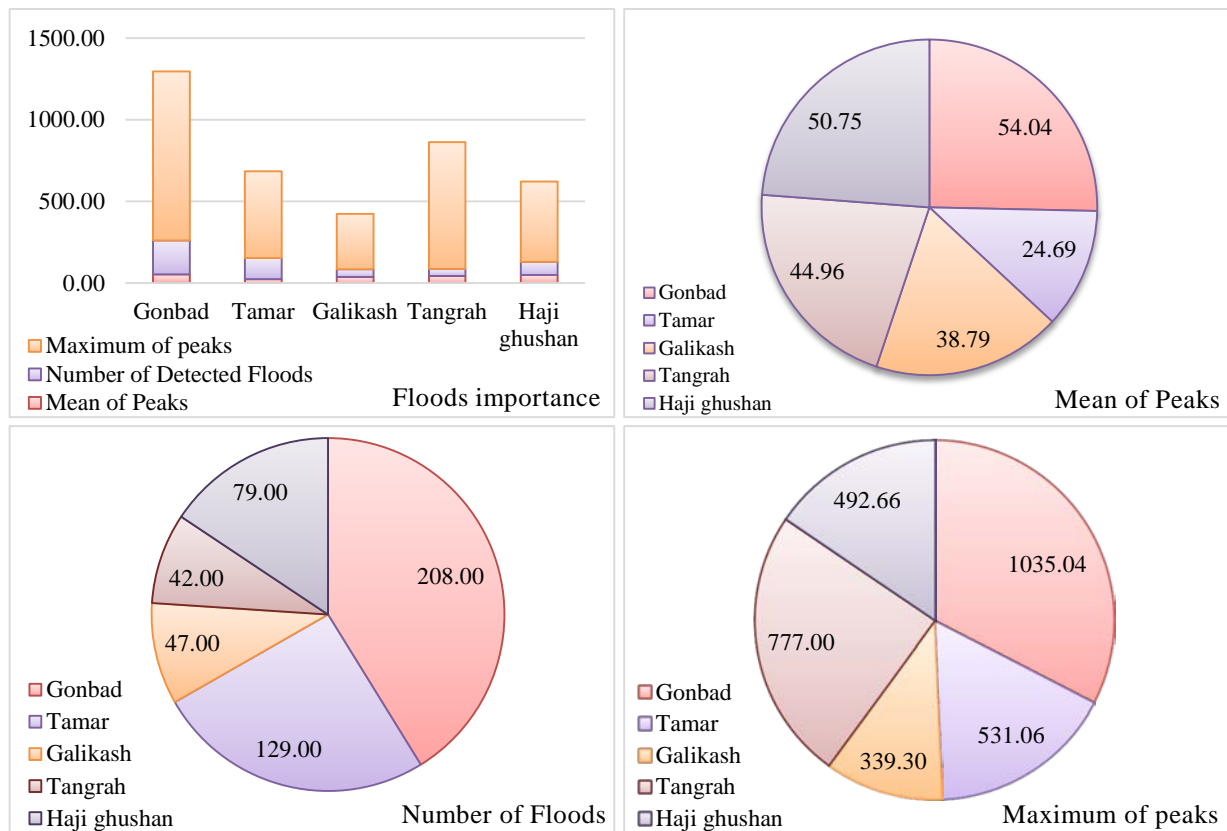
Fig. 4.2. Graphical presentation of floods characteristics in the sub-basins. Mean and maximum of floods are in millimeter and the "Floods importance" chart is the stacked column chart of all three characteristics.

4.2.3. Characteristics determination of flood hazards and statistical assessment

In this section, we will use correlation analysis to detect relationships among factors (Ben Aissia et al., 2012). The correlation is a scale free measure of linear association among x and y variable and is given by formula $r = cov\,(x,y)/s_x s_y$ that the r could be write as r_{xy} too (Zaiontz, 2014). The r could be between 1 and -1 that 1 means x and y are positively correlated. Whereas, if r is close to -1 the x and y are negatively correlated. When r is about zero there is not a significant relationship between x and y (Zaiontz, 2014). To prepare data for analyzing correlations between flood hazards

characteristics and meteorological and LCLU data the mean of floods characteristics and meteorological data for the intervals of 1972, 1986, 2000 and 2014 were calculated. Trends in average flood hazards characteristics data were investigated to detect increasing and decreasing trends to select appropriate factors for correlation analysis. Fig 4.3 shows the trends in floods hazard characteristics in different stations. Regarding the trends in stations with increase in flood characteristics the correlation analysis were done among them with LCLU and precipitation.

4.2.4. Model-based LCLU impact assessment

To provide deeper knowledge regarding LCLU changes impacts on the floods we decide to use a physical based model called Soil and Water Assessment Tool (SWAT); A river basin or watershed, scale model developed by Dr. Jeff Arnold for the USDA Agricultural Research Service (ARS) (Arnold, Srinivasan, Muttiah, & Williams, 1998). This model designed to estimate runoff, soil moisture, evapotranspiration, sediment and nutrient loads and so on (Bossa, Diekkruger, & Agbossou, 2014; Heo, Yu, Giardino, & Cho, 2015). SWAT subdivides the catchment into sub-catchments and Hydrological Response Units (HRUs) and work based on them (Bossa et al., 2014). To applying the SWAT model a 30 m ASTER DEM, daily climate data (precipitation and temperature) from 1980 to 2010, DSMW FAO Soil database and LCLU maps were used. For this study four SWAT model constructed based on different LCLU maps of 1972, 1986, 2000 and 2014 to model surface runoff for the period of 1980 to 2010. We want to consider the LCLU impact on entire of period, henceforth we did not do calibration on the model because calibration based on each one of the four LCLUs could affect the model and provide unrealistic results. The same inputs and different LCLU maps simulated the daily time series of runoff. Finally, to analyze four model results and understanding impacts of LCLU changes the maximum, minimum and mean of simulated discharge series for five sub-basins were calculated and compared.

4.3.   Results and discussion

Several researchers paid attention to the relations among LCLU, CC and flood hazards and invited other researchers for more investigation in this field (Capparelli et al., 2013; Muzik, 2002; F. Wu et al., 2013). To investigate the relations among LCLU, CC and flood hazards characteristics we used correlation analysis. The prepared data for correlation analysis are presented in Table 4.4 to 4.6 and graphically in Fig 4.2 to Fig 4.4. Fig 4.3 presents the LCLU classes areas in whole the watershed and in five sub-basin separately. As can be seen from total graph in Fig 4.3 the range and forest classes have a decreasing trend in the total area of watershed while farmland, built-up, water

and bare land categories had increasing trends. Nevertheless, this condition in analysis of LCLUs in the sub-basins are somehow different and its make analysis of relations with flood characteristics in each sub-basin more interesting.

Table 4.4. LCLU classes area percentage in whole of the watershed and each sub-basin.

	Year	Bare land	Built-up	Farmland	Forest	Range	Water
Total Area of Watershed	1972	0.72	0.09	17.76	21.67	59.76	0.00
	1986	0.73	0.30	27.83	21.05	50.07	0.02
	2000	0.86	0.60	35.35	18.71	44.44	0.04
	2014	0.73	1.18	40.67	18.74	38.47	0.22
Gonbad Sub-basin	1972	0.00	0.37	50.75	39.37	9.48	0.02
	1986		1.35	57.28	35.87	5.41	0.09
	2000		2.49	61.70	34.27	1.32	0.22
	2014		4.15	60.97	33.24	0.92	0.72
Tamar Sub-basin	1972	0.11	0.01	9.57	17.34	72.98	
	1986	0.00	0.04	25.88	19.44	54.65	0.00
	2000	0.03	0.21	36.40	14.94	48.43	0.00
	2014	0.01	0.69	47.69	16.49	35.10	0.01
Galikash Sub-basin	1972	0.01	0.03	18.35	54.35	27.27	
	1986		0.07	32.00	45.74	22.20	
	2000	0.00	0.17	49.16	39.11	11.55	
	2014		0.57	54.83	37.79	6.72	0.08
Tangrah Sub-basin	1972	2.08	0.01	1.99	15.43	80.50	
	1986	2.21	0.02	10.24	15.73	71.81	
	2000	2.56	0.06	14.58	14.91	67.89	
	2014	2.19	0.20	18.68	14.57	64.37	0.00
Haji-ghushan Sub-basin	1972		0.06	26.92	0.37	72.66	
	1986		0.11	30.87	0.36	68.66	0.00
	2000	0.01	0.26	39.17	0.31	60.25	0.00
	2014		0.61	43.42	0.30	55.10	0.56

Table 4.5 and Fig 4.4 show three flood hazards characteristics that in most of the stations have increasing trend. The statuses of the meteorological factors are presented in Table 4.6 and Fig 4.5 too.

Fig. 4.3. LCLU areas in different classes since 1972 to 2014.

Table 4.5. Flood hazards characteristics include average of peak floods, number of floods and maximum of peak floods

	Year	Gonbad	Tamar	Galikash	Tangrah	Haji-ghushan
Floods Peaks (m³)	1972	121.48	37.62	53.17	30.00	
	1986	174.49	31.23	11.30	11.42	203.90
	2000	247.10	93.83	55.77	21.19	121.44
	2014	297.69	120.22	67.16	122.20	172.89
No. Floods	1972	2.00	2.67	1.50	1.14	
	1986	2.93	1.57	0.57	0.64	4.00
	2000	4.57	3.43	1.57	1.07	2.43
	2014	6.27	4.64	1.10	1.00	3.36
Maximum Peaks(m³)	1972	509.85	94.60	167.90	117.00	
	1986	614.00	142.40	81.30	76.40	293.40
	2000	672.42	347.36	317.00	68.10	464.60
	2014	1,035.40	531.06	339.30	777.00	492.66
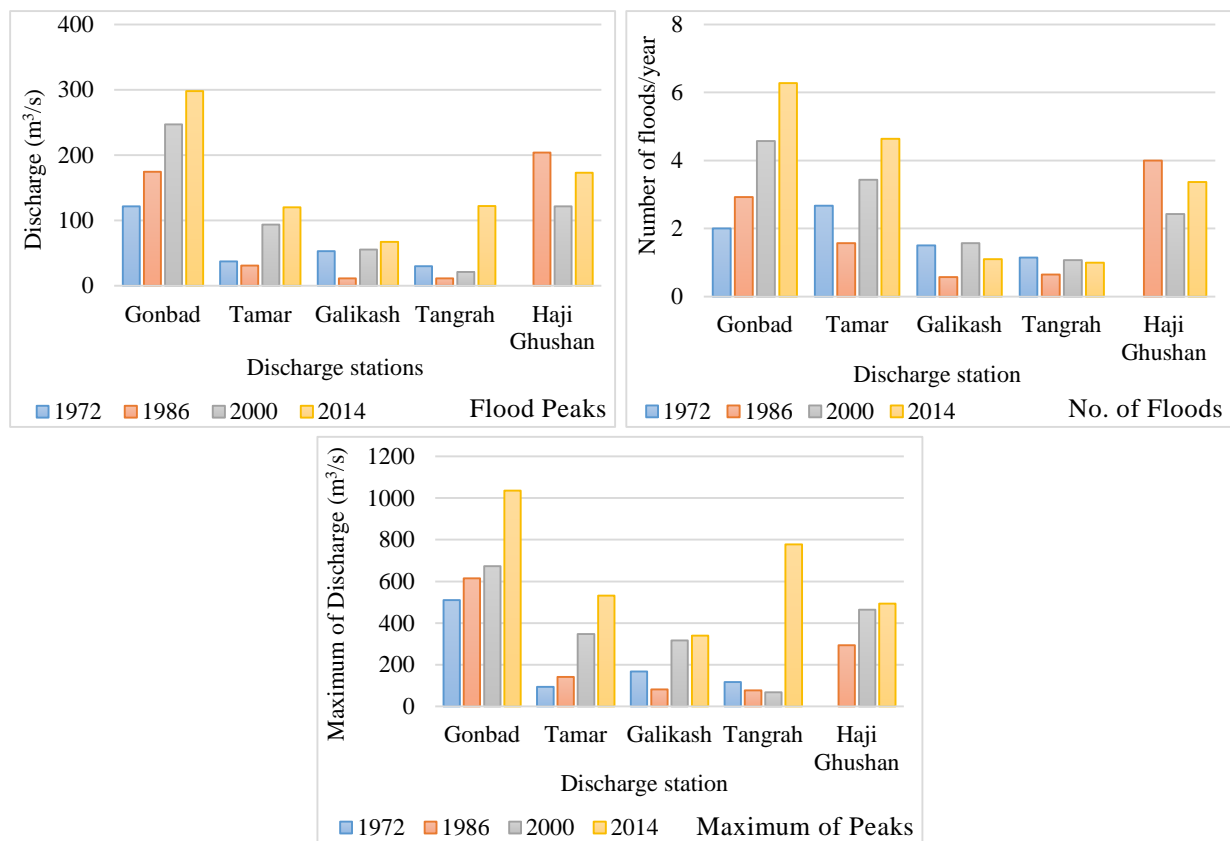
Fig. 4.4. Flood hazards characteristics. Left side peak discharge in total watershed and sub-basins. Right side the number of floods happened per year in total watershed and sub-basins. Down is the maximum of peaks during each period.

Table 4.6. Meteorological factors, precipitations (mm) and temperature (°C).

	Year	Gonbad	Galikash	Tangrah	Tamar	Cheshme-khan	Robat-gharabil	Pishkamar	Dasht
Precipitation	1972	435.41	921.40	940.00	420.51			512.01	
	1986	508.83	696.75	638.02	428.07	237.46	163.96	546.75	63.20
	2000	456.21	805.86	727.39	573.50	230.40	198.34	525.86	108.31
	2014	438.82	737.38	793.50	580.95	238.95	198.77	490.81	260.69
Maximum Temperature	1972	24.91			23.55				
	1986	24.29			24.96	19.77	21.75		19.66
	2000	24.02			24.65	19.40	20.60		19.80
	2014	24.75			24.82	19.75	21.85		20.17
Minimum Temperature	1972	10.55			1.27				
	1986	11.04			9.15	4.08	3.26		3.43
	2000	11.75			10.69	3.36	3.41		3.89
	2014	12.83			11.85	4.15	2.23		4.96
Mean Temperature	1972	17.73			12.41				
	1986	17.66			17.06	11.93	12.51		11.46
	2000	17.88			17.67	11.38	12.00		10.93
	2014	18.79			18.34	11.95	12.04		12.20
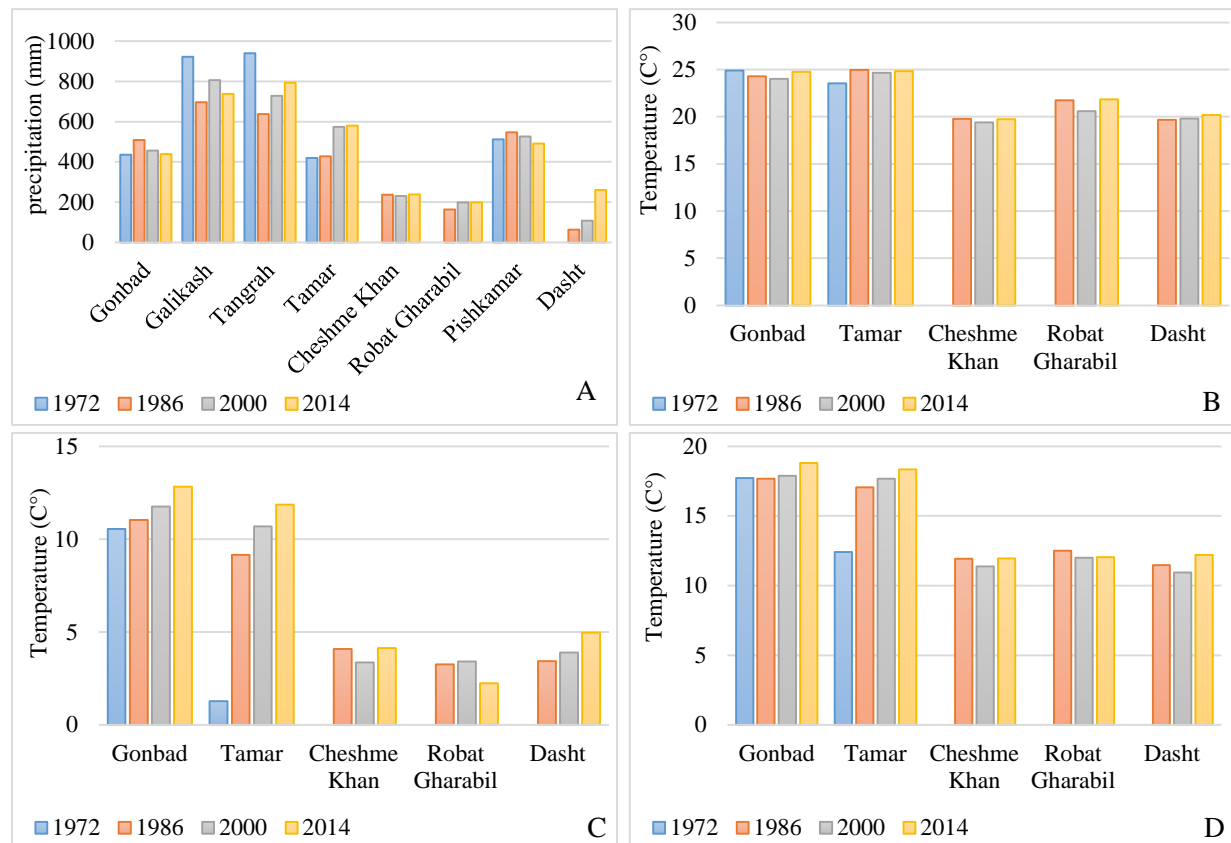
Fig. 4.5. Meteorological data in different stations. A) Precipitation, B) Maximum temperature, C) Minimum temperature and D) is the mean temperature.

Correlation analysis between characteristics of flood hazards, LCLU and CC factors provide important insight into relations among them and detecting the most relevant factor. Based on the trend of the flood hazards characteristics we investigated the relations in the stations that experience an increase in the conditions. Therefore, the selected floods characteristics in each sub-basin are presented in Fig 4.6.
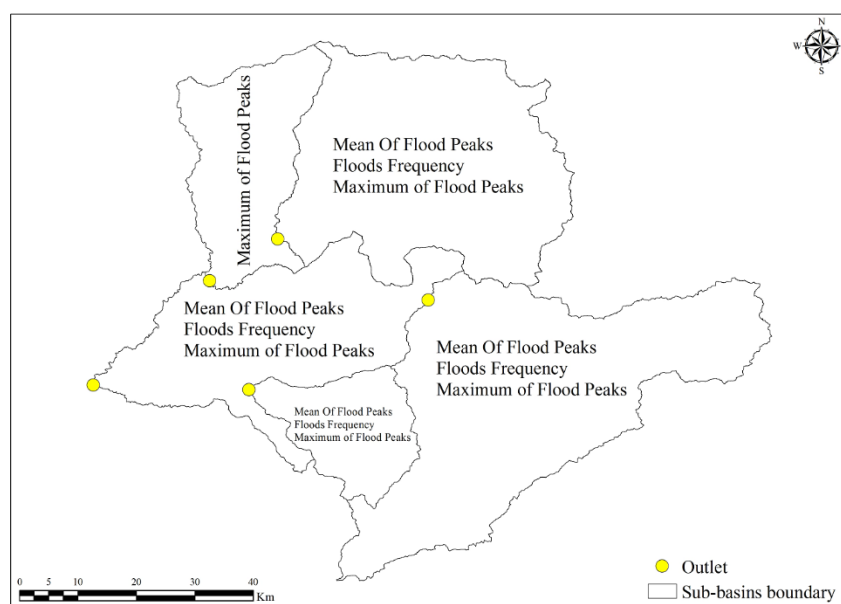
Fig. 4.6. Sub-basin' flood characteristics that experienced increase during time.

Table 4.7, present correlation results of LCLU related classes and precipitation in the whole watershed with flood hazards characteristics in the main outlet. We note that the first significant relation is by LCLU and afterward precipitation. As it is clear from Table 4.7 farmland and built-up classes have 98 and 96 percent correlation with floods peaks. Precipitations in Tamar and Dasht stations with 94 and 91 percent of correlation are in the second rank. From the table it can be seen that relations between floods frequency and the LCLU classes and precipitation are almost same with floods peaks just with small difference that shows more importance of built-up area and Dasht precipitation on the frequency of floods. Analysis of relations with maximum peaks will change the importance order, Dasht precipitation comes to the first rank and after that built-up and farmlands LCLU classes are located. In addition, the bottom of the table shows strong negative correlation in all series with forest and range classes. Overall, these results indicate that as all around the world CC and LCLU have impacts on the flood hazards characteristics. The increase in built-up and farmlands increase the floods characteristics and increasing the forests and rangelands decrease the floods characteristics. but, in this region mean flood peaks and floods frequency are controlled more by LCLU but the maximum of flood peaks are more dependent to CC and its shows also the impact of urban areas in increasing the floods risks.

Table 4.7. Correlation between flood hazards characteristics, LCLU classes and precipitation. "Prcp" = precipitation.

Factor	Flood peaks	Factor	Floods frequency	Factor	Maximum of peaks
Farmland	0.98	Built-up	0.99	Dasht-Prcp	0.99
Built-up	0.96	Farmland	0.96	Built-up	0.98
Tamar-Prcp	0.94	Dasht-Prcp	0.95	Farmland	0.87
Dasht-Prcp	0.91	Tamar-Prcp	0.92	Tamar-Prcp	0.76
Robat-gharabil-Prcp	0.91	Robat-gharabil-Prcp	0.86	Robat-gharabil-Prcp	0.61
Bare land	0.34	Bare land	0.24	Cheshme-khan-Prcp	0.53
Cheshme-khan-Prcp	0.06	Cheshme-khan-Prcp	0.17	Bare land	-0.08
Gonbad-Prcp	-0.19	Tangrah-Prcp	-0.23	Tangrah-Prcp	-0.13
Tangrah-Prcp	-0.33	Gonbad-Prcp	-0.27	Gonbad-Prcp	-0.28
Pishkamar-Prcp	-0.47	Galikash-Prcp	-0.49	Galikash-Prcp	-0.52
Galikash-Prcp	-0.53	Pishkamar-Prcp	-0.57	Pishkamar-Prcp	-0.66
Forest	-0.95	Forest	-0.92	Forest	-0.75
Range	-0.98	Range	-0.96	Range	-0.88

We have divided the entire watershed to five main sub-basins based on the hydrological gauges to reach to a deeper spatial knowledge about role of CC and LCLU changes on the flood hazard characteristics. The five sub-basins are Gonbad, Tamar, Galikash, Haji-ghushan and Tangrah. Firstly, statistical analysis were applied in the sub-basin level to the Gonbad sub-basin that have the same outlet with whole of watershed. Results of impact assessment among flood hazards characteristics with precipitation and LCLU classes in this sub-basin are shown in Table 4.8. IT can be seen from the data that increase in mean flood peaks is firstly related to built-up area and

after that precipitation in Tamar and Dasht stations and the importance of the farmlands in changes are reduced. This result indicates that increase of built-up in the low lands had straight impacts on the floods peaks and it means statistical analysis accurately understands the LCLU change characteristics. The condition in the floods frequency analysis is almost same just the amounts of contributions are somehow increased. In maximum peaks relation analysis, precipitation get the first role and after that LCLU placed. Same as the pervious analysis range and forest areas have a strange negative correlation with mean of peaks and number of floods but their role in maximum peaks reduced.

Table 4.8. Correlation between flood hazards characteristics, LCLU classes and precipitation in Gonbad sub-basin. "Prcp" = precipitation.

Factor	Flood peaks	Factor	Floods frequency	Factor	Maximum of peaks
Built-up	0.98	Built-up	0.99	Dasht-Prcp	0.99
Tamar-Prcp	0.94	Dasht-Prcp	0.95	Built-up	0.96
Dasht-Prcp	0.91	Tamar-Prcp	0.92	Tamar-Prcp	0.76
Robat-gharabil-Prcp	0.91	Robat-gharabil-Prcp	0.86	Farmland	0.68
Farmland	0.91	Farmland	0.85	Robat-gharabil-Prcp	0.61
Cheshme-khan-Prcp	0.06	Cheshme-khan-Prcp	0.17	Cheshme-khan-Prcp	0.53
Gonbad-Prcp	-0.19	Tangrah-Prcp	-0.23	Tangrah-Prcp	-0.13
Tangrah-Prcp	-0.33	Gonbad-Prcp	-0.27	Gonbad-Prcp	-0.28
Pishkamar-Prcp	-0.47	Galikash-Prcp	-0.49	Galikash-Prcp	-0.52
Galikash-Prcp	-0.53	Pishkamar-Prcp	-0.57	Pishkamar-Prcp	-0.66
Forest	-0.95	Forest	-0.91	Range	-0.77
Range	-0.96	Range	-0.92	Forest	-0.81

Floods characteristics in Tamar sub-basin experience increase during time. In this sub-basin, the role of climate in mean of flood peaks and floods frequency is more important than LCLU. Precipitation have the biggest impact and built-up and farmland are after that. Interestingly, correlation analysis with maximum of peaks shows the importance of LCLU greater than precipitation (Table 4.9). The importance of LCLU classes on the maximum peaks is showed clearly in the bottom of table with strong negative correlation with rangelands.

Table 4.9. Correlation between flood hazards characteristics, LCLU classes and precipitation in Tamar sub-basin. "Prcp" = precipitation.

Factor	Flood peaks	Factor	Floods frequency	Factor	Maximum of peaks
Tamar-Prcp	0.97	Robat-gharabil-Prcp	0.92	Built-up	0.95
Robat-gharabil-Prcp	0.96	Dasht-Prcp	0.91	Farmland	0.94
Built-up	0.90	Built-up	0.89	Dasht-Prcp	0.94
Farmland	0.88	Tamar-Prcp	0.85	Tamar-Prcp	0.93
Dasht-Prcp	0.86	Farmland	0.70	Robat-gharabil-Prcp	0.88
Tangrah-Prcp	-0.01	Tangrah-Prcp	0.30	Cheshme-khan-Prcp	0.13
Cheshme-khan-Prcp	-0.06	Cheshme-khan-Prcp	0.04	Tangrah-Prcp	-0.13
Galikash-Prcp	-0.22	Galikash-Prcp	0.02	Gonbad-Prcp	-0.37
Bare land	-0.40	Bare land	-0.12	Galikash-Prcp	-0.40
Gonbad-Prcp	-0.51	Range	-0.66	Bare land	-0.54
Pishkamar-Prcp	-0.68	Forest	-0.73	Forest	-0.58
Forest	-0.73	Gonbad-Prcp	-0.74	Pishkamar-Prcp	-0.64
Range	-0.83	Pishkamar-Prcp	-0.88	Range	-0.92

In Galikash sub-basin, the flood characteristics have increasing trend in flood peaks mean and maximum and in floods frequency are approximately no special trend. In this basin, CC is the most important factor and the LCLU even does not have a strong correlation (Table 4.10). In the maximum of peaks, we will see the impacts of increasing the farmlands area in this region and its impact on the maximum flood peaks after precipitation.

Table 4.10. Correlation between flood hazards characteristics, LCLU classes and precipitation in Galikash sub-basin. "Prcp" = precipitation.

Factor	Flood peaks	Factor	Floods frequency	Factor	Maximum of peaks
Robat-gharabil-Prcp	0.98	Robat-gharabil-Prcp	0.87	Robat-gharabil-Prcp	0.99
Dasht-Prcp	0.80	Galikash-Prcp	0.80	Tamar-Prcp	0.94
Tamar-Prcp	0.67	Tangrah-Prcp	0.66	Farmland	0.80
Tangrah-Prcp	0.62	Tamar-Prcp	0.33	Built-up	0.74
Built-up	0.60	Dasht-Prcp	0.25	Dasht-Prcp	0.73
Galikash-Prcp	0.44	Forest	0.08	Tangrah-Prcp	0.17
Farmland	0.43	Farmland	0.01	Galikash-Prcp	0.03
Cheshme-khan-Prcp	-0.16	Built-up	-0.04	Cheshme-khan-Prcp	-0.27
Forest	-0.29	Range	-0.09	Gonbad-Prcp	-0.66
Range	-0.54	Pishkamar-Prcp	-0.43	Pishkamar-Prcp	-0.71
Pishkamar-Prcp	-0.89	Cheshme-khan-Prcp	-0.75	Forest	-0.71
Gonbad-Prcp	-0.94	Gonbad-Prcp	-0.80	Range	-0.86

In Tangrah basin the peak's mean and maximum have an increasing trend but the number of floods did not changed in a strong way. Tangrah station statistical relationship assessment results in Table 4.11 shows that precipitation is the most relevant factor to increase the flood hazards. In the analysis of mean peaks the built-up have strong correlation after the precipitation. In the flood frequency, the impact of the

precipitation is increased and the number of floods is not actually dependent to LCLU. Whereas, in maximum peak the role of LCLU increase by considering the impact of urban area growth on flood hazards.

In the Haji-ghushan basin, just the maximum of peaks shows increasing trends. In relationship assessment, precipitation has the most important impact and after that, the farmlands area is located (Table 4.12). In addition, the range and forest area have a strong negative impact on maximum peak of floods that presented in the bottom of Table 4.12.

If we now turn to the temperature impacts on the floods hazards, it is more complicated than precipitation and LCLU. Precipitation and LCLU impacts are clear as force factors to increase or decrease the flood hazards. While, temperature impacts could be different based on several temperature properties. But generally in analysis the results we seen that in the whole basin floods characteristics with temperature increase in minimum temperature in the Gonbad and Dasht stations and maximum temperature in Dasht station show a strong relation with mean of flood peaks and floods frequency. In the maximum of peaks property increase of maximum and minimum temperature in Dasht station has shown a significant relation. In addition, Gonbad minimum temperature shows a strong relation with maximum of floods peak. In Tamar sub-basin minimum temperature in increase of all flood characteristics have a great role. Maximum temperature is more related in the floods frequency and maximum peaks. In addition, increase of mean temperature, shows a strong negative correlation with mean of flood peaks.

Table 4.11. Correlation between flood hazards characteristics, LCLU classes and precipitation in Galikash sub-basin. "Prcp" = precipitation.

Factor	Flood peaks	Factor	Floods frequency	Factor	Maximum of peaks
Dasht-Prcp	0.99	Robat-gharabil-Prcp	0.98	Dasht-Prcp	0.97
Built-up	0.95	Tangrah-Prcp	0.81	Built-up	0.95
Farmland	0.60	Galikash-Prcp	0.81	Cheshme-khan-Prcp	0.64
Tamar-Prcp	0.59	Dasht-Prcp	0.55	Farmland	0.63
Robat-gharabil-Prcp	0.57	Tamar-Prcp	0.33	Tamar-Prcp	0.57
Cheshme-khan-Prcp	0.57	Range	0.18	Robat-gharabil-Prcp	0.50
Tangrah-Prcp	0.24	Built-up	0.16	Tangrah-Prcp	0.15
Galikash-Prcp	-0.21	Bare land	0.09	Bare land	-0.27
Bare land	-0.26	Farmland	-0.14	Galikash-Prcp	-0.31
Gonbad-Prcp	-0.54	Cheshme-khan-Prcp	-0.49	Gonbad-Prcp	-0.44
Range	-0.57	Forest	-0.52	Range	-0.60
Forest	-0.78	Pishkamar-Prcp	-0.66	Forest	-0.74
		Gonbad-Prcp	-0.94	Pishkamar-Prcp	-0.81

Table 4.12. Correlation between flood hazards characteristics, LCLU classes and precipitation in Haji-ghushan sub-basin. "Prcp" = precipitation.

Factor	Maximum of peaks
Robat-gharabil-Prcp	0.99
Farmland	0.92
Tamar-Prcp	0.86
Built-up	0.76
Dasht-Prcp	0.76
Gonbad-Prcp	0.10
Pishkamar-Prcp	-0.14
Cheshme-khan-Prcp	-0.22
Tangrah-Prcp	-0.61
Galikash-Prcp	-0.69
Forest	-0.88
Range	-0.92

In Galikash, temperature shows a negative relation with all floods characteristics. The negative relations are exist in Tangrah station too. Whereas, mean and maximum flood peaks had strong positive relation with temperatures. In Haji-ghushan station that experience increase in maximum flood peaks, a meaningful strong positive relation with minimum and mean temperature in Tamar station was seen. In spite of these results, however, it is clear that temperature have its great impacts on hydro-meteorological cycle, and to reach a good knowledge of the straight impact of temperature on floods in this region more detailed research with more detailed data (e.g. hourly data) should be done that was one of our limitations in data section.

Graphical presentation of statistical relations among floods, CC and LCLU are presented in Figs 4.7 to 4.13. From the Fig 4.7 we can see that the most important factor that influence flood characteristics in the Gonbad sub-basin is LCLU while, in other sub-basins the CC paly more important role to control floods characteristics. The graphs in each sub-basin present the contribution of LCLU/CC as the first important factor in the three floods characteristics. In Gonbad in $2/3$ of the assessments, LCLU is important whereas, in Tamar it is contrariwise. In other three sub-basins, the CC is the main factor totally.
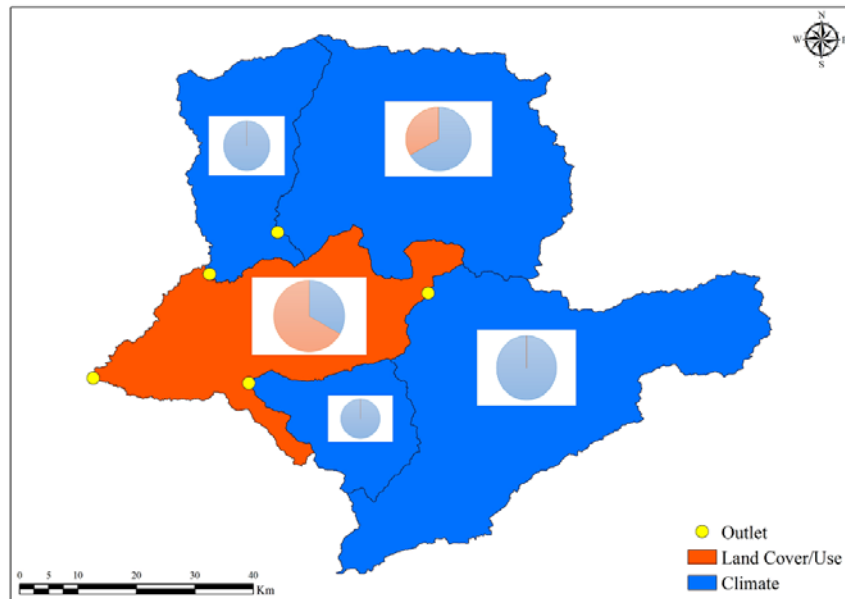
Fig. 4.7. Main control factor in different sub-basins.

The mean percentage of CC contribution for each flood characteristics calculated separately. Fig 4.8 shows an overview of the CC impacts on mean of floods peak. The greatest impact is in Tangrah and the smallest in Haji-ghushan. The results of relationship analysis with floods frequency are shown in Fig 4.9. The largest mean of contribution is in Gonbad and followed by Tamar and Tangrah sub-basins. It can be seen from the Fig 4.10 that in maximum of peaks the CC had the biggest role in Tamar station and Followed by Galikash and Haji-ghushan sub-basins. What is interesting in these images regarding the CC impact on different floods characteristics is that the CC had the greatest impacts on the mean of flood peaks and after that maximum of peaks and finally floods frequency.
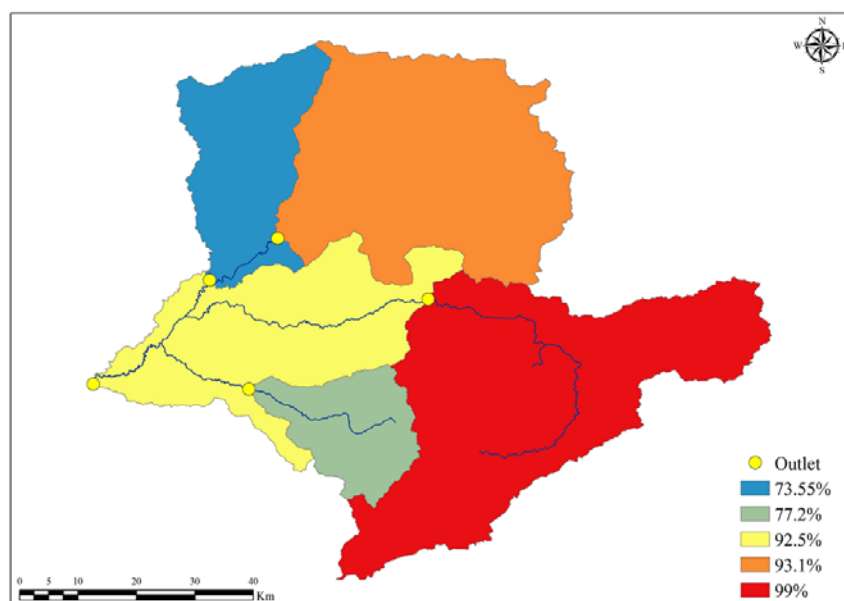

Fig. 4.8. CC contribution in mean of flood peaks in different sub-basins per percent.

Detailed presentation of land cover effects on mean of flood peaks per percent, are presented in the Fig 4.11 to understand how much LCLU is important and what is the difference in sub-basins. As you can see its true that the CC is the main factor in four sub-basin but the LCLU have its impact on mean floods discharge from 60% to about 95%. The Galikash sub-basin has the smallest role of LCLU in the mean of flood peaks. The Tamar sub-basin with around 83% shows a considerable role of LCLU in floods.
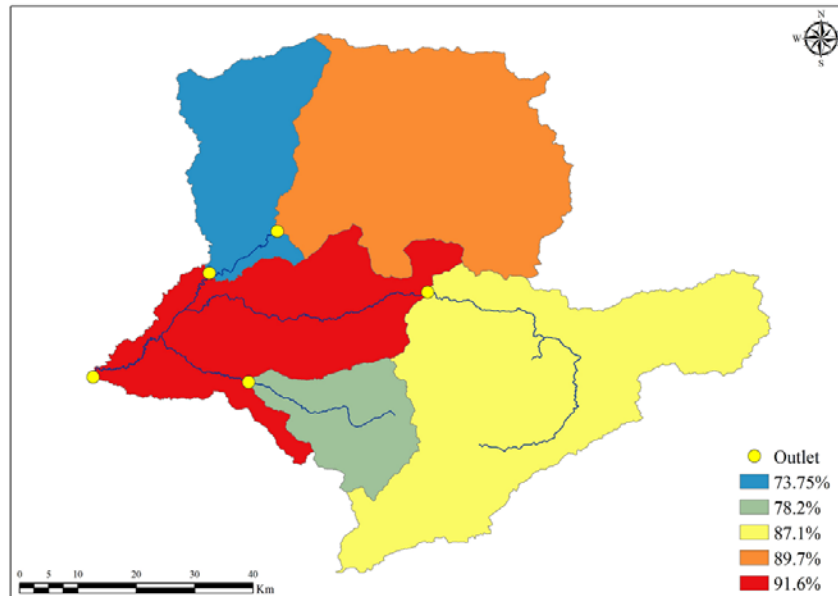

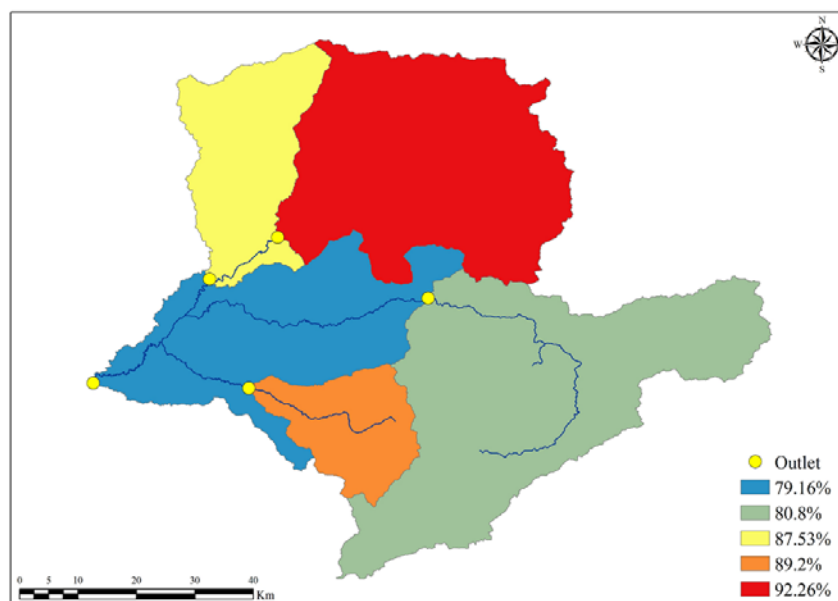Fig. 4.9. CC contribution in frequency of floods in different sub-basins per percent.

Fig. 4.10. CC contribution in Maximum flood peaks in different sub-basins per percent.

Fig 4.12 provides the knowledge about the LCLU contribution in frequency of floods in the sub-basins. What is interesting in this map is that the general role of LCLU in frequency of floods reduced in comparison to mean of flood peaks and it means the

CC has more impact on the frequency of flood occurrence. The results obtained from relationship assessment among maximum flood peaks and LCLU are summarized in Fig 4.13. The more surprising mean of correlations is that the map interestingly shows the impacts of LCLU on increasing the amount of maximum floods. A comparison of three maps reveals that the impact of LCLU in this characteristic is more than others are. In addition, from the figure it is apparent that the LCLU impact is stronger in the Tamar and Haji-ghushan.
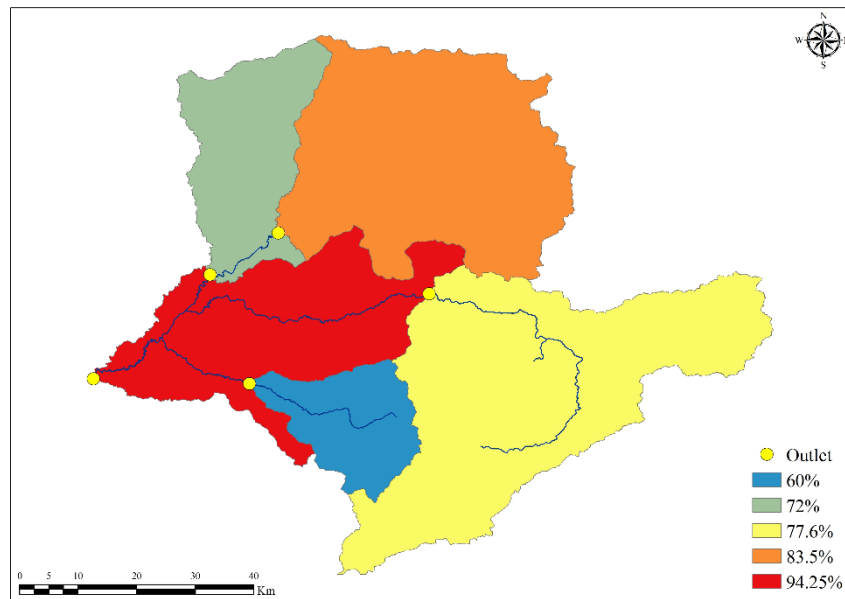

Fig. 4.11. LCLU contribution in mean of floods peaks in different sub-basins per percent.
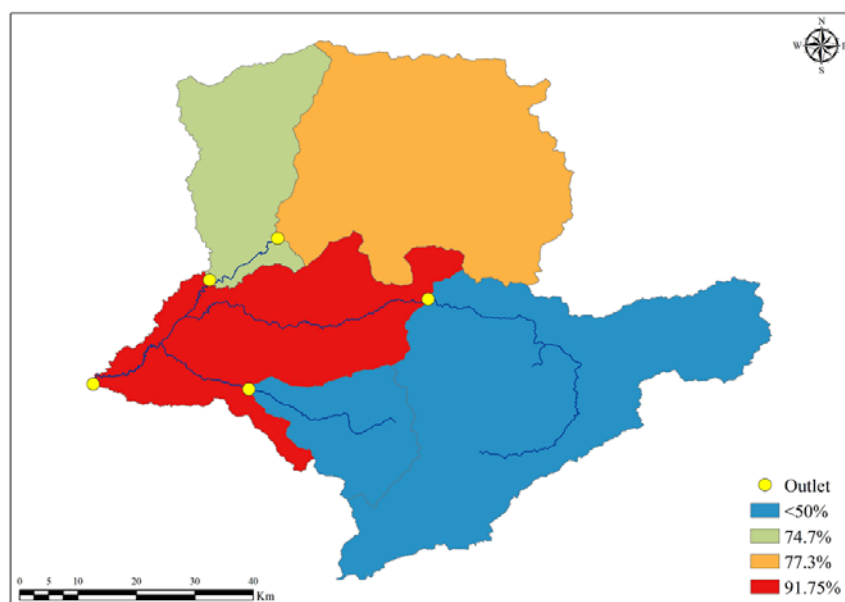

Fig. 4.12. LCLU contribution in frequency of floods in different sub-basins per percent.
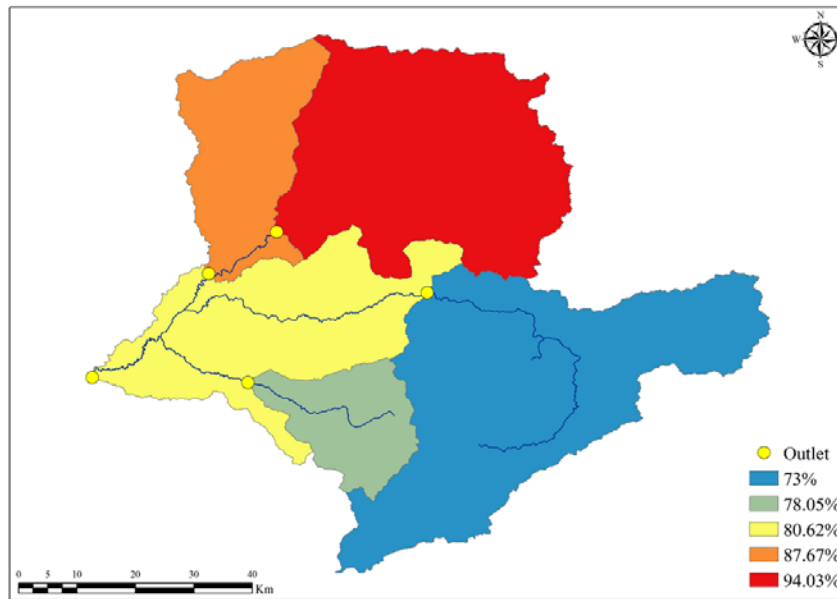
Fig. 4.13. LCLU contribution in Maximum flood peaks in different sub-basins per percent.

Model based LCLU impact assessment results are presented in the Table 4.13 and Figs 4.14 – 4.18. As it is clear from the table and graphs sub-basins have different condition compare to each other. A glimpse to the Fig 4.14 shows that greatest minimum is belong to Tamar sub-basin and after that Haji-ghushan. While, the smallest one is in Tangrah and Galikash, respectively. While, biggest maximum and mean discharges are in Gonbad followed by Haji-ghushan and Tamar. Galikash and Tangrah have the smallest one but their position is different in maximum and mean discharge graphs.

A detailed look in each sub-basin series separately shows that LCLU changes from 1972 to 2014 decreased the minimum of runoff in Tamar sub-basin. This trend is similar in Haji-ghushan and Gonbad sub-basins too. The minimum in Tangrah sub-basin is zero in the entire four-constructed model. While, in Galikash sub-basin the LCLU changes caused increase of minimum runoff (Fig. 4.15). Fig 4.16 present the impact of LCLU changes on mean of simulated surface runoff. From charts, it can be seen that LCLU changes caused increase in mean of daily discharge in all sub-basins. The results of maximum runoff analysis are summarized in Fig 4.17. As shown in figure Tamar, Haji-ghushan, Tangrah and Gonbad sub-basins present increase in maximum runoff regarding the change in LCLU. Whereas, in Galikash sub-basin the maximum of surface runoff decreased.
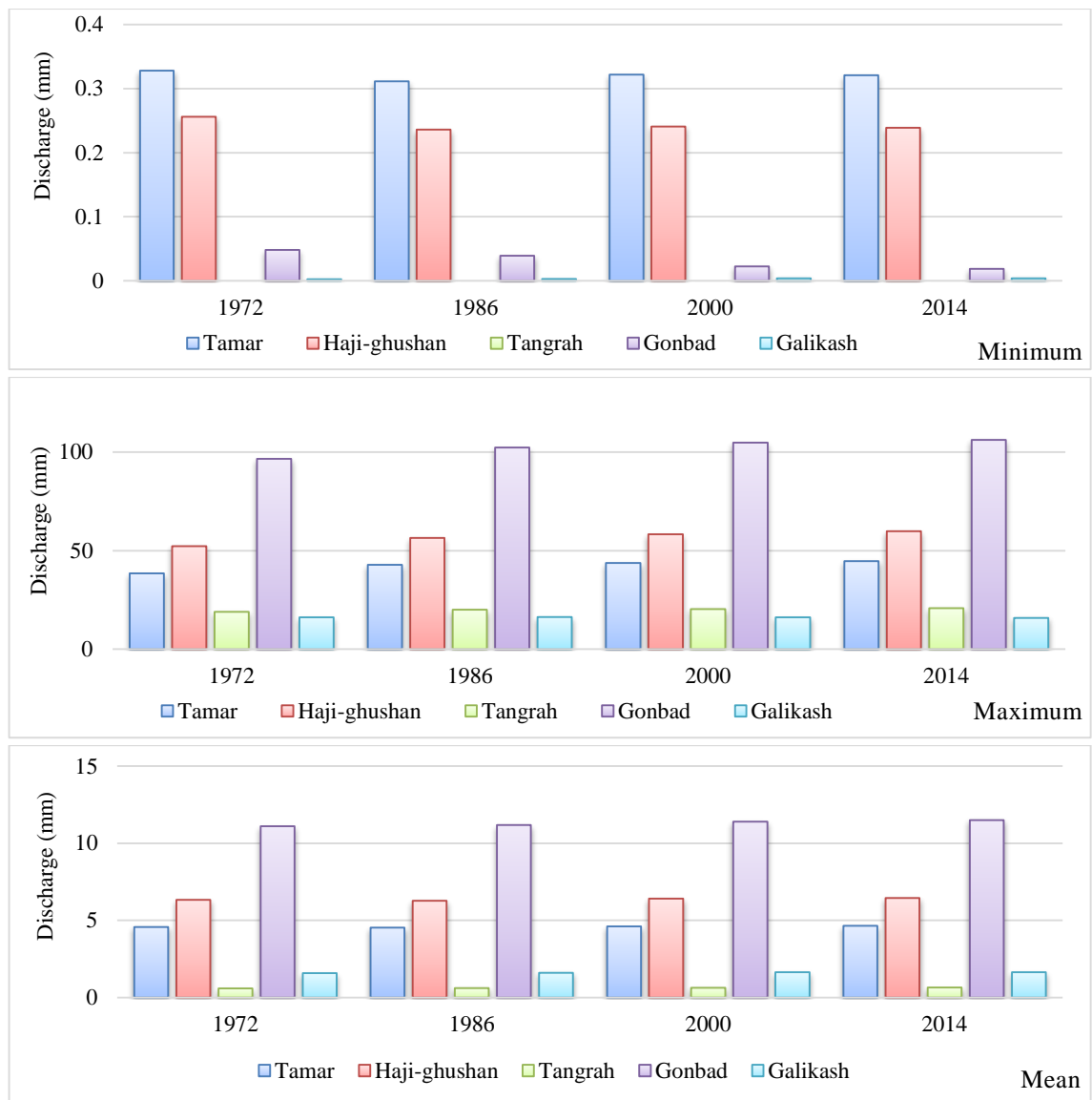
Fig. 4.14. Minimum, maximum and mean discharge in different sub-basins in four constructed model based on LCLU maps of 1972, 1986, 2000 and 2014.

Table 4.13. Daily maximum, minimum and mean of simulated series in sub-basins based on four LCLU maps.

|		1972	1986	2000	2014
Minimum	Sub1	0.33	0.31	0.32	0.32
	Sub2	0.26	0.24	0.24	0.24
	Sub3	0.00	0.00	0.00	0.00
	Sub4	0.05	0.04	0.02	0.02
	Sub5	0.00	0.00	0.00	0.00
Maximum	Sub1	38.45	42.83	43.76	44.72
	Sub2	52.19	56.52	58.36	59.83
	Sub3	18.95	20.11	20.43	20.89
	Sub4	96.53	102.27	104.77	106.21
	Sub5	16.19	16.37	16.25	15.90
Mean	Sub1	4.57	4.53	4.62	4.65
	Sub2	6.33	6.29	6.41	6.45
	Sub3	0.61	0.62	0.63	0.65
	Sub4	11.10	11.18	11.40	11.50
	Sub5	1.58	1.61	1.65	1.65
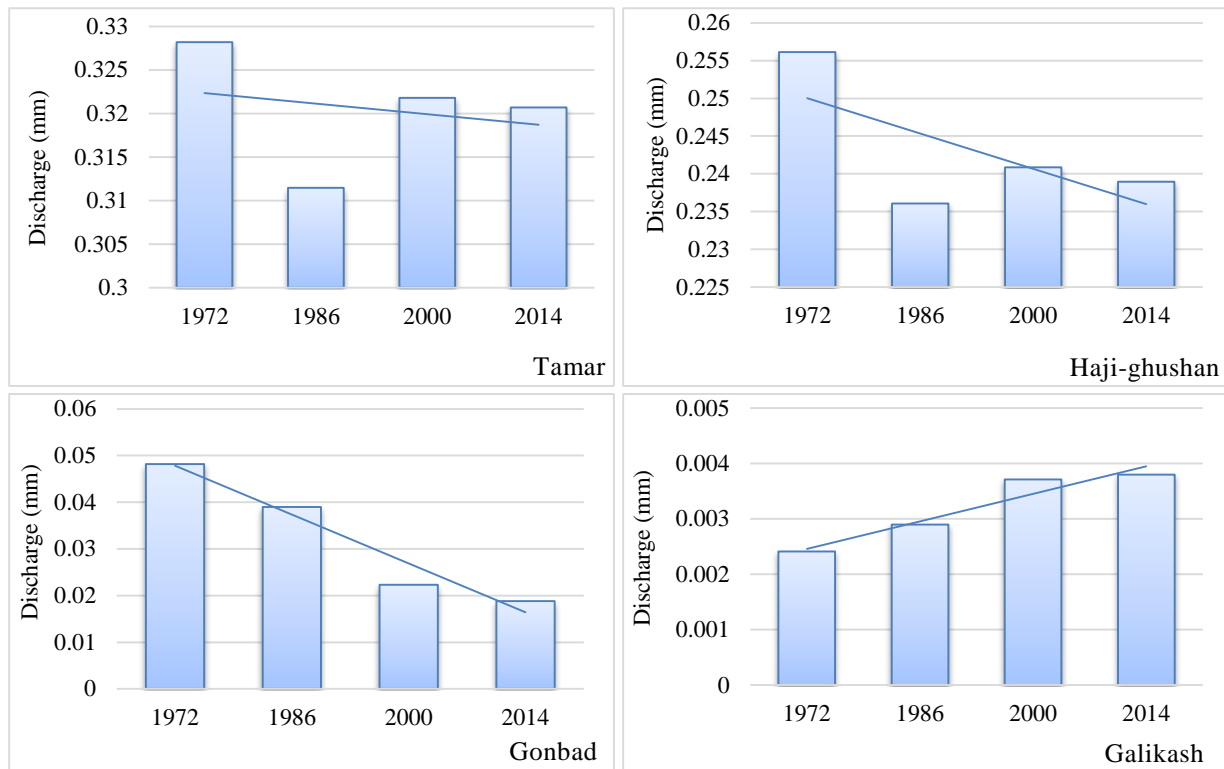
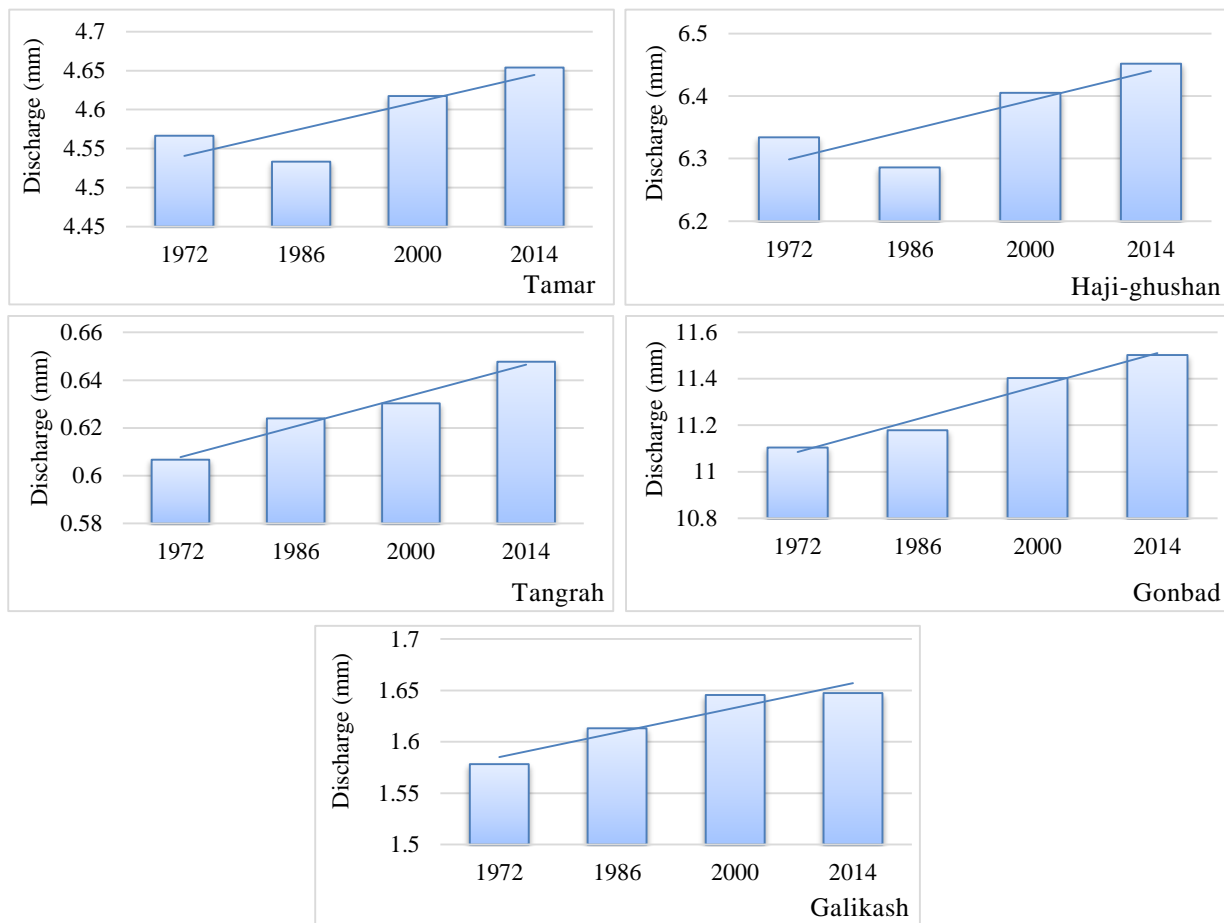Fig. 4.15. Minimum of simulated daily runoff in sub-basins during 1972-2014.

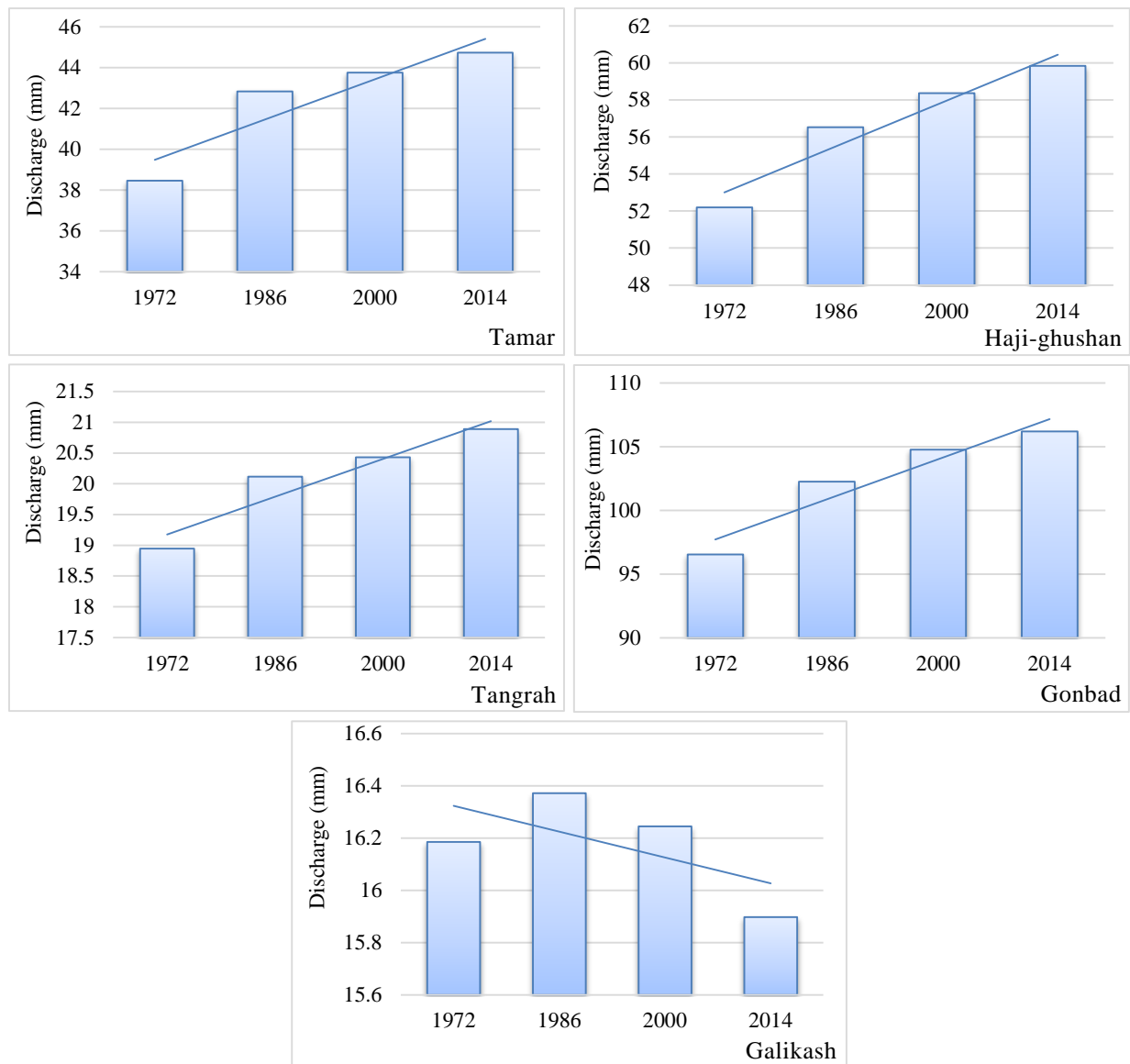Fig. 4.16. Mean of simulated daily runoff in sub-basins during 1972-2014.

Fig. 4.17. Maximum of simulated daily runoff in sub-basins during 1972-2014.

To provide better knowledge in case of LCLU change impacts on the minimum, maximum and mean of surface runoff the percent of change in each time interval are presented in the Fig 4.18. Regarding the minimum of daily runoff Tamar sub-basin experienced five percent reduction in the 1972 to 1986 but this negative percentage decreased in the next intervals. In Haji-ghushan, minimum runoff decreased about 7 percent in the first interval and the graphs shows that there is a slight variation during next intervals. The Tangrah sub-basin minimum as zero is stable in entire of period. While, Gonbad sub-basin graph reveals that there has been a steady rise in percent of minimum discharge reduction (~ 80%). At the end, the Galikash sub-basin graph shows that there has been a steep rise in minimum discharge increase.

Regarding the maximum discharges Tamar and Haji-ghushan sub-basins experienced greatest increase around 15% and followed by Tangrah and Gonbad sub-basins with 10% increase. However, the percentage of maximum daily runoff reduction

in Galikash sub-basin negative intensity. In the final analysis, the figure shows that increasing trends of mean daily discharges are stronger in Tangrah sub-basin (~ 6%) and followed by Tamar, Haji-ghushan, Galikash and Gonbad.
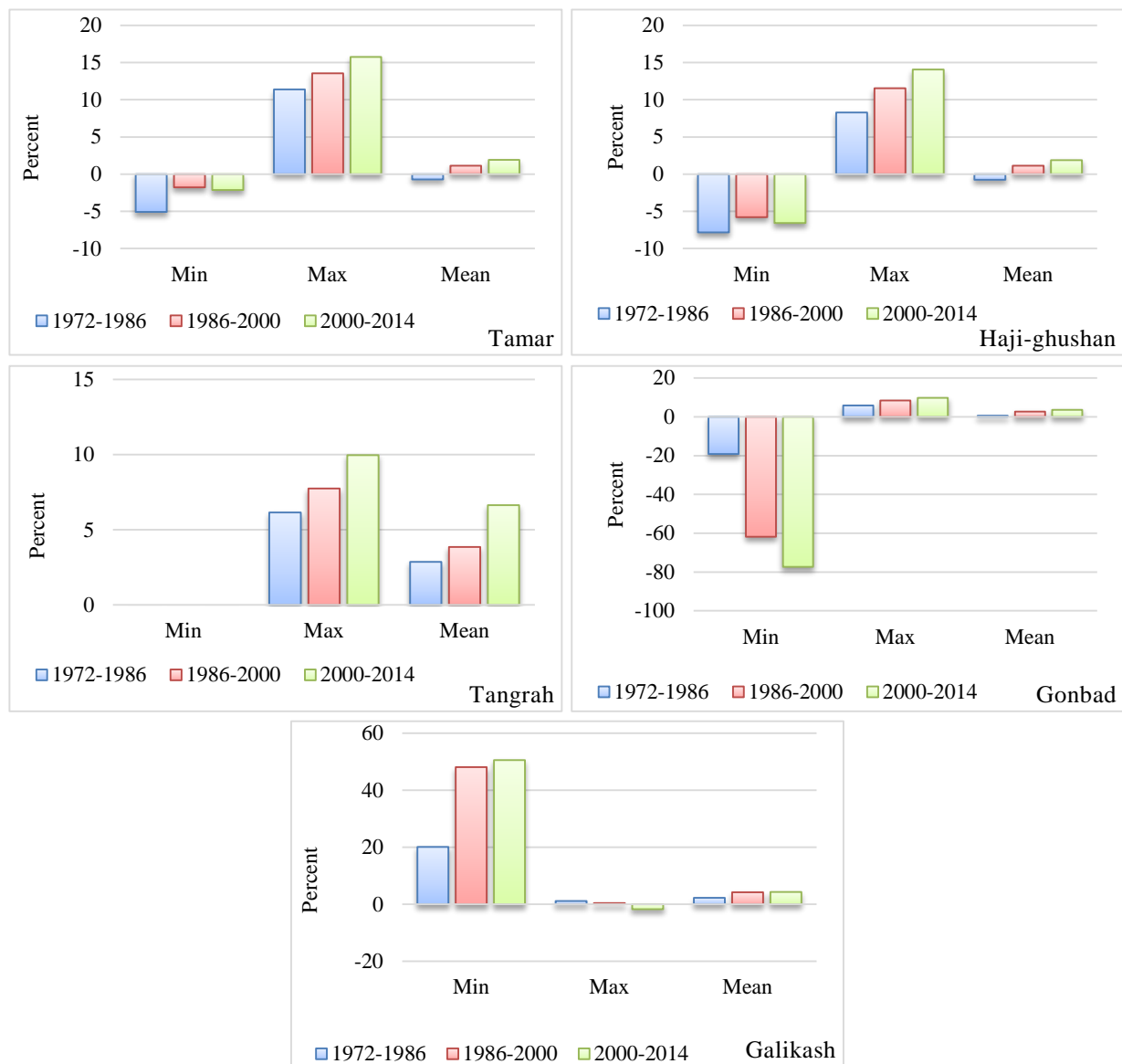
Fig. 4.18. Percentage of daily discharge changes in different sub-basins during LCLUC intervals.

4.4.   Conclusion

The aim of this section is to evaluate and compare the relations and impacts among flood hazards characteristics, CC and LCLUC. We used the historical discharge data to detect floods and providing floods characteristics. After evaluating and presenting the different flood characteristics associated with five gauges considered series, a statistical study was conducted.

The results of this investigation confirmed that in general the CC is more important and play the first role in 80% of sub-basins. The research has also shown that CC has the great impact of the mean of flood peaks in the south sub-basins, the floods frequency in the west and maximum flood peaks in the northeast of the watershed. Regarding the LCLU contribution in floods the biggest contribution for mean of flood peaks and floods frequency is in the low lands while for the maximum of flood peaks moves to the north and northeast sub-basins.

Detailed analysis of results revealed that in LCLU categories the built-up and farmlands had the great positive relation with increase in floods characteristics, but the percentage of significant contribution varying for built-up (60% to 99%) and farmland (60% to 98%) in different sub-basins. Whereas, even in some sub-basins their importance get too lower than this. In the same fashion, for the range and forest classes as the negative factors for flood hazard the percentage of contribution and its intensity varying in different sub-basins from too low to significant levels 60%-98% and 71%-95%, respectively. On other hand, the maximum impacts of CC are also different in sub-basins from 87% to 99%.

In addition, model based LCLU impact assessments were implemented to analysis the role of LCLU changes during these years. To reach to this goal four model based four LCLU map were constructed. The results reveal that LCLU changes caused decrease of minimum discharge in three sub-basin and increase in one sub-basin. However, the mean of discharge increased in all sub-basins by happened changes in LCLU class areas. After all, LCLU changes caused increase in the maximum of daily discharge that could be the most important element in floods considered studies in four sub-basins whereas, it caused reduction in one sub-basin. In addition, it should be mentioned that the greatest role of LCLU changes is in increasing the maximum daily runoff values.

Which factor(s) control floods from the past to the present?

As the result of this section both CC and LCLU factors have important role in floods from past to the present, but the CC play greater role in entire of the basin.

Chapter 5

Conclusion and Summary

> *This chapter as the last one will include the answers to the objectives by the knowledge arising from the results and findings of this research. It will explain some limitations and suggest some directions for probable future works in this filed.*

5.1.   General conclusion and discussion

Flood hazards are the most common and destructive of all natural disasters (Kellens et al. 2013). This fact is also true for the Gorganrood watershed. Flood as a hazard that cause tremendous losses and social disruption worldwide each year, need to be delineated and identified for possible measures to mitigate potential impacts. GISci or GIScience as the abbreviation of Geographic Information Science contains the existing technologies and research areas of geographic information systems (GIS), remote sensing, cartography and quantitative spatial analysis (Walsh, 2015). GIScience, therefore, addresses fundamental issues in the use of digital technology to handle geographic information; namely, information about places, activities and phenomena on and near the surface of the Earth that are stored in maps or images (http://www.geo.oregonstate.edu/gcert) that provides a great foundation for flood hazard studies.

This thesis is compiled in five chapters. The first chapter introduces basics and fundamentals of research include problem statement, research question, research objectives, motivation, methodology and so on. Chapter 2 covered the first section of GIScience procedure for flood hazards assessment in relation to LCLU and CC. in this chapter hydro-meteorological data were analyzed spatially and temporally. Chapter 3 illustrates the LCLU status and dynamics with a comprehensive methodology to prepare deep knowledge about the LCLU changes. Chapter 4 by detecting and analyzing floods characteristics as the last part of the methodology prepared a base to assemble the outcomes from all sections. Ultimately, the relations were assessed and the percentage of contributions of LCLU and CC were assessed. Chapter 5 will elucidate conclusions

and discuss the research objectives. Afterwards, limitations of this thesis are explained and subsequently the suggested direction of future works and recommendations will be presented.

After all, this study set out to analyses and evaluates role of LCLU and CC in flood hazards that is an important issue for a wide range of public, scientific and governmental section of society in the study area. The key strengths of this study that make it different and new from previous studies is that it evaluate the LCLU and CC impacts on the floods together and by both statistical and modelling methods. Published researches did not cover entire of the study area and the analysis period, variables and provided maps are less than this study. In general, therefore, this is the first study to investigate the effect of LCLU and CC in the study area with a systematic, comprehensive and holistic procedure. In light of these considerations, the study has gone some way towards enhancing our understandings of flood hazard in this region and will serves as a base for future studies too.

5.1.1. Objectives

Objective 1: To map and analyze LCLU changes and dynamics in the study area

Application of GIS integrated with remote sensing played a great role in recognizing, classifying and investigating the distribution of LCLU classes. The study area has six categories include bare land, built-up, farmland, forest, range and water. Four Landsat images from 1972 to 2014 were selected in path/row 162/34. The LCLU in the area firstly detected by supervised pixel-based and GEOBIA remote sensing techniques. In pixel-based classification, the maximum likelihood and neural network classifiers provide final map and for the GEOBIA using data mining technique and rule base generation, the image were classified. Afterward, with creating transition matrix, trend surface analysis and intensity analysis in different levels the spatio-temporal dynamics and characteristics of changes were investigated that provide very good knowledge in case of LCLU of the region that can play a great role in geographical and environmental studies of the watershed. In one hand, the farmland category has the greatest increase and is the dominant LCLU in the watershed nowadays. In addition, built-up increased to 9000 hectares while both of them will increase the risk of flood hazards. On other hand, the forest and range categories experienced reduction that it shows less ecosystem service ability in the watershed.

Finally, it should be mentioned that the application of the GIS spatial analysis to investigate changes and dynamics and resistances combined by multi-temporal imagery to monitor the LCLU dynamics offers advance chances for exhaustive explanation of LCLU by means of earth observation data that is an important component in the planning and management of watershed.

Objective 2: To detect trends in hydro-meteorological data.

Trends in hydro-meteorological time series were investigated in different scale as daily, monthly and yearly. Precipitation had experienced changes that could increase the flood risks in the study area. Daily, monthly and yearly precipitation in some stations have upward trend. This trend in yearly series is stronger than daily ones. Temperatures include minimum, maximum and mean had changes that will affect hydrology cycle. Maximum temperature experienced increase in monthly series. Minimum temperature have both upward and downward trend in the daily series. In highlands, Robat-gharabil station gets cooler while Tamar in low lands have upward trend. In monthly series there is not any decreasing trend and Gonbad, Tamar and Cheshme-khan have upward trends and in yearly scale Gonbad and Tamar. Mean temperature have also increasing trends in daily, monthly and yearly series that this increase in monthly series is more spatial distributed. In case of trend intensity, they are more intense in the yearly scale and among temperatures stronger in minimum temperature. Discharge trend analysis shows decrease in 80% of daily data. However, in the monthly and yearly data just 40% of stations present downward trends. These trend and changes means climate change and variation happened in the region and have their impacts on the environment, hydrological cycle, ecosystem service and human life.

Objective 3: To investigate LUCC and CC impacts on floods within the catchment.

The results of this investigation confirmed that in general the CC played the first role in 80% of sub-basins. The research has also shown that CC has the great impact of the mean of flood peaks in the south sub-basins, the floods frequency in the west and maximum flood peaks in the northeast of the watershed. Regarding the LCLU contribution in floods the biggest contribution for mean of flood peaks and floods frequency is in the low lands while for the maximum of flood peaks moves to the north and northeast sub-basins.

Detailed analysis of results revealed that in LCLU categories the built-up and farmlands had the great positive relation with increase in floods characteristics, but the percentage of significant contribution varying for built-up (60% to 99%) and farmland (60% to 98%) in different sub-basins. Whereas, even in some sub-basins their importance get too lower than these do. In the same fashion, for the range and forest classes as the negative factors for flood hazard the percentage of contribution and its intensity varying in different sub-basins from too low to significant levels 60%-98% and 71%-95%, respectively. On other hand, the maximum impacts of CC are also different in sub-basins from 87% to 99%.

5.2. Limitations of the present study

Although, this research was carefully designed and implemented, there were some unavoidable weaknesses:

First, Limitation of remotely sensed images with better spectral and spatial resolution to provide more accurate and detailed LCLU maps.

Second, using the hydro-meteorological data in daily series and limited stations that have less quality in comparison to 3hour or hourly time series with more stations.

5.3.   Directions for future works

This watershed is very important in several viewpoints. Agricultural production, valuable soils, living of about 600 thousand people who are under floods risks in the study area, locating Golestan national park as a UNESCO heritage site in this region with valuable and old forests, high diversity of flora and fauna and endangered species that can be suffered from floods, CC and LCLUC are some important viewpoint. In this regard, more researches are necessary and valuable from several aspects. The findings of this study provide a great worth knowledge in case of environmental conditions and dynamics in the region that could be a strong basement for a big collection of studies.

Regarding the floods hazards and risk analysis, we suggest that use the physical hydrological models to investigate the relations between floods, CC and LCLU and provide better understand in the modeling way too. It would be interesting to simulate the future LCLU and using IPCC scenarios to investigate future conditions of CC and investigate their impacts on the flood hazards in the future.

Bibliography:

Abbaszadeh Tehrani, N., Makhdoum, M. F., & Mahdavi, M. (2011). Studying the Impacts of Land Use Changes on Flood Flows by Using Remote Sensing(RS) and Geographical Information System (GIS) Techniques- a Case Study in Dough River Watershed, Northeast of Iran. *Environmental Research, 1*(2), 1-14.

Abd El-Kawy, O. R., Rød, J. K., Ismail, H. A., & Suliman, A. S. (2011). Land use and land cover change detection in the western Nile delta of Egypt using remote sensing data. *Applied Geography, 31*(2), 483-494. doi: http://dx.doi.org/10.1016/j.apgeog.2010.10.012

Abghari, H., Tabari, H., & Hosseinzadeh Talaee, P. (2013). River flow trends in the west of Iran during the past 40 years: Impact of precipitation variability. *Global and Planetary Change, 101*(0), 52-60. doi: http://dx.doi.org/10.1016/j.gloplacha.2012.12.003

Abino, A. C., Kim, S. Y., Jang, M. N., Lee, Y. J., & Chung, J. S. (2015). Assessing land use and land cover of the Marikina sub-watershed, Philippines. *Forest Science and Technology, 11*(2), 65-75. doi: 10.1080/21580103.2014.957353

Addink, E. A., Van Coillie, F. M. B., & de Jong, S. M. (2012). Introduction to the GEOBIA 2010 special issue: From pixels to geographic objects in remote sensing image analysis. *International Journal of Applied Earth Observation and Geoinformation, 15*, 1-6. doi: 10.1016/j.jag.2011.12.001

Adhikari, S., Southworth, J., & Nagendra, H. (2014). Understanding forest loss and recovery: a spatiotemporal analysis of land change in and around Bannerghatta National Park, India. *Journal of Land Use Science*, 1-23. doi: 10.1080/1747423x.2014.920425

Aldwaik, S. Z., & Pontius Jr, R. G. (2012). Intensity analysis to unify measurements of size and stationarity of land changes by interval, category, and transition. *Landscape and Urban Planning, 106*(1), 103-114. doi: http://dx.doi.org/10.1016/j.landurbplan.2012.02.010

Aldwaik, S. Z., & Pontius Jr, R. G. (2013). Map errors that could account for deviations from a uniform intensity of land change. *International Journal of Geographical Information Science, 27*(9), 1717-1739. doi: 10.1080/13658816.2013.787618

Alexandersson, H. (1986). A homogeneity test applied to precipitation data. *Journal of Climatology, 6*(6), 661-675. doi: 10.1002/joc.3370060607

Alsamamra, H., Ruiz-Arias, J. A., Pozo-Vazquez, D., & Tovar-Pescador, J. (2009). A comparative study of ordinary and residual kriging techniques for mapping global solar radiation over southern Spain. *Agricultural and Forest Meteorology, 149*(8), 1343-1357. doi: 10.1016/j.agrformet.2009.03.005

ArcGIS Help. (2014). Fundamentals of panchromatic sharpening. Retrieved 11.03.2015, 2015, from http://resources.arcgis.com/en/help/main/10.1/index.html#//009t000000mw000000

Arnold, J. G., Srinivasan, R., Muttiah, R. S., & Williams, J. R. (1998). Large area hydrologic modeling and assessment - Part 1: Model development. *Journal of the American Water Resources Association, 34*(1), 73-89. doi: DOI 10.1111/j.1752-1688.1998.tb05961.x

Arundel, S. T. (2005). Using spatial models to establish climatic limiters of plant species' distributions. *Ecological Modelling, 182*(2), 159-181. doi: 10.1016/j.ecolmodel.2004.07.016

Attorre, F., Alfo, M., De Sanctis, M., Francesconi, F., & Bruno, F. (2007). Comparison of interpolation methods for mapping climatic and bioclimatic variables at regional scale. *International Journal of Climatology, 27*(13), 1825-1843. doi: 10.1002/joc.1495

Baatz, M., & Schäpe, M. (2000). Multiresolution segmentation – an optimization approach for high quality multi-scale image segmentation. In J. Strobl, T. Blaschke, & G. Griesebner (Eds.), *Angewandte Geographische Informations-Verarbeitung* (Vol. XII, pp. 12–23): Wichmann Verlag, Karlsruhe

Bakr, N., Weindorf, D. C., Bahnassy, M. H., Marei, S. M., & El-Badawi, M. M. (2010). Monitoring land cover changes in a newly reclaimed area of Egypt using multi-temporal Landsat data. *Applied Geography, 30*(4), 592-605. doi: http://dx.doi.org/10.1016/j.apgeog.2009.10.008

Ben Aissia, M. A., Chebana, F., Ouarda, T. B. M. J., Roy, L., Desrochers, G., Chartier, I., & Robichaud, E. (2012). Multivariate analysis of flood characteristics in a climate change context of the watershed of the Baskatong reservoir, Province of Quebec, Canada. *Hydrological Processes, 26*(1), 130-142.

Benavides, R., Montes, F., Rubio, A., & Osoro, K. (2007). Geostatistical modelling of air temperature in a mountainous region of Northern Spain. *Agricultural and Forest Meteorology, 146*(3-4), 173-188. doi: 10.1016/j.agrformet.2007.05.014

Berakhi, R. O., Oyana, T. J., & Adu-Prah, S. (2014). Land use and land cover change and its implications in Kagera river basin, East Africa. *African Geographical Review, 34*(3), 209-231. doi: 10.1080/19376812.2014.912140

Berezovskaya, S., Yang, D., & Kane, D. L. (2004). Compatibility analysis of precipitation and runoff trends over the large Siberian watersheds. *Geophysical Research Letters, 31*(21), L21502. doi: 10.1029/2004GL021277

Biswal, S., Ghosh, A., Sharma, R., & Joshi, P. K. (2013). Satellite Data Classification Using Open Source Support. *Journal of the Indian Society of Remote Sensing, 41*(3), 523-530. doi: DOI 10.1007/s12524-013-0265-4

Blaschke, T. (2010). Object based image analysis for remote sensing. *Isprs Journal of Photogrammetry and Remote Sensing, 65*(1), 2-16. doi: DOI 10.1016/j.isprsjprs.2009.06.004

Blaschke, T., Feizizadeh, B., & Holbling, D. (2014). Object-Based Image Analysis and Digital Terrain Analysis for Locating Landslides in the Urmia Lake Basin, Iran. *IEEE Journal of Selected Topics in Applied Earth Observations and Remote Sensing, 7*(12), 4806-4817. doi: 10.1109/Jstars.2014.2350036

Boi, P., Fiori, M., & Canu, S. (2011). High spatial resolution interpolation of monthly temperatures of Sardinia. *Meteorological Applications, 18*(4), 475-482. doi: 10.1002/met.243

Bormann, H., Pinter, N., & Elfert, S. (2011). Hydrological signatures of flood trends on German rivers: Flood frequencies, flood heights and specific stages. *Journal of Hydrology, 404*(1–2), 50-66. doi: http://dx.doi.org/10.1016/j.jhydrol.2011.04.019

Bossa, A. Y., Diekkruger, B., & Agbossou, E. K. (2014). Scenario-Based Impacts of Land Use and Climate Change on Land and Water Degradation from the Meso to Regional Scale. *Water, 6*(10), 3152-3181. doi: 10.3390/w6103152

Box, G. E. P., & Pierce, D. A. (1970). Distribution of Residual Autocorrelations in Autoregressive-Integrated Moving Average Time Series Models. *Journal of the American Statistical Association, 65*(332), 1509-1526. doi: 10.2307/2284333

Bronstert, A., Niehoff, D., & Burger, G. (2002). Effects of climate and land-use change on storm runoff generation: present knowledge and modelling capabilities. *Hydrological Processes, 16*(2), 509-529. doi: Doi 10.1002/Hyp.326

Buishand, T. A. (1982). Some methods for testing the homogeneity of rainfall records. *Journal of Hydrology, 58*(1–2), 11-27. doi: http://dx.doi.org/10.1016/0022-1694(82)90066-X

Buishand, T. A., De Martino, G., Spreeuw, J. N., & Brandsma, T. (2013). Homogeneity of precipitation series in the Netherlands and their trends in the past century. *International Journal of Climatology, 33*(4), 815-833. doi: 10.1002/joc.3471

Canty, M., Niemeyer, I., Richter, B., & Stein, G. (1999). Wide-area change detection: The use of multitemporal Landsat images for nuclear safeguards. *JNMM, Journal of the Institute of Nuclear Materials Management, 27*(2), 19-24.

Capparelli, V., Franzke, C., Vecchio, A., Freeman, M. P., Watkins, N. W., & Carbone, V. (2013). A spatiotemporal analysis of U.S. station temperature trends over the last century. *Journal of Geophysical Research: Atmospheres, 118*(14), 7427-7434. doi: 10.1002/jgrd.50551

Chapin Iii, F. S., Zavaleta, E. S., Eviner, V. T., Naylor, R. L., Vitousek, P. M., Reynolds, H. L., . . . Diaz, S. (2000). Consequences of changing biodiversity. *Nature, 405*(6783), 234-242.

Chapman, T. (1999). A comparison of algorithms for stream flow recession and baseflow separation. *Hydrological Processes, 13*(5), 701-714. doi: Doi 10.1002/(Sici)1099-1085(19990415)13:5<701::Aid-Hyp774>3.0.Co;2-2

Chapman, T. G. (1991). Evaluation of Automated Techniques for Base-Flow and Recession Analyses - Comment. *Water Resources Research, 27*(7), 1783-1784. doi: Doi 10.1029/91wr01007

Chavez, P. S. (1989). Radiometric Calibration of Landsat Thematic Mapper Multispectral Images. *Photogrammetric Engineering and Remote Sensing, 55*(9), 1285-1294.

Chebana, F., Ouarda, T. B. M. J., & Duong, T. C. (2013). Testing for multivariate trends in hydrologic frequency analysis. *Journal of Hydrology, 486*(0), 519-530. doi: http://dx.doi.org/10.1016/j.jhydrol.2013.01.007

Chen, C. F., Yue, T. X., Dai, H. L., & Tian, M. Y. (2013). The smoothness of HASM. *International Journal of Geographical Information Science, 27*(8), 1651-1667. doi: 10.1080/13658816.2013.787146

Cleveland, W. S. (1994). *The Elements of Graphing Data*. P.O. Box 1473, Summit N.J. 07902-1473, U.S.A.: Hobart Press,.

Crawford, C. J., Manson, S. M., Bauer, M. E., & Hall, D. K. (2013). Multitemporal snow cover mapping in mountainous terrain for Landsat climate data record development. *Remote Sensing of Environment, 135*, 224-233. doi: 10.1016/j.rse.2013.04.004

Cristobal, J., Ninyerola, M., & Pons, X. (2008). Modeling air temperature through a combination of remote sensing and GIS data. *Journal of Geophysical Research-Atmospheres, 113*(D13), 1-13. doi: Artn D13106

10.1029/2007jd009318

Cunderlik, J. M., & Ouarda, T. B. M. J. (2009). Trends in the timing and magnitude of floods in Canada. *Journal of Hydrology, 375*(3–4), 471-480. doi: http://dx.doi.org/10.1016/j.jhydrol.2009.06.050

Dan Steinberg, M. G. (2006). *CART 6.0 User's Manual.* San Diego: CA: Salford Systems.

Dan Steinberg, P. C. (1997). *Cart-Classification and Regression Tree*. San Diego: CA: Salford Systems.

Danneberg, J. (2012). Changes in runoff time series in Thuringia, Germany – Mann-Kendall trend test and extreme value analysis. *Advances in Geosciences, 31*, 49-56. doi: 10.5194/adgeo-31-49-2012

Das, T. (2009). *Land Use / Land Cover Change Detection: an Object Oriented Approach, Münster, Germany.* (Master of Science (M.Sc.)), University of Münster

Davids, C., & Doulgeris, A. (2007). *Unsupervised change detection of multitemporal Landsat imagery to identify changes in land cover following the Chernobyl accident.* Paper presented at the International Geoscience and Remote Sensing Symposium (IGARSS).

De Roo, A., Odijk, M., Schmuck, G., Koster, E., & Lucieer, A. (2001). Assessing the effects of land use changes on floods in the Meuse and Oder catchment. *Physics and Chemistry of the Earth Part B-Hydrology Oceans and Atmosphere, 26*(7-8), 593-599.

De Roo, A., Schmuck, G., Perdigao, V., & Thielen, J. (2003). The influence of historic land use changes and future planned land use scenarios on floods in the Oder catchment. *Physics and Chemistry of the Earth, 28*(33-36), 1291-1300.

Delbari, M., Afrasiab, P., & Jahani, S. (2013). Spatial interpolation of monthly and annual rainfall in northeast of Iran. *Meteorology and Atmospheric Physics, 122*(1-2), 103-113. doi: 10.1007/s00703-013-0273-5

Dingle Robertson, L., & King, D. J. (2011). Comparison of pixel- and object-based classification in land cover change mapping. *International Journal of Remote Sensing, 32*(6), 1505-1529. doi: 10.1080/01431160903571791

Douglas, E. M., Vogel, R. M., & Kroll, C. N. (2000). Trends in floods and low flows in the United States: impact of spatial correlation. *Journal of Hydrology, 240*(1–2), 90-105. doi: http://dx.doi.org/10.1016/S0022-1694(00)00336-X

Dozier, J. (1989). Spectral Signature of Alpine Snow Cover from the Landsat Thematic Mapper. *Remote Sensing of Environment, 28*, 9-&. doi: Doi 10.1016/0034-4257(89)90101-6

Dragut, L., Tiede, D., & Levick, S. R. (2010). ESP: a tool to estimate scale parameter for multiresolution image segmentation of remotely sensed data. *International*

Journal of Geographical Information Science, 24(6), 859-871. doi: 10.1080/13658810903174803

Du, J. K., Qian, L., Rui, H. Y., Zuo, T. H., Zheng, D. P., Xu, Y. P., & Xu, C. Y. (2012). Assessing the effects of urbanization on annual runoff and flood events using an integrated hydrological modeling system for Qinhuai River basin, China. *Journal of Hydrology, 464*, 127-139. doi: DOI 10.1016/j.jhydrol.2012.06.057

Eckhardt, K. (2005). How to construct recursive digital filters for baseflow separation. *Hydrological Processes, 19*(2), 507-515. doi: 10.1002/hyp.5675

El Kenawy, A., López-Moreno, J. I., Stepanek, P., & Vicente-Serrano, S. M. (2013). An assessment of the role of homogenization protocol in the performance of daily temperature series and trends: application to northeastern Spain. *International Journal of Climatology, 33*(1), 87-108. doi: 10.1002/joc.3410

El Kenawy, A., López-Moreno, J. I., & Vicente-Serrano, S. M. (2012). Trend and variability of surface air temperature in northeastern Spain (1920–2006): Linkage to atmospheric circulation. *Atmospheric Research, 106*(0), 159-180. doi: http://dx.doi.org/10.1016/j.atmosres.2011.12.006

Enaruvbe, G. O., & Pontius, R. G. (2015). Influence of classification errors on Intensity Analysis of land changes in southern Nigeria. *International Journal of Remote Sensing, 36*(1), 244-261. doi: 10.1080/01431161.2014.994721

Erdenetuya, M., Khishigsuren, P., Davaa, G., & Otgontugs, M. (2006). *Glacier change estimation using Landsat TM data.* Paper presented at the Proceedings of the ISPRS Tokyo 2006 Symposium Technical Commission VI

ESRI. (2001). *Getting Started with ArcGIS*: ESRI Press.

Exelis VIS, p. d. c. (2015). Radiometric Calibration. from http://www.exelisvis.com/docs/RadiometricCalibration.html

Farooq, A. (2015). Spectral Reflectance of Land Covers. Retrieved 23 July 2015, from http://www.geol-amu.org/notes/m1r-1-8.htm

Fortin, G., & Hétu, B. (2014). Estimating winter trends in climatic variables in the Chic-Chocs Mountains, Canada (1970-2009). *International Journal of Climatology, 34*(10), 3078-3088. doi: 10.1002/joc.3895

Gao, Y., & Mas, J. F. (2008). A Comparison of the Performance of Pixel Based and Object Based Classifications over Images with Various Spatial Resolutions. *ISPRS Archives, XXXVIII-4/C1*, 1-6.

Gebremicael, T. G., Mohamed, Y. A., Betrie, G. D., van der Zaag, P., & Teferi, E. (2013). Trend analysis of runoff and sediment fluxes in the Upper Blue Nile basin: A combined analysis of statistical tests, physically-based models and landuse maps. *Journal of Hydrology, 482*(0), 57-68. doi: http://dx.doi.org/10.1016/j.jhydrol.2012.12.023

Ghalkhani, H., Golian, S., Saghafian, B., Farokhnia, A., & Shamseldin, A. (2013). Application of surrogate artificial intelligent models for real-time flood routing. *Water and Environment Journal, 27*(4), 535-548. doi: 10.1111/j.1747-6593.2012.00344.x

Ghezelsofloo, A., Deiminiat, A., Shojaee, H., & Lotfi, R. (2010). On the experience of flood control schemes application in the Golestan province (Iran)Environmental Hydraulics (pp. 1-6).

Gocic, M., & Trajkovic, S. (2013). Analysis of changes in meteorological variables using Mann-Kendall and Sen's slope estimator statistical tests in Serbia. *Global and Planetary Change, 100*(0), 172-182. doi: http://dx.doi.org/10.1016/j.gloplacha.2012.10.014

Hadiani, M. O., & Ebadi, A. G. (2007). The Role of Land Use Changing in Uncertainty of Design Flood of Hydraulic Structures (The Case Study about Madarsoo Watershed Basin). *World Appl. Sci. J., 2*(2), 136-141.

Hall, M., Frank, E., Holmes, G., Pfahringer, B., Reutemann, P., & Witten, I. H. (2009). The WEKA data mining software: an update. *SIGKDD Explor. Newsl., 11*(1), 10-18. doi: 10.1145/1656274.1656278

Hancock, S., Baxter, R., Evans, J., & Huntley, B. (2013). Evaluating global snow water equivalent products for testing land surface models. *Remote Sensing of Environment, 128*, 107-117. doi: 10.1016/j.rse.2012.10.004

Hartmann, H., & Andresky, L. (2013). Flooding in the Indus River basin — A spatiotemporal analysis of precipitation records. *Global and Planetary Change, 107*(0), 25-35. doi: http://dx.doi.org/10.1016/j.gloplacha.2013.04.002

Hasan, A., & Schorr, P. (2012). Trend Analysis of Precipitation and Runoff As a Basis of Design and Operation of Pumped Storage Water Supply Infrastructure in New Jersey *World Environmental and Water Resources Congress 2012* (pp. 1559-1564).

Hengl, T., Heuvelink, G. B. M., Tadic, M. P., & Pebesma, E. J. (2012). Spatio-temporal prediction of daily temperatures using time-series of MODIS LST images. *Theoretical and Applied Climatology, 107*(1-2), 265-277. doi: 10.1007/s00704-011-0464-2

Heo, J., Yu, J., Giardino, J. R., & Cho, H. (2015). Impacts of climate and land-cover changes on water resources in a humid subtropical watershed: a case study from East Texas, USA. *Water and Environment Journal, 29*(1), 51-60. doi: 10.1111/wej.12096

Hosseini Asl, A., Matkan, A. A., Javid, F., & Pourali, H. (2008). establishing a Basic GIS Database for Madarsoo Watershed in Golestan (Iran). *Evironmental science, 5*(2), 87-99.

Hosseinzadeh, S. R., & Jahadi Toroghi, M. (2007). Geomorphologic analysis of catastrophic floods of Madarsoo river (north-eastern Iran). *Journal of Geography and regional development, 7*, 89-115.

Houston, J. (2006). Variability of precipitation in the Atacama Desert: its causes and hydrological impact. *International Journal of Climatology, 26*(15), 2181-2198. doi: 10.1002/joc.1359

http://www.kuleuven.be/hydr/pwtools.htm. (2014). Water engineering tools. 2015, from http://www.kuleuven.be/hydr/pwtools.htm

http://www.kuleuven.be/wieiswie/en/person/u0009249. (2014). Water engineering tools. 2015, from http://www.kuleuven.be/hydr/pwtools.htm

Huang, J., Pontius Jr, R. G., Li, Q., & Zhang, Y. (2012). Use of intensity analysis to link patterns with processes of land change from 1986 to 2007 in a coastal watershed of southeast China. *Applied Geography, 34*(0), 371-384. doi: http://dx.doi.org/10.1016/j.apgeog.2012.01.001

Huang, J., Sun, S., & Zhang, J. (2013). Detection of trends in precipitation during 1960–2008 in Jiangxi province, southeast China. *Theoretical and Applied Climatology, 114*(1-2), 237-251. doi: 10.1007/s00704-013-0831-2

Ishak, E. H., Rahman, A., Westra, S., Sharma, A., & Kuczera, G. (2013). Evaluating the non-stationarity of Australian annual maximum flood. *Journal of Hydrology, 494*(0), 134-145. doi: http://dx.doi.org/10.1016/j.jhydrol.2013.04.021

Jabot, E., Zin, I., Lebel, T., Gautheron, A., & Obled, C. (2012). Spatial interpolation of sub-daily air temperatures for snow and hydrologic applications in mesoscale Alpine catchments. *Hydrological Processes, 26*(17), 2618-2630. doi: 10.1002/hyp.9423

Jano, A. P., Jefferies, R. L., & Rockwell, R. F. (1998). Erratum: The detection of vegetational change by multitemporal analysis of LANDSAT data: The effects of goose foraging (Journal of Ecology (1998) 86 (93-99)). *Journal of Ecology, 86*(2), 362.

Jha, M. K., & Singh, A. K. (2013). Trend analysis of extreme runoff events in major river basins of Peninsular Malaysia. *International Journal of Water, 7*(1-2), 142-158.

Joseph, R., Ting, M., & Kumar, P. (2000). Multiple-Scale Spatio–Temporal Variability of Precipitation over the Coterminous United States. *Journal of Hydrometeorology, 1*(5), 373-392. doi: 10.1175/1525-7541(2000)001<0373:MSSTVO>2.0.CO;2

Joyce, K. E., Wright, K. C., Samsonov, S. V., & Ambrosia, V. G. (2009). Remote sensing and the disaster management cycle. In G. Jedlovec (Ed.), *Advances in Geoscience and Remote Sensing* (pp. 317-346): InTech.

Kalivas, D. P., Kollias, V. J., & Apostolidis, E. H. (2013). Evaluation of three spatial interpolation methods to estimate forest volume in the municipal forest of the Greek island Skyros. *Geo-Spatial Information Science, 16*(2), 100-112. doi: 10.1080/10095020.2013.766398

Kang, H. M., & Yusof, F. (2012). Homogeneity Tests on Daily Rainfall Series in Peninsular Malaysia. *Int. J. Contemp. Math. Sciences, 7*(1), 9-23.

Kellens, W., Terpstra, T., & De Maeyer, P. (2013). Perception and Communication of Flood Risks: A Systematic Review of Empirical Research. *Risk Analysis, 33*(1), 24-49. doi: 10.1111/j.1539-6924.2012.01844.x

Klein, A. G., & Isacks, B. L. (1999). Spectral mixture analysis of Landsat thematic mapper images applied to the detection of the transient snowline on tropical Andean glaciers. *Global and Planetary Change, 22*(1-4), 139-154. doi: Doi 10.1016/S0921-8181(99)00032-6

Kliment, Z., Matouskava, M., Ledvinka, O., & Kralovec, V. (2011). Trend Analysis Of Rainfall-Runoff Regimes In Selected Headwater Areas Of The Czech Republic. *J. Hydrol. Hydromech, 59*(1), 36-50. doi: DOI: 10.2478/v10098-011-0003-y

Kolios, S., & Stylios, C. D. (2013). Identification of land cover/land use changes in the greater area of the Preveza peninsula in Greece using Landsat satellite data. *Applied Geography, 40*(0), 150-160. doi: http://dx.doi.org/10.1016/j.apgeog.2013.02.005

Kousari, M. R., Ahani, H., & Hendi-zadeh, R. (2013). Temporal and spatial trend detection of maximum air temperature in Iran during 1960–2005. *Global and*

Planetary Change, 111(0), 97-110. doi: http://dx.doi.org/10.1016/j.gloplacha.2013.08.011

Kramer, S. (2014). J48. Retrieved 2015-09-29, 2015, from http://www.opentox.org/dev/documentation/components/j48

Kriegel, D., Mayer, C., Hagg, W., Vorogushyn, S., Duethmann, D., Gafurov, A., & Farinotti, D. (2013). Changes in glacierisation, climate and runoff in the second half of the 20th century in the Naryn basin, Central Asia. *Global and Planetary Change, 110, Part A*(0), 51-61. doi: http://dx.doi.org/10.1016/j.gloplacha.2013.05.014

Kundzewicz, Z. W., Pinskwar, I., & Brakenridge, G. R. (2013). Large floods in Europe, 1985-2009. *Hydrological Sciences Journal-Journal Des Sciences Hydrologiques, 58*(1), 1-7.

Kundzewicz, Z. W., & Robson, A. J. (2004). Change detection in hydrological records—a review of the methodology / Revue méthodologique de la détection de changements dans les chroniques hydrologiques. *Hydrological Sciences Journal, 49*(1), 7-19. doi: 10.1623/hysj.49.1.7.53993

Kuntiyawichai, K. (2012). *Interactions between Land Use and Flood Management in the Chi River Basin: UNESCO-IHE PhD Thesis*: CRC Press.

Kwon, H. H., Sivakumar, B., Moon, Y. I., & Kim, B. S. (2011). Assessment of change in design flood frequency under climate change using a multivariate downscaling model and a precipitation-runoff model. *Stochastic Environmental Research and Risk Assessment, 25*(4), 567-581. doi: 10.1007/s00477-010-0422-z

Kyriakidis, P. C., & Goodchild, M. F. (2006). On the prediction error variance of three common spatial interpolation schemes. *International Journal of Geographical Information Science, 20*(8), 823-855. doi: 10.1080/13658810600711279

Lambin, E. F., Turner, B. L., Geist, H. J., Agbola, S. B., Angelsen, A., Bruce, J. W., . . . Xu, J. (2001). The causes of land-use and land-cover change: moving beyond the myths. *Global Environmental Change, 11*(4), 261-269. doi: http://dx.doi.org/10.1016/S0959-3780(01)00007-3

Lang, S. (2008). Object-based image analysis for remote sensing applications: modeling reality – dealing with complexity. In T. Blaschke, S. Lang, & G. Hay (Eds.), *Object-Based Image Analysis* (pp. 3-27): Springer Berlin Heidelberg.

Leo Breiman , J. F., Richard Olshen, Charles Stone. (1984). *Classification and Regression Trees*: Pacific Grove: Wadsworth.

Li, J. Z., Feng, P., & Wei, Z. Z. (2013). Incorporating the data of different watersheds to estimate the effects of land use change on flood peak and volume using multi-linear regression. *Mitigation and Adaptation Strategies for Global Change, 18*(8), 1183-1196. doi: 10.1007/s11027-012-9416-0

Li, X., Cheng, G. D., & Lu, L. (2005). Spatial analysis of air temperature in the Qinghai-Tibet Plateau. *Arctic Antarctic and Alpine Research, 37*(2), 246-252. doi: Doi 10.1657/1523-0430(2005)037[0246:Saoati]2.0.Co;2

Li, Z., Liu, W. Z., Zhang, X. C., & Zheng, F. L. (2009). Impacts of land use change and climate variability on hydrology in an agricultural catchment on the Loess Plateau of China. *Journal of Hydrology, 377*(1-2), 35-42. doi: 10.1016/j.jhydrol.2009.08.007

Li, Z. J., & Li, X. B. (2008). Trend and causation analysis of runoff variation in the upper reach of Chaobaihe River Basin in northern China during 1961-2005. *Beijing Linye Daxue Xuebao/Journal of Beijing Forestry University, 30*(SUPPL. 2), 82-87.

Liu, L. L., Liu, Z. F., Ren, X. Y., Fischer, T., & Xu, Y. (2011). Hydrological impacts of climate change in the Yellow River Basin for the 21st century using hydrological model and statistical downscaling model. *Quaternary International, 244*(2), 211-220. doi: 10.1016/j.quaint.2010.12.001

Ljung, G. M., & Box, G. E. P. (1978). On a Measure of Lack of Fit in Time Series Models. *Biometrika, 65*(2), 297-303. doi: 10.2307/2335207

López-Moreno, J. I., Fontaneda, S., Bazo, J., Revuelto, J., Azorin-Molina, C., Valero-Garcés, B., . . . Alejo-Cochachín, J. (2014). Recent glacier retreat and climate trends in Cordillera Huaytapallana, Peru. *Global and Planetary Change, 112*(0), 1-11. doi: http://dx.doi.org/10.1016/j.gloplacha.2013.10.010

Loukas, A., Vasiliades, L., & Dalezios, N. R. (2004). Climate change implications on flood response of a mountainous watershed. *Water, Air, and Soil Pollution: Focus, 4*(4-5), 331-347. doi: 10.1023/B:WAFO.0000044809.79328.9d

Lu, D., Mausel, P., Brondízio, E., & Moran, E. (2004). Change detection techniques. *International Journal of Remote Sensing, 25*(12), 2365-2401. doi: 10.1080/0143116031000139863

Lu, D. S., Li, G. Y., Kuang, W. H., & Moran, E. (2014). Methods to extract impervious surface areas from satellite images. *International Journal of Digital Earth, 7*(2), 93-112.

Łupikasza, E. B., Hänsel, S., & Matschullat, J. (2011). Regional and seasonal variability of extreme precipitation trends in southern Poland and central-eastern Germany 1951–2006. *International Journal of Climatology, 31*(15), 2249-2271. doi: 10.1002/joc.2229

Madugundu, R., Al-Gaadi, K. A., Patil, V. C., & Tola, E. (2014). Detection of land use and land cover changes in dirab region of Saudi Arabia using remotely sensed imageries. *American Journal of Environmental Sciences, 10*(1), 8-18. doi: 10.3844/ajessp.2014.8.18

Mallinis, G., Koutsias, N., & Arianoutsou, M. (2014). Monitoring land use/land cover transformations from 1945 to 2007 in two peri-urban mountainous areas of Athens metropolitan area, Greece. *Science of The Total Environment, 490*(0), 262-278. doi: http://dx.doi.org/10.1016/j.scitotenv.2014.04.129

Mann, H. B. (1945). Nonparametric Tests Against Trend. *Econometrica, 13*(3), 245-259. doi: 10.2307/1907187

Martínez, M. D., Serra, C., Burgueño, A., & Lana, X. (2010). Time trends of daily maximum and minimum temperatures in Catalonia (ne Spain) for the period 1975–2004. *International Journal of Climatology, 30*(2), 267-290. doi: 10.1002/joc.1884

Mas, J. F. (1999). Monitoring land-cover changes: A comparison of change detection techniques. *International Journal of Remote Sensing, 20*(1), 139-152. doi: 10.1080/014311699213659

Matinfar, H. R., & Roodposhti, M. S. (2013). Decision tree land use/ land cover change detection of khoram abad city using landsat imagery and ancillary SRTM data. *Middle East Journal of Scientific Research, 13*(8), 1057-1064.

Matkan, A. A., Shakiba, A., Pourali, S. H., & Azari, H. (2009). Flood Early Warning with Integration of Hydrologic and Hydraulic Models, RS and GIS (Case study: Madarsoo basin, Iran). *World Applied Science Journal, 6*(12), 1698-1704.

Maurer, T. (2013). How to Pan-Sharpen Images Using the Gram-Schmidt Pan-Sharpen Method - A Recipe. *Int. Arch. Photogramm. Remote Sens. Spatial Inf. Sci., XL-1*(W1), 239-244. doi: 10.5194/isprsarchives-XL-1-W1-239-2013

McLeod, A. I., & Li, W. K. (1983). Diagnostic Checking Arma Time Series Models Using Squared-Residual Autocorrelations. *Journal of Time Series Analysis, 4*(4), 269-273. doi: 10.1111/j.1467-9892.1983.tb00373.x

Meng, Q. (2006). Geostatistical prediction and mapping for large area forest inventory using remote sensing data. *2006 UCGIS Summer Symposium.*

Meng, Q. (2014). Regression Kriging versus Geographically Weighted Regression for Spatial Interpolation. *International Journal of Advanced Remote Sensing and GIS, 3*(1), 606-615.

Meng, Q., Liu, Z., & Borders, B. E. (2013). Assessment of regression kriging for spatial interpolation - Comparisons of seven GIS interpolation methods. *Cartography and Geographic Information Science, 40*(1), 28-39. doi: 10.1080/15230406.2013.762138

Merz, R., & Bloschl, G. (2005). Flood frequency regionalisation-spatial proximity vs. catchment attributes. *Journal of Hydrology, 302*(1-4), 283-306. doi: 10.1016/j.jhydrol.2004.07.018

Merz, R., Bloschl, G., & Humer, G. (2008). National flood discharge mapping in Austria. *Natural Hazards, 46*(1), 53-72. doi: 10.1007/s11069-007-9181-7

Mikaeili A.R, Abdoli A, & S.M, A. N. (2005). Physical structure of the Madar-Sou stream in Golestan National Park. *J. Agric. Sci. Natur. Resour, 12*(3), 11.

Modaresi, F., Araghinejad, S., Ebrahimi, K., & Kholghi, M. (2010). Regional Assessment of Climate Change Using Statistical Tests: Case Study of Gorganroud-Gharehsou Basin. *Journal of Water and Soil, 24*(3), 476-489.

Mohammadi, A., Alaghmand, S., & Mosaedi, A. (2008). Study and determination of morphological changes of Dough river in north of Iran using GIS. *The International Archives of the Photogrammetry, Remote Sensing and Spatial Information Sciences, XXXVII*(Part B8).

Mohammadi, A., Mosaedi, A., & Alaghmand, S. (2007). Effects of east-Golestan August 2001 flood on the morphology of the Madarsoo river. *J. Agric. Sci. Natur. Resour, 14*(1).

Muzik, I. (2001). Sensitivity of hydrologic systems to climate change. *Canadian Water Resources Journal, 26*(2), 233-252.

Muzik, I. (2002). A first-order analysis of the climate change effect on flood frequencies in a subalpine watershed by means of a hydrological rainfall–runoff model. *Journal of Hydrology, 267*(1–2), 65-73. doi: http://dx.doi.org/10.1016/S0022-1694(02)00140-3

Naess, L. O., Bang, G., Eriksen, S., & Vevatne, J. (2005). Institutional adaptation to climate change: Flood responses at the municipal level in Norway. *Global*

Environmental Change-Human and Policy Dimensions, 15(2), 125-138. doi: 10.1016/j.gloenvcha.2004.10.003

Nemmour, H., & Chibani, Y. (2010). Support Vector Machines for Automatic Multi-class Change Detection in Algerian Capital Using Landsat TM Imagery. *Journal of the Indian Society of Remote Sensing, 38*(4), 585-591. doi: 10.1007/s12524-011-0060-z

Nie, C., Li, H., Yang, L., Ye, B., Dai, E., Wu, S., . . . Liao, Y. (2012). Spatial and temporal changes in extreme temperature and extreme precipitation in Guangxi. *Quaternary International, 263*(0), 162-171. doi: http://dx.doi.org/10.1016/j.quaint.2012.02.029

Nutini, F., Boschetti, M., Brivio, P. A., Bocchi, S., & Antoninetti, M. (2013). Land-use and land-cover change detection in a semi-arid area of Niger using multi-temporal analysis of Landsat images. *International Journal of Remote Sensing, 34*(13), 4769-4790. doi: 10.1080/01431161.2013.781702

Obot, N. I., Chendo, M. A. C., Udo, S. O., & Ewona, I. O. (2010). Evaluation of rainfall trends in Nigeria for 30 years (1978-2007). *International Journal of the Physical Sciences, 5*(14), 2217-2222.

Ololade, O., Annegarn, H. J., Limpitlaw, D., & Kneen, M. A. (2008). *Land-use/cover mapping and change detection in the rustenburg mining region using landsat images.* Paper presented at the International Geoscience and Remote Sensing Symposium (IGARSS).

Ouellet, C., Saint-Laurent, D., & Normand, F. (2012). Flood events and flood risk assessment in relation to climate and land-use changes: Saint-Francois River, southern Quebec, Canada. *Hydrological Sciences Journal-Journal Des Sciences Hydrologiques, 57*(2), 313-325. doi: 10.1080/02626667.2011.645475

Pakhale, G. K., & Gupta, P. K. (2010). Comparison of Advanced Pixel Based (ANN and SVM) and Object-Oriented Classification Approaches Using Landsat-7 Etm+ Data. *International Journal of Engineering and Technology, 2*(4), 245-251.

Petrow, T., & Merz, B. (2009). Trends in flood magnitude, frequency and seasonality in Germany in the period 1951–2002. *Journal of Hydrology, 371*(1–4), 129-141. doi: http://dx.doi.org/10.1016/j.jhydrol.2009.03.024

Pettitt, A. N. (1979). A Non-parametric Aproach to the Change-point Problem. *Appl. statist, 28*(2), 126-135.

Pontius, R., Gao, Y., Giner, N., Kohyama, T., Osaki, M., & Hirose, K. (2013). Design and Interpretation of Intensity Analysis Illustrated by Land Change in Central Kalimantan, Indonesia. *Land, 2*(3), 351-369.

Poozesh-Shirazi, m., Refahi, H. G., & Shahooei, S. (2000). Application of Answers model for calculating runoff and predicting sedimentation from steep agricultural watersheds in Gorgan catchment and its comparison with other methods common in Iran. *Iranian. J. Agric. Sci., 31*(3).

Prakash, A. (2000). *Thermal remote sensing: concepts, issues and applications.* Paper presented at the ISPRS, Amsterdam.

Qin, Y., Niu, Z., Chen, F., Li, B., & Ban, Y. (2013). Object-based land cover change detection for cross-sensor images. *International Journal of Remote Sensing, 34*(19), 6723-6737. doi: 10.1080/01431161.2013.805282

Rabia, A. H., & Terribile, F. (2013). *Semi-Automated Classification of Gray Scale Aerial Photographs using Geographic Object Based Image Analysis (GEOBIA) Technique*. Paper presented at the European Geosciences Union General Assembly - Geophysical Research Abstracts, Vienna - Austria. http://meetingorganizer.copernicus.org/EGU2013/EGU2013-219.pdf

Renard, B., Lang, M., Bois, P., Dupeyrat, A., Mestre, O., Niel, H., . . . Gailhard, J. (2008). Regional methods for trend detection: Assessing field significance and regional consistency. *Water Resources Research, 44*(8), W08419. doi: 10.1029/2007WR006268

Riggs, G. A., Hall, D. K., & Salomonson, V. V. (1994, 8-12 Aug 1994). *A snow index for the Landsat Thematic Mapper and Moderate Resolution Imaging Spectroradiometer.* Paper presented at the Geoscience and Remote Sensing Symposium, 1994. IGARSS '94. Surface and Atmospheric Remote Sensing: Technologies, Data Analysis and Interpretation., International.

Río, S. d., Herrero, L., Fraile, R., & Penas, A. (2011). Spatial distribution of recent rainfall trends in Spain (1961–2006). *International Journal of Climatology, 31*(5), 656-667. doi: 10.1002/joc.2111

Rogan, J., & Chen, D. M. (2004). Remote sensing technology for mapping and monitoring land-cover and land-use change. *Progress in Planning, 61*(4), 301-325. doi: 10.1016/S0305-9006(03)00066-7

Rogger, M., Kohl, B., Pirkl, H., Viglione, A., Komma, J., Kirnbauer, R., . . . Bloschl, G. (2012). Runoff models and flood frequency statistics for design flood estimation in Austria - Do they tell a consistent story? *Journal of Hydrology, 456*, 30-43.

Saadat, H., Adamowski, J., Bonnell, R., Sharifi, F., Namdar, M., & Ale-Ebrahim, S. (2011). Land use and land cover classification over a large area in Iran based on single date analysis of satellite imagery. *Isprs Journal of Photogrammetry and Remote Sensing, 66*(5), 608-619. doi: 10.1016/j.isprsjprs.2011.04.001

Saboohi, R., Soltani, S., & Khodagholi, M. (2012). Trend analysis of temperature parameters in Iran. *Theoretical and Applied Climatology, 109*(3-4), 529-547. doi: 10.1007/s00704-012-0590-5

Safeeq, M., Mair, A., & Fares, A. (2013). Temporal and spatial trends in air temperature on the Island of Oahu, Hawaii. *International Journal of Climatology, 33*(13), 2816-2835. doi: Doi 10.1002/Joc.3629

Saghafian, B., Farazjoo, H., Sepehry, A., & Najafinejad, A. (2006). Effect of Land Use Change on Floods in Golestan Dam Drainage Basin. *Iran Water resource research, 2*(1), 18-28.

Salarijazi, M., Akhond-Ali, A.-M., Adib, A., & Daneshkhah, A. (2012). Trend and change-point detection for the annual stream-flow series of the Karun River at the Ahvaz hydrometric station. *African Journal of Agricultural Research, 7*(32), 13.

Salford System. (2015, 2015). CART Classification And Regression Trees. Retrieved 2015.09.29, from http://www.salford-systems.com/products/cart

Salman Mahini, A., Feghhi, J., Nadali, A., & Riazi, A. (2009). Tree cover change detection through Artificial Neural Network classification using Landsat TM and

ETM+ images (case study: Golestan Province, Iran). *Iranian Journal of Forest and Poplar Research, 16*(3), 495-505.

Salmi, T., Määttä, A., Anttila, P., Ruoho-Airola, T., & Amnell, T. (2002). Detecting Trends Of Annual Values Of Atmospheric Pollutants By The Mann-Kendall Test And Sen's Slope Estimates -The Excel Template Application Makesens *Publications on air quality* (pp. 1-35). Helsinki: Finnish Meteorological Institute.

Santos, M., & Fragoso, M. (2013). Precipitation variability in Northern Portugal: Data homogeneity assessment and trends in extreme precipitation indices. *Atmospheric Research, 131*(0), 34-45. doi: http://dx.doi.org/10.1016/j.atmosres.2013.04.008

Sepehry, A., & Liu, G.-J. (2006). *Flood Induced Land Cover Change Detection Using Multitemporal ETM+ Imagery*. Paper presented at the 2nd Workshop of the EARSeL SIG on Land Use and Land Cover, Center for Remote Sensing of Land Surfaces, Bonn.

Shalaby, A., & Tateishi, R. (2007). Remote sensing and GIS for mapping and monitoring land cover and land-use changes in the Northwestern coastal zone of Egypt. *Applied Geography, 27*(1), 28-41. doi: 10.1016/j.apgeog.2006.09.004

Sharma, R., Ghosh, A., & Joshi, P. K. (2013). Decision tree approach for classification of remotely sensed satellite data using open source support. *Journal of Earth System Science, 122*(5), 1237-1247. doi: DOI 10.1007/s12040-013-0339-2

Shifteh Some'e, B., Ezani, A., & Tabari, H. (2012). Spatiotemporal trends and change point of precipitation in Iran. *Atmospheric Research, 113*(0), 1-12. doi: http://dx.doi.org/10.1016/j.atmosres.2012.04.016

Sim, L. K., & Balamurugan, G. (1991). Urbanization and Urban Water Problems in Southeast-Asia - a Case of Unsustainable Development. *Journal of Environmental Management, 32*(3), 195-209. doi: Doi 10.1016/S0301-4797(05)80051-9

Singh, A. (1989). Review Article Digital change detection techniques using remotely-sensed data. *International Journal of Remote Sensing, 10*(6), 989-1003. doi: 10.1080/01431168908903939

Soltani, S., Saboohi, R., & Yaghmaei, L. (2012). Rainfall and rainy days trend in Iran. *Climatic Change, 110*(1-2), 187-213. doi: 10.1007/s10584-011-0146-1

Son, N., Chen, C., Chang, N., Chen, C., Chang, L., & Thanh, B. (2014). Mangrove Mapping and Change Detection in Ca Mau Peninsula, Vietnam, Using Landsat Data and Object-Based Image Analysis. *IEEE Journal of Selected Topics in Applied Earth Observations and Remote Sensing, 8*(2), 503-510.

Soo Chin, L., Aik Song, C., & Leong Keong, K. (2010, 25-30 July 2010). *Spatio-temporal variability of precipitation in southeast asia analyzed using the empirical orthogonal function (EOF) technique.* Paper presented at the Geoscience and Remote Sensing Symposium (IGARSS), 2010 IEEE International.

Statistical-Center-of-Iran. (2006). Iranian Population and Housing Census 1385 - Golestan Province General Results. 57.

Suriya, S., & Mudgal, B. V. (2012). Impact of urbanization on flooding: The Thirusoolam sub watershed - A case study. *Journal of Hydrology, 412*, 210-219. doi: 10.1016/j.jhydrol.2011.05.008

Tabari, H., Abghari, H., & Hosseinzadeh Talaee, P. (2012). Temporal trends and spatial characteristics of drought and rainfall in arid and semiarid regions of Iran. *Hydrological Processes, 26*(22), 3351-3361. doi: 10.1002/hyp.8460

Tabari, H., & Hosseinzadeh Talaee, P. (2011). Temporal variability of precipitation over Iran: 1966–2005. *Journal of Hydrology, 396*(3–4), 313-320. doi: http://dx.doi.org/10.1016/j.jhydrol.2010.11.034

Tabari, H., & Hosseinzadeh Talaee, P. (2013). Moisture index for Iran: Spatial and temporal analyses. *Global and Planetary Change, 100*(0), 11-19. doi: http://dx.doi.org/10.1016/j.gloplacha.2012.08.010

Tabari, H., Hosseinzadeh Talaee, P., Ezani, A., & Shifteh Some'e, B. (2012). Shift changes and monotonic trends in autocorrelated temperature series over Iran. *Theoretical and Applied Climatology, 109*(1-2), 95-108. doi: 10.1007/s00704-011-0568-8

Tabari, H., Somee, B. S., & Zadeh, M. R. (2011). Testing for long-term trends in climatic variables in Iran. *Atmospheric Research, 100*(1), 132-140. doi: http://dx.doi.org/10.1016/j.atmosres.2011.01.005

Tabari, H., & Talaee, P. H. (2011). Recent trends of mean maximum and minimum air temperatures in the western half of Iran. *Meteorology and Atmospheric Physics, 111*(3-4), 121-131. doi: DOI 10.1007/s00703-011-0125-0

Tehrani, N., Makhdoum, M. F., & Mahdavi, M. (2011). Studying the impact of land use changes on flood flows by using Remote Sensing (RS) and Geographical information System (GIS) techniques – A case study in Dough river watershed, northeast of Iran. *Environmental Research, 1*(2), 1-14.

Thilagavathi, N., Subramani, T., & Suresh, M. (2015). Land use/land cover change detection analysis in Salem Chalk Hills, South India using remote sensing and GIS. *Disaster Advances, 8*(1), 44-52.

Tian, Y., Ma, L., Lei, X., & Jiang, Y. (2010, 28-31 Aug. 2010). *Analysis of runoff change trend using hydrological time series method.* Paper presented at the Geoscience and Remote Sensing (IITA-GRS), 2010 Second IITA International Conference.

Tjerry, S., Jessen, O. Z., Morishita, K., & Enggrob, H. G. (2006). Flood modelling and impact of debris flow in the Madarsoo River, Iran. *WIT Transactions on Ecology and the Environment, 90*, 69-78. doi: doi:10.2495/DEB060071

Uddin, K., Gurung, D. R., Amarnath, G., & Shrestha, B. (2013). Application of remote sensing and GIS for flood hazard management: a case study from Sindh Province, Pakistan. *American Journal of Geographic Information System, 2*(1), 1-5. doi: 10.5923/j.ajgis.20130201.01

Unkašević, M., & Tošić, I. (2013). Trends in temperature indices over Serbia: relationships to large-scale circulation patterns. *International Journal of Climatology, 33*(15), 3152-3161. doi: 10.1002/joc.3652

USGS. (2013a). How is radiance calculated?   , 2015, from http://landsat.usgs.gov/how_is_radiance_calculated.php

USGS. (2013b). Using the USGS Landsat 8 Product. Retrieved 10.03.2015, 2015, from http://landsat.usgs.gov/Landsat8_Using_Product.php

USGS. (2013c). What are the band designations for the Landsat satellites. Retrieved September 2013, from http://landsat.usgs.gov/band_designations_landsat_satellites.php

Velpuri, N. M., & Senay, G. B. (2013). Analysis of long-term trends (1950–2009) in precipitation, runoff and runoff coefficient in major urban watersheds in the United States. *Environmental Research Letters, 8*(2), 024020. doi: Artn 024020

10.1088/1748-9326/8/2/024020

Vieira, M. A., Formaggio, A. R., Renno, C. D., Atzberger, C., Aguiar, D. A., & Mello, M. P. (2012). Object Based Image Analysis and Data Mining applied to a remotely sensed Landsat time-series to map sugarcane over large areas. *Remote Sensing of Environment, 123*, 553-562. doi: DOI 10.1016/j.rse.2012.04.011

Viola, F., Liuzzo, L., Noto, L. V., Lo Conti, F., & La Loggia, G. (2014). Spatial distribution of temperature trends in Sicily. *International Journal of Climatology, 34*(1), 1-17. doi: 10.1002/joc.3657

Vorovencii, I. (2014). Detection of environmental changes due to windthrows using landsat 7 ETM+ satellite images. *Environmental Engineering and Management Journal, 13*(3), 565-576.

Waheed, T., Bonnell, R. B., Prasher, S. O., & Paulet, E. (2006). Measuring performance in precision agriculture: CART—A decision tree approach. *Agricultural Water Management, 84*(1–2), 173-185. doi: http://dx.doi.org/10.1016/j.agwat.2005.12.003

Waikato, M. L. G. (2015). Weka 3: Data Mining Software in Java. 2015, from http://www.cs.waikato.ac.nz/~ml/weka/

Walsh, K. (2015). Geographic Information Science (CERT) Retrieved 2015.09.29, 2015, from http://gradschool.oregonstate.edu/programs/cg03

Wang, H., Zhang, M., Li, P., Dang, X., Zhu, H., & Chang, L. (2011, 20-22 May 2011). *Long-term trend analysis for the runoff series in Yulin.* Paper presented at the 2011 International Symposium on Water Resource and Environmental Protection (ISWREP).

Wang, S.-q., Liu, E.-p., Zhang, H.-j., & Wu, W. (2011, 19-20 Feb. 2011). *Comparison of Spatial Interpolation Methods for Soil Available P in a Hilly Area.* Paper presented at the 2011 International Conference on Computer Distributed Control and Intelligent Environmental Monitoring (CDCIEM)

Wang, Y., Ren, F., & Zhang, X. (2014). Spatial and temporal variations of regional high temperature events in China. *International Journal of Climatology, 34*(10), 3054-3065. doi: 10.1002/joc.3893

Wang, Z., Jensen, J. R., & Im, J. (2010). An automatic region-based image segmentation algorithm for remote sensing applications. *Environmental Modelling & Software, 25*(10), 1149-1165. doi: http://dx.doi.org/10.1016/j.envsoft.2010.03.019

Wijngaard, J. B., Klein Tank, A. M. G., & Können, G. P. (2003). Homogeneity of 20th century European daily temperature and precipitation series. *International Journal of Climatology, 23*(6), 679-692. doi: 10.1002/joc.906

Willems, P. (2009). A time series tool to support the multi-criteria performance evaluation of rainfall-runoff models. *Environmental Modelling & Software, 24*(3), 311-321. doi: 10.1016/j.envsoft.2008.09.005

Witharana, C., Civco, D. L., & Meyer, T. H. (2014). Evaluation of data fusion and image segmentation in earth observation based rapid mapping workflows. *Isprs Journal of Photogrammetry and Remote Sensing, 87*(0), 1-18. doi: http://dx.doi.org/10.1016/j.isprsjprs.2013.10.005

Wolter, P. T., Berkley, E. A., Peckham, S. D., Singh, A., & Townsend, P. A. (2012). Exploiting tree shadows on snow for estimating forest basal area using Landsat data. *Remote Sensing of Environment, 121*, 69-79. doi: 10.1016/j.rse.2012.01.008

Woods, R., Schmidt, J., & Collins, D. (2009). Estimating the potential effect of land use change on Waikato tributary floods – TopNet model development *NIWA Client Report: CHC2009-155*. New Zealand National Institute of Water & Atmospheric Research Ltd

Wu, C., Huang, G., Yu, H., Chen, Z., & Ma, J. (2014). Spatial and temporal distributions of trends in climate extremes of the Feilaixia catchment in the upstream area of the Beijiang River Basin, South China. *International Journal of Climatology, 34*(11), 3161-3178. doi: 10.1002/joc.3900

Wu, F., Wang, X., Cai, Y., & Li, C. (2013). Spatiotemporal analysis of precipitation trends under climate change in the upper reach of Mekong River basin. *Quaternary International, xxx*, 1-10.

Wu, G., Gao, Y., Wang, Y., Wang, Y. Y., & Xu, D. (2015). Land-use/land cover changes and their driving forces around wetlands in Shangri-La County, Yunnan Province, China. *International Journal of Sustainable Development and World Ecology, 22*(2), 110-116. doi: 10.1080/13504509.2014.915894

www.floodsite.net. (2013). Integrated Flood Risk Analysis and Management Methodologies., from www.floodsite.net.

Xiaolu, S., & Bo, C. (2011). Change detection using Change Vector Analysis from Landsat TM images in Wuhan. *Procedia Environmental Sciences, 11-Part A*, 238-244. doi: http://dx.doi.org/10.1016/j.proenv.2011.12.037

Xu, K., Milliman, J. D., & Xu, H. (2010). Temporal trend of precipitation and runoff in major Chinese Rivers since 1951. *Global and Planetary Change, 73*(3–4), 219-232. doi: http://dx.doi.org/10.1016/j.gloplacha.2010.07.002

Yamani, M., Eyvazi, J. J., & Jahadi, M. (2010). The Investigation of Flood Flows in Madarsoo River In the Catastrophic Floods, 2001 & 2002. *Physical Geography Research Quarterly, 42*(72), 1-20.

Yang, X., & Lo, C. P. (2002). Using a time series of satellite imagery to detect land use and land cover changes in the Atlanta, Georgia metropolitan area. *International Journal of Remote Sensing, 23*(9), 1775-1798. doi: 10.1080/01431160110075802

Yesmin, R., Mohiuddin, A. S. M., Uddin, M. J., & Shahid, M. A. (2014). *Land use and land cover change detection at Mirzapur Union of Gazipur District of Bangladesh using remote sensing and GIS technology.* Paper presented at the IOP Conference Series: Earth and Environmental Science.

Yin, D. M., Cao, X., Chen, X. H., Shao, Y. J., & Chen, J. (2013). Comparison of automatic thresholding methods for snow-cover mapping using Landsat TM imagery. *International Journal of Remote Sensing, 34*(19), 6529-6538. doi: 10.1080/01431161.2013.803631

Yoon, G.-W., Cho, S. I., Jeong, S., & Park, J.-H. (2003). *Object oriented classification using Landsat images*. Paper presented at the The 24th Asian Conference on Remote Sensing, Busan, South Korea.

Yue, S., & Pilon, P. (2004). A comparison of the power of the t test, Mann-Kendall and bootstrap tests for trend detection / Une comparaison de la puissance des tests t de Student, de Mann-Kendall et du bootstrap pour la détection de tendance. *Hydrological Sciences Journal, 49*(1), 21-37. doi: 10.1623/hysj.49.1.21.53996

Yue, S., Pilon, P., Phinney, B., & Cavadias, G. (2002). The influence of autocorrelation on the ability to detect trend in hydrological series. *Hydrological Processes, 16*(9), 1807-1829. doi: 10.1002/hyp.1095

Yuhendra, Alimuddin, I., Sumantyo, J. T. S., & Kuze, H. (2012). Assessment of pan-sharpening methods applied to image fusion of remotely sensed multi-band data. *International Journal of Applied Earth Observation and Geoinformation, 18*(0), 165-175. doi: http://dx.doi.org/10.1016/j.jag.2012.01.013

Zaiontz, C. (2014). Real Statistics Using Excel - Basic Concepts of Correlation. from http://www.real-statistics.com/correlation/basic-concepts-correlation/

Zaksek, K., & Schroedter-Homscheidt, M. (2009). Parameterization of air temperature in high temporal and spatial resolution from a combination of the SEVIRI and MODIS instruments. *Isprs Journal of Photogrammetry and Remote Sensing, 64*(4), 414-421. doi: 10.1016/j.isprsjprs.2009.02.006

Zanganeh, M. E., Mosaedi, A., Meftah Halghi, M., & Dehghani, A. A. (2011). Determination of suitable method for estimating suspended sediments discharge in Arazkoose hydrometric station (Gorganrood basin). *J. of Water and Soil Conservation, 18*(2), 85-103.

Zelinski, M. E., Henderson, J., & Smith, M. (2014). Use of Landsat 5 for change detection at 1998 Indian and Pakistani nuclear test sites. *IEEE Journal of Selected Topics in Applied Earth Observations and Remote Sensing, 7*(8), 3453-3460. doi: 10.1109/Jstars.2013.2294322

Zhang, Q., Li, J., Singh, V. P., & Xiao, M. (2013). Spatio-temporal relations between temperature and precipitation regimes: Implications for temperature-induced changes in the hydrological cycle. *Global and Planetary Change, 111*(0), 57-76. doi: http://dx.doi.org/10.1016/j.gloplacha.2013.08.012

Zhang, Q., Li, J., Singh, V. P., & Xu, C.-Y. (2013). Copula-based spatio-temporal patterns of precipitation extremes in China. *International Journal of Climatology, 33*(5), 1140-1152. doi: 10.1002/joc.3499

Zheng, X., Zhu, J. J., & Yan, Q. L. (2013). Monthly Air Temperatures over Northern China Estimated by Integrating MODIS Data with GIS Techniques. *Journal of Applied Meteorology and Climatology, 52*(9), 1987-2000. doi: 10.1175/Jamc-D-12-0264.1

Zhu, Z., & Woodcock, C. E. (2014). Continuous change detection and classification of land cover using all available Landsat data. *Remote Sensing of Environment, 144*, 152-171. doi: 10.1016/j.rse.2014.01.011

Appendix

Appendix I

Geostatistical Modeling of Air Temperature Using Landsat Thermal Remote Sensing

This appendix regarding the goal of first chapter of the thesis for spatio-temporal analysis of hydro-meteorological data try to investigate the interpolation of temperature using Landsat thermal band in the region with low density of gauges distribution. Using the Landsat instead of for instance MODIS is because many geographical, ecological and bioclimatic research need better resolution of climatic factors and it also help to provide deeper understand in case of "climatic neighborhood" concept. Moreover, According to the snow cover impact on the air temperature and dependency of thermal data's nature to temperature we decided to use the snow covered thermal images in spatial interpolation too. We aimed to investigate the relationship between area of snow covered lands and accuracy of interpolation. To calculate the area of snow cover, band combination and NDSI index were calculated to understand which extent of snow cover could be important in interpolation of air temperature.

At the end, we know that number of our observation stations are to low and considering the Kriging requirements like normal distribution and stationarity is toilsome but we hope to solve this problems in the future studies.

1. Introduction

Spatial interpolation is one of the most often used geographic techniques for spatial data visualization, spatial query of properties, and spatial decision-making processes in geography, earth sciences, and environmental science (Q. Meng, Liu, & Borders, 2013). Indeed, spatial interpolation is often used to predict a value of a variable of interest at unmeasured locations with the available measurements at sampled sites (Kyriakidis & Goodchild, 2006; Q. Meng et al., 2013). Moreover, the spatial interpolation also applies for temperature mapping. Air temperature is one of the input variables for land evaluation and characterization systems, as well as hydrological and ecological models (Benavides, Montes, Rubio, & Osoro, 2007). Benavides et al. (2007) and some others (e.g. X. Li, Cheng, and Lu (2005)) believe that air temperature modeling in mountainous regions is a challenge and it is difficult to obtain precise climatic maps.

Different interpolation methods have been used to model the spatial distribution of air temperature; the most widely used being the inverse distance interpolation

weighting, Voronoi tessellation, regression analysis or, more recently, geostatistical methods (Benavides et al., 2007). The addition of auxiliary variables is often believed to increase the performance of spatial prediction (Q. Meng et al., 2013). Some auxiliary variables that are used whole around the world by researchers in different field of study are Digital Elevation Model (DEM), slope, aspect, distance to sea, solar radiation, land cover, NDVI and so on (Benavides et al., 2007; Boi, Fiori, & Canu, 2011; Jabot, Zin, Lebel, Gautheron, & Obled, 2012; Qingmin Meng, 2006). For example, Kalivas, Kollias, and Apostolidis (2013) applied the slope as the auxiliary data to interpolate the forest volume as an interesting topic for forest managers. Alsamamra, Ruiz-Arias, Pozo-Vazquez, and Tovar-Pescador (2009) interpolated the solar radiation in the southern Spain and used elevation and shadows cast as external variables. Qingmin Meng (2014) used IKONOS bands 2 and 3 that the band 3 was auxiliary data to interpolate the band 2 using regression kriging versus Geographically Weighted Regression method.

In case of temperature, Boi et al. (2011) used five parameters include elevation, sea distance, longitude, latitude and relative elevation to interpolate means of maximum and minimum daily temperatures. Q. Meng et al. (2013) investigated the spatial interpolation of annual maximum temperature in the central Big Sur in California using elevation as the auxiliary variable. Benavides et al. (2007) implemented geostatistical modeling over a mountains region in the Spain to interpolate mean monthly air temperature and used the elevation as an auxiliary data. Arundel (2005) included elevation and slope as independent variables to interpolate the temperature and precipitation. Hengl, Heuvelink, Tadic, and Pebesma (2012) used latitude, longitude, DEM, topographically weighted distance from the coast line, and topographic wetness index, total insolation and MODIS LST images to provide daily temperature maps. They found that MODIS time series of LST images could be successfully combined with ground measurements of temperatures to produce more accurate and more detailed predictions of daily temperature (Hengl et al., 2012). A problem in their study was regarding the MODIS images that had 10-30% missing pixels. Cristobal, Ninyerola, and Pons (2008) measured the role geographical and remotely sensed predictors in air temperature interpolation in the Catalonia, Spain. They used altitude, latitude, continentality and solar radiation as geographical variables and LST and NDVI in Landsat TM, ETM+, AVHRR and MODIS images. They identifies that combined geographical and remotely sensed variables provide better results and among these variables the LST and NDVI are the most powerful remote sensing predictors. Zheng, Zhu, and Yan (2013) recently performed monthly air temperature interpolation using MODIS LST and NDVI.

In the same way, as remotely sensed data can provide a valuable source of information to understand spatial phenomena (Joyce, Wright, Samsonov, & Ambrosia, 2009) and ability of thermal remote sensing in deals with the thermal characteristics of earth surface (Prakash, 2000) we decide to use thermal band of Landsat to enhance the

performance of temperature interpolation. The Landsat images were selected because of better resolution in comparison to MODIS because many geographical, ecological, biological and bioclimatic spatial studies need higher resolution information in their studies (Attorre, Alfo, De Sanctis, Francesconi, & Bruno, 2007; Zaksek & Schroedter-Homscheidt, 2009).

In this section we have to goals: First, to use Geostatistics and thermal remote sensing bands as an ancillary data to spatially predict mean air temperature in four season winter (March), spring (May), summer (August) and autumn (November) in a complex topographic region of North-east of Iran. Second, use cold season images as a great distinction of this study vice versa most of studies that use warm season images. Most of the warm season acquired images are not cloudy and been used in many studies; but in the north east of Iran as like as many areas in the high latitudes, ground surface of satellite images acquired in cold seasons (if sky be cloud free) are covered by snow.

According to the snow cover area (SCA) impact on the air temperature and dependency of thermal data's nature to temperature we decided to use the snow covered thermal images in spatial interpolation. We aimed to investigate the relationship between area of snow covered lands and accuracy of interpolation. In this regard we used four approximately cloud free Landsat thermal bands , two for 1986 December and two others for December of 1999 to evaluate these relationships in a complex topographic region of North-east of Iran. In other word, second part aimed to investigate the relations between amount of snow cover area in the thermal remote sensing images as auxiliary data and spatial interpolation of mean air temperature using Geostatistics.

2. Introduction

2.1. Study area and datasets

Study area is located in the northeastern part of Iran and covers an area of 18000 km^2 (Fig. 1). It is located between the latitude of 36° 43' and 38° 07'N and the longitude of 54° 19' and 56° 25'E. It included most of Gorganrood watershed and parts of Atrak and Gharasoo watersheds. The altitude range is between -30 to 2956 meters above sea level. This region is very important in several viewpoints that explained in the first chapter.

For each section of the appendix, two categories of data were used mean air temperature data (Table 1) as station points and Remote Sensing images as raster. In the first part: Monthly mean air temperature data for November 1988, August 1999, May 2000 and March 2009 of eight stations, were selected (Table 1; Fig. 1). Unlike many researches that only investigate the temperature interpolation in the coldest and warmest month we used thermal bands of four cloud free Landsat Thematic Mapper (TM) and Enhanced Thematic Mapper (ETM+) images (path 162, row 34) for March

of 2009, May of 2000, August of 1999 and November of 1988 on behalf of four season (Fig. 2 and 3). TM and ETM+ sensor thermal bands are in the 10.40-12.50 µm with spatial resolution of 120/60 m (USGS, 2013c).

For the second section, thermal bands of four approximately cloud free Landsat Thematic Mapper (TM) and Enhanced Thematic Mapper (ETM+) images (path 162, row 34) for December 1986 and 1999 were the raster data of the research (Fig. 4 and 5). TM and ETM+ sensor thermal bands are in the 10.40-12.50 µm with spatial resolution of 120/60 m (USGS, 2013c).

The images from the EROS Data Center have already been processed to a standard-level of geometric and terrain accuracy (http://landsat.usgs.gov/Landsat Processing_Details.php). Therefore, images were selected and downloaded from the United States Geological Survey's (USGS) National Center for Earth Resources Observation and Science (http://glovis.usgs.gov).

Table 1. Meteorological Stations

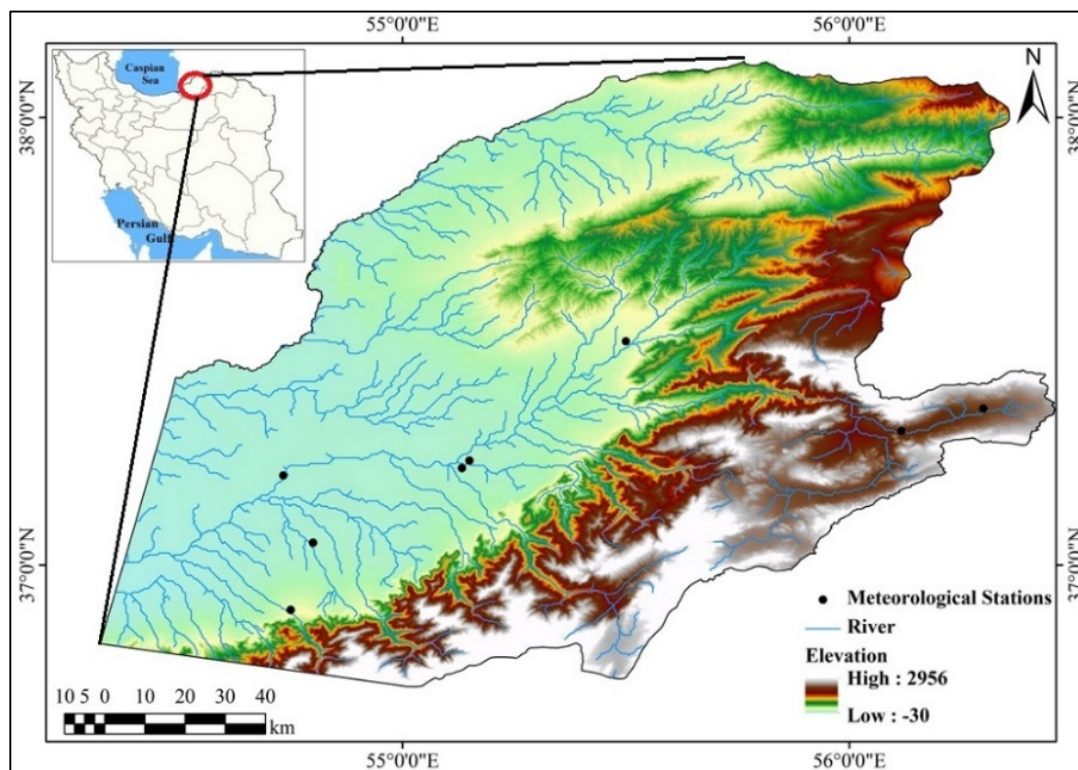| Station	Latitude	Longitude	Elevation(m)
Tamar	37° 29´	55° 30´	132
Gonbad	37° 14´	55° 09´	36
Araz-kuse	37° 13´	55° 08´	34
Bhalke Dashli	37° 04´	54° 47´	24
Fazel-abad	37° 54´	54° 45´	210
Sad-gorgan	37° 12´	54° 44´	12
Ghafar-haji	37° 00´	54° 08´	-22
Cheshme-khan	37° 18´	56° 07´	1250
Robat-gharabil	37° 21´	56° 18´	1450

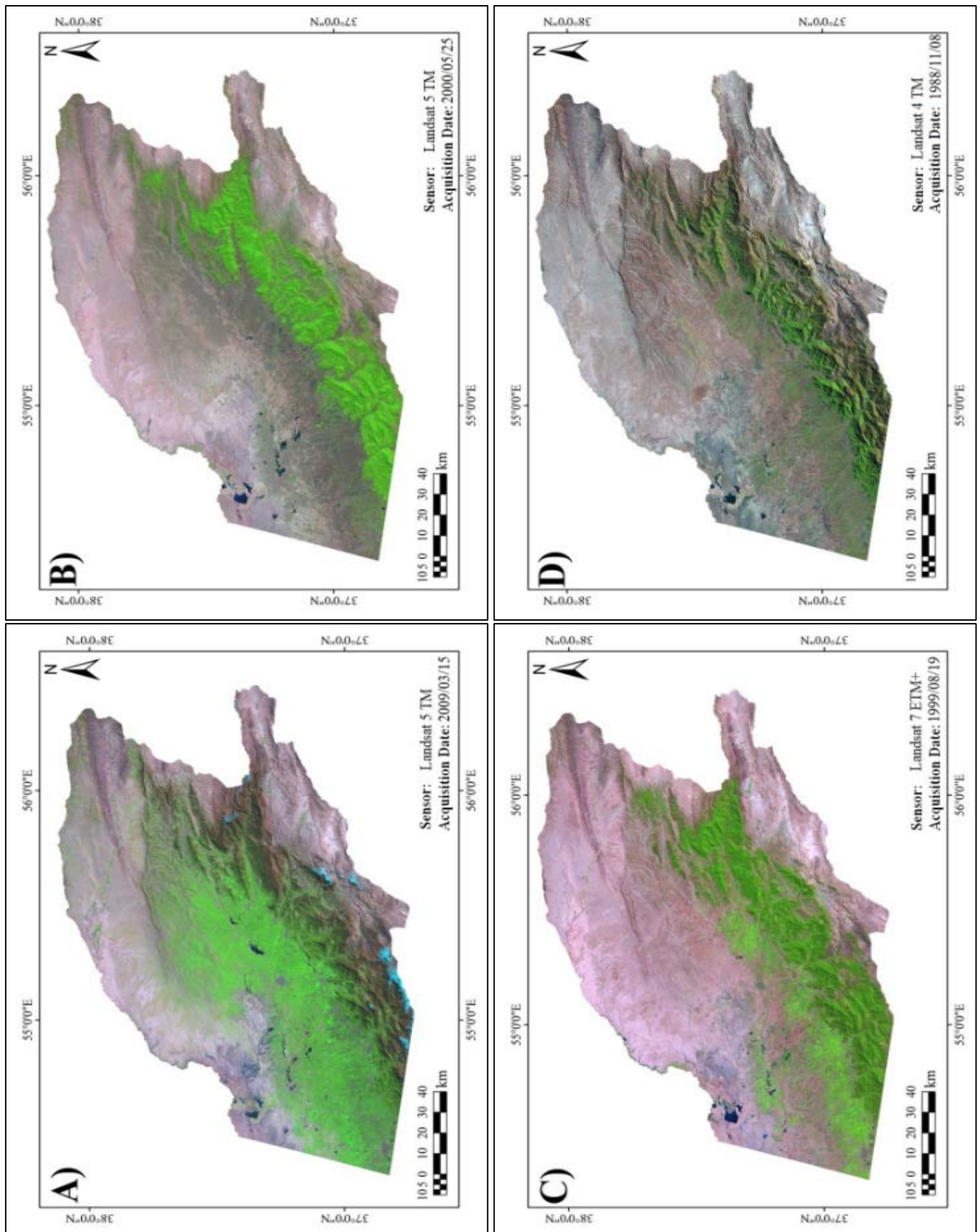Fig. 1. Location of study area and meteorological stations

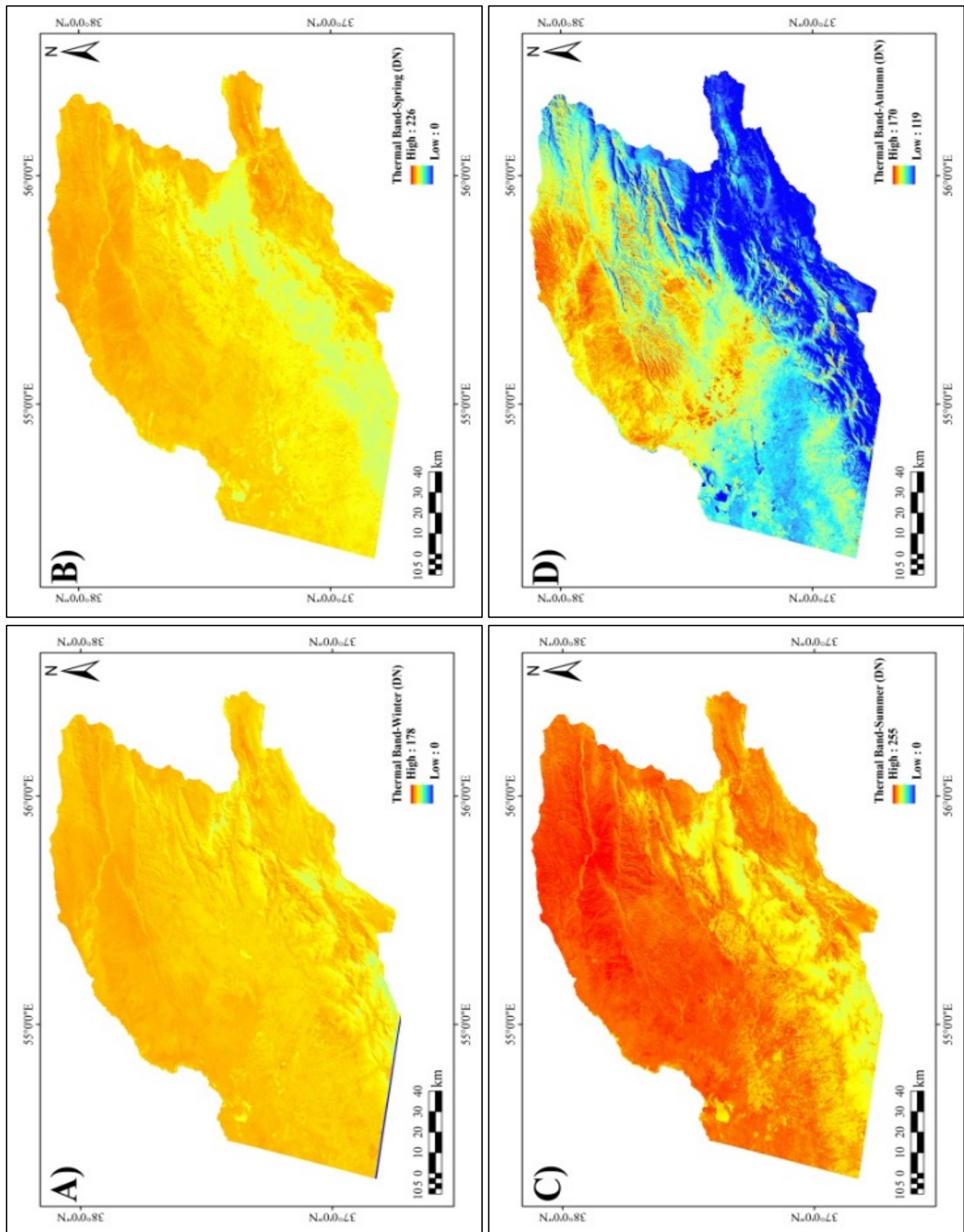Fig. 2. Satellite images of the study area in A) March, B) May, C) August and D) November

Fig. 3. Satellite images thermal bands of the study area in A) March, B) May, C) August and D) November
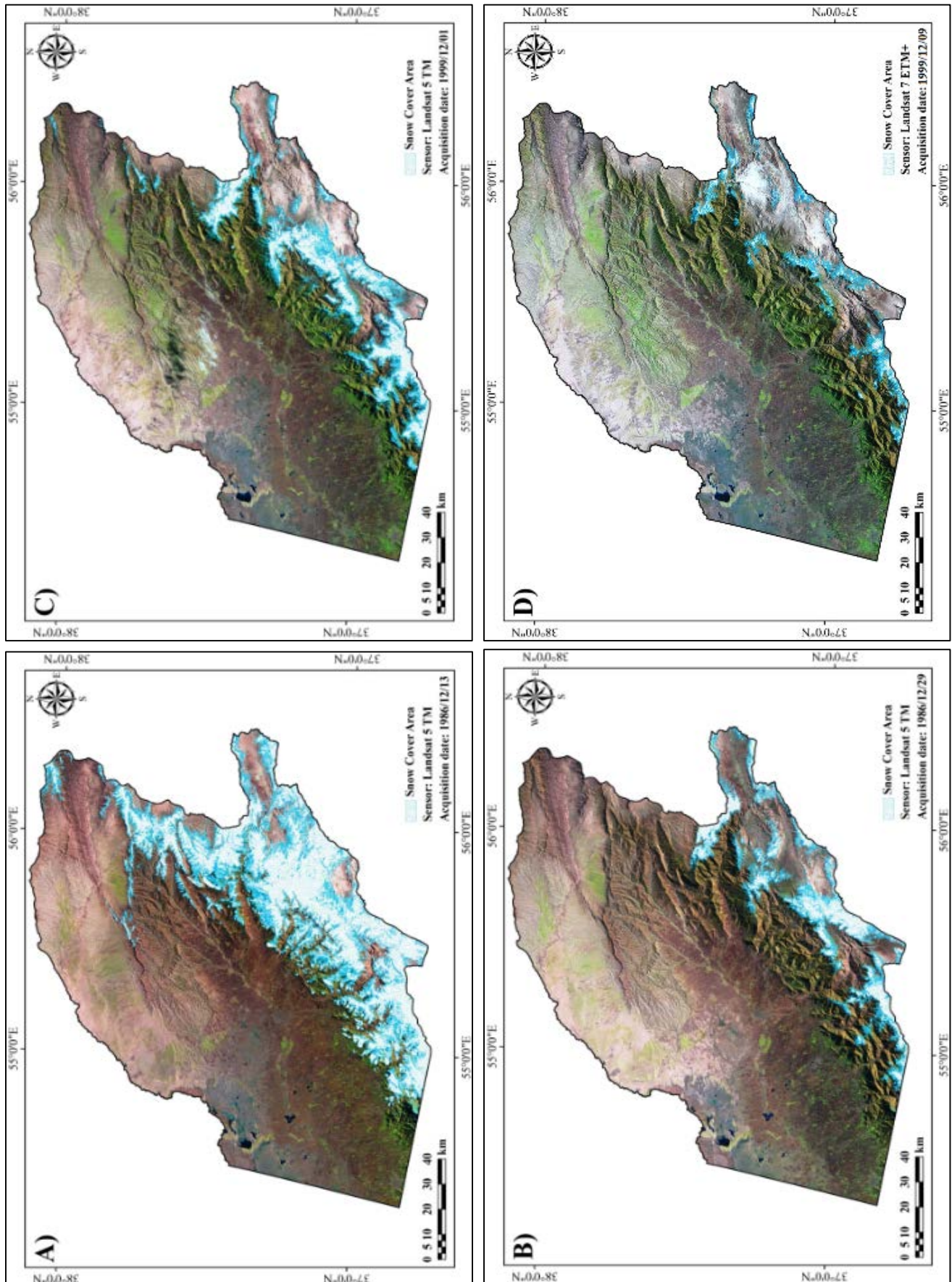
Fig. 4. Satellite images of the study area with SCA in A) 1986 first image (3786.9 Km^2), B) 1986 second image (1003 Km^2), C) 1999 first image (1261.4 Km^2) and D) 1999 second image (367.2 Km^2)
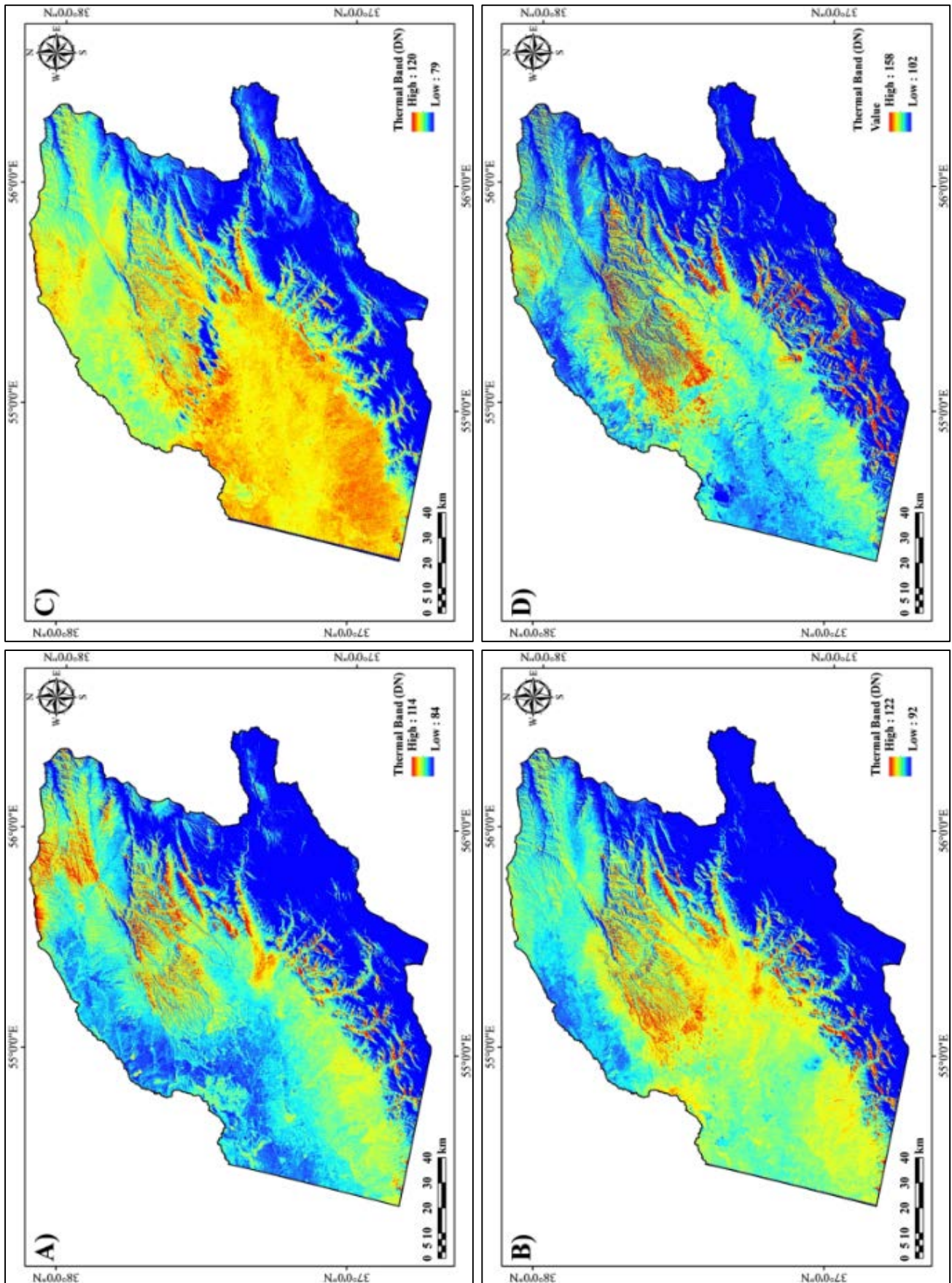
Fig. 5. Landsat thermal bands of the study area A) 1986 first image, B) 1986 second image, C) 1999 first image and D) 1999 second image.

2.2. Geostatistics: Kriging/Co-Kriging

As a brief description, Kriging is a geostatistical interpolation method derived from regionalized variable theory. It assumes that the distance, direction or both between observations which show spatial correlation can be employed to explain variation in the surface (Chen et al. 2013). Kriging can offer the best linear unbiased estimates with an accurate description of the spatial structure of the data and valuable information about estimation error distributions (Chen et al. 2013; Oliver and Webster 1990). A clear improvement to ordinary space–time kriging includes the use of ancillary data to aid in the estimation process, referred to as external drift (Wentz et al. 2010). Co-kriging is a versatile statistical approach for spatial point estimation, especially, when both primary and auxiliary attributes are available. If each component of z(s0) satisfies the intrinsic hypothesis that assumes that stationarity of the differences between pairs of data points exists in the first and second moments, then Co-kriging is unbiased and defined by equations 1, 2, and 3 (Meng 2006; Meng et al. 2013).

$$\hat{z}(s_0) = \sum_{j=1}^{n} z(s_j) \Lambda_{j\bullet} \tag{1}$$
$$\sum_{j=1}^{n} \Lambda_{j\bullet} = I \tag{2}$$
$$\sum_{\emptyset=1}^{v} \Gamma(s_i, s_j) + \Psi = \Gamma(s_i, s_0) \quad i = 1, \dots, n \tag{3}$$

Where I is an identity matrix $= [1, 0, \dots, 0]^T$, T indicates a transpose, and $\Lambda_{j\bullet}$ are the weights associated with the prediction. $z(s_j)$ is the vector $z_1(s_j)\dots z_m(s_j)$. $\Gamma(s_i, s_j)$ and $\Gamma(s_i, s_0)$ are the cross variograms and Ψ is the Lagrange Multiplier for i from 1 to n (Qingmin Meng, 2006; Q. Meng et al., 2013). We used the original thermal bands of Landsat and not the LST or NDVI as the auxiliary data to reduce the input data preparing time and provide a bigger range of values in the predictor variable. At the end, the ordinary and simple kriging and Co-kriging with and without transformations (regarding season data properties), optimization and stable model were implemented and tested and the results of them were compared to select the best output of anyone.

2.3. Validation and comparison

The leave-one-out cross-validation is a commonly applied method in Geostatistics because no reserved data are required for the data validation (Benavides et al., 2007). The number of sampled sites with climatic data is usually not very large and they are sparse throughout the study area, so all the sampled data are used for the spatial prediction in order to improve the precision of the predictions (Benavides et al., 2007). In this regards, results were compared by goodness-of fit statistics such as Mean Error (ME), Root Mean Square Error (RMSE), Mean Standardized Error (MSE), Average Standard Error (ASE) and Root Mean Square Standardized Error (RMSSE) (ArcGIS

Help, 2014; Benavides et al., 2007; Chen, Yue, Dai, & Tian, 2013; Delbari et al., 2013; Q. Meng et al., 2013; S.-q. Wang, Liu, Zhang, & Wu, 2011).

$$ME = \frac{1}{n}\sum_{i=1}^{n}[Z(x_i) - Z'(x_i)] \tag{4}$$

$$RMSE = \sqrt{\frac{1}{n}\sum_{i=1}^{n}[Z(x_i) - Z'(x_i)]^2} \tag{5}$$

$$MSE = \frac{\sum_{i=1}^{n}[Z(x_i) - Z'(x_i)]/\sigma(x_i)}{n} \tag{6}$$

$$ASE = \sqrt{\frac{1}{n}\sum_{i=1}^{n}[Z'(x_i) - \sum_{i=1}^{n}Z'(x_i)/n]^2} \tag{7}$$

$$RMSSE = \frac{1}{n}\sum_{i=1}^{n}[Z_1(x_i) - Z_2(x_i)]^2 \tag{8}$$

Where $Z(x_i)$ is the measured value of the sample points, and its fitted values is $Z'(x_i)$; Standard value of them is $Z_1(x_i)$ and $Z_2(x_i)$ respectively and $\sigma(x_i)$ is standard deviation (ArcGIS Help, 2014; Kalivas et al., 2013; S.-q. Wang et al., 2011)

The ME measures the bias of the prediction and should be close to zero for unbiased methods. It indicates whether the model is, on average, producing estimates that are overestimating or underestimating the observed values. In a well-adapted model, ME and SME should be close to zero for unbiased methods. The RMSE measure the average precision of the prediction and should be as small as possible. The model that performs the best will be the one with the smallest RMSE. This would suggest that the predictions are impartial and close to the respective real values. The values of ASE are used in order to evaluate the prediction divergence from real values. Therefore, ASE should be the same as RMSE, in order to evaluate the divergence of predictions correctly. If the value of the ASE is greater than that of the RMSE this suggests that the variability of the predictions is overestimated. Conversely, if the RMSE is greater than the ASE the variability of the predictions are underestimated. The values of RMSSE should be close to 1. If the RMSSE are greater than 1, then the variability of the predictions is underestimated; if the RMSSE are less than 1, the variability of the predictions is overestimated (ArcGIS Help 2014; Kalivas et al. 2013; Wang et al. 2011).

The ME, RMSE, ASE, SME and RMSSE were calculated to check the performance of each state of interpolations. Therefore, results based on described above rules was compared.

2.4. Image Processing: Snow Cover Mapping

Methods for snow-cover mapping can be categorized into three types: manual interpretation, classification-based, and index-based methods (Yin, Cao, Chen, Shao, & Chen, 2013). Manual-based methods are the most accurate; however, they are difficult and time-consuming to perform and require the skills of experienced specialists (Yin et

al., 2013). Index-based methods, where the normalized difference snow index (NDSI) is frequently used, take advantage of the spectral feature of snow cover characterized as strong reflection in visible/near-infrared wavelengths and nearly total absorption of middle-infrared wavelengths (Crawford, Manson, Bauer, & Hall, 2013; Dozier, 1989; Hancock, Baxter, Evans, & Huntley, 2013; Riggs, Hall, & Salomonson, 1994; Yin et al., 2013).

In this regard, to mapping the snow cover area we followed some steps: spectral characteristics and bands combination to better visualization of snow cover and calculate NDSI to combine the manual interpretation and index-based methods.

2.4.1. Spectral Characteristics and Bands Combinations:

According to Erdenetuya et al. (2006) and (Bakr, Weindorf, Bahnassy, Marei, & El-Badawi, 2010), to recognize snowy areas with regards to snow spectral characteristics, band combination was used and snow affected regions were extracted in 4,3,2 and 3,2,1 and 5,4,3 combinations as showed in Fig 6 and 7.
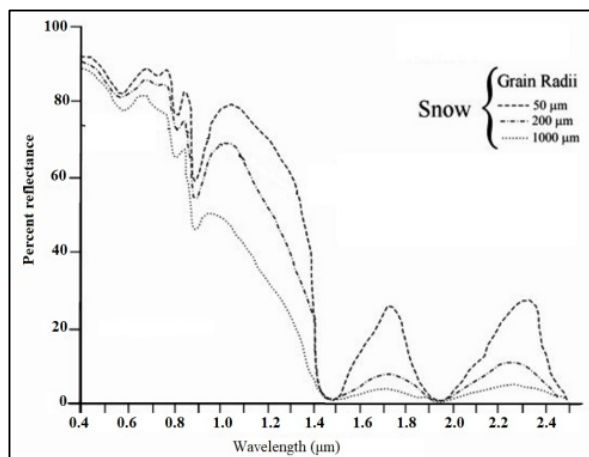

Fig. 6. Snow spectral reflectance. Snow shows variation in spectral reflectance according to the size of crystals in μ (Farooq, 2015)
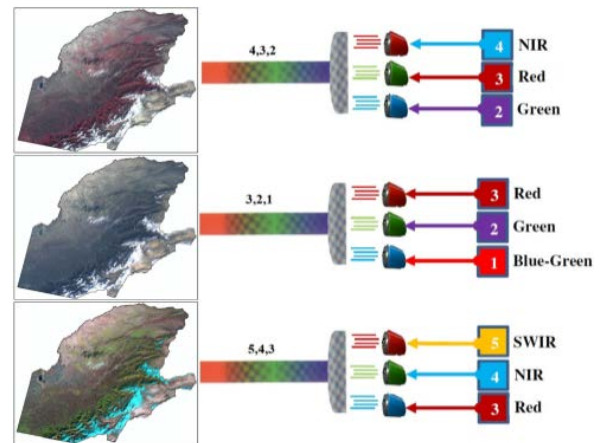
Fig. 7. Landsat band combination to show snow cover (Erdenetuya, Khishigsuren, Davaa, & Otgontugs, 2006).

2.4.2. NDSI:

As indicated above, the NDSI is the ratio of the difference in reflectance in the infra-red and the visible to the sum of the two, to estimate the fractional snow cover (Crawford et al., 2013; Dozier, 1989; Hancock et al., 2013; Riggs et al., 1994). In order to distinguish snow from similarly bright soil, rock and cloud we have calculated NDSI by following formulae:

$$NDSI = ((TM2 - TM5))/((TM2 + TM5)) \tag{1}$$

Where: TM2 and TM5 are Landsat band data (Crawford et al., 2013; Dozier, 1989; Erdenetuya et al., 2006; Klein & Isacks, 1999; Riggs et al., 1994; Wolter, Berkley, Peckham, Singh, & Townsend, 2012).

3. Result and Discussion

In this study, due to low density of meteorological stations, we used the thermal bands of remote sensing imageries from Landsat. Fig 8 and 9 show four maps of winter to autumn predicted mean temperature derived from Kriging and Thermal Co-kriging (TCK). Kriging shows interior regions warm while, there are two warm areas in the center and west (plains to the coastal area) in the TCK output. In spring and summer both of them has the same trend and the warm area is in the center (plain) and for the summer warm area move somehow to the west (to the coast). In the autumn, the kriging shows a descending gradual from west to east but in the TCK warm area located in the north part of the region (hills) with some spatial distribution. On the other hand, the cool parts in all seasons are in the east part of the study area (mountains) and spread over the north and an area in the west in spring.
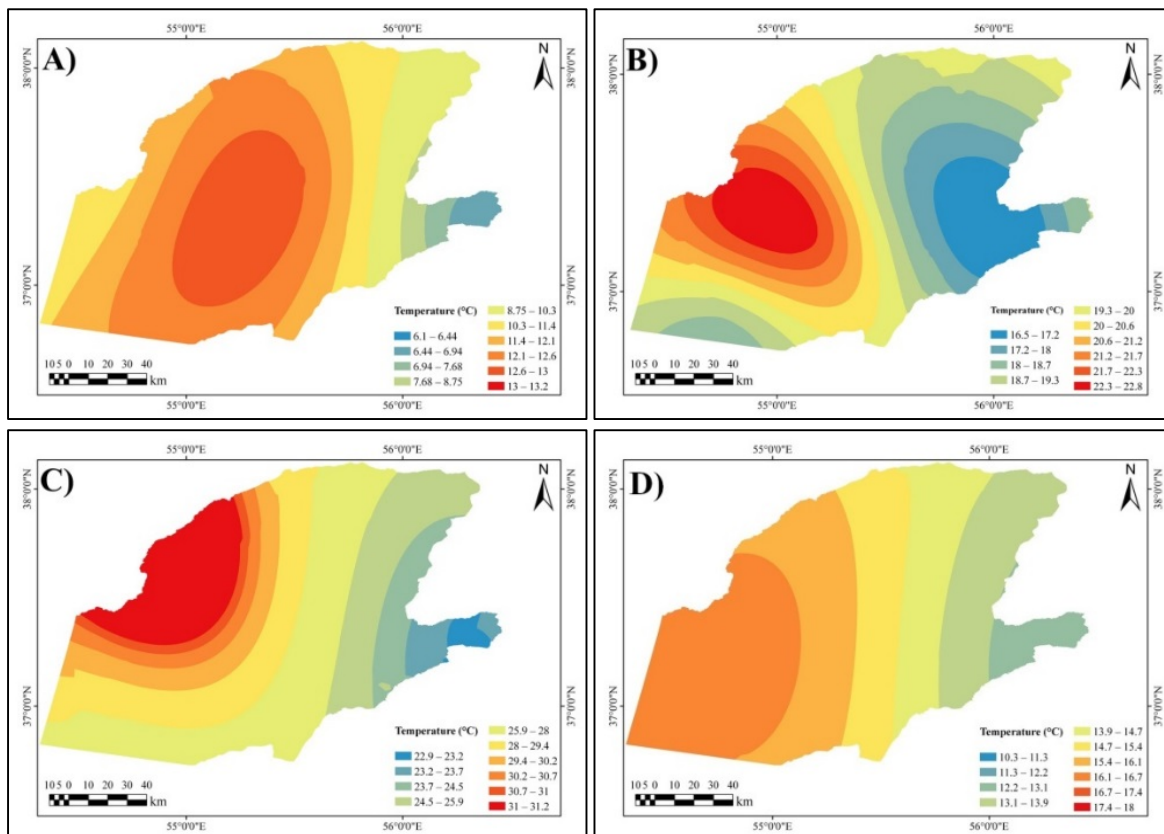

Fig. 8. Models of predicted mean air temperature for Kriging: (A) winter, (B) spring, (C) summer, (D) autumn.

Comparing statistics in the table 2 shows the difference between main data, kriging and TCK. In Min, the difference between TCK and main data in winter, spring and autumn is less than kriging but in the summer, the kriging is closer to the main data.

While, For the Max kriging is more similar to the main data in winter, spring and autumn and for the summer the TCK is closer. The winter, spring and summer for the kriging and autumn for the TCK are closer to the main data in the Mean parameter. In the S.D. variable, winter and autumn for TCK and spring and summer for kriging are more similar to the main data.
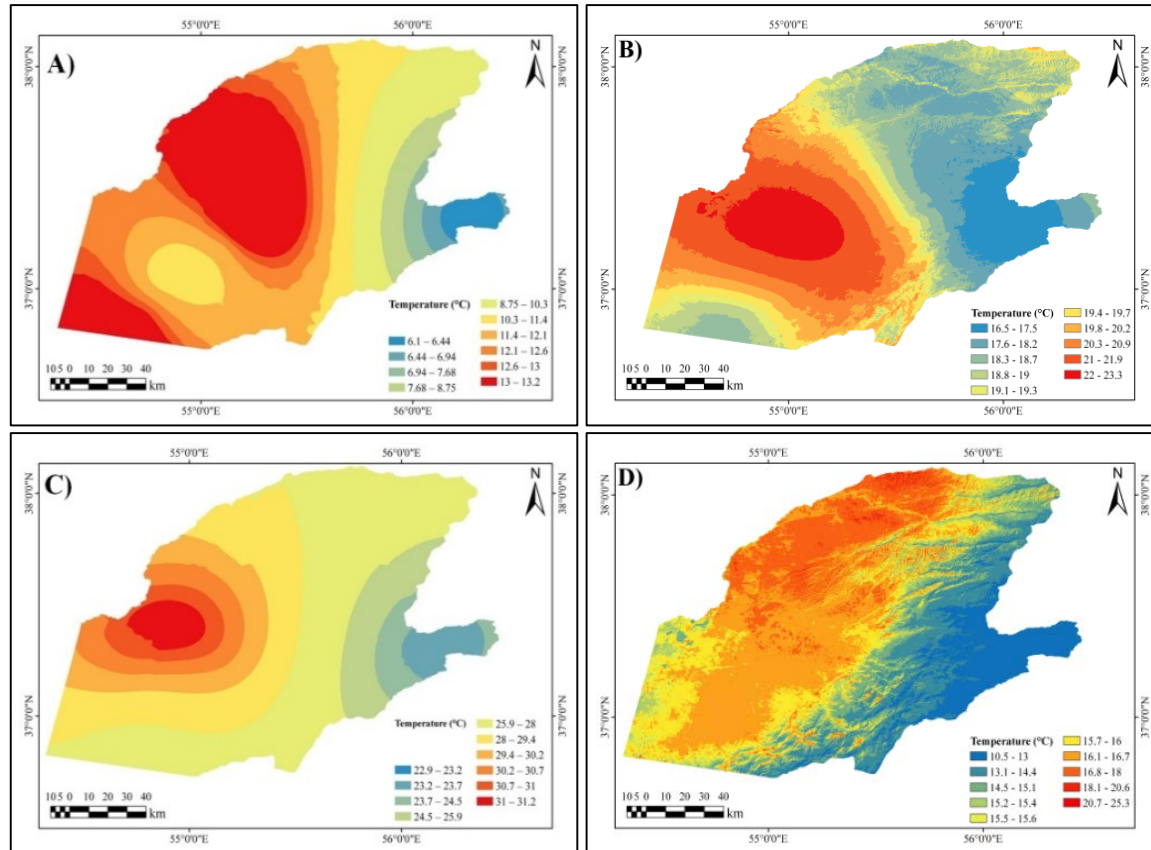

Fig. 9. Models of predicted mean air temperature with TCK: (A) winter, (B) spring, (C) summer, (D) autumn.

Table 2. Statistics of the predicted temperatures

Geostatistics Method		Winter	Spring	Summer	Autumn
Main Data					
	Min	6.1	16.5	22.9	10.3
	Max	13.2	22.8	31.2	18
	Mean	10.87	19.8	27.76	15.18
	S.D.	2.91	2.26	3.14	2.73
Kriging					
	Min	6.62	16.41	23.11	12.24
	Max	12.87	22.85	32.76	16.68
	Mean	10.86	19.53	27.84	14.87
	S.D.	1.69	1.54	3.00	1.34
Thermal Co-Kriging					
	Min	6.094	16.49	23.24	10.63
	Max	14.68	23.20	31.24	19.60
	Mean	11.08	19.43	27.59	14.97
	S.D.	2.12	1.40	2	1.55

Evaluation results based on ME, RMSE, MSE, RMSSE and ASE as goodness-of fit statistics can be seen in Table 3.

For optimality and validity of the models if the root-mean-squared prediction error is smaller for a particular model therefore it is the optimal model. However, when comparing to another model, the root-mean-squared prediction error may be closer to

the average estimated prediction standard error. This is a more valid model, because when we predict at a point without data, we have only the estimated standard errors to assess our uncertainty of that prediction. We also must check that the root-mean-square standardized is close to one (ArcGIS 10 help 2013).

Table 3. Results of ME, RMSE, MSE, RMSSE and ASE.

Geostatistics Method	Winter	Spring	Summer	Autumn
Kriging				
ME	0.00	0.30	-0.13	0.04
RMSE	1.37	1.01	1.40	2.04
MSE	0.01	0.14	-0.30	0.01
ASE	2.13	1.33	1.49	2.14
RMSSE	0.70	0.80	1.02	0.95
Thermal Co-Kriging				
ME	-0.13	0.24	-0.04	0.11
RMSE	1.08	1.04	1.48	1.90
MSE	-0.03	0.10	0.00	0.05
ASE	1.69	1.27	1.78	2.11
RMSSE	0.95	0.86	0.93	0.90

In light of these considerations and as can be understood from Table 3, TCK is optimal for the winter and autumn and valid for the winter and kriging is optimal for spring and summer and valid for summer. In addition, it has to be emphasized that, in general inspections of the results TCK getting more score in the winter and spring, and kriging in summer and autumn. Furthermore, spatial distribution of standard errors maps for kriging and TCK are shown in Fig 10 and 11.
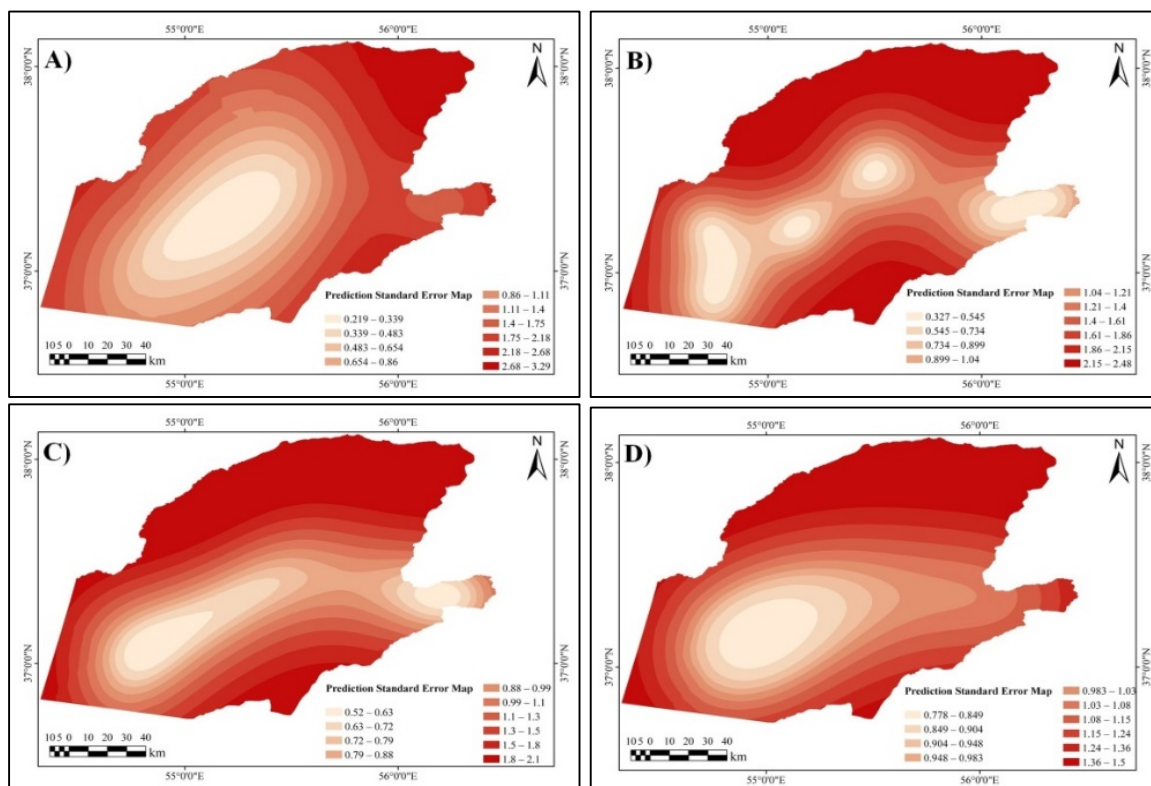

Fig. 10. Standard errors maps of mean air temperature with Kriging: (A) winter, (B) spring, (C) summer, (D) autumn.
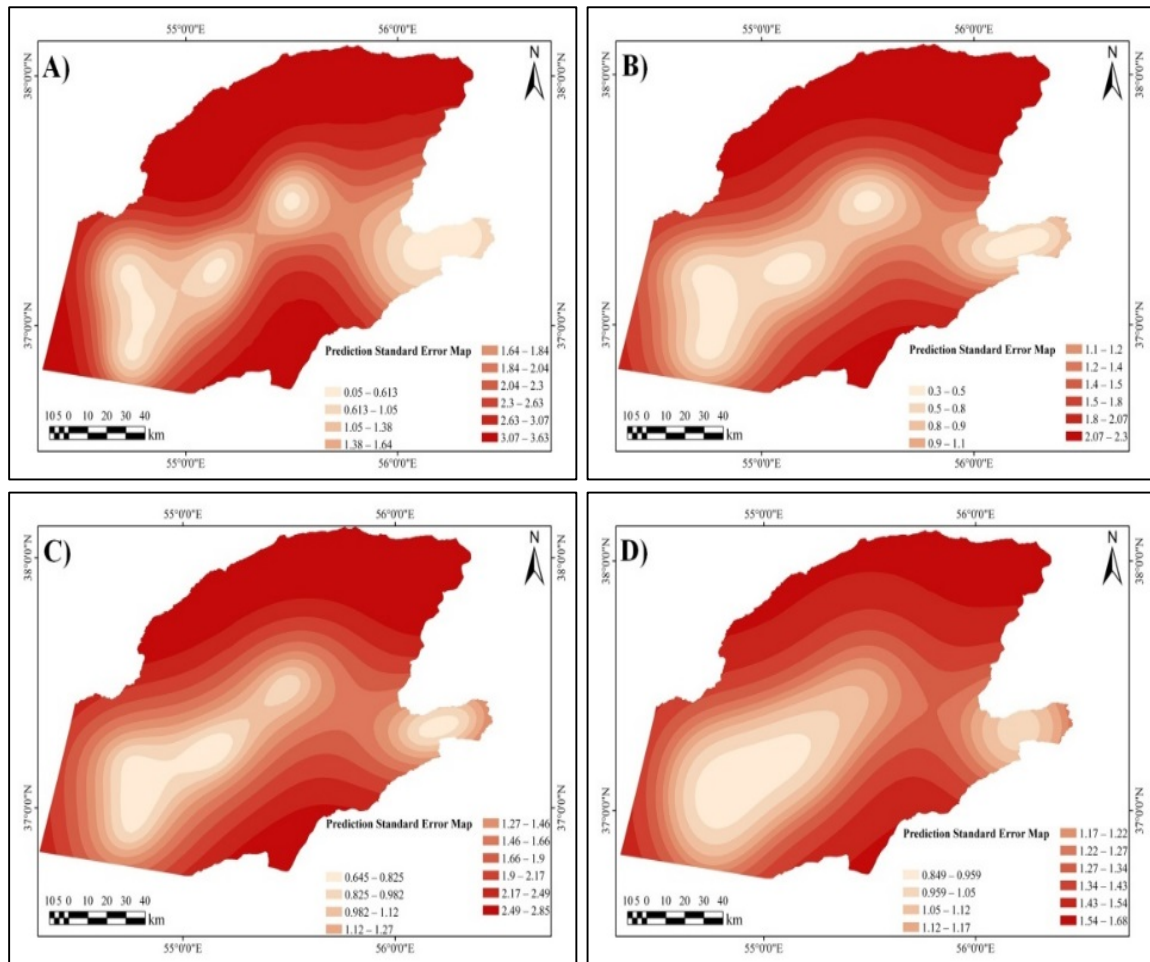
Fig. 11. Standard errors maps of mean air temperature with Thermal Co-Kriging: (A) winter, (B) spring, (C) summer, (D) autumn.

In the following, we studied impact of snow cover extent in images on Geostatistical modeling of air temperature. The areas of snow cover in each image are presented in the Table 4. As can be seen from the table, the greatest area is in of Fig 12 shows predicted maps with best results in ME, RMSE, ASE, MSE and RMSSE for each Geostatistical combination.

Table 4. Snow covered area in each image

Sensor / Acquisition date	Snow cover area (Km^2)
TM / 1986.12.13	3786.9
TM / 1986.12.29	1003
TM / 1999.12.01	1261.4
ETM+ / 1999.12.09	367.2

The maps reveal that thermal images create significant impacts and patterns on the interpolation results. Generally, cold temperature spread in the east of the region and the warm air temperature is in the interior and somehow north-west. Moreover, a very significant point is that using thermal satellite bands as auxiliary data show the impacts of elevation, aspect and land cover/use in interpolated air temperature maps.
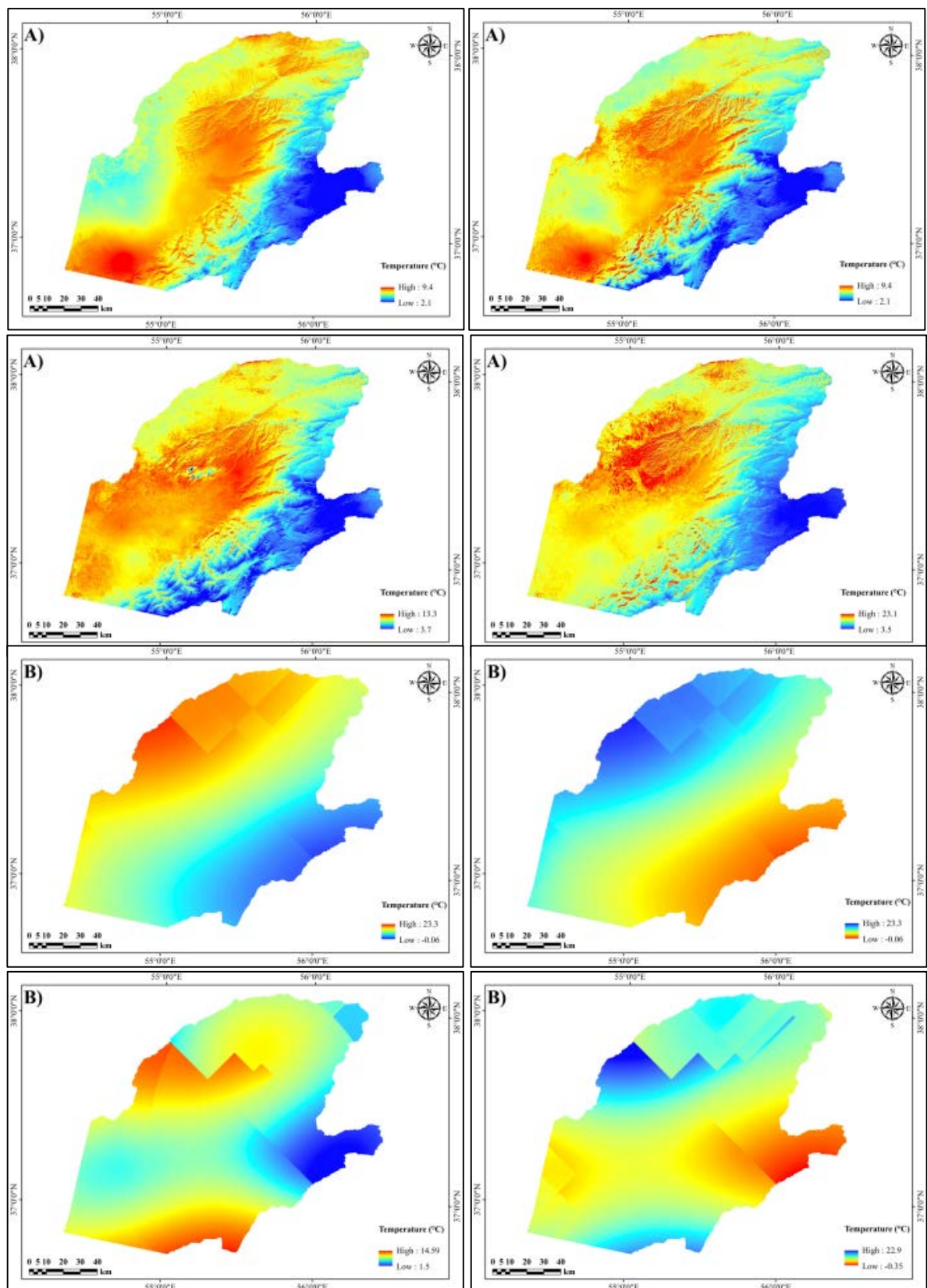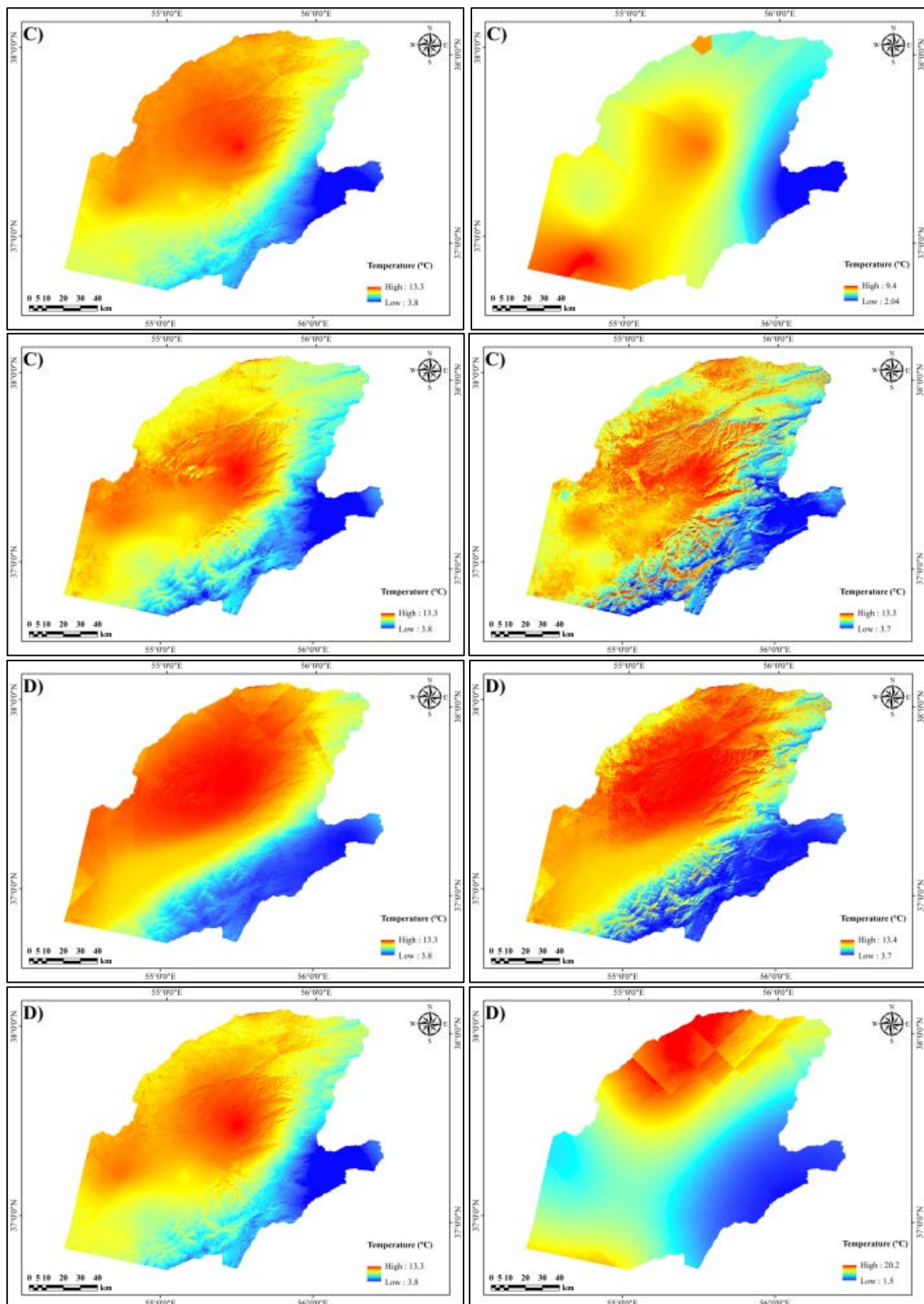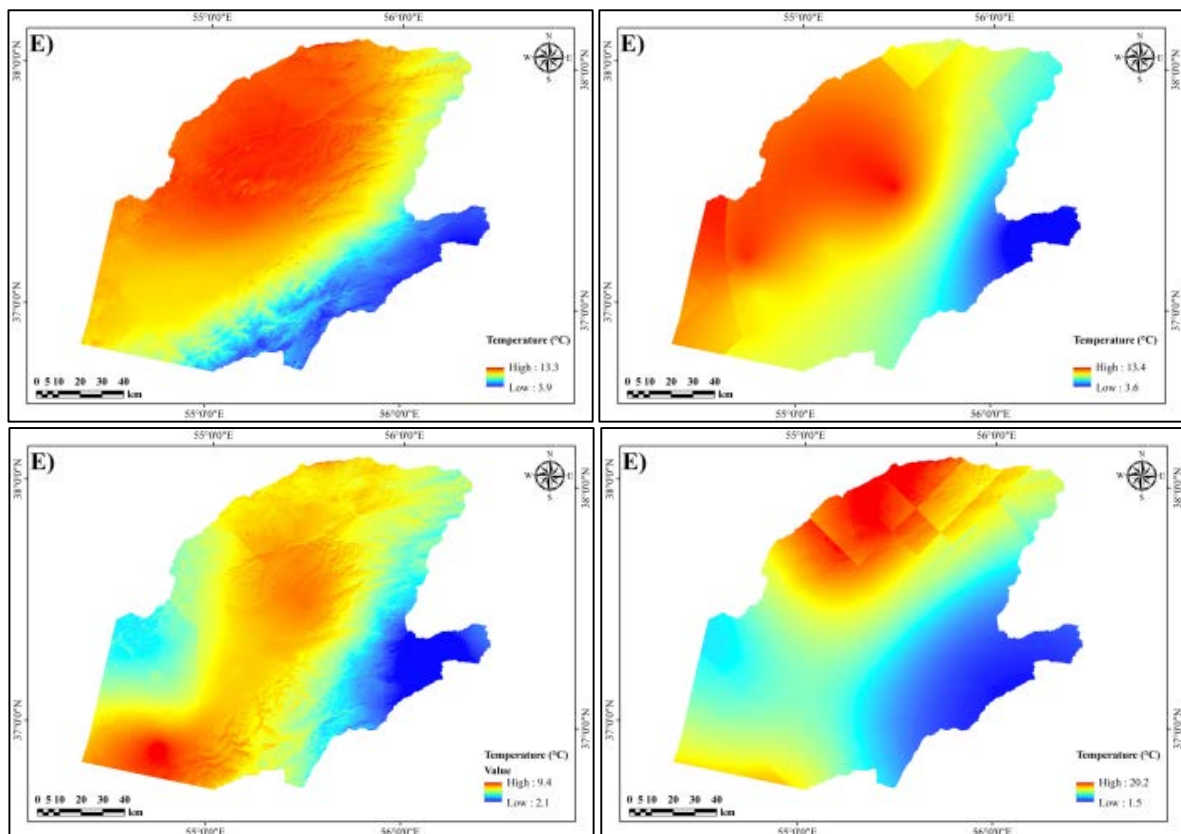
Fig. 12. Predicted maps for TCK1986 with more snow covered image in the left column. Second column is belonging to TCK1986 with low snow cover image. Third column show the results of 1999 interpolation with more snow affected image and fourth column is TCK1999 with second thermal image. In addition, A) is ME, B) RMSE, C) MSE, D) RMSSE and E) ASE.

Evaluation and comparing goodness-of fit statistics in Table 5 shows the difference between TCK outputs based on snow cover area.

Table 3. Results of ME, RMSE, MSE, RMSSE and ASE.

Geostatistics Method		TCK1986-1	TCK1986-2	TCK1999-1	TCK1999-2
Best ME					
	ME	0.00	0.00	-0.01	-0.01
	RMSE	1.50	1.20	2.80	2.03
	MSE	0.05	0.01	0.12	0.10
	RMSSE	0.70	0.64	0.90	0.50
	ASE	-0.30	-0.40	0.15	-1.70
Best RMSE					
	ME	-0.16	0.23	-0.60	-0.60
	RMSE	0.78	0.82	1.30	1.30
	MSE	-0.05	-0.52	-0.48	-0.48
	RMSSE	1.70	3.01	1.94	1.94
	ASE	-0.03	0.40	0.41	0.41
Best MSE					
	ME	-0.28	-0.11	-0.35	-0.14
	RMSE	2.70	1.36	2.80	2.33
	MSE	-0.01	0.00	0.00	0.00
	RMSSE	0.85	0.56	0.89	0.74
	ASE	-0.08	-0.60	0.50	-0.38
Best RMSSE					
	ME	0.41	-0.35	-0.80	-0.69
	RMSE	2.82	0.97	3.20	2.38
	MSE	-0.02	0.16	-0.10	-0.13
	RMSSE	0.87	0.98	1.00	1.01
	ASE	-0.04	0.00	0.50	0.29
Best ASE					

ME	-0.21	-0.35	-0.20	-0.62
RMSE	1.80	0.97	2.70	2.31
MSE	0.01	0.16	0.01	-0.13
RMSSE	0.79	0.98	0.86	0.79
ASE	-0.02	0.00	-0.01	0.01

As mentioned before for optimality and validity of the models if the root-mean-squared prediction error is smaller for a particular model therefore it is the optimal model (ArcGIS Help, 2014). However, when comparing to another model, the root-mean-squared prediction error may be closer to the average estimated prediction standard error (ArcGIS Help, 2014). This is a more valid model, because when we predict at a point without data, we have only the estimated standard errors to assess our uncertainty of that prediction. We also must check that the root-mean-square standardized is close to one (ArcGIS Help, 2014). In light of these considerations and as can be understood from Table 3, in spatial interpolation of 1986 the best-unbiased output is belonging to TCK1986-2 but the most accurate is TCK1986-1. TCK with less snow-affected image in 1986 provide precise standard error too. On the other hand, in 1999 TCK1999-1 show better results in amount of bias while accuracy with other TCK is the same. In addition, the TCK1999-1 provides more accurate standard error. Totally, comparing the results reveal that in Geostatistical modeling of December 1986 the TCK with more snow cover area had the best ME, RMSE and MSE conversely interpolated used less snow cover image had best RMSSE and ASE. For 1999 interpolation, TCK1999-1 is better for ME, MSE, RMSSE and is similar to 1999-2 in RMSE and ASE. Furthermore, if we decided based on RMSE and other statistics in one image, TCK1986-1 is the best for year 1986 and for 1999, the results are similar. In addition, the spatial distribution of standard error for predicted maps with best results in ME, RMSE, ASE, MSE and RMSSE in each Geostatistical combination are showed in the Fig 13.
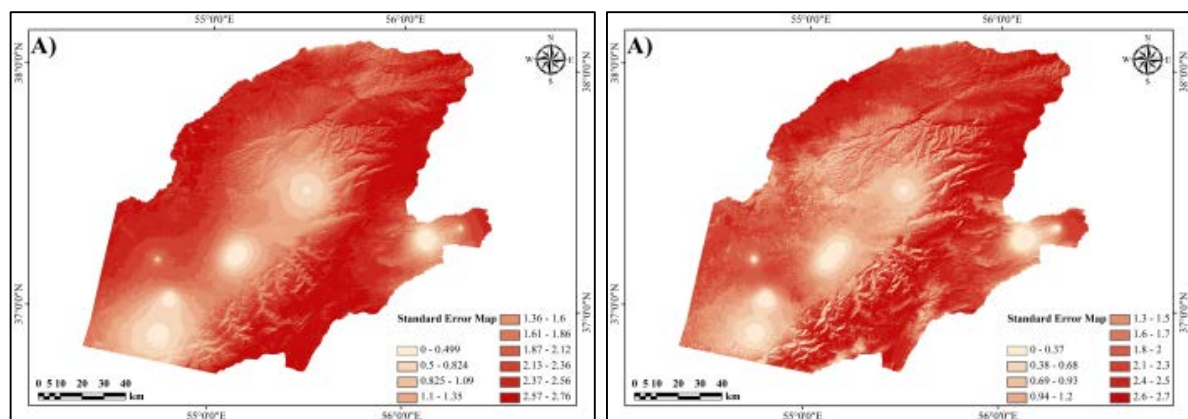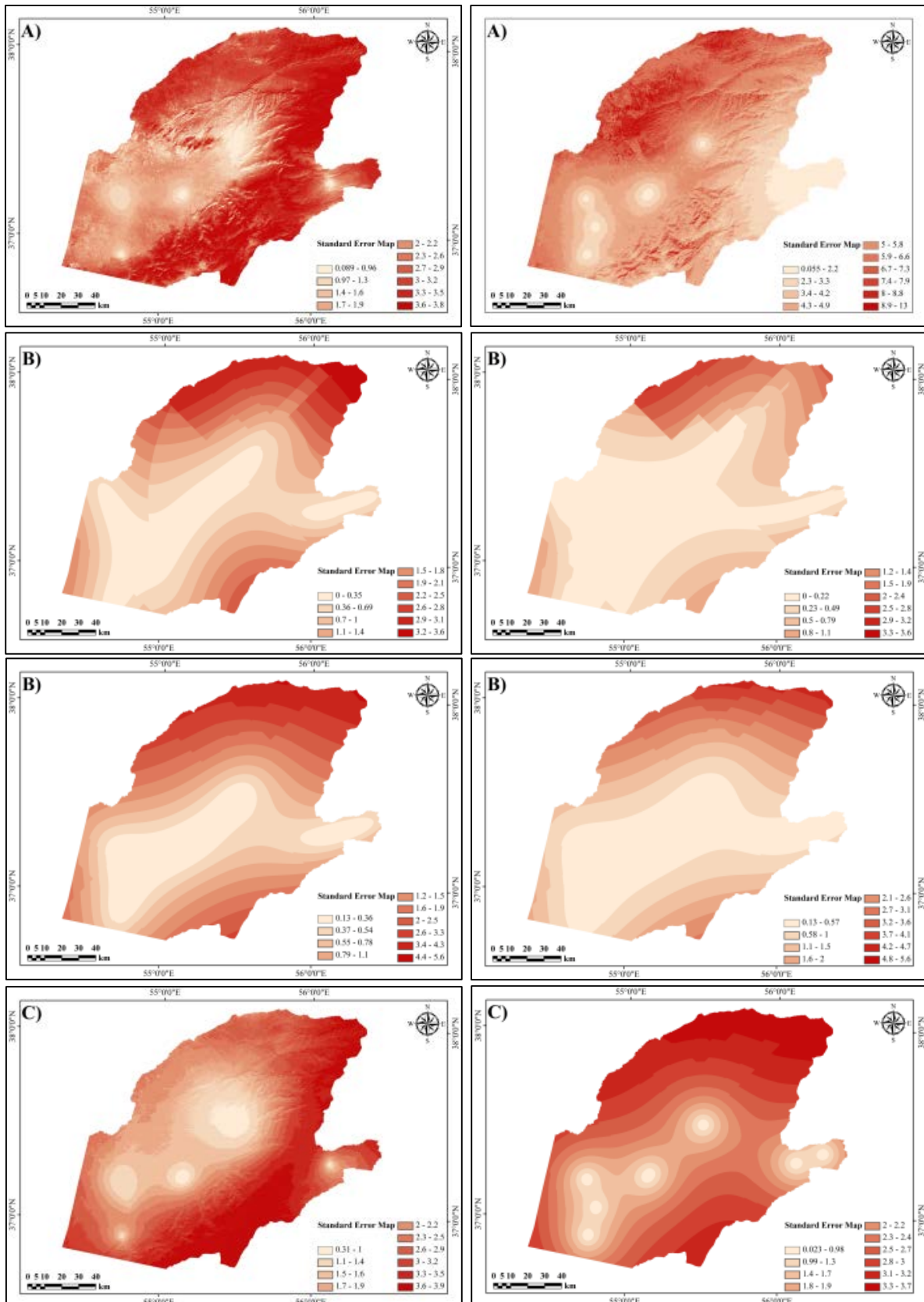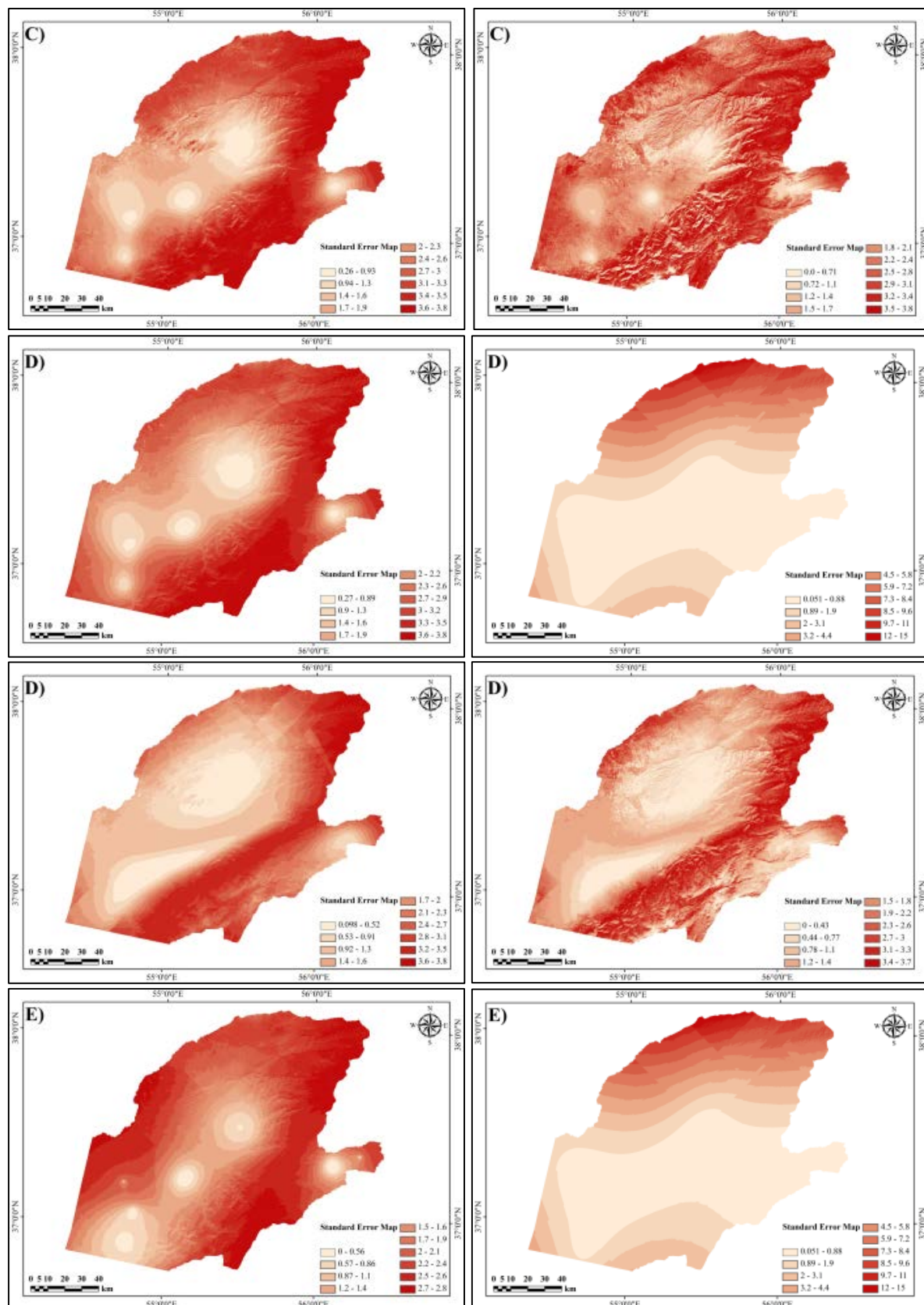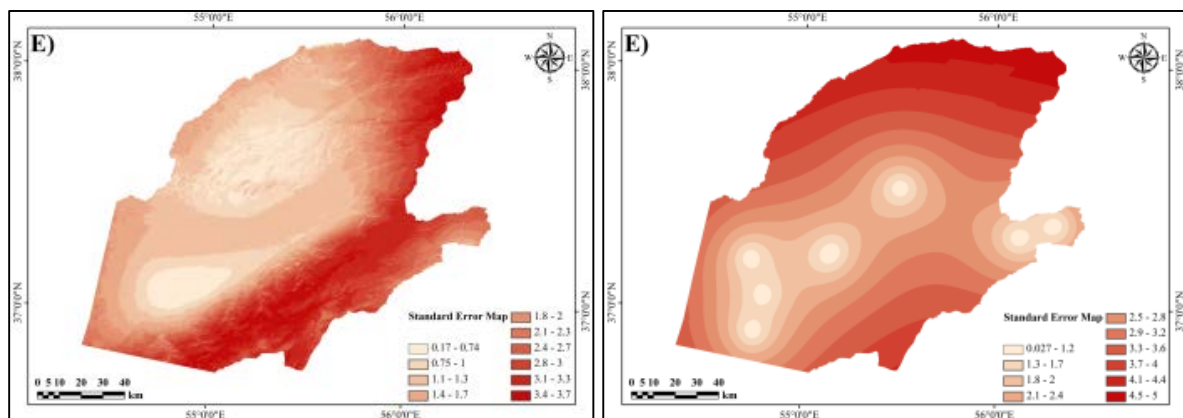
Fig. 13. Standard error maps for TCK1986 with more snow covered image in the left column. Second column is belonging to TCK1986 with low snow cover image. Third column show the results of 1999 interpolation with more snow affected image and fourth column is TCk1999 with second satellite image. In addition, A) is ME, B) RMSE, C) MSE, D) RMSSE and E) ASE.

4. Conclusions and Future Works

Developing Remote Sensing data (including thermal bands) is taking place at an unprecedented rate nowadays. In line with this development, satellite images can be relatively easily in access. Owing to this, we decided to first use the thermal bands of the TM and ETM+ sensors as auxiliary data to enhance the mean temperature interpolation quality in the complex regions with less meteorological stations and second evaluate the impact of snow-covered area in thermal images on air temperature interpolation. First section results reveals that, for this region with mentioned images the TCK has shown good performance for winter and autumn instead of kriging, though its result for the spring and summer is good too. While, second section results shows that, TCK for December of 1986 provide better results with more snow affected thermal image. While, in 1999 although different results was obtained but the best selected output did not show impacts of different snow cover area. It should be recalled that, in 1999, the snow cover areas are 1261.4 km^2 and 367.2 km^2 and they did not show difference in predicted results. While in 1986 first SCA is 3786.9 km^2 and second one is 1003 km^2. Therefore, we conclude that, maybe 3000 km^2 is the impact threshold.

Future direction of this research include testing and use of different spatial interpolations and Geostatistics methods, thermal bands for different regions and time periods. It is recommended to provide thermal inputs of Geostatistics methods using different sampling methods to reduce calculation volumes. Furthermore, check the usefulness of the method for other geographical factors that need to be interpolated. It is worth noting, that this study could open a new window to "climatic neighborhood" concept using future studies. At the end, it should be mentioned that we know the number of our observation stations are to low and considering the kriging requirements

like normal distribution and stationarity is toilsome but this problem exist in many regions in the world.

Personal Data:

- **First name:** Masoud
- **Surname:** Minaei
- **Academic degree:** PhD Student of University of Vienna
- **Date of birth:** Sep. 22, 1984 - Iran
- **E-mail:** minaiy.gis@gmail.com

Education:

03/2012 – Present: University of Vienna: PhD Student.
Field of Study: Geographic Information Science

09/2006 – 10/2009: University of Tehran: Master of Science.
Field of Study: Remote Sensing and Geographic Information Systems

02/2003 - 07/2006: University of Tabriz: Bachelor of Science
Field of Study: Geography

09/2001 – 06-2002: Andishe School: Pre-university.
09/1998 – 06/2001: Motahari High School: Diploma.

Honors and Awards:

✓ Top rank among Iranina PhD students in Austria, by the Union of Islamic Students Associations in Vienna.
✓ Introduced as a scientific elite by the Iranian National Elite Institute. Website: http://bmn.ir
✓ Elite graduated from Tehran University. In MSc.
✓ Ranked 1 among students of Geography and Climatology, University of Tabriz. In Bachelor.
✓ Honor of some champions and medals (at the University of Tabriz) in sport (Running).

Publications:

Book:

Minaei M, Faraji Sabokbar H.A, Rahmani M. (2010). Applicable Teaching of Fuzzy Logic (With Mention to Geography). Ministry of science publication. Tehran, Iran.

S.K Alavipanah, **Minaei M**, Nasiri H - Translation a book titled: Hyperspectral Remote sensing (principals and applications), Written by Marcus Borengasser et al., CRC Press, translated in Persian, Published in Nourbakhsh Press, (2010), Tehran, Iran.

Journals:

Maghsoudi M, Alavipanah S.K, Bagheri s, **Minaei M** (2010). Investigation of tectonic role in development of landforms (Case study Ghalajeh Synclinal). Accepted for publication in Journal of Geographical Environment. University of Tehran. Iran. (In Persian).

Fraji Sabokbar H.A, **Minaei M,** Ghodsi R (2009). Implementation of Agricultural Land Use Planning Model in Iran Using GIS, Fuzzy Logic and AHP(Case Study Freydun Shar Region in Esfahan Province). Journal of Geographical Environment. No.1. University of Tehran. Iran. (In Persian).

Maghsoudi M, Bagheri s, **Minaei M** (2009). Evaluation of tectonic role on appearing and change of alluvial fans. Journal of Geography and Regional Development. No. 12. Iranian Geographical Association and Ferdowsi university of Mashad. Mashhad. Iran. (In Persian).

Ziyari K, Hosseini S.A, Hosseini S.M, **Minaei M** (2008). The development in the concept of the paradigm and the planning of land use. Accepted for publication in Journal of humanities science, Modares University. Tehran. Iran. (In Persian).

Conference:

Minaei M, Kainz W, Abbasiyan A, Aghajani, M (2015) Remote Sensing Rangeland Detection using Geographic Object Based Image Analysis and Data Mining. National Conference on Advanced Research of Natural Resources Management. 16 April 2015- Malayer, Iran.

Minaei M, Kainz W, Hosseini S.A, Hoseini S.M (2014) Providing Agricultural Cadastral Maps Using Geographic Object Based Image Analysis and GIS in Different Agricultural Lands. Iranian Conference of Geographical Science, 20 May 2014 – Tehran, Iran.

Minaei M, Kainz W, Hosseini S.A, Hoseini S.M (2014) Urban Growth and Dynamics in the East of Gorganrood Watershed - 1972 to 2014. Iranian Conference of Geographical Science, 20 May 2014 – Tehran, Iran.

Minaei M, Kainz W, Minaei F (2013) Visualization and Spatio-Temporal Analysis of Drought using SPI and DI. The 2nd International Conference on Plant, Water, Soil and Weather Modeling. 8-9 May 2013. Kerman. Iran.

Davudi M, **Minaei M,** Jorjani H.A. (2008). Study the trend of annual extreme and average precipitation in Iran. Presented in 1st Iranian Geography Student Congress (IGSC). 28-29 oct 2008. Tehran. Iran.

Workshop:

- ✓ Workshop on the use of SWAT-CUP for SWAT model calibration, validation, sensitivity analysis, and uncertainty analysis held by EAWAG Aquatic Research Institute. 5-6 October 2015. Zurich, Switzerland.
- ✓ Ecohydrology: an essential tool for proper management of natural resources held by University of Malayer, April 2015, Malayer, Iran
- ✓ 4th advanced training course in land remote sensing workshop held by European Space Agency (ESA). 01-05 July 2013. Harokopio University. Athens, Greece.

Skils

- ✓ Scientific knowledge of the processing and analysis of multisensor, multitemporal and multispectral imagery.
- ✓ Software familiarity with ERDAS, ENVI, eCognition, ArcGIS, QGIS
- ✓ Ability to draft technical documents, analytical reports, and publications in English.
- ✓ Demonstrated ability to communicate effectively to produce high-quality analytical reports and present methods, techniques, and findings.
- ✓ Familarity with Laser Scanning
- ✓ Familarity with drones

Language:

- ✓ English: Fluent (IELTS 6)
- ✓ Persian: Mother tongue
- ✓ Kurdish: Fluent